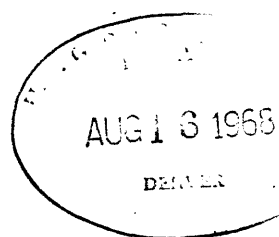


68-97

THE GEOLOGIC CLASSIFICATION OF THE METEORITES

by

Donald Parker Elston



A Dissertation Submitted to the Faculty of the

DEPARTMENT OF GEOLOGY

In Partial Fulfillment of the Requirements
For the Degree of

Doctor of Philosophy

In the Graduate College

THE UNIVERSITY OF ARIZONA

1 9 6 8

Murray carbonaceous chondrite; Specimen No. 635.1, 32.7 g;

Arizona State University Meteorite Collection, Tempe, Arizona.



Murray carbonaceous chondrite

ACKNOWLEDGMENTS

The opportunity to study meteorites was made possible through support provided by the Training Act of the United States Geological Survey. Results presented here summarize dissertation work at the University of Arizona, Tucson, undertaken in partial fulfillment of requirements for the PhD degree in geology. I wish to acknowledge the support of the faculty of the Geology Department of the University of Arizona, in particular Professor Spencer R. Titley, faculty and dissertation advisor, and Professors Paul E. Damon, Robert L. DuBois, John M. Guilbert, and Evans B. Mayo.

The work was made possible by the existence of excellent meteorite collections at Arizona State University, Tempe, and at the University of Arizona. I wish to thank Professor Carleton B. Moore, Director of Research, Center for Meteorite Studies at Arizona State University, for the extended loan of several meteorites, for numerous fruitful discussions and manuscript review, and for bringing to my attention unpublished data of his that led to correlations of the hypersthene and bronzite chondrites with the Ga-Ge II and III group irons, respectively. I also wish to acknowledge and thank Dr. Michael B. Duke, U. S. Geological Survey, for making available thin sections of a number of pyroxene-plagioclase achondrites, and for his review of an early version of this manuscript.

Much of the photographic work was done by Mr. B. D. Lindsay, Jr. The preparation of figures and tables was carried out at facilities at

the Center of Astrogeology, U. S. Geological Survey, Flagstaff, Arizona. Thanks are extended to the staff of the Water Resources Division Office of the U. S. Geological Survey, Tucson, for providing office space and administrative support.

The meticulous work of Geoffrey P. Elston, who painstakingly measured and catalogued map data that led to plots of the size-frequency distribution of materials in the Murray carbonaceous chondrite, is gratefully acknowledged. The wholehearted and unselfish support of my wife, Shirley, is directly responsible for the existence of this manuscript.

TABLE OF CONTENTS

	Page
LIST OF ILLUSTRATIONS	ix
LIST OF TABLES	xii
ABSTRACT	xiv
1. INTRODUCTION	1
2. THE METEORITE CLASSES	4
Descriptive Classification	4
Proposed Genetic Classification	5
3. EVIDENCE FOR GENETIC GROUPINGS	9
Compositional and Mineralogical Characteristics	9
Chemical Compositions	9
Distribution of Elements	10
Individuality of the Chondrite Classes	16
Correlations between Chondrites and Achondrites	20
Petrologic Evidence for the Metamorphism of Chondrites	23
Chemical-petrologic Classification of the Chondrites	23
Mineralogic-petrologic Classification of the Calcium-poor Stony Meteorites	26
Correlation of Irons and Pallasites with Chondrites	30
Ga-Ge Groups	30
Correlations with the Chondrites	36
Summary	41
4. CHONDRITES, THE FIRST ROCKS	42
Introduction	42
Murray Carbonaceous Chondrite	43
Circumstances of Fall	43
General Characteristics	44
Paragenetic and Textural Studies	48
Recognition of Components 1, 2, and 3 in other Chondrites	76
Chondrule Formation and Chondrite Accretion	84
Aggregation of Solids	84
Inferred Character of Early Solar System	86

TABLE OF CONTENTS--Continued

	Page
Possible Enrichment of Volatile Elements in Inner Part of Component 1 Dust Cloud	91
Evidence for a Common Parent Material	92
Elemental Abundances in Carbonaceous Meteorites and the Solar Photosphere	92
Uniformity of Fe and the Rare Earth Elements in Chondrites	95
Evidence for a Genetic Relationship between Components 2 and 3 in the Chondrites	96
Model for Accretion of Chondrites and Formation of Parent Bodies	98
Character of Parent Bodies for the Chondritic Meteorites	102
5. CALCIUM-RICH ACHONDRITES	106
Pyroxene-plagioclase Achondrites	106
Diopside-olivine and Augite Achondrites	107
Rare Earth Elements and Oxygen Isotopes in Stony Meteorites and Terrestrial Materials	109
Uniformity of REE in Chondrites	109
Calcium-poor and Calcium-rich Achondrites	113
Meteorites and Terrestrial Mantle Materials	115
Reflectance Characteristics of Stony Meteorites and the Moon	116
Remanent Magnetism in Meteorites	118
Summary	127
6. METEORITE BRECCIAS	128
Monomict and Polymict Breccias	128
General Descriptions and Definitions of Terms	128
Dense Impactites	157
Classification of the Meteorite Breccias	169
Volatile-rich Breccias	173
Volatile-poor Breccias	174
Interpretation of Record in Breccias	174
Comet-asteroid and Interasteroidal Collisions, Breakup of Asteroids, and Formation of Lunar Basins	174
Recent Cratering of the Moon	184
Tektites, and Lunar and Terrestrial Craters	189
APPENDIX I. Sources of Data for Table 4 - Elemental Abundances of Meteoritic Materials	198
APPENDIX II. Notes and References for Table 20	208

TABLE OF CONTENTS--Continued

	Page
APPENDIX III. List of Brecciated Meteorites Arranged in Genetic Groupings	214
APPENDIX IV. Ages of Selected Stones and Irons used for Estimating the Ages of Collision Events Outlined in Table 21	220
REFERENCES CITED	227

LIST OF ILLUSTRATIONS

Figure	Page
1. Relationship between oxidized iron, and iron as metal and sulfide in analyses of observed falls in chondrites. . .	17
2. Olivine composition, determined by X-ray diffraction, showing compositional hiatus in olivine-bronzite and olivine-hypersthene chondrites	19
3. Plot of CaO (weight percent) against FeO/FeO+MgO (mole percent) for the achondrites	22
4. Variation of Ga and Ge contents of iron meteorites	32-33
5. Relation between Ga and Ge concentrations in iron meteorites	35
6. Frequency distribution of the mole-ratios Fe/Fe+Mg in 63 individual olivine crystals (fig. 6a) and 16 individual pyroxene crystals (fig. 6b), Murray carbonaceous chondrite	49-50
7. Preliminary microgeologic maps of Murray carbonaceous chondrite	52-55
8. Size distributions of accretionary and pre-accretionary aggregates, particles and grains in the Murray carbonaceous chondrite	57-58
9. Compound pre-accretionary chondrule (component 2), Murray carbonaceous chondrite	61-62
10. Accretionary chondrule (component 3) containing particles, granules, and hollow spherules of matrix material, Murray carbonaceous chondrite	65-66
11. Accretionary chondrule containing several hollow matrix spherules, Murray carbonaceous chondrite	68
12. Fragmented, hollow matrix spherule that forms the nucleus of an irregular, accretionary aggregate (component 3), Murray carbonaceous chondrite	69

LIST OF ILLUSTRATIONS--Continued

Figure	Page
13. Yellow, limonitic stained accretionary chondrule (component 3), enclosed by a shiny black sheath of matrix material (component 1), Murray carbonaceous chondrite	71
14. Compound accretionary chondrule (component 3), Murray carbonaceous chondrite	72
15. Mighei carbonaceous chondrite	78
16. Mokoia pigeonite chondrite (carbonaceous)	79
17. Karoonda pigeonite chondrite	81
18. Holbrook hypersthene chondrite	83
19. Phase diagram for the system H-O-Mg-Si, from thermochemical calculations	87
20. Xenon and radiogenic ^{129}Xe contents for mineral phases and chondrule samples from the Bruderheim hypersthene chondrite	90
21. Rb-Sr values for the Peace River hypersthene chondrite, for four of its chondrules, and for carbonaceous and pigeonite meteorites	93
22. Schematic model of a carbonaceous meteorite (cometary) parent body	103
23. Schematic model of a volatile-poor chondrite (asteroidal) parent body	105
24. Absolute rare earth abundances for stony meteorites and for selected terrestrial materials	110-112
25. Development of milkiness in plagioclase of pyroxene-plagioclase achondrites with brecciation	119-122
26. Johnstown hypersthene achondrite (diogenite)	131
27. Carbon-bearing Norton County enstatite achondrite (aubrite)	132
28. Unbrecciated and brecciated pallasites	135

LIST OF ILLUSTRATIONS--Continued

Figure	Page
29. White achondrite (enstatite?) spherules and fragment in Juvinas eucrite.145-152
30. Morristown calcium-rich mesosiderite	160
31. Index map of moon and full moon photograph181-182

LIST OF TABLES

Table	Page
1. Modified Prior-Mason classification of the meteorites	6
2. Proposed genetic classification of the meteorites	7
3. The chemical compositions of the meteorites	In Pocket
4. Elemental abundances of meteoritic materials	11
5. Enrichment-depletion factors in the volatile-poor chondrites and achondrites relative to the carbonaceous chondrites	12
6. Relative abundance and distribution of trace and minor elements in stony meteorites	13
7. Summary of some mineralogical and compositional characteristics of the calcium-poor meteorites	21
8. Chemical-petrologic classification and proper names of the chondrites	24
9. Mineralogic-petrologic classification of the calcium-poor stony meteorites	27
10. Chondrites formerly and presently classed as olivine-pigeonite chondrites	29
11. Ranges of concentrations of Ga, Ge and Ni associated with the Ga-Ge groups in the metal phase of meteorites	31
12. Correlations between chondrite classes and Ga-Ge groups	37
13. Ga and Ge contents of the separated metal phase of enstatite, bronzite and hypersthene chondrites	39
14. Analysis of Murray carbonaceous chondrite	46
15. Abundance of particles and components in map areas of Murray carbonaceous chondrite	56

LIST OF TABLES--Continued

Table	Page
16. Mineral assemblages (components) in selected chondrites	77
17. Elemental abundances (atomic percent) for lunar mare and uplands materials, and for calcium-rich achondrites	108
18. Values of natural remanence (NRM) for various meteorites and meteorite classes	123
19. Provisional classification of the mesosiderites, and irons with silicate inclusions	137-139
20. Preliminary classification of meteorite breccias	170-172
21. Ages of stones and irons, and apparent correlations among proposed genetic groups	176
22. Generalized collision history inferred from the meteorite breccias and the ages of stones and irons	177

ABSTRACT

The meteorite classes of Prior and Mason are assigned to three proposed genetic groups on the basis of a combination of compositional, mineralogical, and elemental characteristics: 1) the calcium-poor, volatile-rich carbonaceous chondrites and achondrites; 2) the calcium-poor, volatile-poor chondrites (enstatite, bronzite, hypersthene, and pigeonite), achondrites (enstatite, hypersthene, and pigeonite), stony-irons (pallasites, siderophyre), and irons; and, 3) the calcium-rich (basaltic) achondrites. Chondrites are correlated with calcium-poor achondrites and the silicate phase of the pallasitic meteorites on Fe contents of olivine and pyroxene; and with metal of the stony-irons and irons on the basis of trace elements (Ga and Ge). Transitions in structure and texture between the chondrites and achondrites are recognized. The Van Schmus-Wood chemical-petrologic classification of the chondrites has been modified and expanded to a mineralogic-petrologic classification of the chondrites and calcium-poor achondrites.

Chondrites apparently are the first rocks of the solar system. Paragenetic and textural relations in the Murray carbonaceous chondrite shed new light on the manner of accretion, and on the character of dispersed solid materials ("dust", and chondrules and metal) that existed in the solar system before accretion.

Two pre-accretionary mineral assemblages (components) are recognized in the carbonaceous chondrites and in the unequilibrated

volatile-poor chondrites. They are: 1) a "low temperature" water-, rare gas-, and carbon-bearing component; and, 2) a high temperature anhydrous silicate and metal component. Paragenetic relations indicate that component 2 materials predate chondrite formation. An accretionary assemblage (component 3) also is recognized in the carbonaceous chondrites and in the unequilibrated volatile-poor chondrites. Component 3 consists of very fine grains of olivine and pyroxene, which occur as pervasive disseminations, as small irregular aggregates of grains, and as large subround to round, finely granular accretionary chondrules. Evidence in Murray indicates that component 3 silicates precipitated abruptly and at low pressures, possibly from a high temperature gas, in an environment that contained dispersed component 1 and 2 materials. All component 3 aggregates in Murray contain component 1 material, most commonly as flakes, and locally as tiny granules and larger spherules, some of which are hollow and some of which were broken prior to their mechanical incorporation in accretionary chondrules. Accretion may have occurred as ices associated with dispersed water-bearing component 1 materials temporarily melted during the precipitation of component 3 silicates, and then abruptly refroze to form an icy cementing material.

Group 1 materials may be cometary, and group 2 materials may be asteroidal. Schematic models are proposed.

Evidence is reviewed for the lunar origin of the pyroxene-plagioclase achondrites. On the basis of natural remanent magnetism, it is suggested that the very scarce diopside-olivine achondrites may be samples from Mars.

A classification of the meteorite breccias, including the calcium-poor and calcium-rich mesosiderites, and irons that contain silicate fragments, is proposed. A fragmentation history of the meteorites is outlined on the basis of evidence in the polymict breccias, and from gas retention ages in stones and exposure ages in irons. Cometary impacts appear to have caused the initial fragmentation, and possibly the perturbation of orbits, of two inferred asteroidal bodies (enstatite and bronzite), one and possibly both events occurring before 2000 m.y. ago. Several impacts apparently occurred on the inferred hypersthene body in the interval 1000 to 2000 m.y. ago. Major breakups of the three bodies apparently occurred as the result of interasteroidal collisions at about 900 m.y. ago, and 600 to 700 m.y. ago. The breakups were followed by a number of fragmentation events between hypersthene and bronzite materials on less than 100 m.y. intervals.

The apparent breakup history has implications for lunar and terrestrial geology. The major lunar basins may have been excavated by materials produced during the apparent major breakups, which would suggest ages for the lunar basins of about 900 m.y. and less.

A correlation between the four terrestrial tektite fields and four large (about 100 km) lunar ray craters is proposed. An explanation is offered for the formation of terrestrial craters that are apparently related with the three older tektite fields, and for the lack of an associated crater for the fourth, very young and very extensive tektite field. If the proposed correlations are valid, the Copernican System, the youngest of the lunar geologic systems, has a time span of about 35 m.y.

CHAPTER 1

INTRODUCTION

The capture of meteorites by the earth can hardly be entirely accidental or random because although 1800 meteorites have been collected as falls and as finds in the last 150 years or so, less than two dozen discrete classes of meteorites are recognized. In most meteorites the materials belong to a single meteorite class. Some meteorites, however, are brecciated and contain materials of two or more classes. In such cases, the mixtures are physical records of past events in the history of the meteorites.

The meteorites have arrived in the vicinity of the earth through some combination of circumstances or events, which presumably includes formation and storage in a parent body, followed, in most but not in all cases, by involvement in one or more fragmentation events and injection into earth-crossing orbits. If the discrete meteorite classes can be arranged in genetic groupings, we may better understand the source or sources of the meteorites, the character of the parent materials and bodies, and something of the fragmentation histories. The meteorite classes are now grouped only according to texture and phase (chondrite, achondrite, stony-iron, and iron), and not according to compositional and mineralogical characteristics that may have genetic significance.

The theme that is developed in Chapters 2, 3, 4, and 5 is that a number of the individual meteorite classes are genetically related.

Three broad genetic groups are proposed. One group includes material that appears to have been preserved with little change from the time of the formation of the solar system, and such material may be of cometary origin. A second proposed genetic group includes compositionally related materials of several meteorite classes; the materials appear to have undergone varying degrees of metamorphism, recrystallization, and fractionation, and they may be the debris of a small number of asteroidal bodies. The third proposed genetic group includes materials that appear to have been derived principally from the moon, but one or two meteorites of this group may have been derived from Mars. In Chapter 6, brecciated polymict meteorites are described and classified. They are interpreted to be mechanical mixtures that record comet-asteroid and interasteroidal collisions, and impact of the moon by cometary and asteroidal materials.

The concept of a geologic classification of the meteorites involves two principal parts: 1) a genetic classification; and, 2) a classification of the meteorite breccias. The validity of the genetic classification is developed: a) from compositional evidence that indicates the meteorites are derived from a limited number of sources and source bodies; and, b) from textural and paragenetic evidence that indicates the chondrites are the starting mixtures from which other types of meteorites have evolved. The genetic classification leads to implications regarding the pre-fragmentation character of the meteorite parent bodies, and the distribution of materials in the solar system. The classification of the meteorite breccias, and interpretation in light of the genetic classification, leads to an outline of the

fragmentation histories of the meteorite parent bodies. The geologic classification of the meteorites developed here hopefully can serve as a useful and flexible model for better understanding the meteorites, and solar system history.

CHAPTER 2

THE METEORITE CLASSES

Descriptive Classification

Classification of the meteorites began in the 19th century with the recognition of irons, stones, and stony-irons, following which there evolved two complicated, competing systems. One system recognized "type" meteorites. In the other system, meteorites were classed on a combination of mineralogical, compositional, and structural characteristics. The latter culminated in the Rose-Tschermak-Brezina (R.T.B.) system, in which 76 classes were recognized (Brezina, 1904). The R.T.B. classification, which is summarized by Mason (1962a, p. 47-50), contains the names of a number of meteorite classes that are still in use today. Mason (1962a) points out that the R.T.B. classification is unsatisfactory in that the multiplicity of classes has tended to obscure the essential similarity of many of the chondritic meteorites.

A revised and simplified version of the Rose-Tschermak-Brezina classification was proposed by the British meteoritist G. T. Prior (1920). Prior's classification has become widely used because it allows for rapid cataloging with a minimum of mineralogical and chemical investigations. In it, as in the R.T.B. classification, four groups of meteorites are recognized, -- the chondrites, achondrites, stony-irons, and irons. Prior's classification was modified by Mason (1962b), who recognized two additional chondrite classes, the carbonaceous chondrites

and the pigeonite chondrites. Mason (1967a) subsequently proposed that the pigeonite chondrite class be abandoned, but it is retained in this paper for reasons given later.

The Prior-Mason classification of 1962 is reproduced in slightly modified form in Table 1. The chondrites are arranged in order of increasing average metal contents. To maintain uniformity in classification, a class of carbonaceous achondrites is formally recognized here; elsewhere, achondritic carbonaceous meteorites currently are classed as carbonaceous chondrites and are called Type I carbonaceous chondrites (Wiik, 1956; Mason, 1963a). Other modifications in Table 1 include subdivision of the achondrites into calcium-poor and calcium-rich subgroups, and subdivision of the mesosiderites into calcium-poor and calcium rich subclasses.

The Prior-Mason classification is descriptive because the meteorite classes are grouped either on the basis of structure (chondrites, achondrites), or on the relative amount of silicate and metal (stony-irons, irons). Grouping in this manner does not allow for the possibility that physically and structurally similar materials may have formed and resided in different parent bodies. The format of the Prior classification is expanded into a proposed genetic classification to allow for this possibility.

Proposed Genetic Classification

The proposed genetic classification is summarized in Table 2. Support for the validity of the classification is developed in

Chapters 3, 4, and 5. Inferred sources shown in Table 2 are derived from discussions in the three chapters that follow.

CHAPTER 3

EVIDENCE FOR GENETIC GROUPINGS

Compositional and Mineralogical Characteristics

Chemical Compositions

The chemical compositions of the meteorites (Table 3, in pocket) are summarized in the format of the proposed genetic classification. In the stony meteorites, compositional hiatuses with respect to water and carbon, and calcium, separate the three proposed genetic groups. In the calcium-poor groups, the individual chondrite classes exhibit fairly characteristic contents of disseminated metal; the volatile-poor achondrites are coarsely crystalline silicates in which very sparse metal occurs in breccia; and the stony-irons and irons contain abundant metal, which mainly displays textures that are attributable to slow cooling and crystallization in a parent body. Some chemical similarities and relationships exist between the chondrites and the calcium-poor achondrites, pallasites, and irons. The chondrites are mixtures of silicates, metal, and sulfides that can serve as sources for the other types of meteorites.

The carbonaceous meteorites, chondrites and achondrites, are rich in rare (noble) gases (Signer and Suess, 1963) as well as in water (Table 3). On the basis of textural and paragenetic relationships, which are discussed in Chapter 4, the gases and water appear to be intrinsic to carbonaceous matrix materials of unmetamorphosed

(unequilibrated) chondrites, both volatile-rich and volatile-poor. The carbonaceous achondrites (Type I of Wiik, 1956) have been shown by Ringwood (1966, Fig. 1) to have elemental abundances that are similar to elemental abundances of the solar photosphere. Ringwood suggests that carbonaceous achondrite materials may be closely related to the dust particles of the primordial solar nebula, but he cautions they are not to be regarded as unaltered samples of this primitive dust because they appear to have undergone a mild thermal and metamorphic history.

Studies described in Chapter 4 support this idea.

Distribution of Elements

Abundances of some major, minor, and trace elements in the chondrites and achondrites are listed in Table 4, and enrichment-depletion factors relative to the carbonaceous chondrites are given in Table 5. The relative enrichments and depletions of groups of elements that have similar melting points are summarized in Table 6. Elemental discontinuities exist. The carbonaceous achondrites are enriched, relative to the carbonaceous chondrites, in the low melting point elements Cs, Rb, K, Na, Li, and Ba; the carbonaceous achondrites are slightly depleted in Sr and the higher melting point elements. Curiously, the low melting point elements Rb, K, Na, Li, Ba, and Sr are enriched in the more highly metamorphosed, volatile-poor chondrites relative to the otherwise volatile-rich carbonaceous meteorites. The calcium-poor achondrites are depleted in these elements relative to the volatile-poor chondrites. The pyroxene-plagioclase achondrites are greatly depleted in Cs relative to the chondrites; substantially to slightly depleted in Rb, K,

Table 5.--Enrichment-depletion factors in the volatile-poor chondrites and achondrites relative to the carbonaceous chondrites.^{1/}

Element	Calcium-poor volatile-poor		Calcium-rich		
	Chondrite (Average)	Achondrite (Average)	Nakhlite	Howardite	Eucrite
Cs	0.5	0.3	--	--	0.09
Rb	1.9	0.6	1.7	--	0.1
K	1.9	0.3	2.7	0.5	1.1
Na	1.5	1.2 ^{2/} 0.7 ^{3/}	0.8	0.6	0.8
Li	4.4	1.6	--	--	16
Ba	2.8	1.7	--	5.8	10
Sr	1.7	0.8	6.1	3.8	8.5
Ca	1	0.6	8.4	4.3	5.6
Mg	1.1	1.5	0.6	0.6	0.4
Al	1.1	0.4	0.8	0.5	0.6
Si	1.3	1.7	1.7	1.7	1.7
Fe ^{4/} <u>5/</u>	0.6 1	0.5 0.5	1 0.7	0.8 0.6	0.8 0.6
Ni	1	0.1	--	0.1	--
Sc	0.9	1.1	6.6	1.9	3.1
Y	1.5	0.8	2.1	--	12
La	0.9	0.3	4.9	--	11
Ce	1	0.9	6.7	4.6	8.4

^{1/}. Enrichment and depletions relative to carbonaceous chondrites are calculated from data in Table 4.

^{2/}. Average of 3 meteorites.

^{3/}. Average of 2 meteorites.

^{4/}. In silicate only.

^{5/}. In silicate, metal, and sulfide.

Table 6.--Relative abundance and distribution of trace and minor elements in stony meteorites.

Elements	Melting Point °C	Carbonaceous chondrite	Volatile-poor chondrite	Nakhlite	Howardite-eucrite
Cs	28	Background	Depleted	Depleted	Greatly depleted
Rb, K, Na	38-97	"	Enriched	Substantially enriched	Greatly depleted- slightly depleted
Ca	842	"	Background	More highly enriched	
La, Ce and the other rare earths	804-1652	"	"	Enriched	Enriched-more highly enriched

and Na; and enriched to highly enriched in Li, Ba, Sr, Ca, and the rare earths.

If chondrites are the starting materials, a conclusion that is drawn from evidence presented in Chapter 4, the distribution of elements in the different meteorite groups and classes (Tables 5 and 6), may be partly the result of an uneven distribution of elements in the solar system at the time of accretion as well as the result of post-accretion fractionations in parent bodies. If the volatile-rich carbonaceous meteorites are essentially unmetamorphosed, nearly primitive materials, they should be rich in the volatile element Cs. This then raises the question as to why Rb through Sr (Tables 5 and 6) are enriched in the volatile-poor chondrites relative to the volatile-rich carbonaceous chondrites. Appeal to an enrichment of these volatile elements in the chondrites during the metamorphism of a parent chondritic material which initially contained uniform quantities of the minor elements does not seem warranted because Cs is depleted, and Ca and the rare earths are unenriched. A possible solution is that the Rb through Sr group of elements was enriched in the region of accretion of the volatile-poor chondrites. Depletions in the calcium-poor achondrites relative to the chondrites (Table 5) would be expected if these achondrites are the products of metamorphism and recrystallization of chondritic silicates.

An elemental discontinuity exists between the calcium-rich and calcium-poor meteorites in respect to Ca and the rare earths. These elements may have been enriched from normal chondritic abundances as the result of differentiation processes in the parent bodies. The calcium-poor achondrites, in contrast, are not enriched in Ca and the rare

earths. They contain rare earth abundances similar to, and markedly less than, those of the chondrites (Chapter 5), which is considered evidence for the genetic relationship between the chondrites and calcium-poor achondrites. The marked depletions seem to indicate that rare earths can be lost during the slow crystallization that appears to have been required for the development of the very coarsely crystalline pyroxene of the hypersthene and enstatite achondrites. Rare earths, thus lost, would presumably become available for incorporation in differentiated silicates. However, the possibility exists that the high Ca and rare earth abundances for the calcium-rich achondrites may be inherited from chondritic materials that were enriched in these elements at the time of accretion.

An apparent elemental discontinuity exists within the calcium-rich achondrites with respect to Rb and K, which are enriched in the diopside-olivine achondrites and are depleted in the pyroxene-plagioclase achondrites relative to the carbonaceous chondrites. Because Rb and K are also enriched in the volatile-poor chondrites, the possibility arises that the parent material of the diopside-olivine achondrites may have had Rb and K contents similar to volatile-poor chondrites, and possibly that parent material of the pyroxene-plagioclase achondrites may have been depleted in Rb and K. If meteorites can be identified in respect to general source areas in the solar system, and if the manner of accretion can be outlined, then the possibility of an uneven distribution of volatile elements at the time of accretion can be examined.

Individuality of the Chondrite Classes

The chondrite classes have been shown by Ringwood (1961; 1966, Fig. 4) and by Mason (1962a, 1965) to occupy discrete compositional fields when the weight percent of oxidized iron that resides in silicates is plotted against the weight percent of iron in metal and sulfide (Fig. 1). Such a plot shows the existence of distinct hiatuses between, and essentially defines the existence of, five discrete classes of chondrites. The plot also shows that although the relative amounts of oxidized iron and iron in metal vary widely, the total iron content remains approximately constant. Prior (1916) summarized the relationship between the metal and silicates as follows: "the less the amount of nickel-iron in chondritic stones the richer it is in nickel and the richer in iron are the magnesium silicates". This has become known as "Prior's rule" or "rules" -- because two relationships are noted.

Four of the five meteorite classes (Fig. 1) can be intersected by a single line of essentially constant iron content. One class, the hypersthene chondrites, can be intersected by a line of lower total iron content. The compositional difference was first noted by Urey and Craig (1953) in "superior" analyses of ordinary chondrites (hypersthene and bronzite chondrites), and it led to the proposal that the chondrites be classed in a high-iron or H-group (bronzite), and a low-iron or L-group (hypersthene). Members of the low-iron group tend to cluster into two subgroups, and the L-group has recently been subdivided into L- and LL-groups (Keil and Fredriksson, 1964). Ringwood (1966) concludes that the plot of oxidized iron versus metallic iron shows that there is no doubt

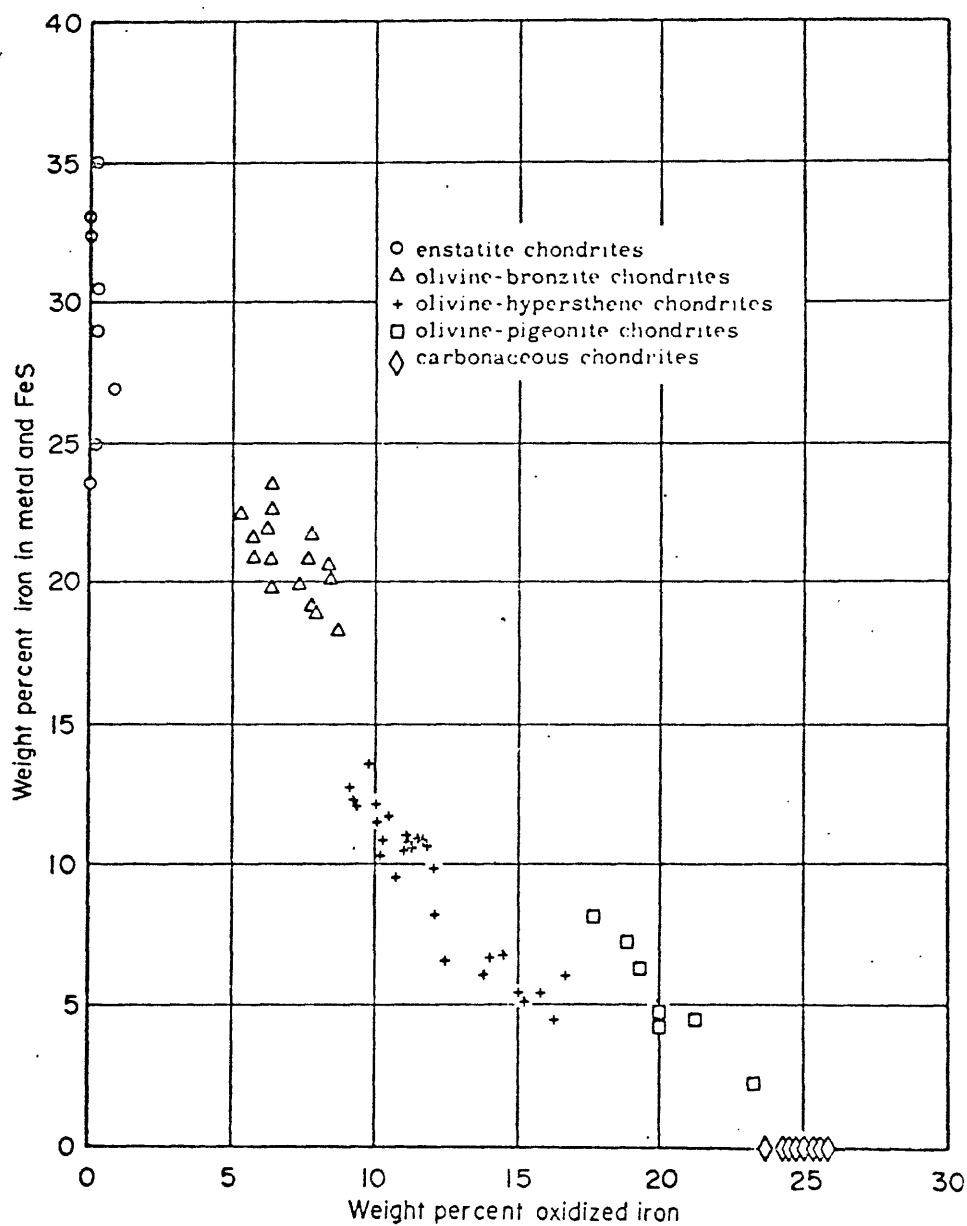


Fig. 1.--Relationship between oxidized iron, and iron as metal and sulfide in analyses of observed falls in chondrites.

From Mason (1962a, b).

as to the validity of Prior's rules, if broadly applied, and that the group concept of Urey and Craig is also supported.

Figure 1 is in part derived from the chemical determination of iron contents of the chondritic silicates. Much detailed petrographic and microprobe work has been done in the last few years on the olivine and pyroxene of the chondrites and a substantial body of data now exists, a large part of which is reported in Mason (1963b) and in Keil and Fredriksson (1964). Mason has shown that a narrow but distinct compositional hiatus exists in olivine of the bronzite and hypersthene chondrites (Fig. 2), and Keil and Fredriksson have shown that a similar hiatus exists for pyroxenes of these chondrites. Thus, on the basis of content of metal and the composition of olivine and pyroxene, the hypersthene and bronzite chondrites have been shown to be discrete classes of chondrites.

A large compositional hiatus separates the enstatite chondrites from the bronzite chondrites. The dominant mineral of the enstatite chondrites is pyroxene that is essentially free of iron, and olivine is absent (Mason, 1962a, 1966).

In the pigeonite chondrite class, which includes meteorites previously classed as Type III carbonaceous chondrites (those low in carbon and high in olivine; Wiik, 1956), a calcium-poor clinopyroxene characteristically occurs with the major olivine (Mason, 1962a, 1967a). Mason at first considered the clinopyroxene to be pigeonite on the basis of its X-ray diffraction pattern and its refractive indices, but later considered it to be a phase distinct from pigeonite, formed by the inversion of the proto-form and not by direct crystallization from a melt.

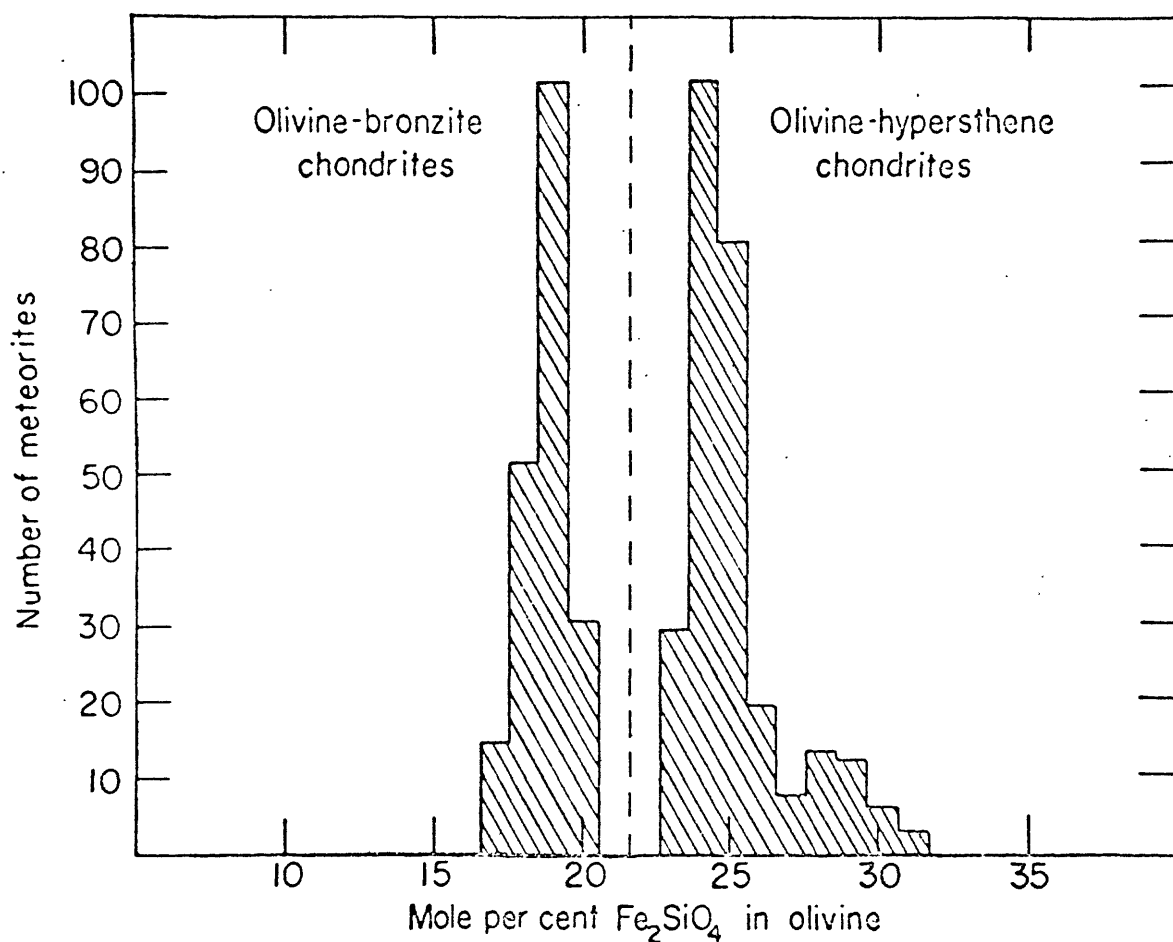


Fig. 2.--Olivine composition, determined by X-ray diffraction, showing compositional hiatus in olivine-bronzite and olivine-hypersthene chondrites.

From Mason (1963b).

Mason (1967a, p. 315) notes that the low-calcium clinopyroxene, while characteristic of the Type III carbonaceous chondrites, is not confined to them but is also present in many other chondrites, particularly the unequilibrated chondrites of Dodd and Van Schmus (1965). For this reason, Mason has proposed that the term pigeonite be abandoned. However, it is retained here to designate a discrete class of chondrites (as shown by Fig. 1), a class that is characterized by clinopyroxene, by iron-rich to iron-free olivine, by relatively sparse carbonaceous matter, and by low metallic nickel-iron contents. Textural, paragenetic, and compositional data summarized in Chapter 4 confirm that the "pigeonite" class belongs neither to the carbonaceous nor to the hypersthene chondrites.

In summary, five discrete classes of chondrites are recognized on the basis of distinct compositional and mineralogical characteristics (Fig. 1; Table 7). The mineralogical classification of Prior and Mason is used for the classification of the chondrites because, as will be shown in Chapter 4, the precipitation of "essential" olivine and "essential" or "characteristic" pyroxene (enstatite, bronzite, hypersthene, and pigeonite), was the event responsible for accretion of the chondrites.

Correlations between Chondrites and Achondrites

The compositions of the achondrites fall into discrete groups (Fig. 3). Olivine and pyroxene of the various calcium-poor achondrites and certain of the stony-irons (pallasites, siderophyre) are compositionally similar to the olivine and pyroxene of various chondrite

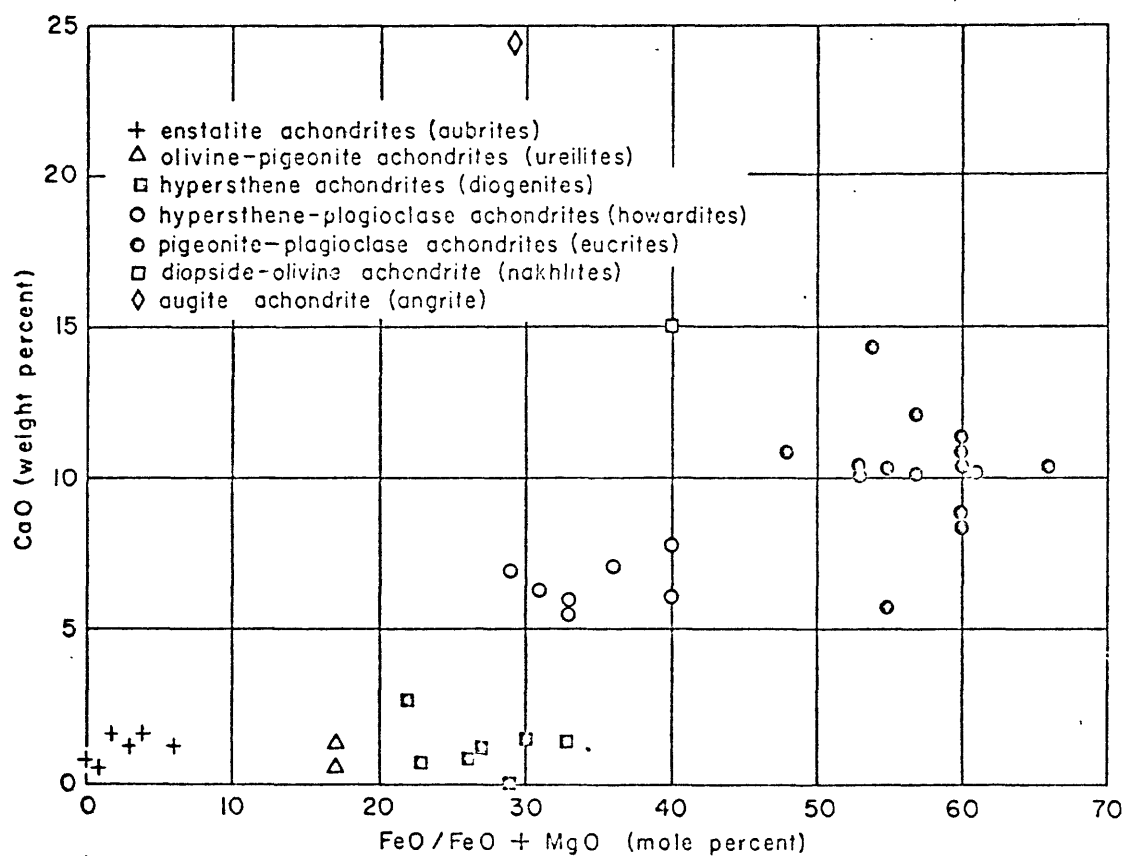


Fig. 3.--Plot of CaO (weight percent) against FeO/FeO+MgO (mole percent) for the achondrites.

From Mason (1962a).

classes (Tables 1 and 2; Fig. 3). The mineralogical characteristics and proposed correlations are summarized in Table 7. Possibly related achondritic silicates include iron-poor, calcium-poor silicates that occur as inclusions in irons, and as fragments in the brecciated MgSiO_3 mesosiderites.

Petrologic Evidence for the Metamorphism of Chondrites

Chemical-petrologic Classification of the Chondrites

Differences in texture in different chondrites, observed as a decreasing distinctness in chondrule structure and outline, have been attributed to thermal metamorphism in the chondrite parent body (Wood, 1962a; 1963a, Plates 2 and 3). A small number of little-metamorphosed, "unequilibrated" hypersthene and bronzite chondrites have been identified and described (Dodd and Van Schmus, 1965; Dodd and others, 1967). Detailed textural and mineralogical characteristics observed within and between chondrules and matrix in individual chondrites have been ordered in respect to relative degree of metamorphism, or "thermo-chemical equilibration". A detailed petrographic study of a large number of chondrites by Van Schmus and Wood (1967) has led to a chemical-petrologic classification of the chondrites (Table 8).

The chemical-petrologic classification of Van Schmus and Wood (Table 8) recognizes the mineral classes of Prior, but defines the chondrite classes on the basis of chemical characteristics (which are reflected in the mineralogy), and from the expression of Prior's rules (which also are reflected in the mineralogy). Each of the mineral or "chemical" classes has been subdivided by Van Schmus and Wood (1967)

Table 8.--Chemical-petrologic classification and proper names of the chondrites.^{1/}

a. Classification of the chondrites

Chemical group	Petrologic type					
	1	2	3	4	5	6
E	E1 --	E2 --	E3 1*	E4 4	E5 2	E6 6
C	C1 4	C2 16	C3 8	C4 2	C5 --	C6 --
H	H1 --	H2 --	H3 7	H4 35	H5 74	H6 44
L	L1 --	L2 --	L3 9	L4 18	L5 43	L6 152
LL	LL1 --	LL2 --	LL3 4	LL4 3	LL5 7	LL6 21

*Number of examples of each meteorite type now known is given in its box

b. Proper names for chondrites

Petrologic type						
	1	2	3	4	5	6
E	*	*	Enstatite chondrites			
C	Carbonaceous chondrites			C4	*	*
H	*	*	H3*	Bronzite chondrites		
L	*	*	L3*	Hypersthene chondrites		
LL	*	*	LL3*	Amphoterite chondrites		

Z

Z

*--Unpopulated.

Z--Ordinary chondrites.

*--Unequilibrated ordinary chondrites

^{1/}. From Van Schmus and Wood (1967, tables 3 and 4). Fayalite and ferrosillite contents of olivine and pyroxene of the chondrites are summarized in Table 7.

into a series of petrologic classes, numbered in order of increasing metamorphism. Of ten criteria used by Van Schmus and Wood, the first four they list are:

1. Homogeneity of silicate mineral compositions. Heterogeneous olivine and pyroxene crystals indicate a high degree of disequilibrium, and the crystals tend to become more homogeneous in composition with progressive degrees of equilibrium. (The "heterogeneity" will be shown, in Chapter 4, to be the result of the accretionary process.)
2. Pyroxene. The ratio of low-calcium monoclinic pyroxene to orthorhombic pyroxene in chondrites correlates (decreases) with progressive recrystallization of a chondrite. Van Schmus and Wood (1967) note that the monoclinic state is the natural product of the quenching necessary to produce chondrules, and that orthorhombic pyroxene may represent the inversion of the metastable monoclinic state under conditions of sustained high temperature (metamorphism), although they note that this is not a unique interpretation.
3. Feldspar. Grains of sodic plagioclase are evident only in well recrystallized chondrites. According to Mason (1967a), some plagioclase may be produced during the inversion of clinopyroxene to orthopyroxene, the components of the plagioclase being in solid solution in the clinopyroxene, but most plagioclase appears originally to have been glass; a brown transparent or turbid glass is a common constituent of plagioclase-free chondrites, which microprobe analysis has shown to have the

composition of albite (Fredriksson and Reid, 1965). Mason (1967a) notes that devitrification of the glass produces disordered, so-called high temperature plagioclase.

4. "Igneous" glass. Van Schmus and Wood (1967) note that glass is found in some chondrules of (apparently) unmetamorphosed and little metamorphosed chondrites, and it is considered by them as evidence for the quenched state of the chondrules. Chondrule glasses studied by Fredriksson and Reid (1965) and Van Schmus (1966) have had compositions that are rich in Na, Al, and Si, and are poor in Fe, Mg, and Ca. Van Schmus and Wood remark that this primary glass is absent from more recrystallized chondrites.

Mason (1966) has described mineralogical and textural characteristics for the enstatite chondrites which lead to the implication that progressive metamorphism of enstatite chondrite material may have been responsible for the enstatite achondrites.

Mineralogic-petrologic Classification of the Calcium-poor Stony Meteorites

It is proposed here that the chemical-petrologic classification of Van Schmus and Wood (1967) be re-ordered to a mineralogic-petrologic classification and expanded to include the achondrites (Table 9). The format is adapted from the proposed genetic classification (Table 2). The volatile-rich carbonaceous meteorites are set apart. For reasons summarized in Table 9 and for reasons developed in Chapter 4, it is proposed that some of the hydrous clays of the carbonaceous achondrites may be the products of low temperature alteration (chloritization), in a

Table 9.--Mineralogic-petrologic classification of the calcium-poor stony meteorites.^{1/}

<u>Mineralogic Class</u>	<u>Symbol</u>	Petrologic class and type						
		Chondrite					Achondrite	
		1	2	3	4	5	6	7
Carbonaceous	C	14	x	x	x	x	2	3
Pigeonite	P	2	8	-	-	-	1 ^{2/}	5
Hypersthene(low)	H _l	-	4	3	7	21(?)	1(?) ^{3/}	9 ^{4/}
Hypersthene(high)	H _h	-	9	18	43	151(?)	(?)	
Bronzite	B	-	8	35	74	44(?)	-	1 ^{5/}
Enstatite	E	-	1	4	2	5(?)	1(?)	9

1/. Modified and expanded from Van Schmus and Wood (1967). The petrologic class that is shown for the chondrites is one less numerically than in the original scheme. Class 5 chondrites may contain some essentially achondritic materials such as the Shaw meteorite, and the enstatite chondrite Jajh deh Kot Lalu (Mason, 1966), which have been placed, provisionally, in a new petrologic class that is established to bridge the gap between the volatile-poor chondrites and the coarsely crystalline calcium-poor achondrites. The number of representatives in class 5 is subject to revision because of possible re-assignment to class 6.

Class 5 carbonaceous achondrites contain high temperature materials. Tonk contains 0.40 weight percent Ni-Fe (W.A.K. Christie, in Wilk, 1956), and the presence of olivine in Orgueil has been confirmed by Kerridge (1968). Metal and olivine occur in the carbonaceous chondrites, and because chondrites apparently are the first rocks (Chapter 4), the carbonaceous achondrites are inferred to be chloritized carbonaceous chondrite material, -- the product of low temperature metamorphism in a volatile-rich environment. Classes 2-5 may not exist for the carbonaceous meteorites.

- 2/. Chassigny. A possibly recrystallized olivine-pigeonite chondrite (Mason, 1962a), which contains "nascent chondrules" (Jeremine and others, 1962), interpreted here as relict chondrules.
- 3/. Shaw meteorite; an amphoterite that is considered to be a recrystallized hypersthene chondrite (Fredriksson and Mason, 1967).
- 4/. Includes 8 hypersthene achondrites (diogenites), and calcium-poor pyroxene from the mesosiderite Bondoc Peninsula.
- 5/. Achondrite fragment in brecciated Breitscheid bronzite chondrite (Wlotzka, 1963).

volatile-rich environment, of olivine and pyroxene of the carbonaceous chondrites.

Two petrologic classes of calcium-poor achondrites are recognized. One class includes achondritic meteorites that retain vestiges of chondrite parentage, for example, the presence of disseminated metal in a carbonaceous achondrite (Tonk), or the presence of relict chondrules (Chassigny). A number of the amphoterites may belong to this transitional class. The other class of achondrites (volatile-poor) includes materials that apparently have undergone extensive recrystallization.

The pigeonite chondrites are recognized as distinct from the carbonaceous chondrites for reasons given earlier, and in light of evidence developed in Chapter 4. Former and present members of the pigeonite chondrite class are listed in Table 10.

The five-fold petrologic subdivision of the Van Schmus-Wood classification is retained for the chondrites, but the petrologic classes are numerically decreased by one because the carbonaceous achondrites are not considered to be the starting materials. In a few cases, the petrologic and mineralogic assignments of Van Schmus and Wood (1967) have been revised (Tables 9 and 10). Some of their assignments, apparently based mainly on texture, appear to have equated a lack of obvious chondrules with a relatively high degree of metamorphism. As will be shown in Chapter 4, the lack of obvious chondrules is not the result of metamorphic processes in several texturally primitive chondrites, but rather appears to be the result of the accretionary process. It is possible that re-examination of the chondrites in light of information

Table 10.--Chondrites formerly and presently classed as olivine-pigeonite chondrites.

	Mason (1962a)	Carbon ^{1/} (Wt. percent)	Van Schmus and Wood, 1967	This Paper
Bali	--		--	?2/
Chainpur	x ^{3/}	0.57	LL(?) -3	H ₁ (?) -2 ^{2/}
Coolidge	--		C-4	B-2(?) ^{4/}
Felix	x ^{3/}		C-3	P-2
Grosnaja	x ^{3/}		C-3	P-2
Kaba	x ^{3/}		C-2	P-1
Kainsaz	--		C-3	P-2
Karoonda	x	0.10	C-4	P-2(?) ^{5/}
Krymka	--		--	?2/
Lance	x ^{3/}		C-3	P-2
Mokoia	x ^{3/}	0.75	C-2	P-1
Ngawi	x		LL(?) -3	H ₁ (?) -2 ^{2/}
Ornans	x		C-3	P-2
Tieschitz	x	0.34	H-3	B-2
Vigarano	x ^{3/}		C-3	P-2
Warrenton	x	0.30	C-3	P-2

Average: 0.41

1/. From Moore and Lewis (1965), and C. B. Moore (personal communication, 1966).

2/. Listed as a pigeonite chondrite by Hey (1966).

3/. Noted as carbonaceous by Mason (1962a).

4/. Classed as C-4 by Van Schmus and Wood (1967) on the basis of bulk composition and texture. An Arizona State University specimen, examined by this author, displays an accretionary texture that is analogous to accretionary textures in the carbonaceous and pigeonite chondrites. However, olivine (probably accretionary) falls in the fayalite range of the bronzite chondrites (Mason, 1963c). Because of the foregoing, Coolidge is returned to the class originally assigned to it by Mason, and reduced in number to petrologic class 2.

5/. Classed as C-4 by Van Schmus and Wood (1967) on the basis of homogeneous olivine composition (Mason, 1963c). Reclassified here as P-2 because the homogeneous olivine composition appears to be due mainly to the presence of a uniformly fine grained accretionary matrix, and to a paucity of pre-accretionary and accretionary chondrules, rather than the result of metamorphism of chondrule-bearing materials.

and relationships developed in Chapter 4 may result in additional re-assignments of petrologic class.

Correlation of Irons and Pallasites with Chondrites

Ga-Ge Groups

Irons. Gallium concentrations in iron meteorites were discovered to fall into three distinct groups by Goldberg and others (1951). Later, germanium concentrations in irons also were found to occur in distinct groups, a high correlation between gallium and germanium concentrations was shown, and four Ga-Ge groups were defined (Lovering and others, 1957; Table 11). Plots of the data of Lovering and others (1957) are shown in Figure 4a, b.

As shown in Figures 4a and 4b, the Ga-Ge groups crosscut nickel concentrations and thus crosscut structure in the irons that is developed as the result of nickel content. Only very low nickel-irons (hexahedrites; less than about 6 percent Ni) and very high nickel-irons (Ni-rich ataxites; mostly above about 15 percent Ni) fall into single Ga-Ge groups. Except for these, no distinctive, unambiguous relationship appears to exist between nickel content and Ga-Ge content. One group of irons, Ga-Ge group I, exhibits a narrow range of nickel values, almost as if homogenization, perhaps through convective mixing, had occurred.

The work of Lovering and others (1957), which apparently revealed four Ga-Ge groups, also revealed the existence of a number of irons in which the Ga and Ge values were anomalous with respect to the

Table 11.--Ranges of concentrations of Ga, Ge and Ni associated with the Ga-Ge groups in the metal phase of meteorites.^{1/}

<u>Ga-Ge group</u>	<u>Percent of meteorites studied</u>	<u>Range of concentrations</u>		
		<u>Ga (ppm)</u>	<u>Ge (ppm)</u>	<u>Ni (%)</u>
I	10	80-95	300-420	6.5-7.1
II	27	40-62	130-230	5.3-9.6
III	33	8-24	15-80	7.1-13.5
IV	17	< 1-3	< 1	7.7-22.2
Anomalous	13	---	---	---

^{1/}. From Lovering and others (1957), as summarized by Wasson (1967a).

Fig. 4.--Variation of Ga and Ge contents of iron meteorites.

Variation of gallium contents (a) and germanium contents (b) of iron meteorites plotted in respect to nickel contents (from Lovering and others, 1957).

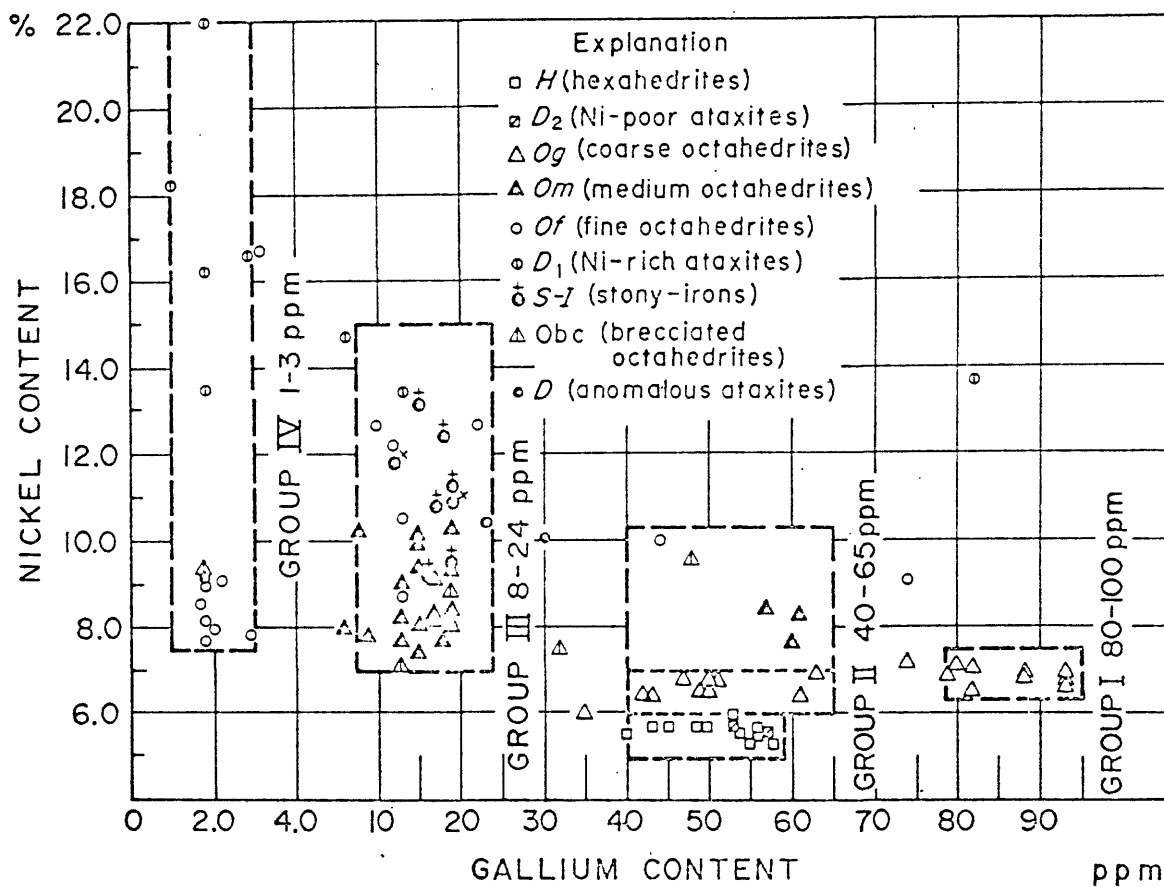


Fig. 4a.--Variation of gallium contents of iron meteorites.

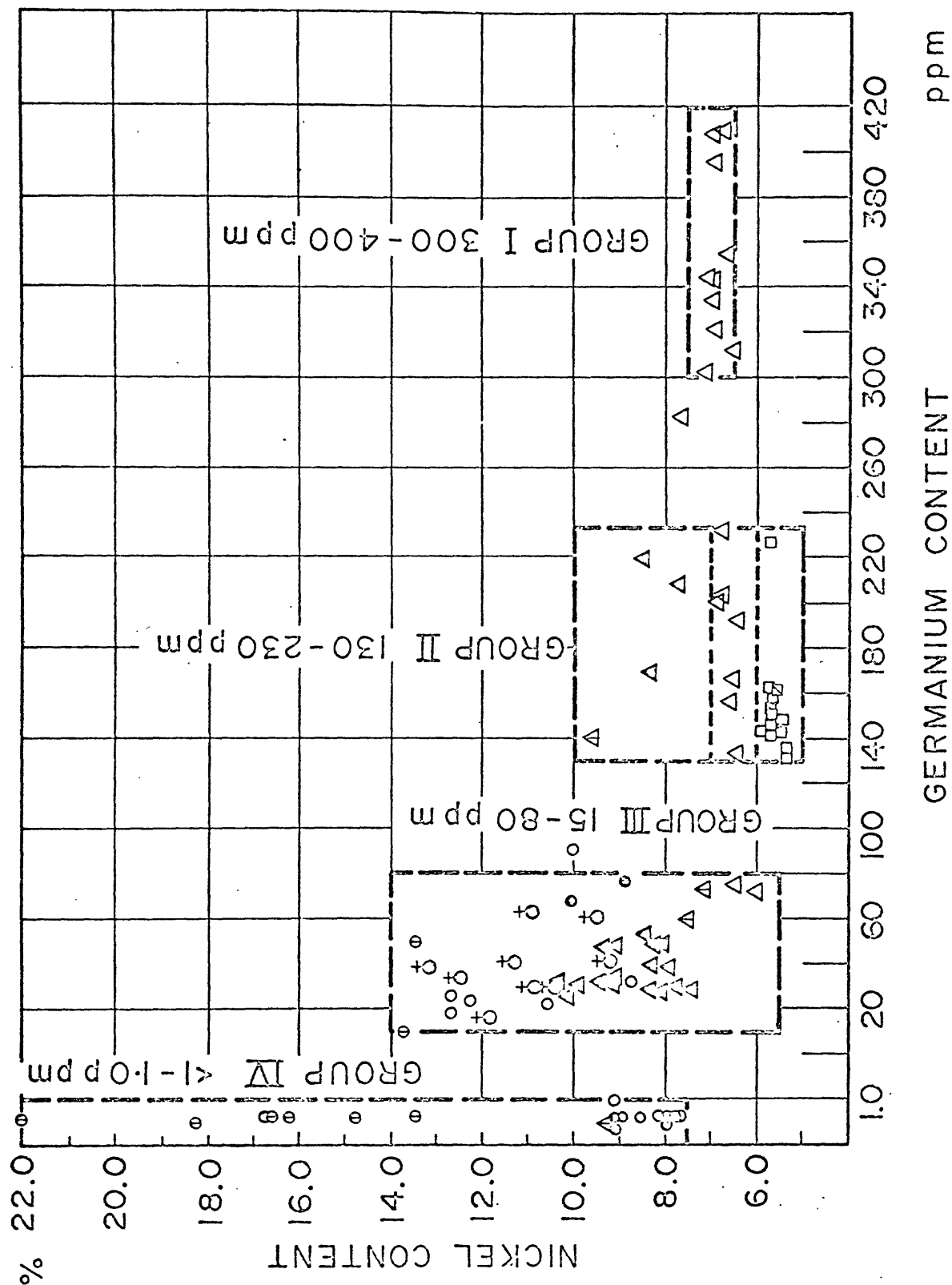


Fig. 4b.--Variations of germanium contents of iron meteorites.

group boundaries that they defined. Recent work by Wasson (1967a) has shown additional irons with anomalous values, and also has resolved two subgroups of group IV in the region of low Ga and Ge values (Fig. 5). The uniformity in nickel and Ga-Ge contents in groups IVa and IVb suggests closely related and probably very limited sources. However, in terms of absolute abundances of Ga and Ge, the differences between the subgroups, and between group IV and the anomalous irons, are very small. For this reason groups IVa, IVb, and the anomalous irons may as well have been derived from different parts of an inhomogeneously mixed core or segregation of a single parent body, as from cores or segregations of two or three different bodies.

Pallasites. Only one Ga-Ge group is represented in the metal phase of the pallasites. Eight pallasites analyzed by Lovering and others (1957, Table 9) contain Ga and Ge of group III. Seven of these belong to the low fayalite (Fa 11 to 13) group of pallasites (Mason, 1963b, p. 10), and one is a high fayalite group (Fa 17 to 20) pallasite (Springwater; Fa 18; Mason, 1963b, p. 10). In addition, one low fayalite pallasite (Geroux) has an "anomalously" low Ge content for group III (9 ppm; Goldstein and Short, 1967a, Table 1), one which falls in the group of "anomalous" irons that occupies the interval between groups III and IV (Fig. 5).

The analytical data clearly indicate that the pallasites belong to Ga-Ge group III (as defined by Lovering and others, 1957), and thus that the apparent compositional gap in the fayalite contents of the pallasites may be the result of incomplete sampling. Furthermore, the low Ge pallasite, Geroux, and irons with a spectrum of Ga-Ge values that

Fig. 5.--Relation between Ga and Ge concentrations in iron meteorites.

Individual plots are for 34 meteorites for which new data are reported by Wasson (1967a). The rectangular fields are the locations of Ga-Ge groups I, II and III as given by Lovering and others (1957).

From Wasson (1967a), who also shows in this plot that two discrete subgroups (IVa and IVb) of Ga-Ge group IV exist.

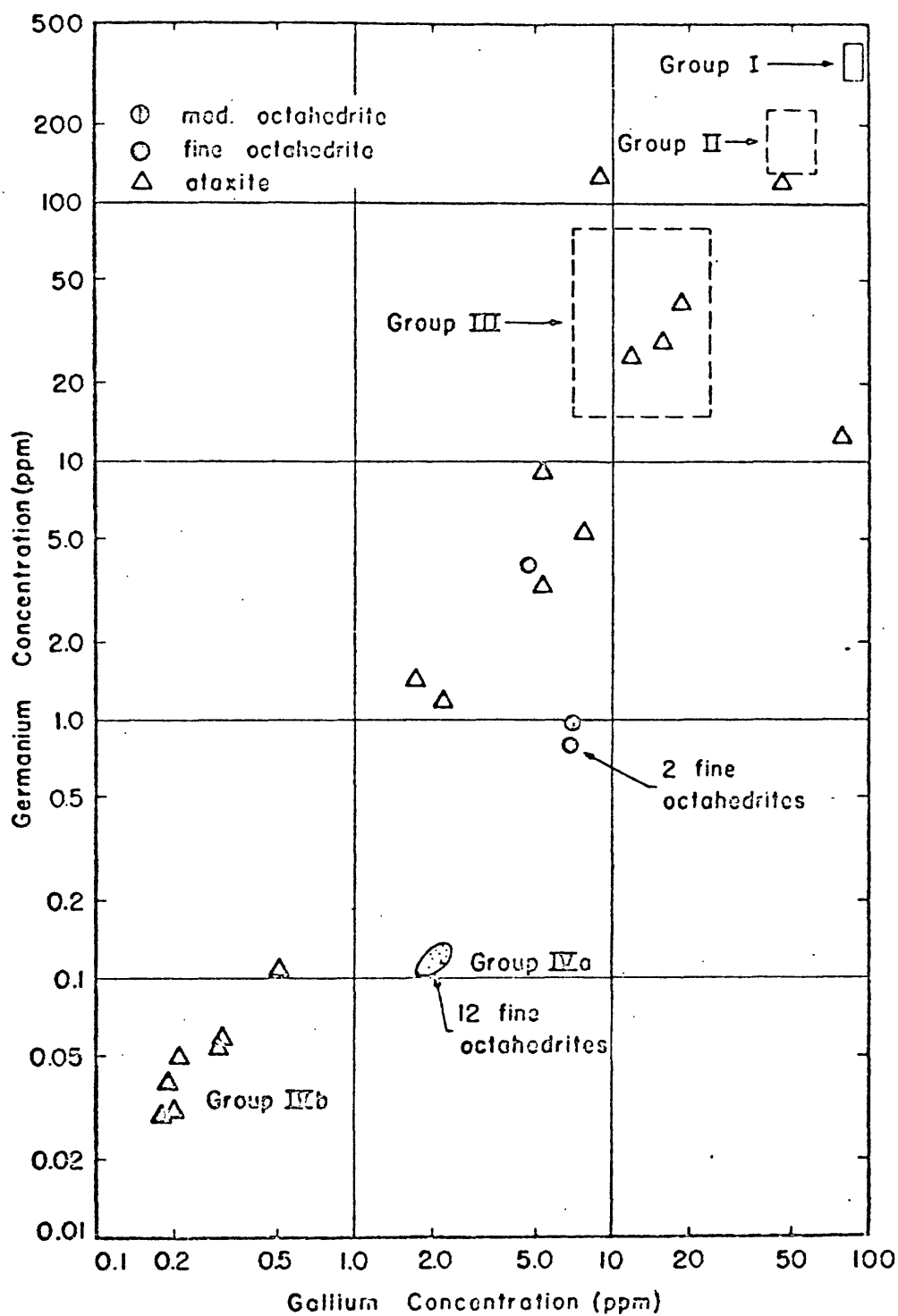


Fig. 5.--Relation between Ga and Ge concentrations in iron meteorites.

lie between Ga-Ge groups III and IV, indicate that the boundary of group III needs to be lowered, at least to the narrow, apparent, compositional hiatus near 1 ppm Ge (Fig. 5). Because only a very small compositional hiatus would remain between groups III and IV, groups III and IV may be members of a genetically related group of irons. If this is the case, clustered values within groups III and IV could be interpreted to be materials derived from restricted parts of a single parent body.

Correlations with the Chondrites

Correlations exist between the enstatite, hypersthene, and bronzite chondrites, and the Ga-Ge group I, II, and III irons, respectively (Table 12). The fundamental assumptions are: 1) that the original Ga and Ge contents of metal in the chondrites was low, and that Ga and Ge originally resided principally in the silicate matrix; and, 2) that metamorphism of the chondrites and fractionation of the metal occurred, during which Ga and Ge in the bulk meteorite were selectively acquired by the metal phase. The resulting Ga and Ge contents of the irons then would be a function of the original bulk contents of Ga and Ge in the chondrites, and the amount of metal in the individual chondrite classes that was available to accept or scavenge Ga and Ge during metamorphism and fractionation.

The calculated Ga and Ge values for metal assumed to have been fractionated from chondritic material (Table 12) were arrived at by assuming that the Ga and Ge values for the bulk meteorite are transferred to the metal during metamorphism and fractionation. The metal makes up a certain average percent of the chondrite (Table 3). Thus, if

Table 12.--Correlations between chondrite classes and Ga-Ge groups.

Class	Chondrites			Fractionated metal		
	Bulk Ga (ppm)	Number of meteorites	Bulk Ge (ppm)	Number of meteorites	Percent Ni-Fe ¹ / ₂	Calculated Ga and Ge concentrations in nickel-iron
						$\frac{\text{Ga}}{\text{Ge}}$ (ppm)
Enstatite high group low group	19.2	(2) ³ / ₃	47.5	(2) ³ / ₃	21.5	221
	12.3	(2) ³ / ₃	26	(2) ³ / ₃		121
Hypersthene	5.5	(4) ⁴ / ₄	10.1	(11) ⁵ / ₅	8.2	123
Bronzite	5.1	(2) ⁴ / ₄	12.0	(3) ⁵ / ₅	19.1	63
Pigeonite high group low group	10.5 6.4	(3) ⁴ / ₄ (2) ⁴ / ₄	18.5 10.0	(2) ³ / ₃ (2) ⁵ / ₅	3.5	300 183
						529 286
Carbonaceous chondrite achondrite	8.1 9.6	(2) ³ / ₃ (2) ³ / ₃	25.2 33.6	(2) ³ / ₃ (2) ³ / ₃	0.16 0.13	- -

1/. From table 1 and 3, this paper.
 2/. As defined by Lovering and others (1957).
 3/. Fouché and Smales (1967, table IV).
 4/. Greenland (1965, table 1); Lancé, in nominal
 high group of pigeonite chondrites, based
 on Greenland's analysis, would be in low
 group (6.8 ppm) based on Fouché and Smales
 (1967), who also show 6.5 ppm Ga and 19.0
 Ge for Ornans.

5/. Greenland and Lovering (1965,
 table 1 and 2).

bulk Ga-Ge values are similar, as in the bronzite and hypersthene chondrites, the chondrite class with the lower average metal content would show a stronger enrichment in Ga and Ge in the fractionated metal. Such appears to have occurred in the hypersthene and bronzite chondrites, as is shown by the correlation of the calculated Ga and Ge values with Ga-Ge II and III groups of Lovering and others (1957).

"Fractionated metal" of the enstatite chondrites correlates in part with Ga-Ge group I, but for some of the enstatite chondrites, the calculated Ga-Ge concentrations fall in Ga-Ge group II (Table 12). The reason for this is not understood, but it may be due to original inhomogeneities in the chondrite mix, or possibly to loss of some of the Ga and Ge from chondritic material as the result of a partial fractionation of metal. No apparent correlation exists between the pigeonite chondrites and Ga-Ge group III and IV irons, and there simply may be none. If irons exist that are related to the pigeonite chondrites, they would be expected to display high Ga and Ge values that could be anomalous to Ga-Ge group I.

Bulk values of Ga and Ge for the carbonaceous meteorites are shown in Table 12 to emphasize the point that the Ga and Ge in unmorphosed chondrite material resides in the matrix, and that this can be an adequate source for the Ga and Ge in fractionated metal. In the volatile-poor chondrites the Ga and Ge reside, to varying degrees, in the metal (Table 13), so some transfer of Ga and Ge from matrix to metal appears to have taken place. Metal of the enstatite chondrites shows a three-fold enrichment in Ga and Ge relative to the bulk meteorite, whereas metal of the bronzite and hypersthene chondrites shows a

Table 13.--Ga and Ge contents of the separated metal phase of enstatite, bronzite and hypersthene chondrites^{1/}.

<u>Class</u>	<u>Number of meteorites</u>	<u>Average Ga (ppm)</u>	<u>Range of values</u>	<u>Average Ge (ppm)</u>	<u>Range of values</u>
Enstatite	4	62	(52-71)	157	(113-212)
Bronzite	8	11.3	(6.2-17.2)	64	(62-67)
Hypersthene	9	11.4	(3.4-26.0)	125	(92-169)

^{1/}. From Fouché and Smales (1967, table II).

two-fold enrichment in Ga and a five- to twelve-fold enrichment in Ge relative to bulk values (Tables 12 and 13). In all cases, the Ga-Ge values of metal separated from the chondrites lie below values of the Ga-Ge group I, II, and III irons, which would allow additional Ga and Ge to be acquired during fractionation to arrive at the values of the Ga-Ge groups of irons.

The correlation between Ga-Ge groups II and III and the hypersthene and bronzite chondrites (Table 12) was brought to my attention by Dr. C.B. Moore (personal communication, 1966). Unpublished analyses by C.B. Moore, H. Brown, and C.R. McKinney revealed that the Ge in the metal phase of five bronzite chondrites was significantly lower than the Ge in the metal phase of two hypersthene chondrites. This relationship has since been clearly shown in recently published data of Fouché and Smales (1967; Table 13).

In summary, a correlation exists that allows for the development of Ga-Ge group I, II, and III irons as materials fractionated from chondrites which contained certain bulk values of Ga, Ge, and metal. A discrepancy in correlation exists with respect to some of the enstatite chondrites. No correlation exists for the pigeonite chondrites. Values for irons possibly derived from pigeonite chondrite materials could lie in or between groups I and II. "Anomalous" irons of Wasson (1967a) having Ga and Ge values less than group III as defined by Lovering and others (1957), are included in group III because of relations in the pallasites. Because only a very narrow compositional gap exists between the expanded group III and the clustered group IV irons, groups III and IV are provisionally considered to be members of a single genetic group.

Summary

Compositional characteristics, both groupings and discontinuities, serve to identify three groups of meteorites. Within the groups, compositional, textural, and mineralogical characteristics serve to identify individual meteorite classes. Five discrete classes of chondrites and calcium-poor achondrites are recognized, principally on the basis of compositions of the silicate minerals. Compositional transitions in the silicates are lacking between the chondrite classes, but on the basis of mineralogical similarities, there appear to be correlations between the chondrites, the calcium-poor achondrites, and the pallasitic meteorites. Correlations also appear to exist between three classes of chondrites and Ga-Ge group I, II, and III irons. The correlations suggest that genetic interrelationships exist among the chondrites, achondrites, pallasites, and irons, and that they have been derived from several discrete parent bodies.

CHAPTER 4

CHONDRITES, THE FIRST ROCKS

Introduction

The interrelated problems of chondrule formation and chondrite accretion have long been recognized as key problems in meteoritics. Several hypotheses have been proposed for the primary origin of chondrules, and several models exist for chondrite formation. Recent discussions, and proposed solutions, may be found in Mason (1962a), Wood (1963b), Anders (1964), Urey (1964), and Ringwood (1966).

No solution yet proposed can account for the general and the detailed chemical, mineralogical, and textural characteristics that are displayed by the five classes of chondrites. A solution to chondrule formation and chondrite accretion should apply both to the volatile-rich and to the volatile-poor chondrites. Because the volatile-rich carbonaceous chondrites (Type II of Wiik, 1956) have apparently undergone the least alteration and metamorphism of the five classes of chondrites, key evidence and relationships between chondrules and matrix should be best preserved in them. This has proven to be the case. It is the purpose here to review detailed paragenetic relationships and textural characteristics in the Murray carbonaceous chondrite which shed new light on chondrule and chondrite formation.

Paragenetic and textural data derived from Murray reveal that two assemblages of materials existed prior to accretion (one low

temperature; one high temperature), and that precipitation of a third assemblage (high temperature) was responsible for accretion. The relations lead to the recognition of two types of chondrules, -- one that formed prior to accretion and one that formed at the time of accretion. The formation of metal is associated with the formation of pre-accretionary chondrules. Evidence is preserved in the assemblages which indicates that accretion of Murray occurred at low temperatures and pressures. On the basis of reconnaissance examinations, the textural and paragenetic relations that are described for Murray are provisionally extended to the other carbonaceous chondrites, to the pigeonite chondrites, and to the hypersthene chondrites. A setting and a model for the accretion of solid materials is proposed which appears to be in accord with the general chemical, mineralogical, and textural characteristics of the chondrites.

Murray Carbonaceous Chondrite

Circumstances of Fall

Murray fell on September 20, 1950 at approximately 1:35 A.M., C.S.T., following the north to south passage of a brilliant fireball across southern Illinois, and its explosion over western Kentucky at an altitude of about 46 kilometers (Horan, 1953). The specimen of Murray that is described here is in the Collection at Arizona State University, Tempe, Arizona (no. 635.1, 32.7 g). It is a fragment from the largest specimen that was recovered (H. H. Nininger, personal communication, 1967), which was about 15 cm in the longest dimension (Horan, 1953,

Fig. 2). The specimen was heard to fall, and was recovered after embedding itself to a depth of about 15 cm in a hard packed path only 26 feet from a house.

The trajectory of the fireball through the atmosphere and its orbital elements were calculated by C. P. Olivier under the assumption of parabolic heliocentric velocity (Horan, 1953); the observed velocity of the bolide, based on six estimates, is reported as 71 kilometers per second, and the inclination of its path to the ecliptic is reported to have been 68° . The high inclination and large heliocentric velocity suggest an encounter with cometary material in a near-parabolic orbit.

General Characteristics

Murray is a dark, compact meteorite that has a specific gravity of 2.81 ± 0.02 (Horan, 1953). The fusion crust on the specimen studied is a fraction of a millimeter thick; no alteration effects are apparent in material that directly underlies the crust. About four-fifths of the meteorite is black, very fine-grained to locally amorphous-appearing, hydrated matrix material. The matrix serves as a bonding agent for disseminated grains, compound particles, and finely granular aggregates of olivine, pyroxene, and metal. Most of the high temperature magnesium silicates occur as irregular to locally nearly spherical aggregates of very fine grains or crystals, and as fine, pervasive disseminations. Several irregular to subround clusters of magnesium silicate crystals are partly to entirely limonite stained. Except for this very local staining, the meteorite appears extremely fresh, unlike some specimens

of Murray in the Collection of the U.S. National Museum which apparently were collected after rains had occurred in the area.

The specimen of Murray described here is similar in texture and in general appearance to the several dozen specimens of Murray that are in the Collection of the U.S. National Museum in Washington, D.C. Murray also is texturally very similar to a specimen of the Mighei carbonaceous chondrite (Arizona State University Collection), and to specimens of the Crescent and Bells carbonaceous chondrites, which were examined through the courtesy of Mr. O.E. Monnig, Fort Worth, Texas. The textural and paragenetic relations described for Murray are thus considered to be representative for the carbonaceous chondrites (Type II).

The chemical composition of Murray (Table 14) has been determined by Wiik (1956). Its water content, about 12.5 weight percent, is very near the average value for the carbonaceous chondrites reported by Wiik. The black carbonaceous matrix of Murray, analyzed by electron microprobe techniques, is reported by Fredriksson and Keil (1964) to consist mainly of layer lattice silicates; the composition of the matrix is reported to be: 13 to 14 percent Si; ~ 22 percent Fe; 9 to 10 percent Mg; ~ 0.5 percent Ca; 0.5 to 1 percent Al; ~ 1 to 4 percent Ni; and ~ 1 to 4 percent S. Fredriksson and Keil (1964) found nickel to be fairly homogeneously distributed in the matrix, and at places found strong positive correlations between nickel and sulfur. At these places they considered the fine grained material to be pentlandite, but where the sulfur content was too low for pentlandite, the material was considered by them to be a sulfate rather than a sulfide. Fredriksson and

Table 14.--Analysis of Murray carbonaceous chondrite.^{1/}

<u>Oxides</u>	<u>Weight Percent</u>		<u>Weight Percent</u>
SiO ₂	28.69	NiO	1.50
MgO	19.77	CoO	0.08
FeO	21.08		
Al ₂ O ₃	2.19	<u>Metal</u>	
CaO	1.92	Fe	0.002/
Na ₂ O	0.22	Ni	0.002/
K ₂ O	0.04	Co	0.00
Cr ₂ O ₃	0.44		
MnO	0.21	<u>Other</u>	
TiO ₂	0.09	FeS	7.67
P ₂ O ₅	0.32	C	2.78
H ₂ O+	9.98	Loss on ign.	0.623/
H ₂ O-	2.44	Sum	100.04

- ^{1/}. From Wiik (1956, Table 1, p. 280-281). Wiik notes that the FeO is only a calculated number, obtained by subtraction of the metallic iron and the troilite iron from the total iron. Wiik also notes that the FeS tends to be too high because all S was calculated to that compound, and accordingly the FeO tends to be too low. Because FeO is not known, Fe₂O₃ also could not be determined; it was realized, however, to³ almost certainly be present in the chlorite reported by Kvasha (1948) in carbonaceous chondrites.
- ^{2/}. A small amount of metallic nickel-iron actually is present in Murray.
- ^{3/}. Wiik considers this to be an approximate estimation of the amount of organic matter.

Keil report that some sulfur can be leached from the matrix with distilled cold water.

Murray is rare gas-rich (Signer and Suess, 1963) as well as water-rich. The water and the rare gases probably are retained in the layer lattice silicates. Silicates in the matrix of the carbonaceous chondrites (Type II) have been identified as serpentine (Wöhler, 1860); chlorite or serpentine (Kvasha, 1948); tubular material characteristic of the chrysotile variety of serpentine (Mason, 1962a, Fig. 27, p. 66); and "Murray F" and "Haripura M" which give "chlorite" or "chrysotile" X-ray powder spacings that do not match the X-ray patterns of terrestrial chlorites and serpentines in detail (DuFresne and Anders, 1962; 1963, p. 504). About three-fourths of the Orgueil carbonaceous achondrite (Type I) consists of hydrated, iron-rich aluminum-poor septechlorite (Boström and Fredriksson, 1966), which Mason (1967b) believes is probably best described as a ferric chamosite; for reasons given in Table 9, this material may not be the same as the layer lattice silicates of the carbonaceous chondrites (Type II).

The carbonaceous chondrites have been described as heterogeneous mixtures of two discrete mineral assemblages. DuFresne and Anders (1962, 1963) note the existence of: 1) a high temperature assemblage that consists mainly of olivine, pyroxene, and subordinate metallic iron, and 2) a low temperature assemblage of "characteristic" minerals that consists principally of complex hydrated magnesium-iron silicates and subordinate pentlandite.

Electron microprobe investigations of randomly selected silicate grains in Murray have revealed that olivine is about four times more

abundant than pyroxene (Fredriksson and Keil, 1964). The olivine and pyroxene were found to vary widely in composition, in agreement with results reported by Ringwood (1961), DuFresne and Anders (1962), and Wood (1967a) on olivine and pyroxene in other carbonaceous chondrites. Fredriksson and Keil (1964) report that the $\text{Fe}/\text{Fe}+\text{Mg}$ ratios in Murray range from 0.003 to 0.902 moles in olivine, and from 0.004 to 0.454 moles in pyroxene (Fig. 6). The frequency distributions of the mole ratios $\text{Fe}/\text{Fe}+\text{Mg}$ in the olivine and pyroxene grains analyzed by Fredriksson and Keil show a lack of correspondence with the Fe contents of olivine and pyroxene of the ordinary chondrites, which led these workers to conclude that the olivine and pyroxene of Murray were not derived from the ordinary chondrites. The analyses show that the majority of the olivine and pyroxene grains in Murray have very low-iron contents (0 to .02 moles). Recent electron microprobe analyses of olivine and pyroxene in Murray by Wood (1967a) have generally supported these results.

Spherules of metallic iron, up to 20 microns across, were found by Fredriksson and Keil (1964) as inclusions in olivine grains that have low $\text{Fe}/\text{Fe}+\text{Mg}$ ratios. The nickel contents of the metallic spherules were found to range from 5 to 9 weight percent, whereas the nickel content of the olivine was found to be less than 50 parts per million.

Paragenetic and Textural Studies

Recognition of three mineral assemblages (components). Any hypothesis or model that deals with the origin of chondrules and the accretion of chondrites should be founded on evidence in both the

Fig. 6.--Frequency distribution of the mole-ratios $\text{Fe}/\text{Fe}+\text{Mg}$ in 63 individual olivine crystals (Fig. 6a) and 16 individual pyroxene crystals (Fig. 6b), Murray carbonaceous chondrite.

Part B of Fig. 6a gives the values from 0 to 0.08 moles on a larger scale. H, L, and LL represent the averages and ranges in composition of olivines and rhombic pyroxenes in H-, L-, and LL-group chondrites (Keil and Fredriksson, 1964). From Fredriksson and Keil (1964, Fig. 1 and 2, p. 207-208).

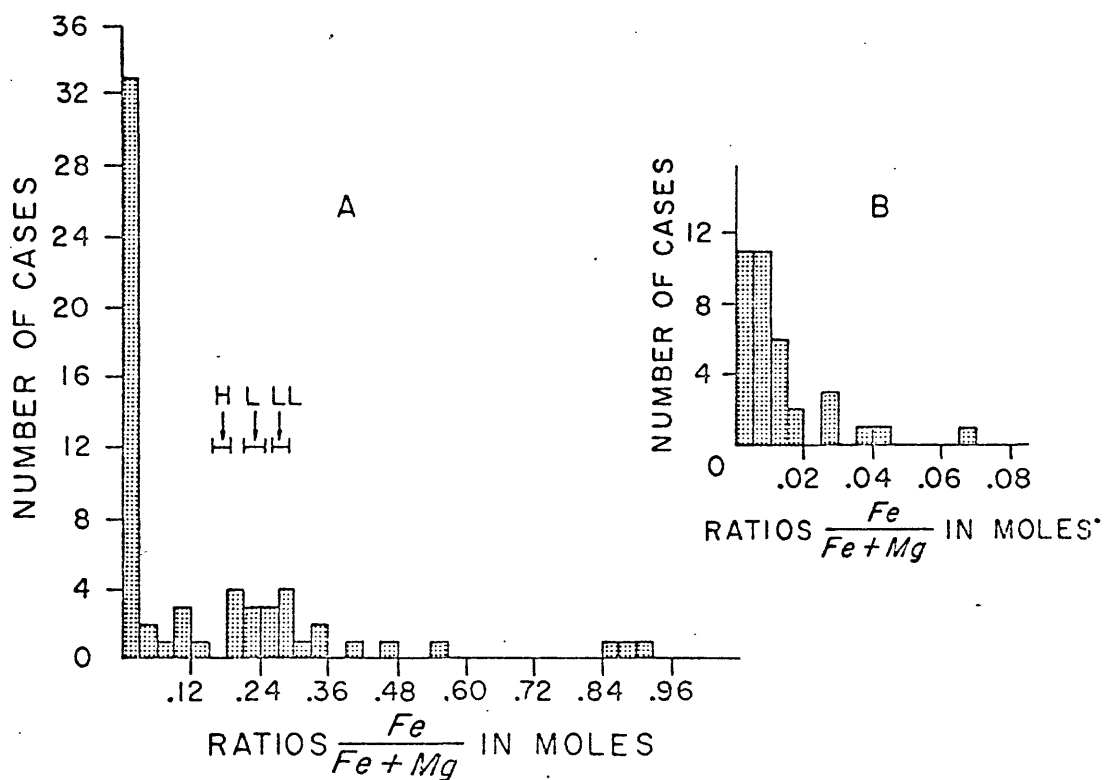


Fig. 6a.--Frequency distribution of the mole-ratios $Fe/Fe+Mg$ in 63 individual olivine crystals, Murray carbonaceous chondrite.

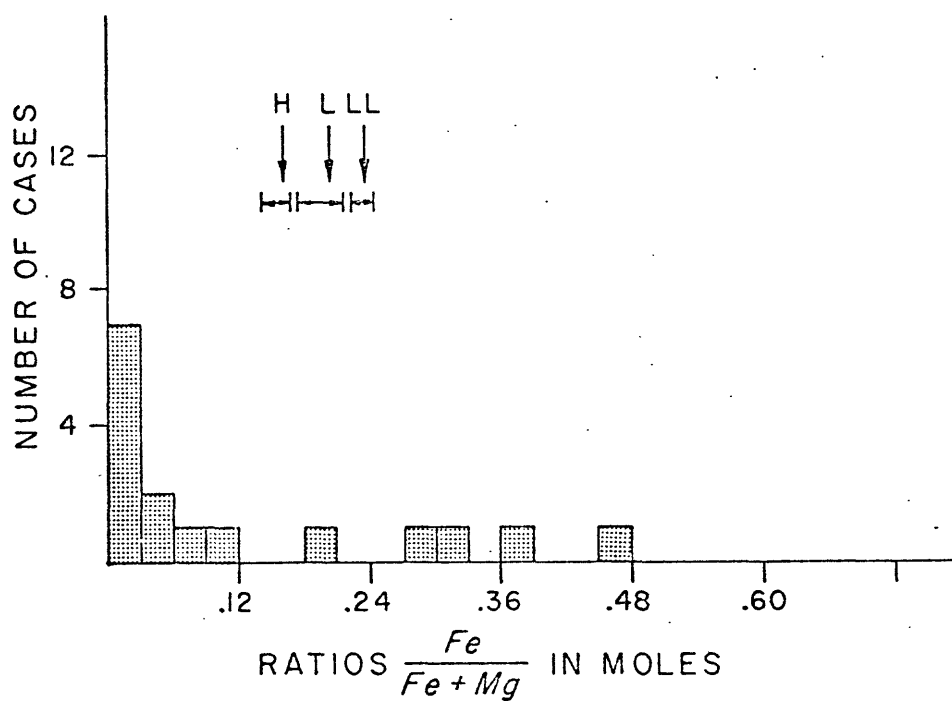


Fig. 6b.--Frequency distribution of the mole-ratios $Fe/Fe+Mg$ in 16 individual pyroxene crystals, Murray carbonaceous chondrite.

chondrules and the chondrites. Not yet considered in any model for accretion are textural characteristics of the mineral assemblages, and paragenetic relationships between grains, aggregates of grains, chondrules, and mineral assemblages.

Investigations consisted of "microgeologic" mapping on photographic enlargements of two near-orthogonal surfaces of Murray. The maps (Fig. 7a, b) show the distribution and sizes of grains, aggregates of grains, and particulate materials of the mineral assemblages; and the paragenetic relationships of these to one another. Textural data (Table 15, Fig. 8) have been extracted from the maps by measuring the area of each discrete grain, or aggregate of grains, that was larger than about 0.05 mm^2 . A small amount of petrographic work was done on mineral grains from fragments that had spalled off the specimen to verify the visual identifications that were made under the binocular microscope during mapping, and for general correlation of the mapped materials with the composition of materials described for Murray by Fredriksson and Keil (1964).

Three mineral assemblages, which formed at different times and presumably at different places, are recognized in Murray (Fig. 7). These are: 1) a pre-accretionary low temperature assemblage; 2) a pre-accretionary high temperature assemblage; and, 3) an accretionary high temperature assemblage. The low temperature assemblage, component 1, forms the black, very fine-grained, volatile-rich matrix. It makes up about 82 percent of the area of the rock and is the material in which components 2 and 3 are embedded (Fig. 7, Table 15). Component 1 matrix

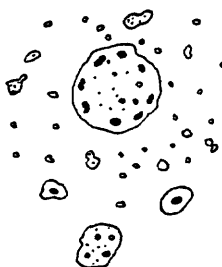
Fig. 7.--Preliminary microgeologic maps of Murray carbonaceous chondrite.

Maps and base photographs of end view (Fig. 7a) and side view (Fig. 7b) showing: a) the distribution of disseminations, aggregates, and chondrules of finely granular, high temperature accretionary magnesium silicates (component 3), and of disseminated coarser grains and chondrules of high temperature, pre-accretionary magnesium silicates and metal (component 2), in low temperature, hydrous, carbonaceous matrix materials (component 1); and, b) the distribution of component 1 matrix materials as granules and spherules in, and as sheaths and rinds around, component 3 accretionary aggregates. Specimen no. 635.1, Arizona State University Collection.

Explanation

Component 3: Accretionary high temperature materials.

a. Unaltered, finely granular low-iron magnesium silicates.



Small irregular aggregates to large nearly spherical chondrules (about 0.1 mm to about 2.5 mm), consisting of tiny (commonly about 0.01 mm to 0.02 mm), clear, fresh-appearing grains of essentially iron-free magnesium silicate, apparently mainly olivine; intergranular material is probably large glassy. Aggregates characteristically contain intimately admixed black flakes, and locally granules and hollow spherules, of matrix materials (component 1), which range in size from about 0.01 mm to 0.3 mm. Some component 3 aggregates contain nuclei of relatively large (0.2 mm to 0.6 mm) grains of olivine or pyroxene (component 2). A few component 3 aggregates contain matrix spherules as central nuclei, but in some aggregates, matrix spherules are irregularly to symmetrically disposed in the medial to outer parts of accretionary chondrules. Paragenetic and textural relations indicate that component 1 and 2 materials were mechanically incorporated in component 3 aggregates. Additionally, component 1 granules and spherules may owe their form and their existence to the process that resulted in precipitation and aggregation of component 3 silicates.

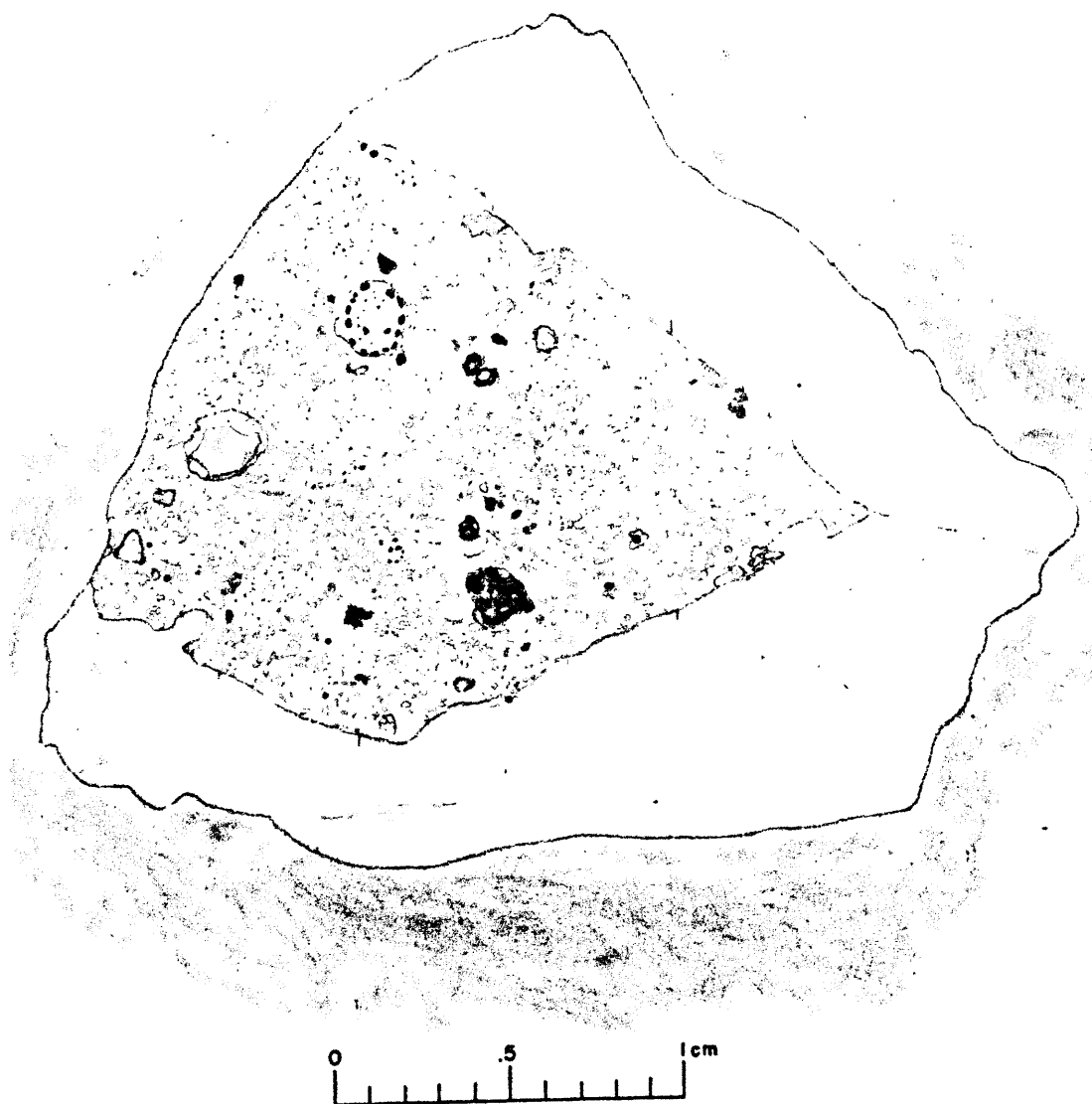


Fig. 7a₁.--Preliminary microgeologic map of end view of
Murray carbonaceous chondrite.

Fig. 7.--Continued

Component 3: Accretionary high temperature materials (Continued).

b. Altered, finely granular low-iron magnesium silicates.

Similar to component 3a, but aggregates and chondrules of essentially iron-free magnesium silicate grains are partly to entirely stained various shades of brown, yellow, and orange. Some aggregates appear to contain rusty relicts of component 1 matrix material, but in most stained aggregates, included matrix material is not apparent. Most stained aggregates are relatively large. Paragenetic relations indicate that aggregation and most of the staining pre-date precipitation of component 3a materials. The staining may be the result of limonitic alteration accompanying dehydration of layer lattice silicates of formerly included matrix material. The altered aggregates may have been briefly heated by the source medium, probably a gas, that was responsible for the general precipitation of the component 3 accretionary aggregates.

c. Unaltered, finely granular high-iron magnesium silicates.

Relatively large (0.2 mm to 2 mm) aggregates and chondrules of finely granular, medium to dark brown, iron-rich magnesium silicates. Included matrix material is not apparent, possibly because of the general darkness of the aggregates. One aggregate locally is limonite-stained or altered. The dark aggregates tend to be clustered. Several are enclosed by thin, dense, dull black rinds of matrix material, and in turn are embedded in sooty-, amorphous-appearing matrix material that is deficient in disseminated component 3a material. One component 3c aggregate is enclosed by a sheath of component 3a material, indicating, as in the case of component 3b, formation before the precipitation of component 3a materials.

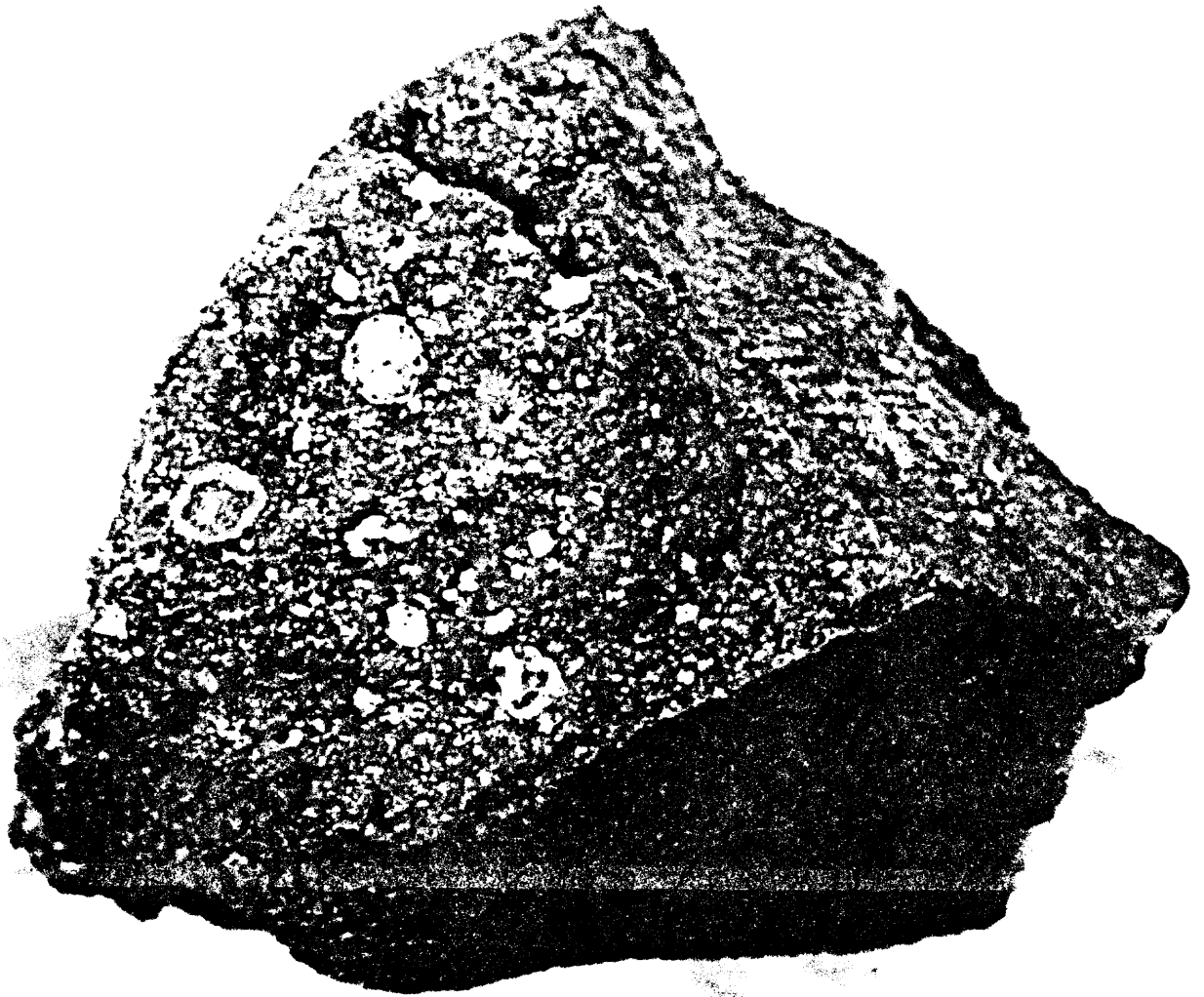
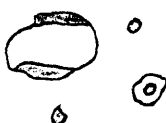


Fig. 7a₂.--Photographic base for microgeologic map of end view of
Murray carbonaceous chondrite.

Fig. 7.--Continued

Component 2: Pre-accretionary high temperature materials.

Heterogeneous assortment of grains and chondrules of olivine, pyroxene, and metal that are irregularly distributed through component 1 matrix material, and that locally are incorporated in component 3 accretionary aggregates and chondrules. Finely granular metal is closely associated and appears to be genetically related to component 2 silicate grains and chondrules, locally occurring in individual grains, and in one case on component 2 silicates in a compound component 2 chondrule. Depositional sequence recorded in the compound chondrule shows the successive formation of a zoned chondrule, deposition of metal, and deposition of coarsely granular silicates, apparently separated by intervals during which partial fragmentation occurred.



- a. Grains and fragments of grains, of clear to very pale brown (iron-free to iron-poor) olivine and pyroxene, mostly about 0.2 mm to 0.7 mm. They occur as isolated grains in component 1 matrix; as the nuclei of several component 3 aggregates; and in a compound component 2 chondrule where they partly enclose metal and zoned silicates.



- b. Irregular fragment of zoned or barred, clear (iron-free) magnesium silicate, probably olivine. In part overlain by components 2a and 2d in a 2 mm compound chondrule. Consists of thin, parallel, resistant layers of clear silicate, separated by soft, milky-white intervals that probably contain Na- and Al-rich glass.



- c. Grains and fragments of grains, of pale to moderately dark brown (moderate- to moderately high-iron) olivine and pyroxene, mostly about 0.2 mm to 0.8 mm, which occur as isolated grains in component 1 matrix.



- d. Metal, apparently nickel-iron, which occurs as sparse very tiny droplets (on the order of 0.01 mm) disseminated in component 1 matrix; as droplets in a few component 2 grains; and as a finely granular deposit on component 2b material in a compound component 2 chondrule.

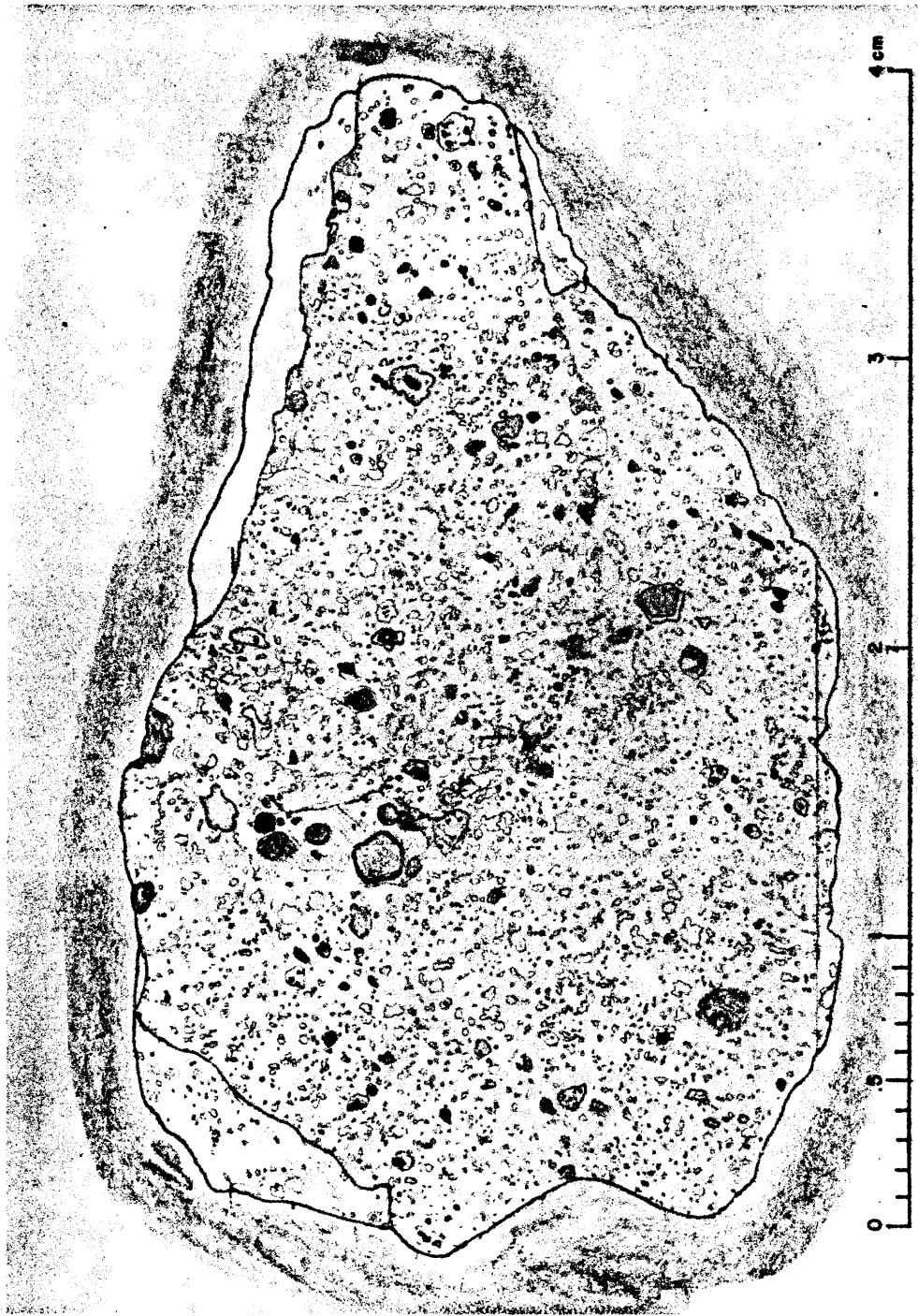



Fig. 7b₁.--Preliminary microgeologic map of side view of Murray carbonaceous chondrite.


Fig. 7.--Continued


Component 1: Pre-accretionary low temperature materials.


Black, very fine-grained, hydrous matrix material. Consists mainly of layer lattice silicates and subordinate nickel-bearing sulfides (Fredriksson and Keil, 1964). The layer lattice silicates presumably contain the approximately 12.5 weight percent H_2O reported by Wiik (1956), and they may also be the sites of retention of Murray's abundant rare gases (Signer and Suess, 1963). Wiik (1956) reports 2.78 weight percent carbon, and a loss on ignition of 0.62 weight percent, which he attributes to organic material.

In addition to matrix material that serves as a general fine grained cement, matrix material occurs as:

- 

a. Flakes, granules, and hollow spherules ranging from about 0.01 mm to 0.3 mm, which are incorporated in component 3a aggregates.
- 

b. Compact, dull rinds, and vitreous-appearing sheaths that enclose, respectively, component 3c and component 3b aggregates.
- 

c. A dense, black, subangular fragment, about 0.7 mm, in the matrix, which may be a piece of pre-solar system "rock".
- 

d. Sooty- and amorphous-appearing material that is deficient in disseminated component 3a material and that encloses several component 3c aggregates.



Fig. 7b₂.--Photographic base for microgeologic map of side view,
Murray carbonaceous chondrite.

Table 15.--Abundance of particles and components in map areas of Murray carbonaceous chondrite.

	Map area of Fig. 7a (2.27 cm ²)		Map area of Fig. 7b (6.62 cm ²)	
	Number of particles or grains	Percent of total area	Number of particles or grains	Percent of total area
<u>Component 3 (Accretionary high temperature silicates)</u>				
Unaltered, low-iron (a) ^{1/}	1600	15.95	3207	12.99
Altered, low-iron (b)	23	1.89	46	1.17
Unaltered, high-iron (c) ^{2/}	--	--	18	1.47
	<u>1623</u>	<u>17.84%</u>	<u>3271</u>	<u>15.63%</u>
Average:	16.7%			
<u>Component 2 (Pre-accretionary high temperature silicates and metal)</u>				
Low-iron chondrules (a,b)	14	0.63	44	0.38
High-iron chondrules (c)	7	0.26	6	0.07
Metal (d)	<u>5</u>	<u>0.41</u>	<u>7</u>	<u>0.04</u>
	26	1.30%	57	0.49%
Average:	0.8%			
<u>Component 1 (Pre-accretionary low temperature matrix materials)</u>				
Matrix granules and spherules in, and rinds of matrix mater- ial around, component 3 aggre- gates; black fragment in matrix (a,b,c)	59	0.56	31	0.40
Sooty amorphous matrix (d)	--	--	2	1.28
Very fine-grained matrix, undivided (e)	<u>--</u>	<u>80.30</u>	<u>--</u>	<u>82.20</u>
	59	80.86%	33	83.88%
Average:	82.4%			

^{1/}. Letters are keyed to materials described in figure 7.

^{2/}. These aggregates display a finely granular texture. They are pre-accretionary in respect to the abundant aggregates of iron-free magnesium silicates. They appear to have been formed elsewhere and transported to the site of accretion of Murray.

Fig. 8.--Size distributions of accretionary and pre-accretionary aggregates, particles, and grains in the Murray carbonaceous chondrite.

a. Plots of data from Figure 7a. Irregular aggregates of unaltered accretionary magnesium silicate (component 3) show two pronounced peaks, which make up about 3 and 4 percent of the total meteorite. This is nearly one-half of the 16 percent total area occupied by component 3 material. The aggregates, if they were spherical, would have diameters of about 0.1 and 0.2 mm, respectively. Altered accretionary aggregates and pre-accretionary particles of components 2 and 1 have sizes that mostly fall under the area of the larger sized accretionary peak.

b. Plot of data from Figure 7b. The occurrence, again, of two prominent peaks in unaltered accretionary material indicates a true bimodal distribution in the sizes of accretionary aggregates. Note that altered accretionary silicates and most of the pre-accretionary particles lie under the larger of the unaltered peaks. In addition, the sizes of finely granular iron-rich aggregates (component 3c) are mostly larger than materials that form the larger sized accretionary peak.

Explanation

Component 3.--Finely granular accretionary aggregates of high temperature magnesium silicates.

- a. Unaltered, low-iron
- b. Altered, low-iron
- c. Unaltered, high-iron

Component 2.--Pre-accretionary high temperature materials.

- a. Grains and fragments (chondrules), low-iron
- b. Compound chondrule
- c. Grains and fragments (chondrules) high-iron
- d. Metal

Component 1.--Pre-accretionary low temperature matrix.

- a. Flakes, granules and hollow spherules in component 3a
- b. Rinds and sheaths around components 3b, c
- c. Fragment in matrix

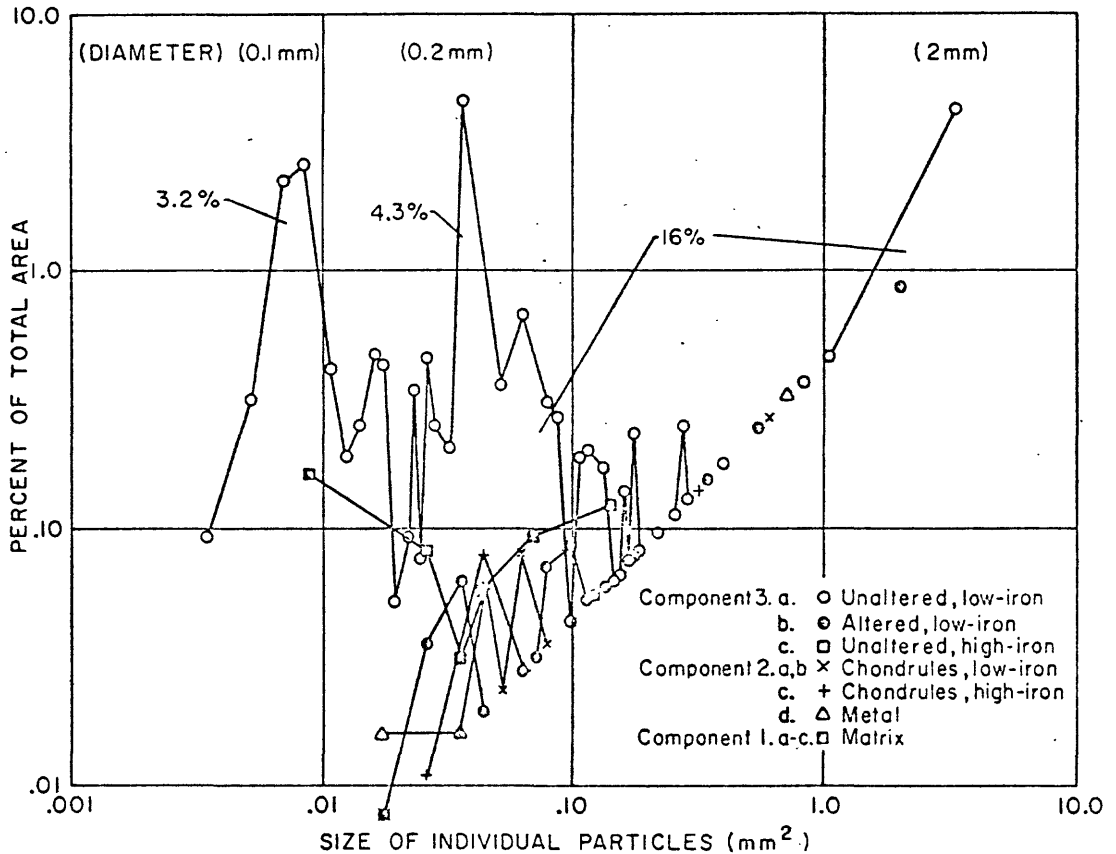


Fig. 8a.--Size distributions of accretionary and pre-accretionary aggregates, particles, and grains in the Murray carbonaceous chondrite. Plots of data from Figure 7a.

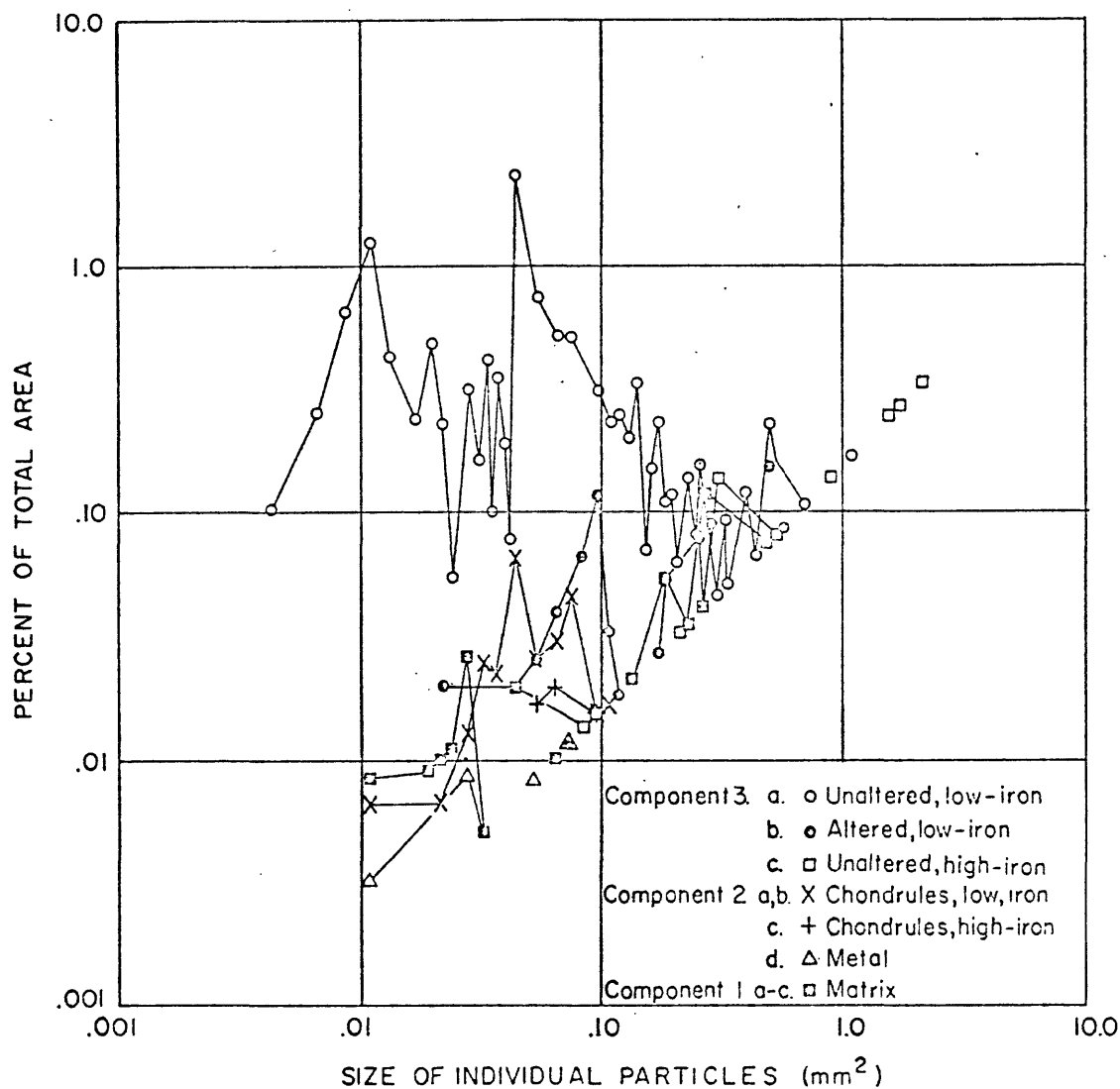


Fig. 8b.--Size distributions of accretionary and pre-accretionary aggregates, particles, and grains in the Murray carbonaceous chondrite. Plot of data from Figure 7b.

material, from descriptions of Fredriksson and Keil (1964), consists mainly of layer lattice silicates and subordinate nickel-bearing sulfides.

The pre-accretionary high temperature assemblage, component 2, consists of scattered, relatively large (mostly 0.2 to 0.8 mm, but locally 2 mm across) grains and chondrules of magnesium silicate. Metal also makes up a very small part of component 2 material. It occurs as a few very tiny droplets in the matrix (commonly on the order of 0.01 mm across), as a finely granular coating on a compound component 2 chondrule, and locally as droplets within component 2 grains of olivine(?). About one percent of the area of the rock is component 2 material (Table 15).

The accretionary high temperature assemblage, component 3, consists of small to large aggregates of tiny magnesium silicate grains or crystals. The grains in most of the aggregates are clear and are essentially iron-free. Some aggregates, however, are made up of pale brown to dark brown grains that appear relatively iron-rich. The aggregates of fine crystals make up most of the high temperature silicates in Murray, and constitute about 17 percent of the rock by area (Table 15). Individual crystals in the aggregates commonly are about 0.01 to 0.02 mm across, but in the larger accretionary aggregates some crystals approach 0.1 mm across. The aggregates appear as "dirty" clusters of (diversely oriented?) grains or crystals. The aggregates are loosely bound together, in part by apparent adhesion between grain surfaces, in part by intergranular glassy(?) materials, and in part by intergranular matrix material (component 1) which is present in all aggregates. The

aggregates range in size from less than 0.1 mm to as much as 2.5 mm across. The small aggregates are extremely irregular in shape. The largest aggregates are most regular in shape and some exhibit oval to nearly circular cross-sections. It is in these, here designated accretionary chondrules, that evidence is most clearly preserved on the manner of aggregation or accretion.

The very abundant, clear, component 3 magnesium silicate crystals are correlated with the abundant low-iron (less than about 0.02 moles Fe) olivine and pyroxene analyzed by Fredriksson and Keil (1964). Olivine and pyroxene of higher iron content that was analyzed by them appears to correlate with pale brown to dark brown magnesium silicates, which have been mapped both as component 2 and 3 materials (Fig. 7). For purposes of mapping, a distinction was made between magnesium silicates that were clear or only a very slightly tinted shade of brown, and silicates that were pale brown to dark brown. This arbitrary distinction has been referred to, respectively, as low-iron and high-iron silicates, and has been recognized in both component 2 and component 3 materials (Fig. 7 and Table 15).

Paragenetic relations in component 2 materials. Component 2 magnesium silicates are recognized by one or a combination of features. Most commonly they may be recognized as discrete, fairly conspicuous grains or chondrules that are of relatively large size. Some grains contain droplets of metal. Some display internal structure such as zoning. Some are compound chondrules that consist of zoned or barred silicate, granular silicate, and finely granular metal (Fig. 9). Component 2 grains commonly occur as isolated grains in component 1 matrix

Fig. 9.--Compound pre-accretionary chondrule (component 2), Murray carbonaceous chondrite.

a. General view, showing relationship to enclosing matrix and to component 3 aggregates. Distribution of various component 2 magnesium silicates and metal within fragment is shown in Figure 7a. Long dimension of chondrule is about 2 mm.

b. Detailed view of chondrule. Zoned or barred olivine(?) is white; medium gray areas in upper left and center are finely granular metal; irregularly surfaced, medium to dark gray material above and below central metallic area is coarsely granular olivine or pyroxene; light gray material at bottom and top center is a soft, punky sheath containing very fine specks of matrix(?) material, and thus is considered to be component 3 material.

c. Detailed view of barred or zoned silicate. Finely granular metal occupies cavity. Relatively coarse, granular component 2 magnesium silicate is at upper margin of chondrule. Note crisp character of finely crystalline aggregates of component 3 in the adjacent ground-mass, and the presence of included black matrix material in the aggregate at the left.

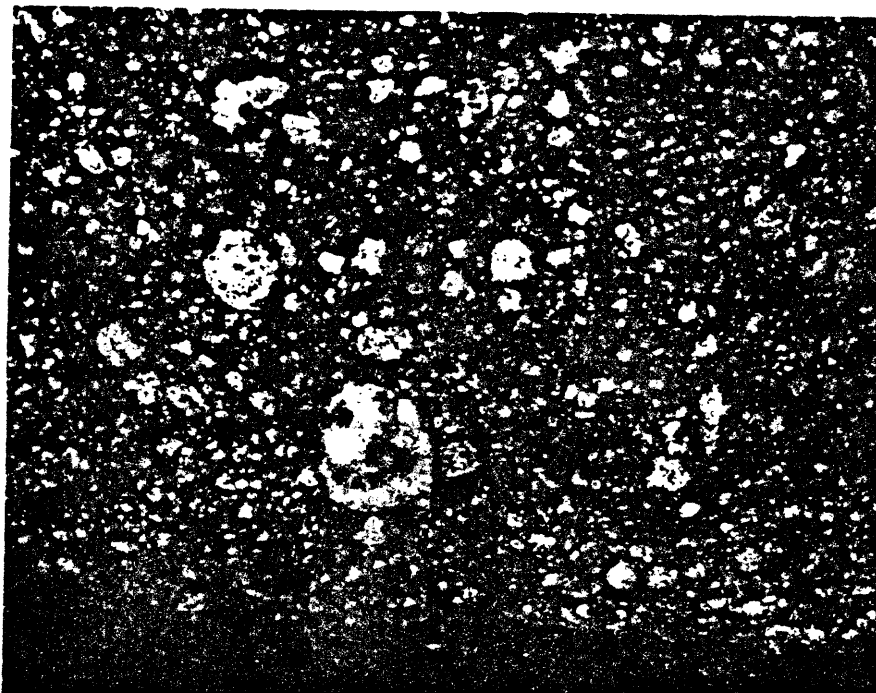


Fig. 9a.--General view of compound pre-accretionary chondrule (component 2), Murray carbonaceous chondrite.

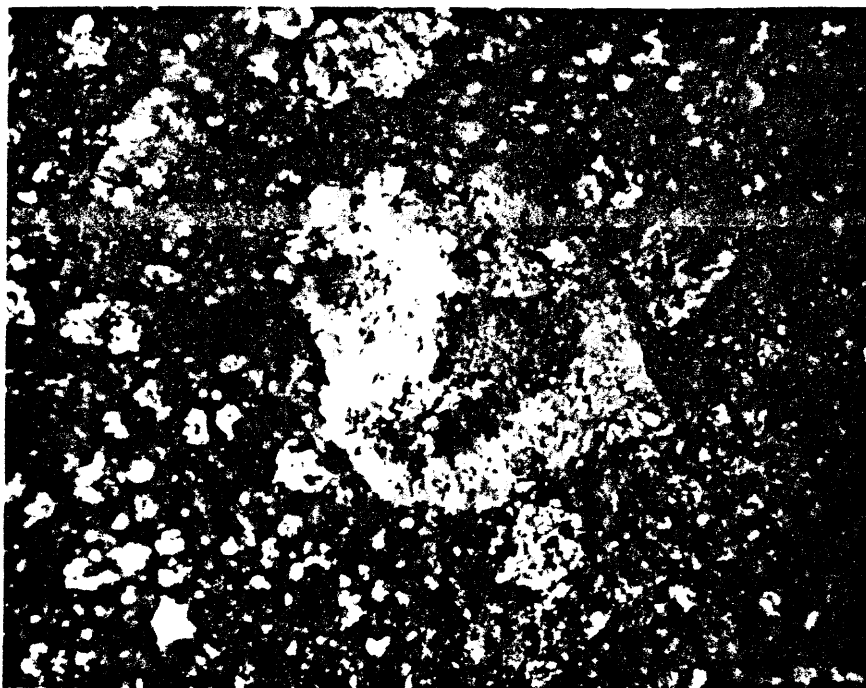


Fig. 9b.--Detailed view of compound pre-accretionary chondrule (component 2), Murray carbonaceous chondrite.



Fig. 9c.--Detailed view of barred and granular silicates and finely granular metal in compound component 2 chondrule, Murray carbonaceous chondrite.

material; they also occur as central to near-central nuclei in a number of accretionary component 3 aggregates (Fig. 7). Component 2 grains show only crisp unaltered contacts with enclosing component 1 and component 3 materials. Some of the grains and chondrules were broken prior to their incorporation in Murray. The distribution and contact relations of grains of component 2 silicate and metal relative to component 1 and 3 materials (Fig. 7) indicate that component 2 materials were in existence, and apparently were cold, prior to the formation of Murray.

Associational and overlap relations within a compound component 2 chondrule indicate that component 2 silicates and metal are genetically related. Steps in the development of one component 2 chondrule (Fig. 9) appear to have been: 1) formation of a zoned silicate chondrule; 2) fragmentation; 3) deposition of finely granular metal; 4) fragmentation(?); 5) deposition of fairly coarse, clear grains of magnesium silicate; 6) fragmentation(?); 7) deposition of a (now) soft light gray, amorphous-appearing sheath that appears to contain finely dispersed matrix material; 8) loss(?) of part of the sheath; and, 9) incorporation of the compound chondrule in Murray. Steps 1 through 5, and possibly step 6, apparently occurred in and near the high temperature environment that gave rise to component 2 materials.

Paragenetic relations in component 3 materials. Most component 3 aggregates are not "altered" or limonite stained, and appear exceedingly fresh. The contacts of aggregates, and of the grains in aggregates, with enclosing and included matrix materials are crisp, and contact metamorphic effects are not apparent. All unaltered aggregates contain matrix material, as flakes, granules, and hollow spherules.

Matrix spherules form the nucleus of some aggregates; in other aggregates, component 2 grains form the nucleus; in a few cases there is a compound nucleus. Thus, both component 1 and 2 materials existed prior to the precipitation of grains of component 3 magnesium silicate, prior to their aggregation as tiny clusters and as accretionary chondrules, and prior to their precipitation as fine disseminations in the matrix of Murray, a process that led to the formation of Murray.

Conditions under which precipitation of the finely granular component 3 materials, and hence accretion, occurred may be deduced from evidence within several of the component 3 aggregates. In one large accretionary chondrule (Fig. 10), the included matrix material occurs as flakes, well rounded tiny granules, and as larger spherules. The size of matrix particles increases from the interior toward the margin of the chondrule, and a number of relatively large (about 0.1 to 0.2 mm), hollow spherules of matrix material were incorporated as a bead-like girdle beneath the periphery of the chondrule. The matrix spherules are oriented. Some spherules are slightly oblate and their short axes lie normal to the adjacent chondrule margin; they exhibit raised equatorial septa or "belts" which parallel the adjacent margin of the chondrule (Fig. 10b, c, d). The textural relations indicate that the matrix spherules were mechanically rolled up in the accretionary chondrule before the chondrule was incorporated in Murray. The equatorial septa appear to have been formed prior to the incorporation of the spherules in the chondrule, which if true would indicate that a rolling-up process was responsible for the formation of the matrix spherules as well as the chondrule, and that this process, operating shortly before accretion of

Fig. 10.--Accretionary chondrule (component 3) containing particles, granules, and hollow spherules of matrix material, Murray carbonaceous chondrite.

a. General view of 2.5 mm beaded chondrule showing relationship to the matrix, and to other chondrules.

b. Detailed view of chondrule showing disseminated fine matrix particles and scattered larger matrix granules in the central to intermediate parts, and a girdle of matrix spherules (about 0.2 mm across) lying close to the periphery of the chondrule. Note the slightly oblate appearance of the spherules and the medial raised belts or septa that are oriented parallel to the adjacent chondrule margin. Spherules at the 5-, 6-, 10- and 2-o'clock positions are broken and display central cavities. An isolated grain of component 2 olivine(?) is present in the matrix at about the 9-o'clock position.

c. Matrix spherules at the 2- and 3-o'clock positions which display, respectively, a partly collapsed cavity, and a raised septum. Note the crisp contact of the magnesium silicate crystals of the chondrule with enclosing matrix material, and grain of component 2 olivine(?) in contact with the accretionary chondrule near the belted matrix spherule.

d. Matrix spherule, at the 10-o'clock position, showing a well developed central cavity. This spherule appears to have been broken prior to its incorporation in the accretionary chondrule. Note the fine matrix material that is disseminated in the accretionary chondrule. Note, also, the small accretionary aggregates and the tiny, almost individual grains of clear magnesium silicate (component 3) disseminated in the matrix.

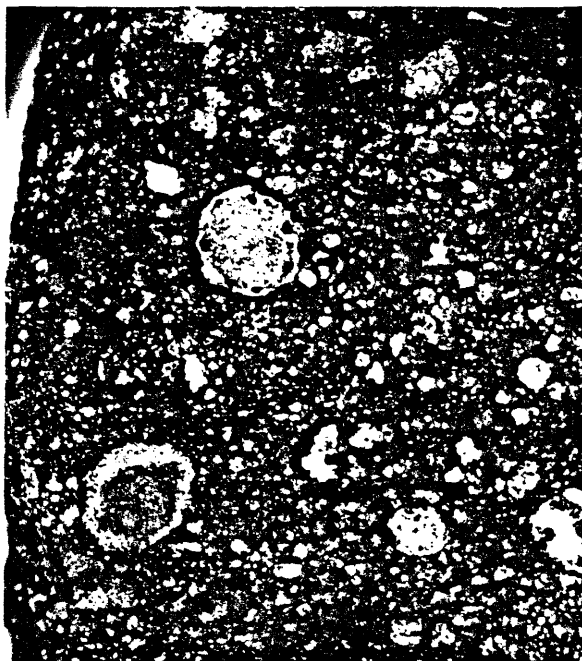


Fig. 10a.--General view of large accretionary chondrule,
Murray carbonaceous chondrite.

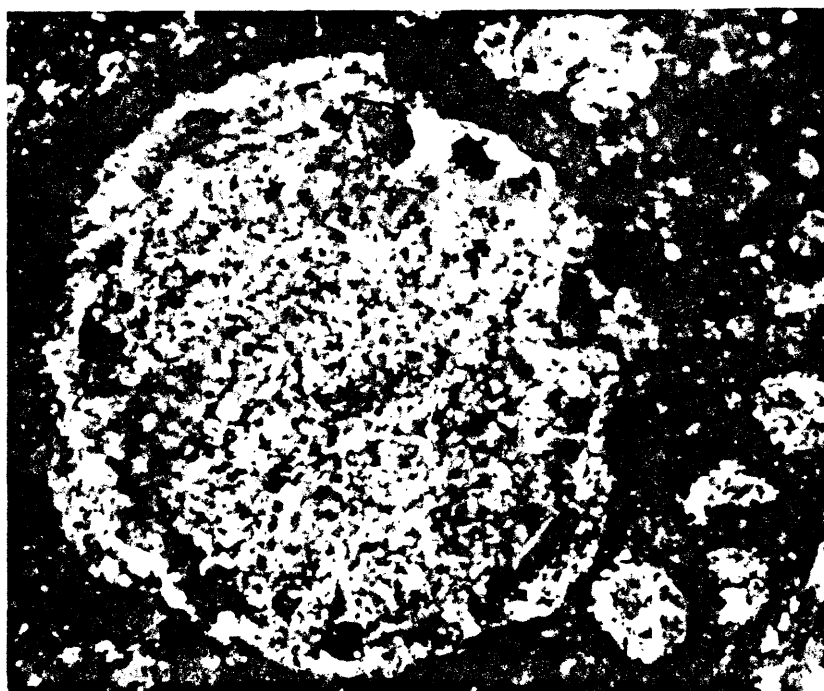


Fig. 10b.--Detailed view of large accretionary chondrule,
Murray carbonaceous chondrite.



Fig. 10c.---Detailed view of hollow, belted matrix spherules in accretionary chondrule, Murray carbonaceous chondrite.

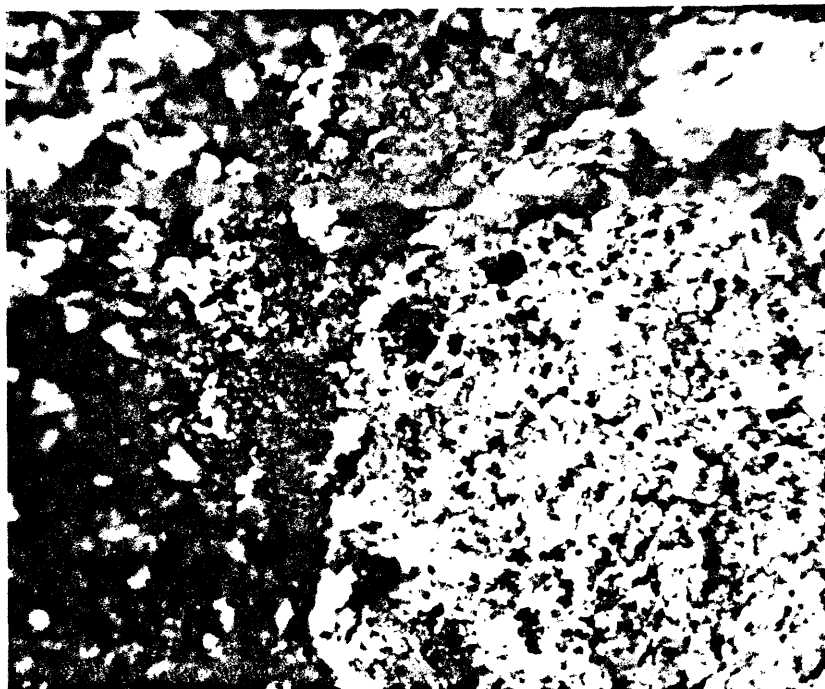


Fig. 10d.---Detailed view of hollow, belted matrix spherules in accretionary chondrule, Murray carbonaceous chondrite.

the chondrule, may have been responsible for the preferred orientations of the spherules at their time of capture by the accretionary chondrule. Formation of the spherules and the accretionary chondrule occurred as the result of a dynamic process that operated in a free environment. The process led to the formation of the matrix spherules from low temperature materials, and their mechanical incorporation in accretionary aggregates during precipitation of high temperature silicates.

Hollow matrix spherules have been observed in several accretionary aggregates (Fig. 10, 11, 12). Although the matrix spherules are now extremely fragile, some were broken to their now-hollow centers prior to their incorporation in the component 3 aggregates (Fig. 10d, 12). The thinness of the spherule walls (Fig. 11), and the pre-accretion fracturing, indicate that the spherules must have once been considerably stronger than they now are, and that they almost certainly were brittle. To account for both the strength and the brittleness, the central voids may once have been occupied by icy nuclei, and the matrix material of the spherules also may have contained interstitial ice. The matrix spherules may have been tiny balls of icy dust. Preservation of the hollow matrix spherules is attributed to low pressures at, and since, the time of accretion, -- and to an armoring effect in the accretionary aggregates by the enclosing grains of magnesium silicate, which are in grain to grain contact (Fig. 11).

Some accretionary aggregates of clear magnesium silicate are limonite stained or "altered"; most of these aggregates lack finely-disseminated matrix material that characterizes the unaltered accretionary aggregates. The limonite staining may be the product of

Fig. 11.--Accretionary chondrule containing several hollow matrix spherules, Murray carbonaceous chondrite.

a. General view. Chondrule (about 1.2 mm in long dimension) contains at least five hollow matrix spherules. Note the highly irregular but crisp contact of the accretionary aggregate with the enclosing matrix material. General view of this chondrule is shown in lower right-hand part of Figure 10a.

b. Detailed view of one of the hollow matrix spherules showing the extreme thinness of the wall. Preservation of such fragile particles is attributed to low pressures in the parent body at the time of accretion, to low pressures since accretion, and to an armoring effect by the enclosing granular crystals of magnesium silicate, which are in grain to grain contact.

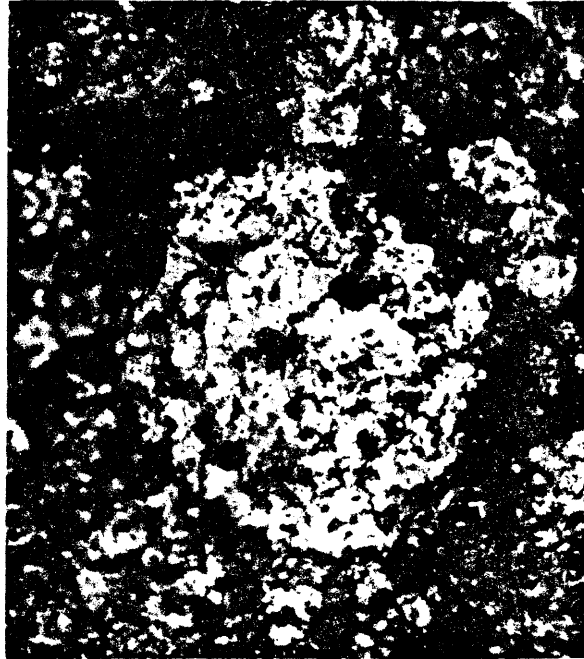


Fig. 11a.--Thin walled hollow matrix spherules in an accretionary chondrule, Murray carbonaceous chondrite.

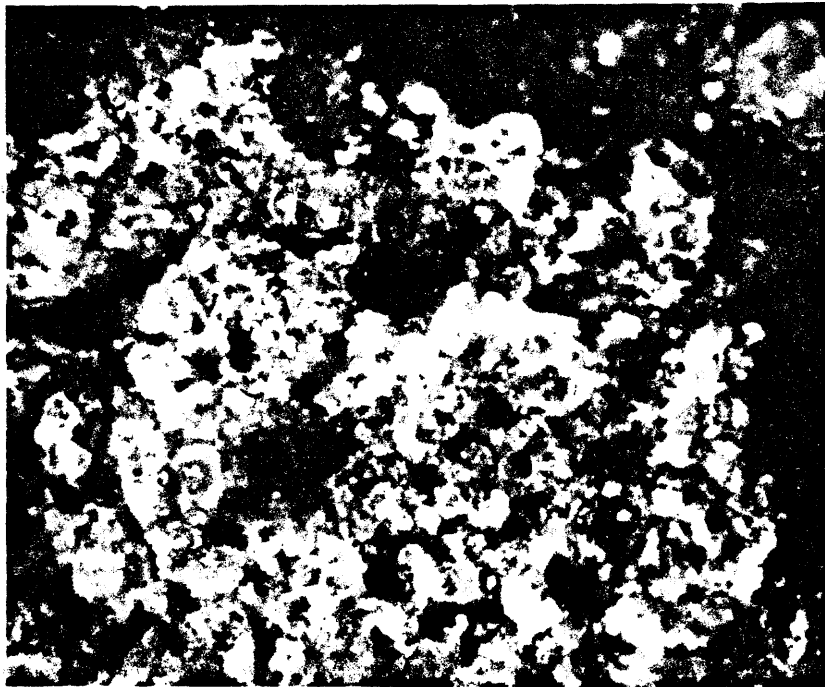


Fig. 11b.--Thin walled hollow matrix spherules in an accretionary chondrule, Murray carbonaceous chondrite.

Fig. 12.--Fragmented, hollow matrix spherule that forms the nucleus of an irregular, accretionary aggregate (component 3), Murray carbonaceous chondrite.

Aggregate is about 0.6 mm across. Location is very near left central edge of map (side view, Fig. 7b) of Murray. Relations suggest that the spherule was brittle. It may have contained an icy nucleus in order to sustain fracturing and to survive during its incorporation as a nucleus in this accretionary aggregate. Note that other matrix material also is present in this aggregate.



Fig. 12.--Fragmented hollow matrix spherule, Murray carbonaceous chondrite.

the oxidation of formerly contained hydrated matrix materials because some altered aggregates contain "rusty" relicts(?) of included matrix material. A number of altered aggregates are embedded in matrix material of Murray, and in most, alteration effects were not observed to extend into the enclosing matrix, which suggests that alteration largely occurred prior to accretion. Some post-accretion alteration appears to have occurred in and around a few limonite-stained aggregates. One of these is a compound component 3--component 1 chondrule (Fig. 13), in which a nucleus of bright yellow-stained accretionary component 3 material is enclosed by a sheath of shiny black matrix material. The sheath, which differs in texture from enclosing matrix and which apparently contains grains of component 3 silicate (Fig. 13), appears to have been acquired after the central-most part of the accretionary aggregate formed but before the aggregate was incorporated in Murray. Matrix material of Murray that encloses this compound chondrule is not obviously altered in detail, but a subtle alteration halo in the enclosing groundmass, which appears as a diffuse, gray patch in Figure 10a, is present.

Accretion of the limonite-stained aggregates apparently occurred shortly prior to the precipitation of some of the unaltered accretionary (component 3) materials. This may be deduced, for example, from relations preserved in a compound accretionary chondrule (Fig. 14). In this chondrule, limonite staining in the inner part appears to have soaked through and locally "altered" part of an enclosing sheath of unaltered component 3 material. This is considered evidence that the process of alteration was going on immediately prior to the acquisition

Fig. 13.--Yellow, limonitic stained accretionary chondrule (component 3), enclosed by a shiny black sheath of matrix material (component 1), Murray carbonaceous chondrite.

Overall compound chondrule is about 0.6 mm across; nucleus is about 0.2 mm. Sheaths such as this apparently were acquired during the general accretionary process, prior to accretion of Murray. "Murray F" material (DuFresne and Anders, 1962) is reported to have enclosed olivine or pyroxene, presumably in a manner similar to the sheathing material shown here. Post-accretion alteration of the enclosing matrix is revealed by the presence of a diffuse halo (see Fig. 10a).



Fig. 13.--Altered compound chondrule, Murray carbonaceous chondrite.

Fig. 14.--Compound accretionary chondrule (component 3), Murray carbonaceous chondrite.

About 2.25 mm across. Unaltered sheath of component 3 magnesium silicate crystals, containing admixed matrix material, encloses yellowish-brown limonite-stained ("altered") core in which matrix material is not evident. Limonitic staining extends from the core to the lower margin of the chondrule, apparently having soaked through part of the unaltered sheath. General view is shown in Figure 10a.



Fig. 14.--Compound accretionary chondrule, Murray carbonaceous chondrite.

of the unaltered sheath, and continued (in this case) for a short time after acquisition of the unaltered sheath.

Paragenetic relations that are outlined in Figure 7 indicate that the local limonitic alteration of accretionary aggregates is pre-terrestrial, and also mostly pre-dated the formation of Murray. The reason for the alteration is not directly evident from paragenetic and textural relations in Murray. Perhaps the simplest way for the altered aggregates to have become limonite stained is to appeal to a brief heating, sufficient to melt ices possibly associated with included matrix material. Heating after formation of the aggregates, prior to their incorporation in Murray, may have permitted oxidation of included matrix material by the presumably associated volatiles. Heating perhaps could have occurred in a warm region near the source medium of the high temperature component 3 magnesium silicates.

A few dark, finely granular aggregates of medium to dark brown (moderate- to high-iron) magnesium silicates (component 3c) are present in Murray (Fig. 7b). They are considered to be component 3 materials on the basis of their texture, their paragenetic relations to component 1 matrix materials and to unaltered component 3a materials, and because they very locally also are limonite stained or altered. Some component 3c aggregates are enclosed by smooth, dense, black rinds of matrix(?) material, and are embedded in sooty appearing matrix material. Some aggregates or chondrules are partly to entirely enclosed by sheaths of component 3a material. Most are comparatively large aggregates. They precipitated from a source medium that differed compositionally from the one that was responsible for precipitation of the dominant iron-free

component 3 silicates of Murray. Precipitation and aggregation elsewhere, and transportation to the site of accretion of Murray is indicated from the paragenetic and textural relations, and the composition. Whereas altered component 3 materials may have formed and have been altered in the region of accretion of Murray, the essentially unaltered, relatively high-iron aggregates (component 3c) may have formed away from the immediate region of accretion of Murray.

Component 3c aggregates are similar to the dominant, dark brown, finely crystalline (apparently accretionary) aggregates in the Vigarano pigeonite chondrite; in Vigarano, apparently iron-free finely crystalline (accretionary?) aggregates are subordinate, which is the reverse of the relationship in Murray. The implication from this is that the medium which gave rise to component 3 silicates at any one place, although broadly uniform (iron-rich, iron-poor), locally differed greatly in iron composition from the medium which gave rise to the olivine and pyroxene of the discrete classes of chondrites.

Textural relations within and between components. Accretionary aggregates occur in three principal sizes (Fig. 8): 1) a few, large (1 to 2 mm across) chondrules; 2) abundant smaller subround to irregular aggregates (commonly on the order of 0.2 mm across); and, 3) very abundant, tiny, irregular aggregates, which if they had circular cross-sections would have diameters of about 0.1 mm and less. The large and intermediate-sized aggregates, on the basis of their external form, and locally on the basis of internal gradations in the size of included matrix material (from fine to coarse from the center to the periphery), are interpreted to have undergone transport in the accretionary

environment prior to their incorporation in Murray. The smallest aggregates, which are pervasively disseminated in the matrix of Murray, exhibit extremely irregular contacts with enclosing and included matrix materials. They are inferred to record the moment of accretion of Murray. This interpretation, based on textural considerations, is supported by the marked bimodal size distribution of unaltered aggregates (Fig. 8); the great abundance of tiny aggregates and disseminated grains (Table 15, Fig. 7); and the virtual absence of any other high temperature materials, except for a few droplets of metal, in the very small size range (Fig. 8).

As indicated by the paragenetic relations and as suggested by the size-frequency distributions, transport in the accretionary environment occurred: 1) in a few large (~ 2 mm) accretionary and pre-accretionary chondrules; and, 2) in a large number of accretionary aggregates and pre-accretionary particles in approximately the 0.2 to 0.4 mm size range. Because of this, the medium that gave rise to the precipitation of the finely granular magnesium silicates appears to have been closely associated with the transport of particulate materials that were involved in accretion. The relations are considered evidence that accretion was brought about as the result of a dynamic process, and that formation of chondrules, both pre-accretionary and accretionary, cannot be the result of in situ or "volcanic" processes in parent material of carbonaceous achondrite (Type I of Wiik, 1956) composition, as has been commonly assumed because of the chemically primitive aspect of the carbonaceous achondrites.

Recognition of Components 1, 2, and 3 in other Chondrites

Components (mineral assemblages) described from the Murray chondrite have been observed during reconnaissance examinations of carbonaceous, pigeonite, and hypersthene chondrite classes (Table 16). As in Murray, finely granular component 3 magnesium silicates are the principal high temperature materials in the Mighei (Fig. 15), Bells, and Crescent carbonaceous chondrites, but these materials appear to be less abundant than in Murray. Large accretionary chondrules were not observed in these meteorites, but a spherical cavity or cast suggests that a relatively large accretionary chondrule may once have been present in the small specimen of Mighei that was examined. Accretionary aggregates comparable in size to the smaller and larger sized materials that form the bimodal peaks of Murray (Fig. 8) appear to be present in all carbonaceous chondrite material that was examined. As in Murray, sparse grains of component 2 olivine or pyroxene, and very sparse grains of metal, are disseminated in the component 1 matrix of these carbonaceous meteorites.

Components 1, 2, and 3 are present in the pigeonite chondrites (Table 16). Component 1 matrix material is less abundant, and finely granular component 3 matrix material is considerably more abundant, than in the carbonaceous chondrites. In Mokoia (Fig. 16), a matrix that consists of tiny grains of magnesium silicate (component 3) and intimately admixed carbonaceous material (component 1) encloses finely granular aggregates and large accretionary chondrules of component 3 material. As in Murray, the component 3 magnesium silicates of Mokoia are clear and are essentially iron-free, and the aggregates and accretionary

Table 16.--Mineral assemblages (components) in selected chondrites.

Chondrite	Mineralogic- petrologic classification ^{1/}	Components		
		<u>1a/</u>	<u>2b/</u>	<u>3c/</u>
Bells ^{2/}	C-1	Dominant	Very scarce	Subordinate
Crescent ^{2/}	"	"	"	"
Mighei ^{3/}	"	"	"	"
Murray ^{3/}	"	"	Scarce	"
Karoonda ^{3/}	P-2(?)	Common	Very scarce silicate Conspicuous metal	Dominant ^{4/}
Mokoia ^{3/}	P-1	"	Scarce	Common ^{5/}
Vigarano ^{3/}	P-2	Subordinate	Subordinate	Dominant
Holbrook ^{6/}	Hh-5	None	Common	"

a/. Carbonaceous matrix material

b/. Chondrules and grains of olivine and pyroxene; metal.

c/. Finely granular olivine and pyroxene as disseminations, aggregates and chondrules.

1/. Revised from chemical-petrologic classification of Van Schmus and Wood (1967). See Table 9.

2/. Specimens of Mr. O. E. Monnig, Fort Worth, Texas.

3/. Arizona State University Collection, Tempe, Arizona. Mighei, specimen no. 211.1; Murray, specimen no. 635.1; Karoonda, specimen, no. 434.5; Mokoia, specimen no. 75.1; Vigarano, specimen no. 590.1.

4/. Mainly very finely granular component 3 and pervasively disseminated component 1.

5/. Principally as aggregates, chondrules, and finely granular disseminations.

6/. University of Arizona Collection, Tucson, Arizona, specimen no. M-819.

Fig. 15.--Mighei carbonaceous chondrite.

General (a) and detailed (b) views showing irregular aggregates and fine disseminations of grains of component 3 magnesium silicate in component 1 matrix. The smooth spherical cavity, which is apparently lined with tiny grains of component 3 silicate, may once have been occupied by a component 3 (accretionary) chondrule (Arizona State University specimen no. 211.1, 4.6 g).



Fig. 15a.--Mighei carbonaceous chondrite, general view.



Fig. 15b.--Mighei carbonaceous chondrite, detailed view.

Fig. 16.--Mokoia pigeonite chondrite (carbonaceous).

General (a) and detailed (b) views showing aggregates, chondrules, and disseminations of component 3 magnesium silicate embedded in porous carbonaceous component 1 matrix. Note the highly irregular contacts between the aggregates and matrix, and that specks of matrix are present in the aggregates and chondrules. Note, also, the well rounded appearance of the accretionary chondrules. They are similar in general form to the large granular (apparently component 3) chondrule in the specimen of the Bjurböle olivine-hypersthene chondrite in the Arizona State University Collection (Arizona State University specimen no. 75.1).



0 1 2 3 4 5
1/2 mm

Fig. 16a.--Mokoia pigeonite chondrite, general view.



mm mm

Fig. 16b.--Mokoia pigeonite chondrite, detailed view.

chondrules contain particles of matrix material. Sparse relatively large grains of component 3 olivine or pyroxene, and tiny grains of metal, are disseminated in the finely granular matrix of Mokoia.

In the pigeonite chondrite Karoonda (Fig. 17), the matrix is almost uniformly very fine-grained. It appears to be an intimate mixture of finely granular magnesium silicates (component 3) and finely disseminated carbonaceous materials (component 1). A few large, finely granular component 3 accretionary chondrules are embedded in the matrix, which is only poorly to moderately well bonded. Conspicuous component 2 metal is disseminated in the component 3--component 1 matrix of Karoonda.

The Vigarano pigeonite chondrite is a fairly dense, dark chondrite, which exhibits a chondritic texture that is similar to that of the unequilibrated ordinary chondrites (such as the Mező-Madaras hypersthene chondrite; see Van Schmus, 1967); the texture also is similar to the texture of the least metamorphosed of the enstatite chondrites (for example, Indarch; Arizona State University specimen no. 63a). In Vigarano, a fine-grained, black, carbonaceous matrix encloses component 2 and 3 chondrules; the matrix appears to be texturally identical to the fine-grained black component 1 matrix of Murray. Component 2 grains and chondrules, and metal, are distributed irregularly through the subordinate matrix. Component 2 silicates are identified on the basis of relatively large grain size, and on internal structure such as zoning. Some of the zoned chondrules, which are enclosed by carbonaceous matrix, were fragmented before accretion. The metal (nickel-iron and troilite?) is very finely granular and occurs as irregularly shaped inclusions and

Fig. 17.--Karoonda pigeonite chondrite.

Consists principally of a finely granular groundmass of admixed component 3 and component 1 materials. Note the hollow spherical granular component 3 chondrule near center. Tiny bright spots are disseminated metal (Arizona State University, specimen no. 434.5, 56.15 g).



Fig. 17.--Karoonda pigeonite chondrite.

as tiny droplets in the matrix. Aggregates of finely granular magnesium silicate are common and they are considered to be component 3 materials. Most are medium to dark brown, and are correlated with the iron-rich olivine which Mason (1962a, 1963c) reports to range from Fa 0 to 60 for the pigeonite chondrites. A few very fine-grained accretionary(?) aggregates are milky-white, and consist of clear, apparently iron-free magnesium silicates. Tiny aggregates and very tiny grains disseminated in the black component 1 matrix also appear to consist both of dark iron-rich and clear iron-free silicates. Black matrix(?) material appears to be present in a few aggregates, but in many fayalite-rich aggregates the presence of included matrix material is not obvious, possibly because of the overall darkness of the aggregates. The dark aggregates are similar to the dark component 3 aggregates that were mapped in Murray (Fig. 7b).

The non-carbonaceous Holbrook meteorite, a light gray, crystalline, spherical, olivine-hypersthene chondrite (Hey, 1966), exhibits component 2 and component 3 materials (Fig. 18). By analogy with the carbonaceous and pigeonite chondrites, component 2 materials are the dense, dark gray, spherical chondrules and the disseminated metal. Component 3 materials are the light gray, finely crystalline materials, which occur: 1) as relatively large, finely granular spherical aggregates, or accretionary chondrules, which are less distinct in outline than the dark gray component 2 chondrules; 2) as smaller, finely granular aggregates of subround to irregular outline; and, 3) as a very finely granular matrix material. The foregoing three-fold character directly parallels the three-fold character of component 3 silicates in

Fig. 18.--Holbrook hypersthene chondrite.

General (a) and detailed (b) views showing pre-accretionary (component 2) materials, consisting of dark gray, well rounded chondrules and metal, embedded in apparent accretionary (component 3) materials. The latter consist of medium gray, round to sub-round granular chondrules (several of which contain nuclei of component 2 metal), medium to light gray, irregular, granular aggregates, and finely granular matrix. The prominent dark gray component 2 chondrule is 3 mm across (University of Arizona, specimen no. M-819).



Fig. 18a.--Holbrook hypersthene chondrite, general view.

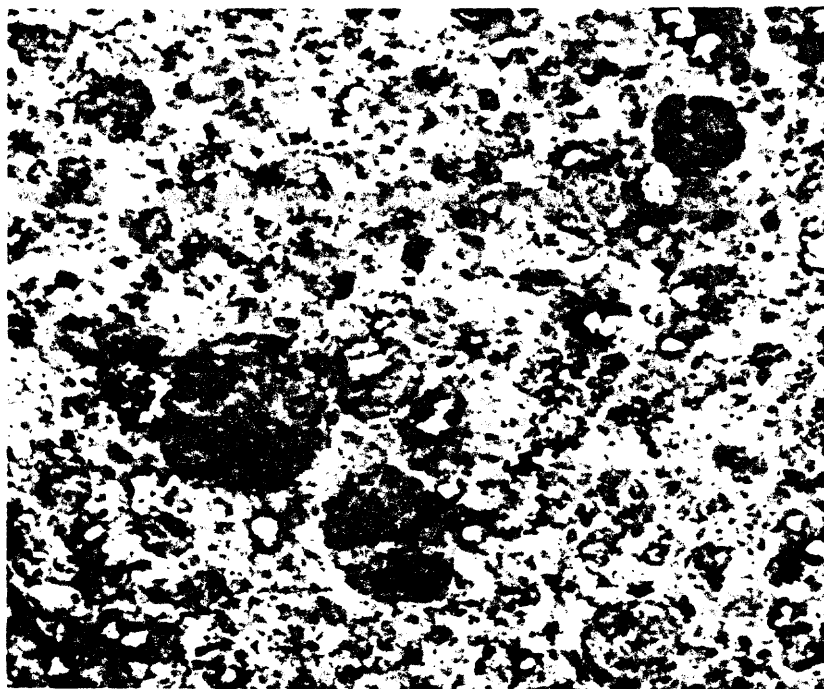


Fig. 18b.--Holbrook hypersthene chondrite, detailed view.

Murray (Fig. 8), except that the very finely granular silicates in Murray are disseminated in component 1 materials, whereas in Holbrook they are in grain to grain contact. Metal locally occurs within the dark gray (component 2) chondrules in Holbrook, which is analogous to the metal in a compound component 2 chondrule in Murray (Fig. 9). Metal in Holbrook also locally forms the nucleus of some finely granular accretionary chondrules, and these may be considered to be compound component 2--component 3 chondrules, which again is analogous to paragenetic relations observed in Murray.

The recognition of component 2 and 3 materials in the volatile-deficient and volatile-poor chondrites implies a common mode of accretion for the chondrites. Although hydrated carbonaceous material is not present in the matrix of Holbrook, some once may have been present prior to its equilibration or metamorphism. For example, the unequilibrated hypersthene chondrite, Mezö-Madaras, which Van Schmus and Wood (1967) classed as an (L)3 chondrite, contains 0.46 weight percent C and 0.79 weight percent $H_2O(+)$ (Jarosewich, 1967). Photographs in Van Schmus (1967) show that the carbonaceous material is matrix material (component 1) which encloses both component 2 chondrules and apparent component 3 chondrules and aggregates.

Chondrule Formation and Chondrite Accretion

Aggregation of Solids

The paragenetic relationships and textural characteristics in Murray cannot be explained as the result of the precipitation of high temperature magnesium silicates from a melt that was in intimate

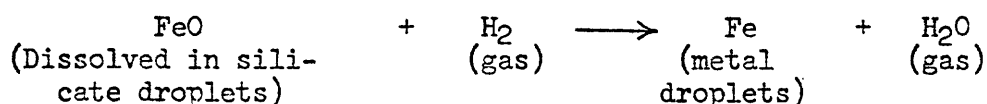
association with volatile-rich matrix materials. Rather, the formation of relatively large accretionary chondrules and smaller irregular aggregates during the course of accretion, and the precipitation of tiny aggregates and grains as disseminations in volatile-rich matrix apparently at the moment of accretion, are uniquely explained if the component 3 silicates were precipitated across a boundary from a high temperature gas, at low pressures, into a cold environment that contained dispersed pre-accretionary low and high temperature materials. Because fragmented, now-hollow matrix spherules in accretionary chondrules in Murray appear to have required the former presence of icy nuclei, free volatiles, as ices, may have been generally associated with dispersed, hydrated, low temperature matrix materials prior to accretion. It is proposed that thawing and refreezing of icy volatiles associated with component 1 materials was responsible for accretion.

Accretion may have occurred as ices associated with component 1 materials melted in the vicinity of precipitation of component 3 materials, following which there was refreezing to form icy chondritic material. The anhydrous component 3 silicates (olivine and pyroxene), on the basis of their small grain size and included component 1 matrix material in component 3 aggregates, must have precipitated abruptly from the high temperature source medium (gas). The formation of accretionary chondrules, and the process of accretion, may have a terrestrial analogy in the rolling up of a dirty snowball where fresh snow overlies relatively warm ground, -- in the terrestrial situation, dirt is picked up at the contact between the cold accreting snowball and the warm earth. In the case of chondrite accretion, the temperature roles were reversed.

Dispersed, very fine-grained, cold background materials adhered to apparently warm, but cooling, grains and aggregates of grains of component 3 magnesium silicate. Accretion of Murray perhaps can be visualized as having occurred as a warm "snowstorm" of fine magnesium silicate crystals, precipitating from a gas in a cold, "dusty" environment, briefly raised temperatures above the melting point of ices, following which there was abrupt refreezing into icy chondritic material. The formation of nearly round accretionary chondrules may be inferred to have occurred where the largest of the accretionary aggregates were virtually rolled along interfaces between the high temperature gas and the low temperature "background" materials, prior to the incorporation of the accretionary chondrules in chondritic material.

Inferred Character of Early Solar System

Because component 1 and 2 materials existed prior to accretion, a low temperature dust cloud and a high temperature region of chondrule and metal formation, and storage, may be inferred to have co-existed in the solar system prior to chondrite formation. Wood (1963b, 1967a) has suggested that chondrules formed in the solar nebula, with reduction of chondrules occurring before accretion by reaction with hydrogen:



However, the precipitation of chondrules as liquid droplets condensing from a gas of solar composition requires high pressures (100 atm total pressure or more, Wood, 1967a; see Fig. 19), and these pressures are much too high for pressures estimated for the primordial nebula

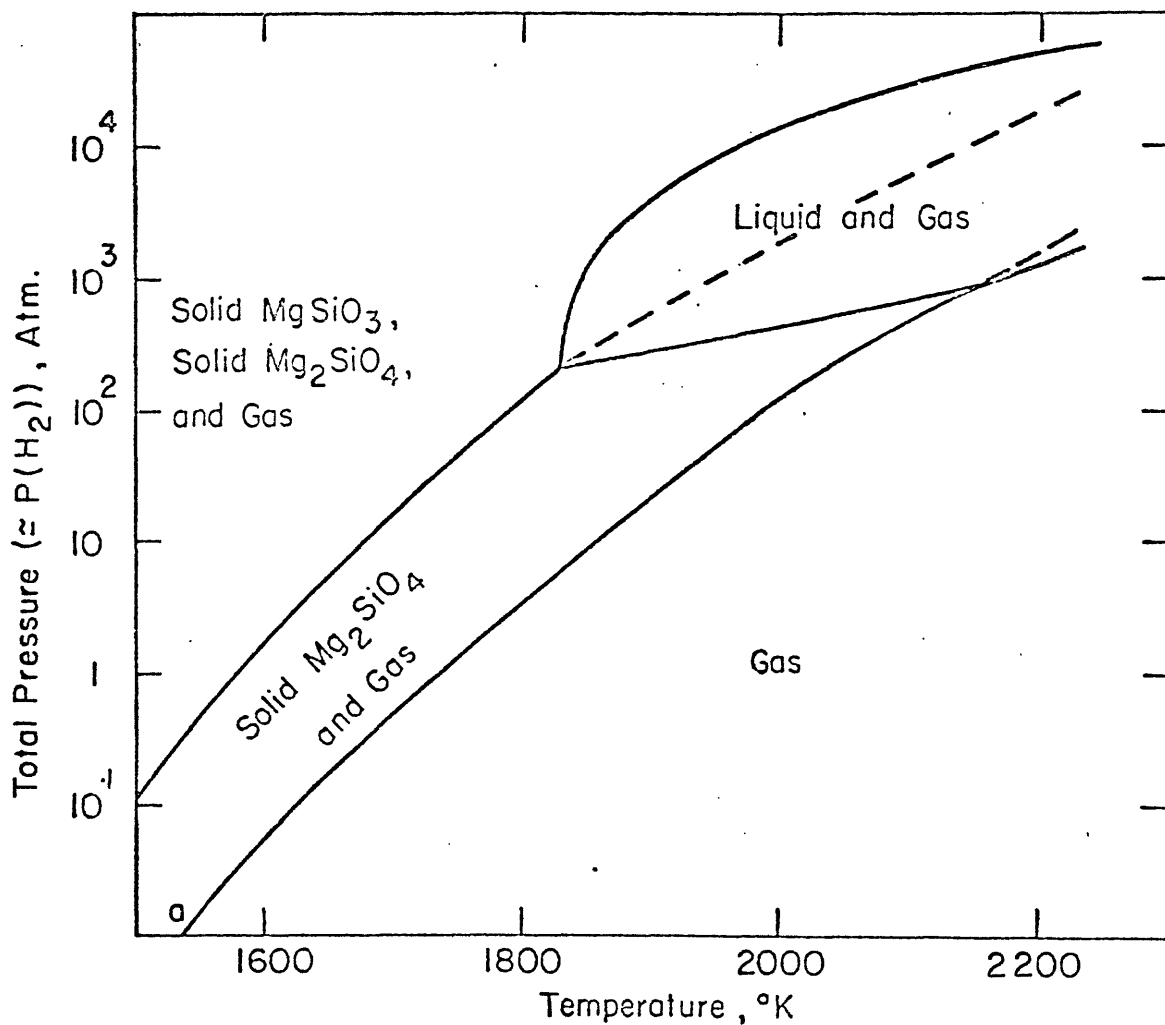


Fig. 19.--Phase diagram for the system H-O-Mg-Si, from thermochemical calculations.

Solar proportions of the four elements are assumed. Liquid condensation is possible only in the "Liquid and Gas" field, at 100 atm. gas pressure. From Wood (1963b, 1967a).

(probably no greater than 10^{-5} to 10^{-4} atm near the present asteroid belt; Cameron, 1966).

Formation of component 2 materials. Component 2 chondrules include massive to barred or zoned grains of magnesium silicate that are on the order of 1 to 2 mm across; some of the massive grains contain tiny droplets of metal, and barred chondrules locally are overlain by finely granular metal. Some component 2 chondrules are granular, and are made up of grains that are on the order of 0.2 to 0.4 mm across. In some chondrites, granular component 2 chondrules are enclosed by sheaths of metal (for example, in the Breitscheid bronzite chondrite; see Wlotzka, 1963, Fig. 10). Some component 2 chondrules are more diversely compound and exhibit zoned and granular silicates, and metal, in varying proportions (Fig. 9). Because of the relatively large size of component 2 grains and chondrules compared to the very fine grain size of component 3 materials; because of the development of texturally complicated compound component 2 chondrules which consist solely of relatively coarse grained high temperature materials; because paragenetic relations show that such component 2 materials clearly are pre-accretionary; and because of regularities in the partition of Fe between component 2 metal and component 3 silicates in the chondrites, which are discussed later, component 2 materials are proposed to have been formed in the vicinity of the protosun rather than in the solar nebula. The formation of component 2 materials in the protosun would allow for the development of a solar gas that was partly to wholly stripped of its Fe, -- a gas that could serve as the source gas for the component 3 silicates.

Support for the pre-accretionary formation of component 2 chondrules in a relatively high temperature environment is seen in the distribution of $^{129}\text{R}_\text{Xe}$ in the Bruderheim hypersthene chondrite. Merrihue (1966) found high $^{129}\text{R}_\text{Xe}/\text{Xe}$ ratios in six chondrules, and lower $^{129}\text{R}_\text{Xe}/\text{Xe}$ ratios in the bulk meteorite and in its troilite, olivine, pyroxene, and feldspar (Fig. 20). If the Bruderheim chondrules are component 2 chondrules, their high $^{129}\text{R}_\text{Xe}$ contents might be explained as the result of formation before accretion, at a time when short-lived radioactive nuclides were producing greater quantities of daughter products; the relatively low total Xe contents of the chondrules then also might be explained as the result of the formation of component 2 chondrules in a volatile-deficient, high temperature region of the early solar system.

Formation of component 3 silicates. Grains of component 3 silicate commonly are much smaller than component 2 grains (about 0.01 to 0.02 mm versus 0.2 to 0.4 mm and larger). Paragenetic and textural relations in Murray indicate that component 3 silicates precipitated at low pressures (a few atmospheres or possibly much less), and that component 3 aggregates and chondrules formed in a dynamic environment in which component 1 and 2 materials were mechanically incorporated during the abrupt precipitation and aggregation of component 3 silicates. Component 3 aggregates include so-called "porphyritic" chondrules, in which relatively large grains of component 2 olivine and pyroxene are embedded in a groundmass of very fine grains of component 3 material. Such accretionary aggregates are compound component 2--component 3 chondrules.

Fig. 20.--Xenon and radiogenic $^{129}\text{R}_{\text{Xe}}$ contents for mineral phases and chondrule samples from the Bruderheim hypersthene chondrite.

The chondrules are labeled BC. Merrihue's data indicate that ^{129}I decay, which resulted in the production of $^{129}\text{R}_{\text{Xe}}$, occurred in situ in the bulk meteorite and its minerals after "solidification and cooling" of the solids because minerals with the smaller gas retentivities display the higher Xe contents. The chondrules are probably all component 2 chondrules. Olivine and pyroxene are probably component 3 materials, and feldspar probably was derived from the devitrification of Na- and Al-rich component 3 glass. Troilite is inferred to have been derived from component 1 sulfides. From Merrihue (1966, Fig. 2).

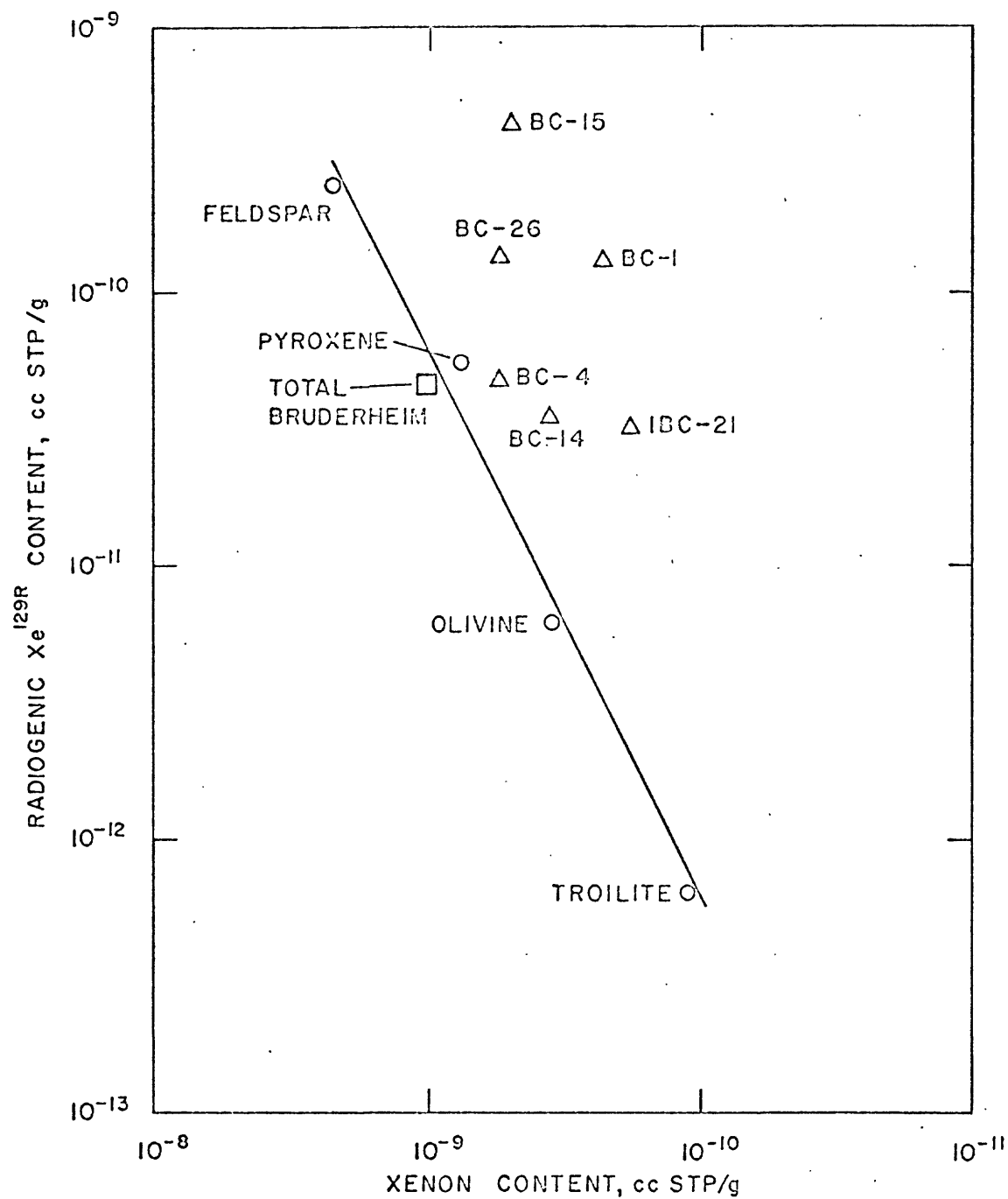


Fig. 20.--Xenon and radiogenic ^{129}Xe contents for mineral phases and chondrule samples from the Bruderheim hypersthene chondrite.

In the phase diagram of Wood (Fig. 19), precipitation of component 3 silicates, and the aggregation of accretionary chondrules, occurred at about 1600°K or less, with the formation of olivine occurring first as the temperature dropped across the gas/gas-solid boundary. This is consistent with the observation that olivine is the dominant high temperature silicate in all classes of chondrites except the enstatite chondrites. Pyroxene of the enstatite chondrites may reflect that precipitation of component 3 silicates occurred from component 3 gas that was at a higher pressure than component 3 gas that was responsible for the accretion of the other classes of chondrites.

Possible Enrichment of Volatile Elements in Inner Part of Component 1 Dust Cloud

Volatile elements may have become irregularly distributed in part of the early solar system prior to accretion as the result of heating in the early sun. Dispersed low temperature component 1 materials, enclosing and presumably collapsing into the region of component 2 chondrule and metal formation, would presumably have lost their volatile elements upon approaching the region of chondrule formation. The volatile elements then might have been precipitated, and reprecipitated, as part of a cyclic process in part of the dust cloud that adjoined the protosun. The postulated region of enrichment may have included H₂O generated during chondrule and metal formation; ammonia, methane, and water originally held as ices in the dust; and volatile elements in the component 1 dust having melting points less than 100°C (such as Rb, K, and Na). An irregular distribution of volatile elements in the inner part of the inferred component 1 dust cloud may have been

the cause of enrichment of the volatile-poor chondrites in Rb, K, Na, Li, Ba, and Sr with respect to the carbonaceous chondrites (Tables 4, 5, and 6).

Rb abundances appear to differ between chondrules and bulk chondrite. Murthy and Compston (1965) found dispersions in the Rb-Sr ratios of chondrules relative to bulk meteorite in the Peace River hypersthene chondrite (Fig. 21). The bulk meteorite displayed Rb-Sr ratios similar to ratios for bulk carbonaceous chondrite, carbonaceous achondrite, and pigeonite chondrite. One Peace River chondrule was found to be deficient in the volatile element Rb, and three chondrules were found to be enriched in Rb. A possible explanation may be that one pre-accretionary component 2 chondrule, and three accretionary component 3 chondrules were analyzed. Component 2 chondrules, presumably formed in a high temperature, high pressure region, might be expected to be deficient in Rb. In contrast, accretionary component 3 chondrules, formed in a low pressure, low temperature region, could possibly trap Rb in glassy phases of the aggregates and in mechanically included Rb-enriched component 1 matrix materials at the time of aggregation, and retain some of the Rb during equilibration. Work on a variety of chondrules and chondrites is needed.

Evidence for a Common Parent Material

Elemental Abundances in Carbonaceous Meteorites and the Solar Photosphere

Ringwood (1966, Fig. 1) has shown that the composition of the carbonaceous achondrites (Type I of Wiik, 1956) is similar to the

Fig. 21.--Rb-Sr values for the Peace River hypersthene chondrite, for four of its chondrules, and for carbonaceous and pigeonite meteorites.

The four Peace River chondrules that were analyzed by Murthy and Compston (1965, Fig. 1) are reported to have shown radiating fibrous structures to the naked eye, were spheroidal or ellipsoidal, and were easily distinguishable from the fine grained matrix. The scatter shown by the plot was much greater than anticipated by them. From the descriptions of the four chondrules, it cannot be ascertained whether all or only part were pre-accretionary chondrules. Peace River is reported by Murthy and Compston as a metamorphosed hypersthene chondrite. Partially recrystallized accretionary chondrules could be fairly prominent in a fine grained matrix and would be susceptible to sampling.

The two "carbonaceous chondrites" on the left are samples of the Mokoia pigeonite chondrite; the central carbonaceous chondrite is Murray; and the two carbonaceous meteorites on the right are specimens of Orgueil carbonaceous achondrite.

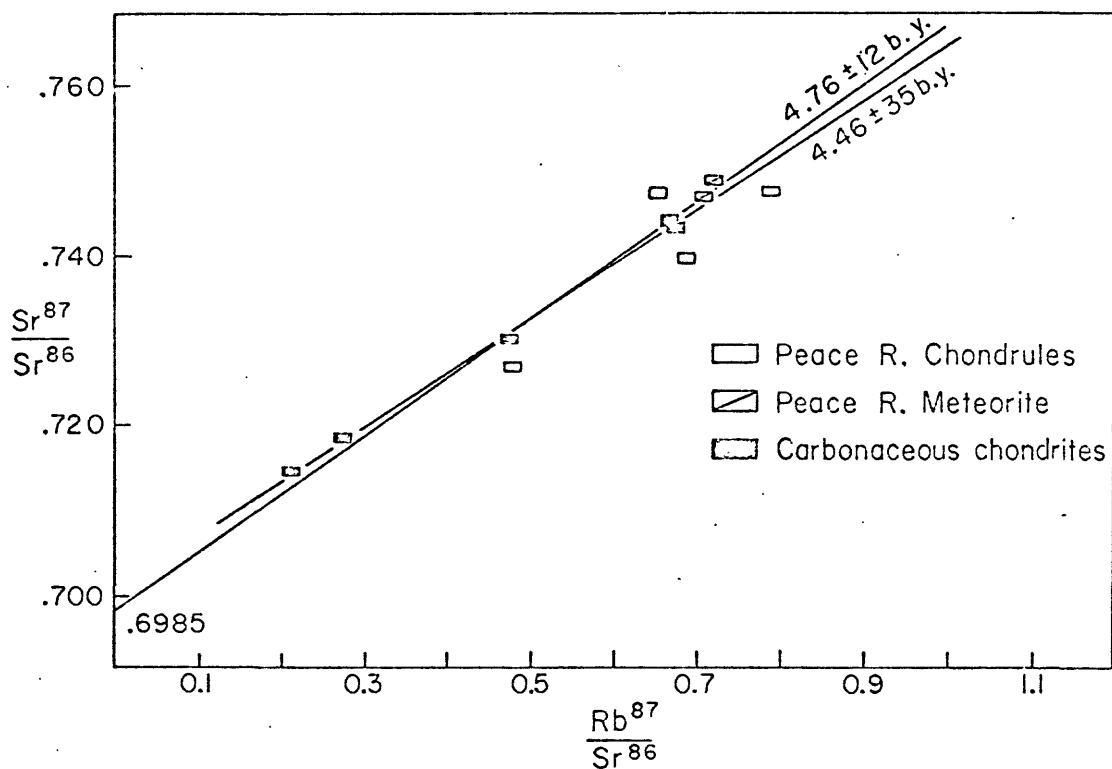


Fig. 21.--Rb-Sr values for the Peace River hypersthene chondrite, for four of its chondrules, and for carbonaceous and pigeonite meteorites.

composition of the solar photosphere. This implies that the sun could have been derived from the elements that make up the carbonaceous meteorites, or that the materials of these meteorites could have been derived from the sun. The general coincidence in elemental abundances would also seem to suggest that the composition of the sun has not changed appreciably as the result of nucleosynthetic processes since the formation of these meteorites. Because the carbonaceous achondrites, of all the meteorites, most closely resemble the solar photosphere in elemental abundance, it would seem to be logical to consider them to be the most primitive of the meteorites, and to assume, therefore, that they represent the starting solid materials in the evolution of the planets and asteroids. The next most elementally primitive meteorites thus would appear to be the carbonaceous chondrites (Type II), which show depletions in volatile elements relative to the carbonaceous achondrites (Tables 3 and 4). Where elemental data were lacking for the carbonaceous achondrites, Ringwood (1966, Fig. 1) used data from the carbonaceous chondrites in demonstrating the elemental similarities between the volatile-rich carbonaceous meteorites and the solar photosphere.

Paragenetic and textural evidence in the carbonaceous chondrites (Type II) indicate, however, that the carbonaceous chondrites cannot be directly derived from carbonaceous achondrite material. Rather, the reverse process seems much more likely because the Tonk carbonaceous achondrite is reported to contain 0.40 weight percent nickel-iron (W.A.K. Christie in Wiik, 1956), and the presence of olivine in the Orgueil carbonaceous achondrite has recently been confirmed

(Kerridge, 1968). The presence of metal (component 2) and olivine (component 2 or 3) in the carbonaceous achondrites can be explained if the carbonaceous achondrites are derived from carbonaceous chondrite material. The greater content of volatile elements in the carbonaceous achondrites may simply be the result of chloritization, in a volatile-rich environment, of the anhydrous magnesium silicates of carbonaceous chondrite material. Chloritization could possibly occur, for example, within a small volatile-rich body.

On paragenetic and textural grounds, the carbonaceous chondrites (Type II) may be considered to be partly devolatilized or dehydrated, but otherwise unmetamorphosed, primitive accretionary materials. In contrast, the carbonaceous achondrites (Type I) may be considered to be chloritized carbonaceous chondrite materials that retain a more primitive elemental aspect because of chloritization, and because of a former position within a small, volatile-rich primitive body. They may be samples, respectively, of near-surface and interior to near-central materials of comets.

Uniformity of Fe and the Rare Earth Elements in Chondrites

The chondrites display fairly uniform Fe contents (Fig. 1 and Table 4). In the carbonaceous chondrites, nearly all the Fe resides in component 1 matrix material (~ 22 percent Fe in Murray matrix; Fredriksson and Keil, 1964). In the enstatite chondrites nearly all the Fe resides in component 2 metal (Table 3). The fairly uniform Fe contents suggest that a common parent material, such as component 1

material of the carbonaceous chondrites, has given rise to the component 2 and 3 materials of the chondrites.

Rare earth element (REE) abundances in the meteorites are briefly discussed in Chapter 5. It is sufficient to note here that the REE abundances are closely similar for all five classes of chondrites (Schmitt and others, 1963; Fig. 24). The essentially uniform REE contents of the chondrites support the inference drawn from the fairly uniform Fe contents of the chondrites, and the similarity in elemental abundances between the solar photosphere and the volatile-rich carbonaceous meteorites, that a common parent material gave rise to the chondrites.

Evidence for a Genetic Relationship between Components 2 and 3 in the Chondrites

Partition of Fe between metal and silicates. One of Prior's "rules" has long noted that a decrease in the Fe content of the silicates of the chondrites is accompanied by an increase in the content of the nickel-iron. The relationship is strikingly well displayed in Figure 1, which for the pigeonite, hypersthene, bronzite, and enstatite chondrites is principally a plot of Fe in component 2 metal versus Fe in component 3 silicates. The dominance of component 3 silicates in the ordinary chondrites may be seen, for example, in Holbrook (Fig. 18). Once the relationship in Fe content between components 2 and 3 is realized, it can be concluded that the medium which gave rise to component 2 pre-accretionary chondrules and metal, also was the medium (gas) which gave rise to the component 3 accretionary silicates. Furthermore, it becomes necessary to conclude that genetic relationships which were

developed prior to accretion during the formation of component 2 materials were grossly preserved during the accretionary event.

An explanation arises from the foregoing for the low Fe content of the L-group (hypersthene) chondrites (Fig. 1). The low Fe content of the hypersthene chondrites is due to a low average metal content, about 7.4 weight percent nickel-iron versus about 18.4 weight percent nickel-iron in the bronzite chondrites (Mason, 1965; Table 3). The low metal content of the hypersthene chondrites simply may be the result of an accidental loss of some component 2 metal during the transport of component 2 materials to the sites of accretion.

The scatter in Fe contents of the enstatite chondrites (Fig. 1) also appears to be explained as the result of differences in the amounts of component 2 metal incorporated at the time of accretion. Because metal is pre-accretionary (component 2), and the silicates of the volatile-poor chondrites appear to be dominantly accretionary (component 3), the differences in metal contents within and between chondrite classes are not explainable as the result of differences in in situ reductions in the parent bodies after accretion.

Prior's rule does not strictly hold for the carbonaceous chondrites because the Fe resides almost entirely in component 1 matrix materials, and the component 3 silicates are essentially iron-free, as in the enstatite chondrites. However, the carbonaceous chondrites contain grains of component 2 silicates that show widely diverse Fe contents, which suggests that the component 2 grains and chondrules were derived from a broad source of component 2 materials.

The fairly uniform Fe content of the chondrites; the presence of minor but compositionally diverse component 2 silicates in the carbonaceous chondrites; and the iron-free component 3 silicates of the carbonaceous chondrites, which indicate a source medium that had been stripped of its Fe as in the enstatite chondrites, are considered evidence that the carbonaceous chondrites formed as the result of the same general process and at the same general time as the other classes of chondrites. The compositional, textural, and paragenetic data and interrelationships are interpreted to reflect that accretion occurred across the solar system as the result of a single, essentially instantaneous event.

Model for Accretion of Chondrites and Formation of Parent Bodies

An eddy of primordial "dust", perhaps derived from a nucleosynthetic event in a supernova that may have occurred about 60 m.y. before accretion (inferred from Xe data of Merrihue, 1966), is assumed to be the parent material of the solar system and is identified with component 1 materials. The dust is inferred to have coalesced into a central condensation, enclosed by a disc of dispersed component 1 materials that continued to spiral-in toward the central condensation. Heating in the nucleus accompanying contraction led to the formation of the protosun. Component 2 chondrules and metal are inferred to have been generated in the outer part of the protosun and temporarily stored in an adjacent ring of chondrule and metal particles. From the diagram of Wood (Fig. 19), temperatures in the region of chondrule formation

were on the order of 1800° to 2000°K , and total pressures were about 10^2 to 10^3 atm.

The inferred ring of component 2 materials presumably increased in mass with the addition of Fe and silicates from in-falling component 1 dust, and Fe and silicates lost from inward-lying solar gas. Rotation of the ring increased with inferred contraction of the protosun and with accompanying contraction of the component 2 ring. At some stage, the rotational angular momentum of the ring may have sufficiently exceeded that of the inward-lying gas so that an unstable situation developed. At this time the chondrule-metal ring, which is assumed to have become debris-choked and dense relative to inward-lying solar gas that had been partly to largely stripped of its Fe, may have begun to creep or slip forward along the chondrule/gas discontinuity, possibly leading to a physical inhomogeneity in the ring and to a rupture. The rupture in turn is inferred to have led to the shedding, together, from the protosun of component 2 materials and component 3 gas, perhaps as a large flap-like, compound filament. Accretion across the solar system is inferred to have occurred along the leading edge of the component 3 part of the filament, with the development to the side of the filament of eddies of accretionary debris, eddies to which direct rotations and angular momentum had been imparted. The primary eddies are inferred to have coalesced into planetesimals, and following dissipation of the filament, eddies of planetesimals and accretionary debris presumably coalesced into planetary eddies, and planets. A number of planetesimal-size bodies may have been lost from the upper and lower edges of the

outer parts of the disc to form the solar system's inferred outlying cometary cloud.

In the foregoing situation accretionary materials in the inner part of the solar system would have been rich in component 2 metal and chondrules, which would give rise to the dense inner planets. In the inner part of the solar system precipitation of component 3 silicates may have been principally from solar gas that had been stripped of its Fe, as in the enstatite chondrites, and component 3 gas pressures may have been high enough to result in the precipitation of pyroxene rather than olivine, again as in the enstatite chondrites. The region of the asteroids, beyond the region of formation of the enstatite chondrites, apparently was the region in which component 2 materials decreased appreciably in abundance, and in which genetically related component 3 gas derived from the protosun had been incompletely stripped of its Fe. Beyond the asteroids, the genetic relationship between component 2 and component 3 materials appears to have been lost, and accretion probably occurred in the manner seen in the carbonaceous chondrites, in which the accretionary mix consists principally of component 1 materials, subordinate component 3 silicates derived from solar gas stripped of Fe, and trace amounts of compositionally diverse component 2 materials.

The recognition of metal as a pre-accretionary material that can be formed as a consequence of early heating in protosolar systems may be a critical feature in the development of solar systems about new suns. The key to solar system formation may very well be the generation and loss of a ring of refractory materials, and inward-lying gas, from a

rotating protosun, with transfer of rotational angular momentum from the protosun to the planetary materials.

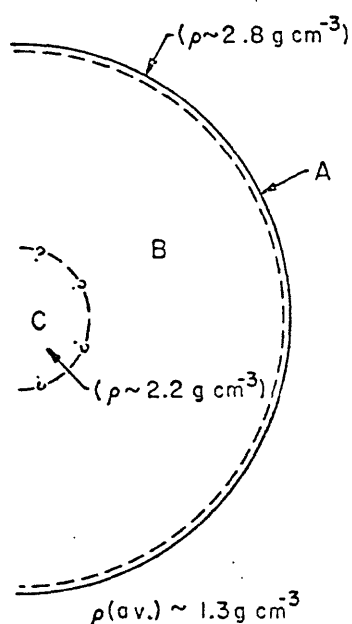
During formation of the planets, primitive atmospheres must have developed as volatiles were lost from volatile-rich matrix materials of the chondrites. The atmospheres must have been fairly extensive, and may have become largely frozen if the sun had not yet evolved to its high temperature stage. Within the largely devolatilized central parts of the early planets, metal became stripped from chondritic materials and metallic cores were formed. As a consequence of metamorphism and fractionation of metal from chondritic materials, nickel, gallium, and germanium in component 1 matrix materials were scavenged by the component 2 metal, giving rise to the nickel abundances and the Ga-Ge groups that are observed in the iron meteorites. Sulfides of component 1 materials probably gave rise to the troilite of the chondrites, pallasites, and irons.

Core formation, accompanied by an increase in rotation, may have been responsible for the formation of planetary satellites by fission, a method of formation of the moon suggested most recently by Wise (1963). A fission origin for the moon is attractive because it would allow for the fractionation of metal from chondritic parent materials prior to fission, and this loss could account for the moon's low average density. The principal objection to a fission origin for the moon is the lack of energy and angular momentum in the present earth-moon system (Wise, 1963, Table 1). To account for this lack, fission may have occurred prior to the high temperature stage of the sun, when the earth presumably would have been surrounded by an extensive frozen primitive

atmosphere. Fission of the moon, or of terrestrial materials that coalesced to form the moon, into such an atmosphere then could have resulted in transfer of angular momentum and energy to the atmosphere, which in turn would be lost with dissipation of the atmosphere when the sun attained its high temperature stage. The formation of planetary satellites, and rings in the case of Saturn, then may be the result of a situation that is similar to that which is proposed for primary accretion in the solar system, -- in which a parent body sheds part of its mass due to rotational instability into enclosing low temperature materials. Planetary satellites may be the result of the fission of discrete satellites, but they also may be the result of the fission of fragments of materials that coalesced during a second stage of cold accretion, a process that needs to be studied further.

Character of Parent Bodies for the Chondritic Meteorites

The inferred structure of small cometary bodies that formed beyond the zone of high component 2 metal content (inner planets and asteroids) is shown in Figure 22. Carbonaceous chondrites may be the partly dehydrated, or ablated, crustal and near-surface materials of comets. Carbonaceous achondrites may be metamorphosed or chloritized, hydrated carbonaceous chondrite materials that occur as dispersed materials in the volatile-rich icy bodies of comets, and that make up cometary cores which possibly have lost most of their free volatiles. The near-solar abundances of elements in the carbonaceous achondrites (Ringwood, 1966, Fig. 1) perhaps may be attributed to a former intimate association with primitive volatile-rich accretionary materials, and to



- A. Carbonaceous chondrite (Type II).
Ablated crustal and near-crustal material;
partly devolatilized but essentially unmetamorphosed.
- B. Icy conglomerate.
Primordial accretionary material. Hydration of
disseminated pre-accretionary and accretionary
olivine and pyroxene increases toward center.
- C. Carbonaceous achondrite (Type I).
Magnesium silicates are essentially all hydrated;
sulfur is in sulfates.

Fig. 22.--Schematic model of a carbonaceous meteorite (cometary) parent body.

the development of hydrated silicates from anhydrous component 3 olivine and pyroxene in which near-solar abundances of elements could be retained.

The inferred structure of parent bodies for the volatile-poor chondrites is shown in Figure 23. Fall data are mainly for materials that are correlated with the inferred hypersthene and bronzite chondrite parent bodies (Tables 1 and 2), and because of this the schematic model most closely approximates a compound hypersthene-bronzite body. Fall data, and correlations in Table 2, suggest that the earth is mainly sampling parts of three small asteroidal bodies. The parent body or bodies for the metal-poor pigeonite chondrites probably possess only small cores, and thus pigeonite body core materials may not have been sampled. Furthermore, the pigeonite chondrites exhibit large differences in accretionary textures, and for this reason the pigeonite chondrite class may include near-surface samples that have been derived from several small, outlying asteroidal bodies.

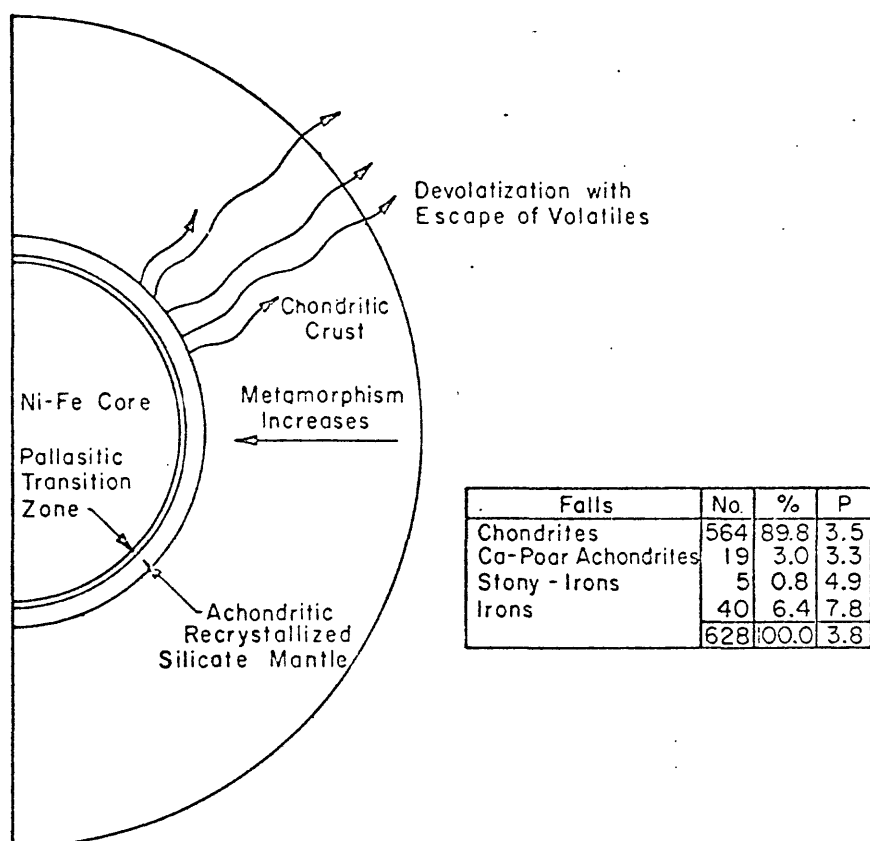


Fig. 23.--Schematic model of a volatile-poor chondrite (asteroidal) parent body.

Proportions calculated from fall data (Hey, 1966; see Table 1). For density data see Wood (1963a).

CHAPTER 5

CALCIUM-RICH ACHONDRITES

Pyroxene-plagioclase Achondrites

The pyroxene-plagioclase achondrites are the most abundant of the achondritic meteorites (Table 1). They include all but three meteorites of the calcium-rich or basaltic achondrite group of Urey and Craig (1953). The character and classification of the pyroxene-plagioclase achondrites have been reviewed and described by Mason (1962a, 1967b), Duke (1963), and Duke and Silver (1967).

Two classes of pyroxene-plagioclase achondrites are recognized, the howardites and eucrites. The howardites are characterized by hypersthene and anorthite (Mason, 1962a) and are polymict breccias (Duke and Silver, 1967); the eucrites consist mainly of pigeonite and anorthite and are mainly monomict breccias. Their chemical compositions are summarized in Table 3.

Duke and Silver (1967) conclude that the principal mineralogical and textural properties of the eucrites and howardites are due to magmatic crystallization, followed by complex fragmentation and recrystallization episodes. Duke (1964) has proposed that the pyroxene-plagioclase achondrites have been derived from the moon. Duke and Silver (1967) review the permissive argument for the lunar origin of howardites and eucrites, and suggest that on the basis of relative iron content, or lightness and darkness of color, and on the basis of

relative degree of brecciation, that the lunar uplands may be of howardite composition and that the maria may be of eucrite composition.

Alpha-scatter analyses of lunar maria and uplands materials obtained during Surveyor Spacecraft Missions V, VI, and VII have revealed that the lunar surface has a composition very similar to that of the pyroxene-plagioclase achondrites (Table 17) and unlike that of the other classes of stony meteorites. The compositional similarity supports the proposal for a lunar origin for the eucrites and howardites. Support also is found in their terrestrial mantle abundances of the rare earth elements, their low values of remanent magnetism, and reflectance characteristics that accompany brecciation, topics which are discussed in other sections of this chapter.

Diopside-olivine and Augite Achondrites

Two diopside-olivine achondrites (Nakhla and Lafayette) and one augite achondrite (Angra dos Reis) are known. Nakhla and Angra dos Reis are falls. Lafayette was found in the Purdue University Museum by O.C. Farrington in 1931 (Mason, 1962a). Lafayette displays an extremely fresh fusion crust, and there is some speculation that it may be a specimen from the Nakhla, Egypt, fall of 1911, which somehow found its way to this country (C.B. Moore, personal communication, 1967). If so, then only two calcium-rich achondrites, both falls, exist that do not belong to the pyroxene-plagioclase class of meteorites (Table 1).

Compositions of the diopside-olivine and augite achondrites are given in Tables 3 and 4. Compositional relations to other achondrites in respect to CaO and $\text{FeO}/\text{FeO}+\text{MgO}$ are shown in Figure 3. Nakhla is

Table 17.--Elemental abundances (atomic percent) for lunar mare and uplands materials, and for calcium-rich achondrites.

Element	Surveyor Spacecraft					
	$V_{1,2}/$ Mare	$VI_{2,2}/$ Sinus Medii	$VII_{2,2}/$ Tycho rim	Pyroxene-plagioclase ^{3/}		Augite ^{3/} (Angra)
	Tranquillitatis			Howardite	Eucrite	Diopside- olivine (Nakhlite)
Si	18.5 ^{±3}	22 ^{±2}	18 ^{±4}	18.3	17.8	18.8
Mg	3 ^{±3}	3 ^{±3}	4 ^{±3}	6.5	4.7	6.9
Fe	} 13 ^{±3}	5 ^{±2}	2 ^{±1}	5.5 ^{4/}	5.3 ^{4/}	6.7 ^{4/}
Ca		6 ^{±2}	6 ^{±2}	3.1	4.1	6.3
Al	6.5 ^{±2}	6.5 ^{±2}	8 ^{±2}	4.4	5.7	0.8
Na	2	2	3	0.8	0.3	0.3
C	3	2	2	--	--	--
O	58 ^{±5}	57 ^{±5}	58 ^{±5}	59.5	59.9	59.7
						58.8

1/. Turkevich and others (1967).

2/. Turkevich (1968).

3/. Calculated from data in table 3.

4/. Fe in metal not included.

described by Prior (1912), and Mason (1962a) reviews the characteristics of the diopside-olivine and augite achondrites. Their contents of the rare earth elements (REE) are shown in Figure 24. The remanent moment of Lafayette is discussed in the section on remanent magnetism.

Rare Earth Elements and Oxygen Isotopes in Stony Meteorites and Terrestrial Materials

Uniformity of REE in Chondrites

The rare earth elements (REE) are lithophile, and appear to migrate chemically as a group (Goldschmidt, 1954). Because they are a long series of chemically similar elements, changes in their abundance across the series may be interpreted with a minimum of assumptions regarding the selective fractionation of individual elements. The average values for the REE are closely similar for all classes of chondrites (Schmitt and others, 1963); the average values for twelve chondrites, which include members of the five chondrites classes, are shown in Figure 24. The similarity of REE abundances in the chondrites indicates that a rather uniform REE abundance existed at the time of accretion in the regions of formation of the volatile-rich and volatile-poor chondrites. The REE abundances, and the slope of the plotted abundances of the chondrites (Fig. 24) can be considered to be primitive. They serve as references for evaluating differences in abundances and abundance slopes in the achondritic meteorites, which may be interpreted, at least in part, to be the results of fractionations in parent bodies.

Fig. 24.--Absolute rare earth abundances for stony meteorites and for selected terrestrial materials.

a. REE abundances of the calcium-rich achondrites and eclogite with respect to the chondrites and calcium-poor achondrites.

Explanation:

- A Angra dos Reis (Schnetzler and Philpotts, 1967).
- Eu Average of Nuevo Laredo and Pasamonte eucrites (Schmitt and others, 1963).
- Ec Roberts Victor mine eclogite (Schmitt and others, 1963).
- N Average of Nakhla and Lafayette diopside-olivine achondrites (Schmitt and Smith, 1963).
- Ho Bununu howardite (Philpotts and others, 1967).
- Sm Serra de Magé eucrite (95 percent feldspar; Philpotts and Schnetzler, 1967).
- Ch Average of twelve chondrites (includes one carbonaceous chondrite; Schmitt and others, 1963).
- Calcium-poor achondrites (Schmitt and others, 1963).
 - En - Norton County (enstatite)
 - Hj - Johnstown (hypersthene)
 - Hs - Shalka (hypersthene)

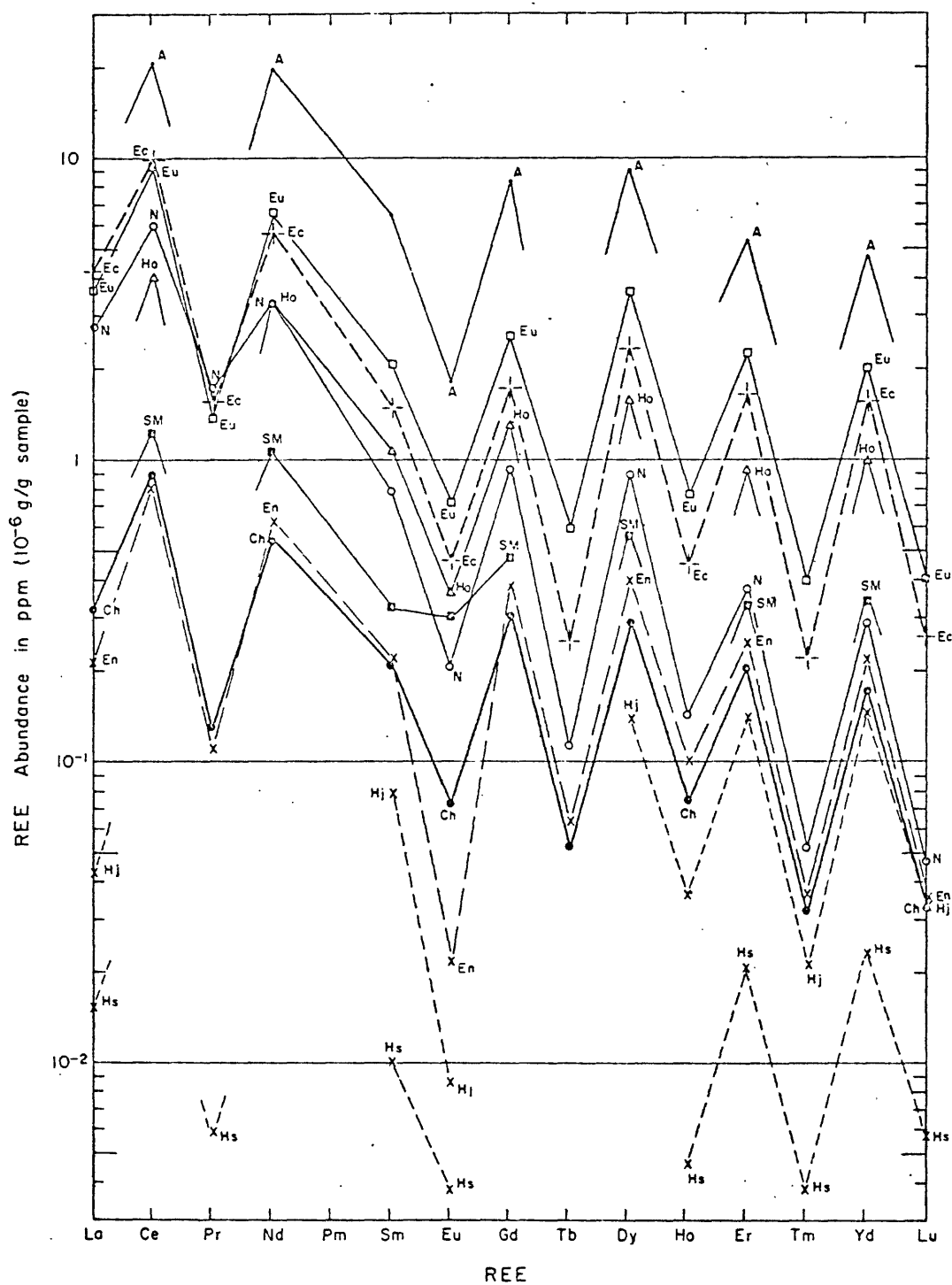


Fig. 24a.--REE abundances of the calcium-rich achondrites and eclogite plotted with respect to the chondrites and calcium-poor achondrites.

Fig. 24b.--REE abundances of the calcium-rich achondrites with respect to various terrestrial mantle materials and chondrites.

Explanation:

- K Kilauea Iki basalt (Schmitt and others, 1963).
- R Average of three Atlantic Ridge basalts (Frey and Haskin, 1964).
- P Wesselton Mine peridotite (Schmitt and others, 1963).
- A Angra dos Reis (Schnetzler and Philpotts, 1967).
- Eu Average of Nuevo Laredo and Pasamonte eucrites (Schmitt and others, 1963).
- Ho Bununu howardite (Philpotts and others, 1967).
- N Average of Nakhla and Lafayette diopside-olivine achondrites (Schmitt and Smith, 1963).
- Ch Average of twelve chondrites (includes one carbonaceous chondrite; Schmitt and others, 1963).

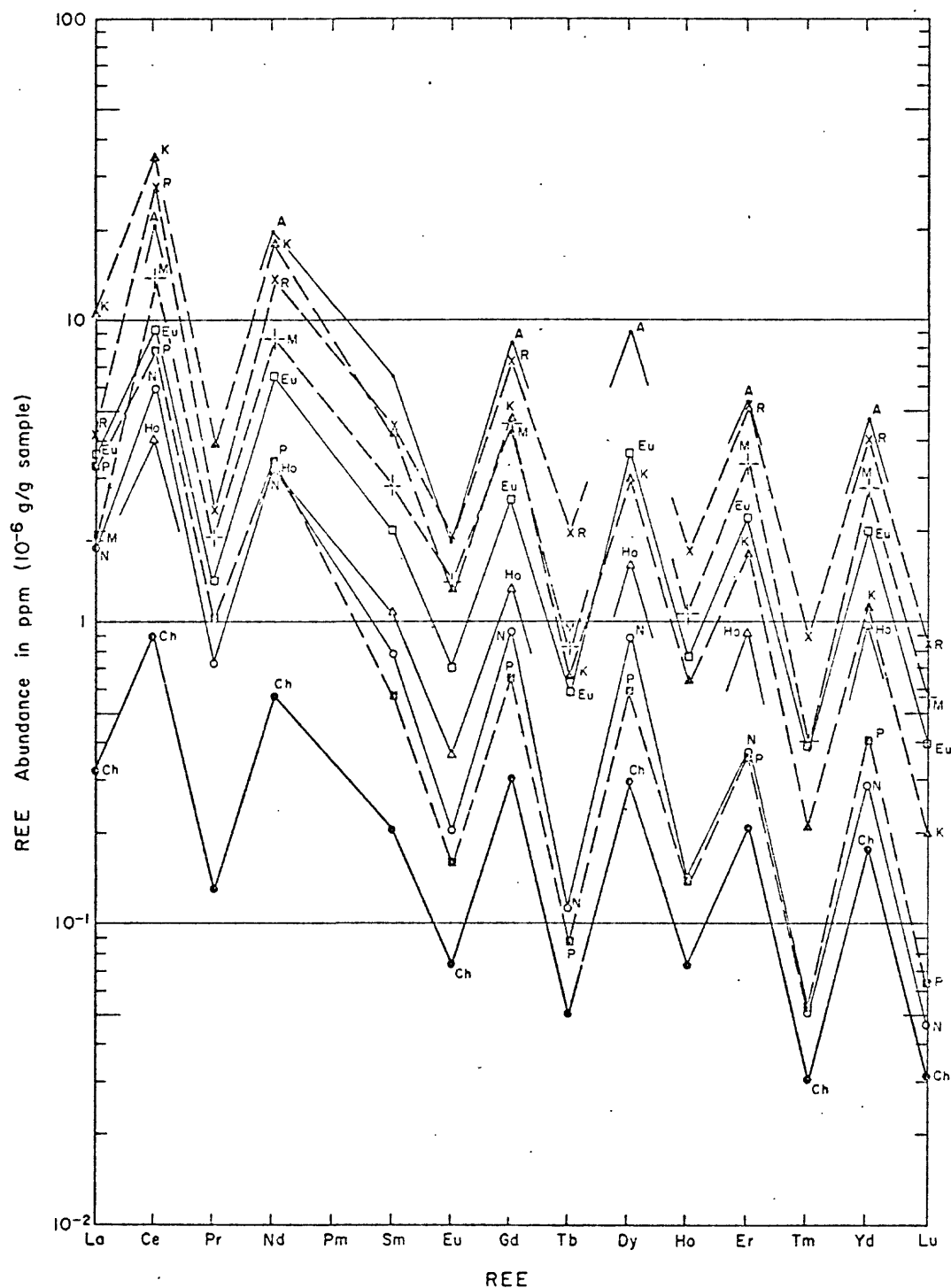


Fig. 24b.--REE abundances of the calcium-rich achondrites plotted with respect to various terrestrial mantle materials and chondrites.

Fig. 24c.--REE abundances of mesosiderite and tektite material plotted with respect to chondrites, howardites, and eucrites.

Explanation:

- T Ivory Coast tektite, composite of ten tektites (Schnetzler and others, 1967).
- M Estherville mesosiderite (Schmitt and others, 1963).
- Eu Average of Nuevo Laredo and Pasamonte eucrites (Schmitt and others, 1963).
- Ho Bununu howardite (Philpotts and others, 1967).
- Ch Average of twelve chondrites (includes one carbonaceous chondrite; Schmitt and others, 1963).

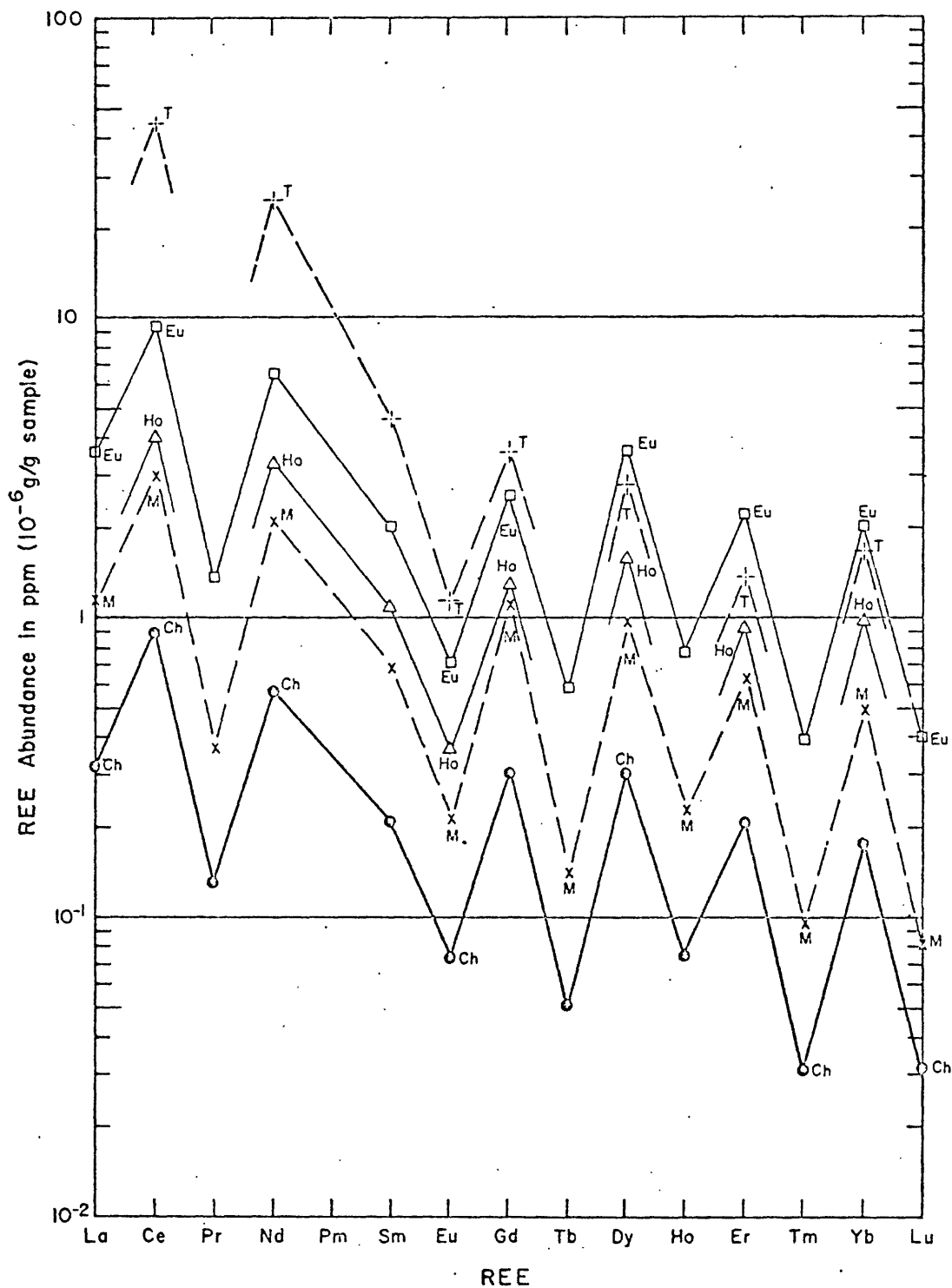


Fig. 24c.--REE abundances of mesosiderite and tektite material plotted with respect to chondrites, howardites, and eucrites.

Calcium-poor and Calcium-rich Achondrites

REE contents. Calcium-poor achondrites have REE abundances similar to or markedly less than the chondrites. The enstatite achondrite, Norton County (Fig. 24a), has an REE abundance very similar to that of the chondrites, but there appears to be some small enrichment in the heavy REE and depletion in the light REE. The hypersthene achondrites, Johnstown and Shalka, show moderate to strong depletions in the REE relative to the chondrites. In contrast, the calcium-rich achondrites are substantially richer in REE than the chondrites. One howardite and two eucrites display relatively high values that have chondrite-like abundance slopes. The relatively low REE content of the Serra de Magé eucrite (Fig. 24a), which is dominantly plagioclase feldspar, suggests that much of the REE of the pyroxene-plagioclase achondrites resides in the pyroxene. There thus appears to be a significant difference in REE contents in the pyroxene of the calcium-poor and the calcium-rich achondrites.

Oxygen isotope ratios. In REE content, the calcium-poor achondrites lie much closer to the chondrites than to the calcium-rich achondrites. However, on the basis of oxygen isotope ratios in pyroxene, the hypersthene achondrites and the pyroxene-plagioclase achondrites are closely similar (Taylor and others, 1965, Fig. 3). Because of this similarity they have been grouped together and have been considered by Taylor and others (1965) to be genetically related. Independent support for the grouping appears to exist because accessory plagioclase feldspar in five hypersthene achondrites (Ang5; Mason, 1963d) is compositionally similar to the feldspar of the

pyroxene-plagioclase achondrites. Taylor and others (1965) tentatively conclude on the basis of similarities of $^{18}\text{O}/^{16}\text{O}$ in pyroxene and plagioclase that the pyroxene-plagioclase achondrites and the hypersthene achondrites exhibit a close genetic relationship, and that the isotopic data are compatible with a hypothesis that these meteorites have arisen through magmatic differentiation from a common parent material. However, the data of Taylor and others (1965) also show that $^{18}\text{O}/^{16}\text{O}$ fractionation apparently has occurred within the eucrites. The Shergotty eucrite shows an $^{18}\text{O}/^{16}\text{O}$ ratio that is similar to that of the ordinary chondrites. Furthermore, the data of Taylor and others show that pyroxene from the Steinbach siderophyre and pyroxene from the calcium-poor Bondoc Peninsula mesosiderite are also essentially identical in $^{18}\text{O}/^{16}\text{O}$ to the pyroxene of the hypersthene achondrites and the pyroxene-plagioclase achondrites. In light of correlations discussed in Chapter 3 (Table 7) and outlined in Figure 2; in light of large differences in REE abundances between the calcium-poor and calcium-rich achondrites; and because the oxygen isotope groups outlined by Taylor and others (1965) cannot be interpreted in an internally consistent and unique manner regarding their origin, it is suggested that similarities in $^{18}\text{O}/^{16}\text{O}$ ratios do not necessarily reflect genetic associations in the meteorites. Fractionation of ^{18}O can and does occur as the result of magmatic processes. Taylor and Epstein (1963) report finding appreciable $^{18}\text{O}/^{16}\text{O}$ variations in the very latest stages of crystallization of the Skaergaard intrusion. Thus, fractionation is a process that can occur in different bodies. It is suggested that the hypersthene achondrites, Bondoc Peninsula pyroxene, and pyroxene of the siderophyre meteorite,

are products of fractionation and recrystallization of parent hypersthene chondrite material, following the correlation of Table 2, during which some of the REE and ^{180}O were lost from the system.

Meteorites and Terrestrial Mantle Materials

The REE values for two eucrites and one howardite bracket the values for eclogite from South Africa (Fig. 24a). Other materials that originated in the mantle (Fig. 24b) have REE values that are similar to or greater than those of the pyroxene-plagioclase achondrites. Atlantic Ridge basalt and experimental Mohole basalt display chondritic abundance slopes. Kilauea Iki basalt shows enrichment in light REE and depletion in heavy REE relative to a chondritic abundance slope. The apparent fractionation may have occurred during storage of the basalt in a magma chamber at a depth of about 39 kilometers prior to eruption (see Eaton and Murata, 1960; and Richter and Eaton, 1960, for a description of the event). Wesselton Mine peridotite also shows apparent fractionation, -- enrichment in light REE and depletion in heavy REE, relative to a chondrite abundance slope. The peridotite, even where greatly depleted in REE, displays abundances that are greater than those in the chondrites. The apparent fractionation of the REE in Kilauea Iki basalt and the peridotite is antithetic to the apparent fractionation in the calcium-poor achondrites. Enrichment of the light REE and depletion of the heavy REE in mantle materials may be the result of differentiation. In the calcium-poor achondrites, general depletion of the REE with selective depletion of the lighter REE may be the result of in situ recrystallization of chondritic silicates.

The REE plots shown in Figures 24a and 24b show that the calcium-rich achondrites in general, and that the pyroxene-plagioclase achondrites in particular, are closely similar to terrestrial mantle materials in REE abundances. The pyroxene-plagioclase achondrites, augite achondrite, and eclogite appear to display a fairly primitive REE abundance slope, whereas the diopside-olivine achondrites appear to be fractionated in a manner similar to terrestrial peridotite.

The calcium-rich mesosiderites, which are discussed in the chapter that deals with breccias, appear to be mechanical mixtures of calcium-poor and calcium-rich meteoritic materials. They display unfractionated REE values that are intermediate between the chondrites and the calcium-rich achondrites (Fig. 24c). Tektite glass, which may be lunar in origin, displays abundances similar to the pyroxene-plagioclase achondrites in the heavier REE, but shows strong enrichment in the light REE. The enrichment may be the result of the process that led to formation of the tektites.

Reflectance Characteristics of Stony Meteorites and the Moon

The optical properties of the moon have been explained principally in terms of the optical characteristics of powdered materials. Deductions from the moon's thermal properties (Wesselink, 1948), deductions from its optical properties (Dollfus, 1962; Hapke and Van Horn, 1963; Hapke, 1966), and Surveyor photographs (for example, see Shoemaker and others, 1967), strongly suggest that at least a thin layer of powder exists at the moon's surface. Optical investigations on powders by Hapke (1968) have shown that materials at the lunar surface apparently

are silicates that contain significant amounts of lattice iron; the silicates are similar compositionally to terrestrial ferro-basalts (and to the pyroxene-plagioclase achondrites) and are materials that appear to have been modified by proton irradiation. As shown by Hapke (1968, Fig. 1), irradiation decreases the intensity of reflection, increases positive polarization, and reddens the spectrum of olivine basalt powders, and he has shown that such powders display a striking fit to intensity, polarization, and spectrum characteristics of the moon.

The general fit described by Hapke, however, does not explain differences in reflectance of materials in different lunar geologic environments, in particular the reason why intrinsically dark lunar mare materials become lighter colored where they presumably are brecciated and reside in crater wall, rim, and ray materials. Also not fully explained is the reason for the apparent loss of reflectance with the passage of time where the materials do not reside in steep slopes.

The reflectance characteristics of stony meteorites have been investigated by Elston and Holt (1967; in preparation). The rocks studied included carbonaceous, pigeonite, and hypersthene chondrites; and hypersthene, enstatite, pyroxene-plagioclase, and diopside-olivine achondrites. Reflectance characteristics were measured on fresh surfaces; on disaggregated material in the $<1 \text{ mm} - >300 \text{ mesh}$ range, and on finely ground powders ($<300 \text{ mesh}$). Only one class of meteorites, the pyroxene-plagioclase achondrites, display reflectance characteristics that parallel those observed in inferred lunar breccias.

Increased reflectance is developed in the pyroxene-plagioclase achondrites with brecciation, and the increase is due to the development

of milky in the abundant plagioclase that characterizes this class of meteorites (Fig. 25a-h). Where unbrecciated, the plagioclase is clear and cleavage-free; where partly brecciated, some of the feldspar is milky and some is clear. The highest reflectance occurs where the rock is coarsely brecciated and where large fragments of milky plagioclase are preserved in a comminuted groundmass. Where finely brecciated the reflectance decreases to about the level of that measured in partly brecciated material. Furthermore, disaggregation of the high albedo materials from their parent rock results in a marked decrease in reflectance. Disaggregation by micrometeorite bombardment may be partly responsible for the decrease in reflectance of lunar ray and rim materials with the passage of time, and from Hapke's work, a part of the loss in reflectance also may be due to irradiation. On the basis of reflectance characteristics, the pyroxene-plagioclase achondrites are the only meteorites that can be correlated with general and with specific lunar reflectance characteristics.

Remanent Magnetism in Meteorites

The natural remanent magnetic moments (NRM) have been investigated and summarized for the major classes of meteorites (DuBois and Elston, 1967; in preparation). Values of total remanence for the various classes of meteorites are summarized in Table 18. Although demagnetization studies are incomplete, some preliminary results may be summarized:

1. The carbonaceous chondrites appear to have a low remanence.

However, they are capable of obtaining a much higher remanent

Fig. 25.--Development of milkiness in plagioclase of pyroxene-plagioclase achondrites with brecciation.

a, b. Unbrecciated Moore County eucrite; general and detailed views. Note clear, cleavage-free plagioclase (bytownite).

c, d. Moderately brecciated Juvinas eucrite. Note scattered large, milky-white plagioclase grains; pyroxene is dark.

e, f. Well brecciated Sioux County No. 2 eucrite, showing angular composite fragment consisting of milky plagioclase in fault contact with dark pyroxene fragment, and comminuted salt and pepper matrix.

g, h. Highly brecciated Stannern eucrite. Locally displays slickensides in fine breccia, and parallel, sheared, plate-like aggregates of milky plagioclase and pyroxene. Northwest-trending veinlet is intrusive metal; northeast-trending veinlet is glassy material.

Specimens are from the Arizona State University Collection, Tempe, Arizona.

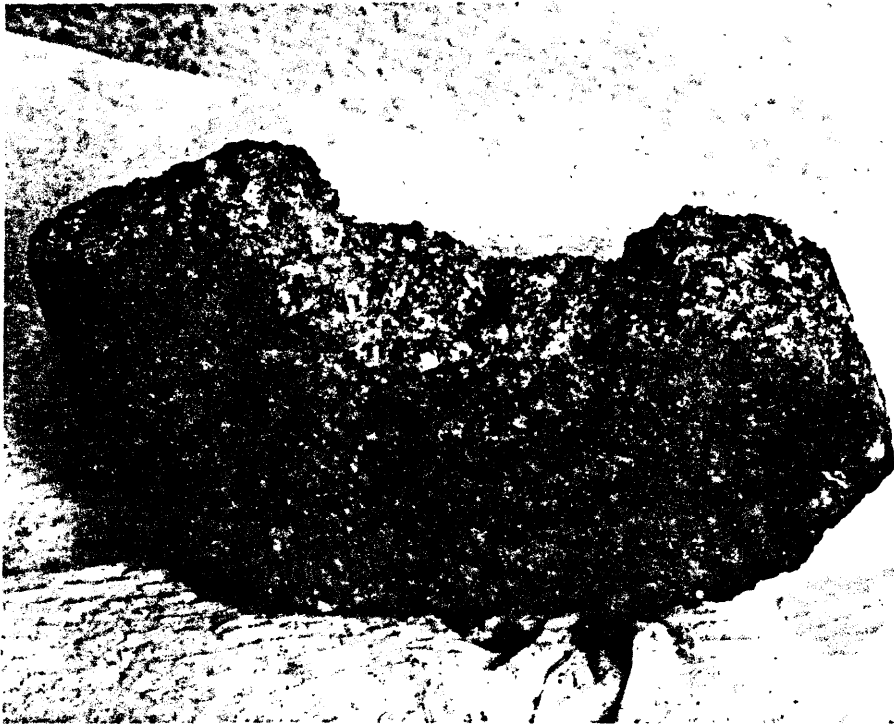


Fig. 25a.--Moore County eucrite, general view.



Fig. 25b.--Moore County eucrite, detailed view.



Fig. 25c.--Juvinas eucrite, general view.



Fig. 25d.--Juvinas eucrite, detailed view.



Fig. 25e.--Sioux County No. 2 eucrite, general view.

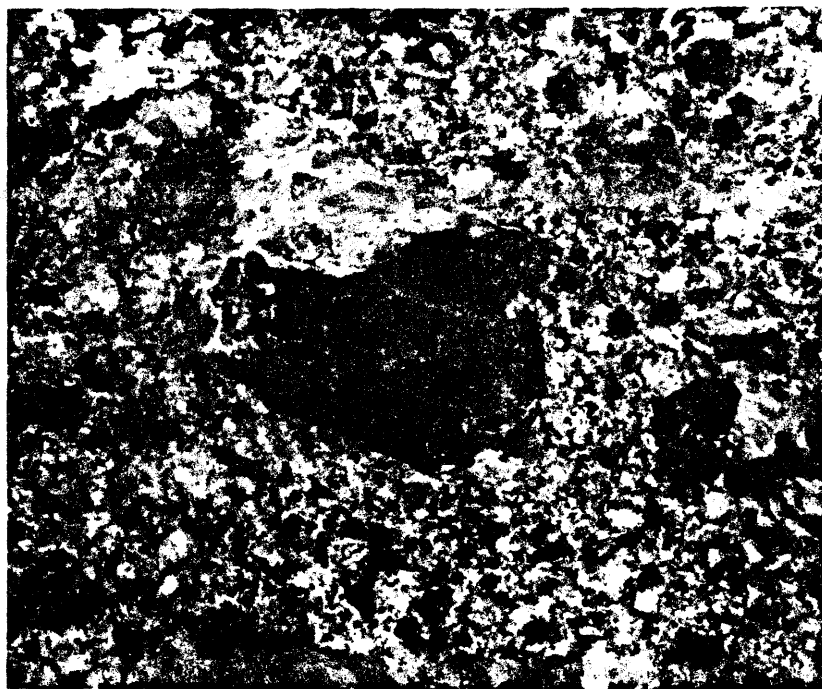


Fig. 25f.--Sioux County No. 2 eucrite, detailed view.



Fig. 25g.--Stannern eucrite, general view.



Fig. 25h.--Stannern eucrite, detailed view.

Table 18.--Values of natural remanence (NRM) for various meteorites and meteorite classes.^{1/}

Class	Number (and name) of meteorites	Natural remanent moment (emu/cm ³)
<u>Calcium-poor meteorites</u>		
Carbonaceous chondrite	1 (Mighei)	1.5×10^{-5}
	1 (Murray) ^{2/}	1.2×10^{-3}
Pigeonite chondrite	1 (Karoonda)	1.3×10^{-4}
	1 (Mokoia)	$\sim 2.5 \times 10^{-4}$
	1 (Mokoia) ^{3/}	3.4×10^{-2}
Hypersthene chondrite	17	9.2×10^{-3}
Hypersthene achondrite	2 (Bondoc pyroxene)	1.6×10^{-3}
	1 (Johnstown)	1.8×10^{-5}
Irons (Ga-Ge group II)	1	1.6×10^{-4}
Bronzite chondrite	12	3.1×10^{-2}
Pallasite (Ga-Ge group III)	1 (Bendock, metal phase)	7.0×10^{-4}
Iron (Ga-Ge group III) (Ga-Ge group IV)	2	4.1×10^{-4}
	1	4.4×10^{-3}
Enstatite achondrite	2	1.6×10^{-5}
Iron (Ga-Ge group I)	10 (Canyon Diablo)	1.16×10^{-2}
	14 (Odessa)	6.6×10^{-3}
<u>Calcium-rich meteorites</u>		
Pyroxene-plagioclase		
Eucrite	15	1.2×10^{-5}
Howardite	1 (Washougal)	8.5×10^{-5}
Diopside-olivine	1 (Lafayette)	1.6×10^{-3}

^{1/}. Adapted from summary table in DuBois and Elston (in preparation).^{2/}. Moment resides principally in the fusion crust.^{3/}. Reason for the high remanence is unknown.

moment following heating in the earth's magnetic field, which suggests that the carbonaceous chondrites may not have been subjected to substantial magnetic fields either during their formation or during storage in their parent bodies, and which is compatible with the concept developed in Chapter 4 that they formed at low temperatures.

2. The pigeonite chondrites, which have the lowest metal contents of the volatile-poor chondrites, appear to have fairly low remanent moments.
3. The hypersthene chondrites, which have metal contents that are intermediate to the pigeonite and the bronzite chondrites, exhibit intermediate values of remanence. The moments in the bronzite and hypersthene chondrites have been shown by Stacey and Lovering (1959) and Stacey and others (1961) to be thermoremanent moments, probably acquired while cooling in the magnetic field of the parent body. The correlation between relative metal contents and strength of moment between the hypersthene and bronzite chondrites may be due simply to the difference in metal contents; additionally, some of the difference may have been due to a stronger magnetic field in the bronzite parent body that may have been the result of a larger fluid metallic conducting core.
4. Ga-Ge group II irons, which are correlated with the hypersthene chondrites, may have lower remanent moments than Ga-Ge group III irons, which are correlated with the bronzite chondrites.

5. The high moments of Ga-Ge group I irons may be matched by relatively high moments in the enstatite chondrites.
6. The pyroxene-plagioclase achondrites show low to very low moments but are capable of acquiring considerably stronger moments if heated and cooled in the earth's magnetic field, which implies that the pyroxene-plagioclase achondrites crystallized in a parent body that was characterized by a weak magnetic field. On the basis of the direction of remanence relative to the plane of crystal layering, Lovering (1959) reports that the Moore County eucrite formed at about 10°N or 10°S magnetic latitude. One of three large (~ 100 km), young lunar ray craters at 10°N or 10°S (Langrenus, Theophilus, or Copernicus), possibly could be the source of the Moore County eucrite, if the pyroxene-plagioclase achondrites are lunar.
7. Pyroxene of the Bondoc Peninsula mesosiderite exhibits a relatively strong remanence that is comparable to the remanence in the hypersthene chondrites. Johnstown, however, has a lower remanence that is comparable to the pyroxene-plagioclase achondrites. It is not known if the remanence of Johnstown is a saturation moment. The low moment of the enstatite achondrites very possibly is a saturation moment in silicate that is essentially iron-free.
8. The diopside-olivine achondrite Lafayette exhibits a fairly strong remanence. The specimen that was measured is unbrecciated, contains no apparent metal, and displays two sawed surfaces and a narrow section of fusion crust. Although

demagnetization studies on fusion crust and interior material have not been made, it may be that most of the remanence resides in the iron-rich silicates of this meteorite.

Nakhla has been found to have a K-Ar age of 1.5 b.y. (Stauffer, 1962), which is young compared to K-Ar ages commonly reported for the pyroxene-plagioclase achondrites (on the order of 3 to 4 b.y.). Because of the apparent lack of brecciation, the nakhlites do not appear to have undergone gas loss due to mechanical causes; it is possible, however, that gas loss due to heating, perhaps during a close approach to the sun, may have occurred. The relatively young age, if valid, and the high remanence, if valid, would suggest that the nakhlites were derived from a parent body that was different than the parent body of the eucrites and howardites.

A possible parent for the nakhlites would be Mars, which because of its size probably is differentiated. From its mean density of about 4 g/cm^3 (Brandt and Hodge, 1964, Table 15.1-2), and as inferred from the volatile-poor chondrites and related materials (Fig. 23), Mars probably has a metallic core. However Mars now has no appreciable magnetic field (Smith and others, 1965), which would suggest that its core is no longer fluid and conducting. When fluid and conducting, the core presumably was responsible for a magnetic field. If Nakhla is martian material, and if the K-Ar age of Nakhla is correct, then Mars (or the parent body of the nakhlites) was undergoing

differentiation about 1.5 b.y. ago, at which time it possessed a magnetic field that may have been adequate to have protected life at the surface.

Summary

The calcium-rich achondrites are differentiated materials that appear to be principally lunar in origin. General composition, trace element characteristics (REE), relatively high abundance, reflectance characteristics, and remanent magnetic characteristics suggest that the pyroxene-plagioclase achondrites are lunar. Magnetic characteristics and age data suggest that the nakhlites may be derived from a different parent body, possibly Mars.

CHAPTER 6

METEORITE BRECCIAS

Monomict and Polymict Breccias

General Descriptions and Definitions of Terms

Many meteorites were mechanically broken prior to their fall on earth. Unbroken fusion crusts enclose disrupted accretionary textures in a large number of chondrites, and enclose disrupted crystallization textures in most achondrites, in some pallasites, and in some irons, attesting to the pre-fall brecciation.

Chondrites. Many chondrites are simple or monomict breccias, breccias that consist of one class of chondritic materials as defined in Table 2. In many chondrites, brecciation is clearly imposed on the accretionary textures and thus post-dates chondrule and chondrite formation. Glassy veins and blackening are common. No evidence is known to link post-accretion brecciation with magmatic processes in the parent bodies of the chondrites. The simplest explanation appears to be that the brecciation was the result of one or more mechanical fragmentation events, impacts or collisions, which ultimately led to the capture of the chondritic materials by the earth. The assumption is supported by relations preserved in several polymict breccias which exhibit mixtures of different classes of meteoritic materials.

Some monomict chondrite breccias exist which have been called polymict breccias, but which here are recognized as accretionary

breccias. Wahl (1952) applied the term polymict to a number of chondrites that display relatively large inclusions which differ texturally from the main chondritic groundmass. One of these "polymict" chondrites, for example, is the unequilibrated chondrite Parnallee, which is classed as an H_1 -2 chondrite in the mineralogic-petrologic classification (Table 9). Parnallee (no. 93a, Arizona State University Collection) displays prominent inclusions of apparent chondritic material that are enclosed by component 1 and 3 materials. Inspection of the "achondritic" inclusions reveals that they are finely granular and they appear to be no more than aggregates of component 3 material that have undergone fragmentation before incorporation in Parnallee. Parnallee thus is considered to be an accretionary breccia, -- a special type of monomict breccia which formed as the result of the aggregation of compositionally similar but texturally diverse materials at the time of accretion. Fracturing accompanying the inferred loss of Parnallee, or other chondrites, from their parent bodies would, as defined here, give rise to monomict chondrite breccias if the fractured materials belong to the same class, or to polymict chondrite breccias if two or more classes of chondritic materials are preserved in the breccia.

The use of the term polymict to describe texturally diverse inclusions in unequilibrated chondrites has continued to the present. Van Schmus (1967) has described the "polymict" structure of the Mezö-Madaras hypersthene chondrite, which is classed as an H_n -2 chondrite in the mineralogic-petrologic classification (Table 9). "Inclusion A" of Van Schmus (1967, Fig. 1) appears to be simply component 1 matrix material that contains disseminated grains of component 3 material. The

component 1 material appears to be traceable laterally into component 1 matrix material that encloses pre-accretionary component 2 and accretionary component 3 chondrules. The "porphyritic" chondrules of Van Schmus (1967) appear to be component 3 accretionary chondrules that contain scattered, relatively large component 2 grains. "Inclusions B and C" of Van Schmus (1967, Fig. 2 and 3) appear to be mainly component 3 accretionary materials that are coarser grained and finer grained, respectively, than "normal" Mezö-Madaras. Van Schmus has shown that compositionally, olivine and pyroxene of inclusions B and C fall within the limits of the hypersthene chondrites. Texturally, Mezö-Madaras is a mixture of materials, which Van Schmus has interpreted to be the result of catastrophic mixing that originated through either impact or volcanic processes. Viewed in light of evidence that is developed in Chapter 4 on the manner of accretion, the texturally diverse component 3 accretionary materials of Mezö-Madaras may be the product of collisions between small masses or bodies of accretionary materials as they were in the process of aggregation during formation of the hypersthene chondrite parent body.

Calcium-poor achondrites. Crystallization textures of the achondrites are, in most cases, highly disrupted (Fig. 25, 26, and 27). Brecciation in the achondrites does not appear to be associated with possible magmatic activity in the meteorite parent bodies. Rather, in a number of cases, small amounts of metal or other foreign materials may be found in the brecciated parts of these meteorites. In Johnstown (Fig. 26), for example, large crystals of hypersthene float in a comminuted matrix of hypersthene. Fine grains and angular fragments of

Fig. 26.--Johnstown hypersthene achondrite (diogenite).

a. Coarsely crystalline hypersthene fragments in a comminuted hypersthene groundmass. Millimeter grid in background.

b. Angular fragment of metal (~ 1 mm) in breccia.

Arizona State University Collection.



Fig. 26a.--Johnstown hypersthene achondrite, general view.

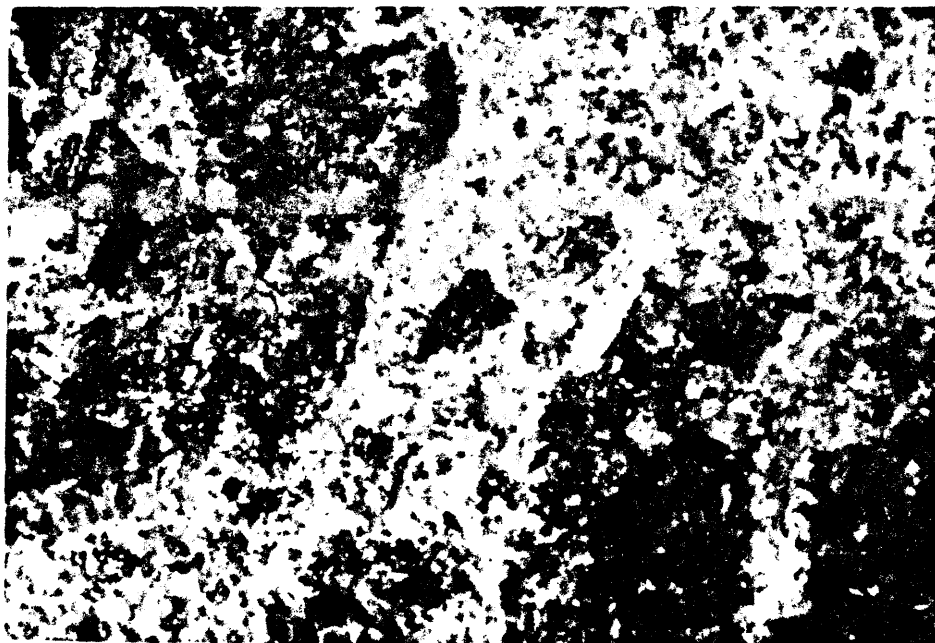


Fig. 26b.--Johnstown hypersthene achondrite, detailed view.

Fig. 27.--Carbon-bearing Norton County enstatite achondrite (aubrite).

Carbonaceous material is intrusive into coarsely crystalline, fragmented enstatite, and is disseminated in granulated, sheared enstatite matrix. Relatively large veinlets intrude milky-appearing enstatite, which is essentially carbon-free in its interior (Fig. 27b). Milkyness appears to correlate with brecciation. A yellowish, sulfur(?) -lined cavity is associated with the intrusive carbon to the right of the relatively large carbonaceous inclusion (Fig. 27b). A small fragment of metal in the carbonaceous material is seen as a bright reflection below the central part of Figure 27a (Arizona State University Collection).

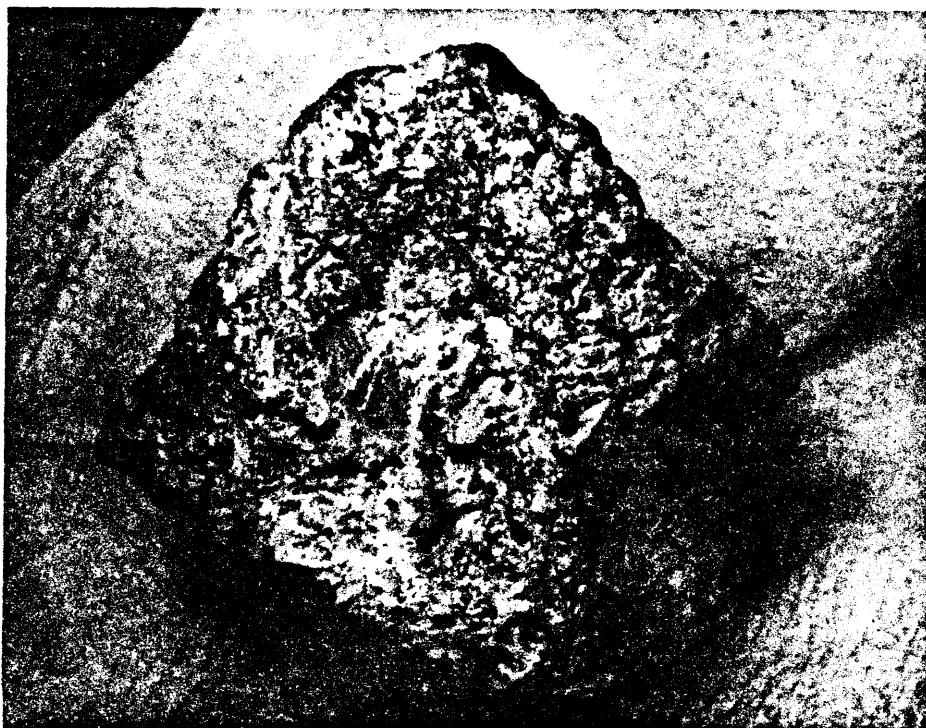


Fig. 27a.--Norton County enstatite achondrite, general view.

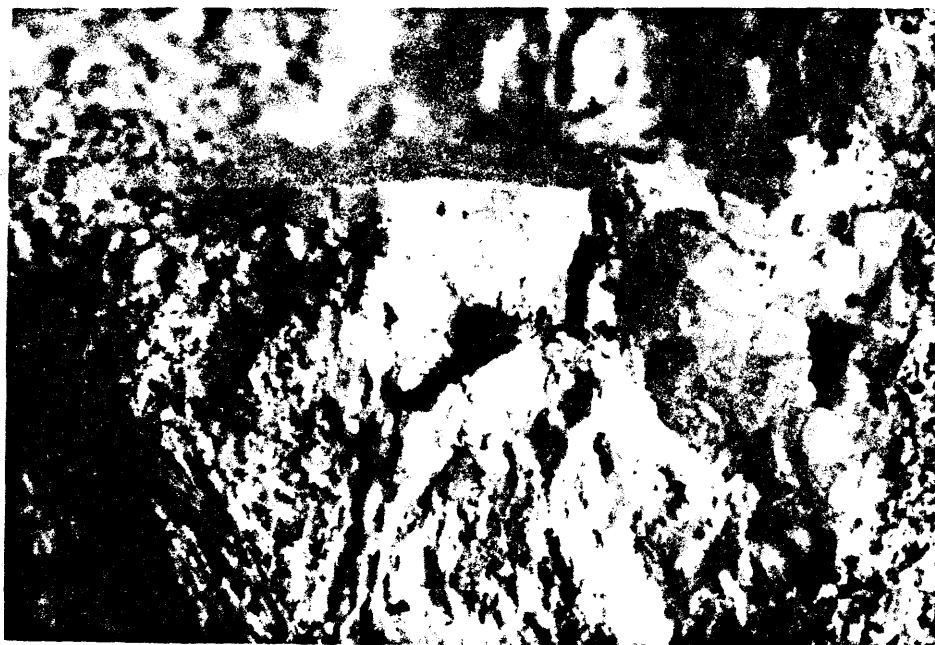


Fig. 27b.--Norton County enstatite achondrite, detailed view.

metal are present in the matrix, but metal is not apparently intrinsic to the hypersthene crystals. The relations suggest that a source of metal underwent fragmentation at the same time as the coarsely crystalline hypersthene. The metal in Johnstown has been found to contain 2.8 percent Ni (see Mason, 1963d, p. 6), which is low for normal meteoritic nickel-iron. An explanation for the low-nickel content may be inferred from studies of metallic spherules from Meteor Crater, Arizona, a number of which were found to have low-nickel contents (Mead and others, 1965). Apparently, impact melting and sudden freezing of shock melted, dispersed droplets of meteoritic nickel-iron results in an irregular distribution of nickel-iron, and commonly in loss of nickel from the metallic droplets.

The Johnstown breccia is inferred to have been developed as the result of an externally caused brecciation event. Because of the presence of metal in the brecciated groundmass, Johnstown is not strictly a monomict breccia. It is classed here as a restricted(?) polymict breccia because its metal may as well have been derived from disrupted nickel-iron of the inferred hypersthene body as from nickel-iron of an impacting material. The term "restricted polymict breccia" is introduced here to allow for the recognition of polymict meteorite breccias which contain materials that may have been derived from different parts of a single parent body.

The Norton County enstatite achondrite (Fig. 27) also is highly brecciated. The large crystals, as in Johnstown, imply a long, slow cooling history prior to brecciation. The brecciation of Norton County was accompanied by the invasion of dispersed carbonaceous material

(0.04 percent carbon; C.B. Moore, personal communication, 1967), and unfractionated primordial rare gases (Eberhardt and others, 1965). The unfractionated rare gases and the carbonaceous material are considered not to have been intrinsic to possible parent body material of Norton County because the carbon-bearing enstatite chondrites display fractionated rare gases (see Anders, 1964, Table 8 and Fig. 25). Because the source of the carbonaceous material and the rare gases in Norton County appears to have been non-enstatite parent body material, Norton County is classed as compound polymict breccia.

Compound polymict breccias, as defined here, are breccias that consist of materials which appear to have been derived from different parent bodies or from different genetic groups. As in Johnstown, there is no evidence to link the brecciation of Norton County with possible magmatic activity in the parent body. Rather, the association of materials and the textures are more simply understood as the products of collision or impact between compositionally diverse materials. The source of the carbon and the unfractionated rare gases in Norton County is inferred to have been cometary material. "Solar" proportions of gases may be retained in the main part of comet bodies, although crustal and "core" materials of comets may be partly fractionated, and show depletions in the lighter rare gases such as are shown by the carbonaceous meteorites (Anders, 1964, Table 8, and Fig. 25).

Pallasites. Pallasites commonly show well developed crystallization textures (Fig. 28a), but in at least two cases (Admire, Eagle Station) the crystallization texture has been disrupted (Fig. 28b). Admire is classed as a monomict breccia because it appears to contain

Fig. 28.--Unbrecciated and brecciated pallasites.

a. Brenham pallasite. Closely packed, sub-rounded to rounded grains of olivine with interstices occupied by nickel-iron and troilite (FeS). Olivine crystals appear to have accumulated prior to the solidification of metallic phases. Specimen is 6 cm across at widest part (U. S. Geological Survey specimen).

b. Admire brecciated pallasite, showing disrupted crystallization texture. Specimen is 7 cm across at widest part (University of Arizona Collection).



Fig. 28a.--Brenham pallasite.



Fig. 28b.--Admire pallasite.

only locally derived materials. No evidence is known to suggest that brecciation accompanied a magmatic event in the parent body.

Irons. Some irons are obviously brecciated. Hey (1966) lists seven brecciated irons, two of which have silicate inclusions. The former are monomict and the latter are restricted(?) polymict breccias. The characteristics of brecciated silicate-bearing irons have been briefly reviewed by Mason (1967c). Mason distinguishes three different types of silicate occurrence: 1) silicates as irregular patches; 2) silicates as minor constituents of troilite or graphite nodules; and, 3) silicates as drop-like inclusions. The second type, for reasons discussed later, are considered to be compound polymict breccias.

The silicate-bearing irons have been arranged, or classified, according to Ga-Ge groups, and inferred Ga-Ge groups (Table 19). Anomalous Ga and Ge values measured in some of these irons possibly may have been the result of collision events. The relatively low-iron silicates in some of the irons, which Mason (1967c) has pointed out are transitional in composition between the enstatite and ordinary chondrites, are probably in some way related to the enstatite or bronzite chondrites.

A fragmented angular silicate inclusion has recently been discovered in the Bishop Canyon iron (C.B. Moore, personal communication, 1968). The pieces form a V-shape and appear to once have been part of a single angular fragment. The fragments lie within a rounded kamacite inclusion, the boundaries of which appear to transect the fine Widmanstätten pattern of the main mass of the meteorite. The relations suggest that nickel-iron was locally melted around the fragment at the

Table 19.--Provisional classification of the mesosiderites, and irons with silicate inclusions.^{1/}

	Olivine ^{2/} Fa	Pyroxene ^{2/} Fs	Plagioclase ^{2/} An	Reference
<hr/>				
CALCIUM-POOR MIXTURES				
<u>Calcium-poor mesosiderites</u>				
Enstatite association ^{3/}				
Bencubbin ^{4/}	P	P		
Enon	6	9	10	a
Mount Egerton ^{5/}				
*Udei Station	5	5	16	a
	6-7	10	15-17	b
Weatherford ^{6/}	P	P		
Winona	5	6	10	c
Hypersthene association ^{3/}				
Bondoc Peninsula ^{7/}	--	19-32	73-97	b
<u>Irons with calcium-poor silicate inclusions</u>				
Ga-Ge group I (Enstatite association)				
Campo del Cielo	5	6	10	a, d
Odessa	3	5	?	a, e
Toluca	5	6	10	a, d
Ga-Ge group II (Hypersthene association)				
Four Corners	4	5	9	a, f
Kendall County ^{8/}	1	1	9	a
*Pitts ^{9/}	5	6	7	a, g
Ga-Ge group III and IV (Bronzite association)				
Bishop Canyon (IVa) ^{10/}	--	--	--	h
Weekeroo Station (III)	None	6	15	a, e, h
Inferred Ga-Ge group I and II				
Copiapo	5	6	10	a
Linwood	4	6	12	a
Persimmon Creek ^{9/}	5	5	8	a
Pine River	4	5	19	a
Woodbine ^{9/}	4	6	9	a
Inferred Ga-Ge group III(?)				
Colomera	None	7	7	a
Kodaikanal	None	14	0	a
Netchaveo ^{11/}	13	12	8	a

Table 19.--Continued

	Olivine ^{2/} Fa	Pyroxene ^{2/} Fs	Plagioclase ^{2/} An	Reference
CALCIUM-RICH MIXTURES				
<u>Calcium-rich mesosiderites</u>				
Hypersthene--pyroxene-plagioclase association ^{3/}				
Mount Padbury ^{12/}	9	--	--	
Bronzite (B) or Hypersthene (H)--pyroxene-plagioclase association ^{3/}				
*Barea	--	--	--	a, i
Clover Springs	--	--	--	a
Crab Orchard	--	--	92	a, i
Dalgaranga (B)	13	--	--	a, k
*Dyarrl Island	--	--	--	a, l
*Estherville (B)	15-20	16-28	88, 96	a, m
Hainholz (H?)	--	18-39	86-98	a, b
*Lowicz (B) ^{13/}				
Mincy	--	--	87	a, n
Morristown (B)	15-35	28-39	84-97	b, j
*Patwar (H) ^{14/}	35	20-35	85-95	a, b
Pinnaroo	--	--	--	
Simondium	--	--	--	a, n
VacaMuerta (H)	--	--	87-96	o
	P	24-40	79-87	b
Veramin	P	19-32	84-94	b
<u>Unclassified</u>				
Budulan				
Lujan(?) ^{15/}				

- 1/. Mesosiderites listed by Hey (1966); asterisk indicates fall. Irons with silicates are from Mason (1967c) except where noted.
- 2/. Percent fayalite (Fa), ferrosilite (Fs), and anorthite (An) contents of olivine, orthopyroxene, and plagioclase feldspar, respectively. P = present.
- 3/. Association of chondrite, achondrite, stony-iron, and iron as shown in the proposed genetic classification (table 2).
- 4/. Clinostatite and a little olivine, nearly iron-free, set in a cryptic, opaque, non-metallic base, that is in turn enveloped in a meshwork of nickel-iron of hexahedrite composition; contains enclaves of enstatite chondrite and hypersthene chondrite (McCall, 1967; Lovering, 1962).
- 5/. Stony-iron of the Shallowater or Pesyanoe enstatite achondrite type (McCall, 1965b).
- 6/. Consists of major clinostatite and minor forsterite (Mason and Nelen, 1967).

Table 19.--Continued

- 7/. Metal encloses and intrudes dark hypersthene (C. B. Moore, personal communication (1966)); an analysis of the pyroxene by H. B. Wiik (personal communication, 1966) revealed no Ca.
 - 8/. All hexahedrites apparently belong to Ga-Ge group II (see Lovering and others, 1957). The essentially iron-free silicates in Kendall County perhaps are enstatite materials emplaced during a collision between the enstatite and hypersthene bodies, which may be inferred from the Bencubbin mesosiderite.
 - 9/. These are considered by Goldstein and Short (1967b) to be irons that would not belong to any Ga-Ge group because of anomalies in band width of Widmanstätten pattern, cooling rates, and exposure ages. It is suggested that the cooling anomalies have been superimposed as the result of a collision.
 - 10/. Angular, broken, relatively dark, crystalline fragment (C. B. Moore, personal communication, 1968).
 - 11/. Mason (1967c) notes that this meteorite was heated in a forge after its discovery, and he postulates that the heating may have altered the original composition of the silicates.
 - 12/. Eucrite, brecciated eucrite, diogenite (hypersthene achondrite), olivine, and nickel-iron; olivine is reported as achondritic inclusions (McCall and Cleverly, 1965; McCall, 1966). Calcium-poor materials may have been in a compound polymict breccia (hypersthene-bronzite?) prior to formation of Mount Padbury.
 - 13/. Classed as a grahamite (calcium-rich? mesosiderite) by Coulson (1940).
 - 14/. Classed as a grahamite by Coulson (1940) who had described it in 1936.
 - 15/. Classed as a mesosiderite (calcium-poor?) by Coulson (1940).
- a). Mason, 1967a.
 - b). Powell and Weiblen (1967).
 - c). Mason and Jarosewich (1967).
 - d). Wasson (1967b).
 - e). Wasson and Kimberlin (1967).
 - f). Lovering and others (1957).
 - g). Cobb and Moran (1965).
 - h). Wasson (1967a).
 - i). Meunier (1872).
 - j). Brezina (1904); Prior (1918); Duke and Silver (1967).
 - k). McCall (1965b).
 - l). Lovering (1962).
 - m). Merrill (1921); Duke (1963); Duke and Silver (1967).
 - n). Prior (1918).
 - o). Prior (1918); Duke and Silver (1967).

time of its brecciation, and intrusion(?), and that this event post-dated development of the Widmanstätten pattern and general solidification of the iron. Bishop Canyon is provisionally classed as a restricted(?) polymict breccia (Table 19).

Compound polymict breccias also appear to exist in the family of irons. This is suggested on the basis of some apparently interrelated compositional and textural anomalies. One of these is the presence of high concentrations of rare gases in some irons (for example, see Krankowsky and Zähringer, 1966). The high concentrations have resulted in calculated K-Ar ages on the order of 10^{10} years (Fisher, 1965). The rare gas-rich irons include Canyon Diablo and Toluca of Ga-Ge group I. The Washington County iron is another rare gas-rich iron; it shows the effects of shock and contains unfractionated rare gases (Anders, 1964, Table 8 and Fig. 25, and discussion). Some of the rare gas-bearing irons contain carbon and troilite nodules, and some of the nodules are diamond-bearing. In Canyon Diablo, diamond locally appears to pre-date terrestrial impact (Carter and Kennedy, 1964, Fig. 1a, c). Carbon nodules commonly appear to interrupt the Widmanstätten pattern of octahedrites. In some cases, cohenite (Fe_3C) encloses carbon nodules and locally appears to cross-cut the Widmanstätten pattern of the enclosing nickel-iron (Carter and Kennedy, 1964, Fig. 5). In other cases, bands of kamacite that swathe or enclose carbon nodules, transect the Widmanstätten pattern, and swathing kamacite also locally outlines carbonaceous veinlets in the nickel-iron. The kamacite, in both cases, appears to post-date the development of the Widmanstätten pattern.

Examples of swathing kamacite may be seen in Wood (1963a, Plate 14a), and in Wasson and Kimberlin (1967, Fig. 6 and 7).

In the Toluca meteorite (University of Arizona specimen no. 8345), a large ($2\frac{1}{2} \times 5^+$ cm) troilite-carbon nodule is bordered by a thin zone of finely granulated, carbonaceous-appearing material. The granulated zone is bordered by swathing kamacite, the outer margin of which in part sharply transects the Widmanstätten pattern of the enclosing nickel-iron. In the main mass of the meteorite, carbonaceous material is present as thin veinlets that commonly follow the Widmanstätten pattern. At places, the veinlets locally appear to cross-cut the Widmanstätten pattern. A few carbon veinlets can be traced into the troilite-carbon nodule. The troilite-carbon nodule and the carbonaceous veinlets thus appear to have been emplaced after the development of the Widmanstätten pattern of Toluca.

Lastly, a curious mineralogical anomaly has been recorded in one iron. The amphibole mineral, richterite ($\text{Na}_2\text{Ca}[\text{Mg}, \text{Fe}]_5 - \text{Si}_8\text{O}_{22}[\text{OH}, \text{F}]_2$), has been described from a carbon or graphite nodule in the Wichita County, Texas, iron (Olsen, 1967). The structurally complex, hydrous mineral almost certainly was not the product of slow cooling in a segregated nickel-iron mass.

The rare gases and the carbon nodules in irons may be genetically related and they may have been introduced during brecciation events. Their introduction after development of the Widmanstätten pattern would account for the discordant textural relations between the inclusions and the Widmanstätten pattern, and for the development of swathing kamacite in zones that locally were melted around the foreign

inclusions. If so, the source of the troilite in the carbon nodules could have been sulfur and sulfide-bearing matrix material of the carbonaceous meteorites, or component 1 materials associated with unequilibrated volatile-poor chondritic material. If the rare gases are unfractionated, the invading material is inferred to have been cometary; if the rare gases are fractionated, the invading material is inferred to have been asteroidal. The introduction of carbon and rare gases into irons parallels, and is an extension of, polymict relations seen in several brecciated carbon- and rare gas-rich stony meteorites.

Calcium-rich achondrites. The pyroxene-plagioclase achondrites have been classed by Duke and Silver (1967) as monomict and polymict breccias, and the terms eucrite applied to the former and howardite to the latter. This has resulted in some differences in the assignment of individual pyroxene-plagioclase achondrites to the eucrite and howardite classes from the assignments listed by Mason (1967b). Mason (1967b, p. 110) classified the pyroxene-plagioclase achondrites on a mineralogical basis, and suggests that:

Howardites: hypersthene dominant over pigeonite

Eucrites: pigeonite dominant over hypersthene

Mason points out that this mineralogical classification has a close correlation with the bulk chemical composition. Furthermore, classification in this manner does not negate the generality that howardites as a group are more thoroughly brecciated than the eucrites. The classification of Mason (1967b) is followed here because on the basis of relations seen on broken surfaces and in thin sections, brecciation appears to be dominantly, if not solely, a post-crystallization feature

of the howardites and eucrites. Because of this, brecciation is not considered to have genetic implications with respect to a mineralogical classification. Duke and Silver (1967) note that they have found evidence in the eucrites which suggests that the brecciation mechanism may have been unrelated to the magmatic process.

The brecciated pyroxene-plagioclase achondrites are classified in the manner proposed for the other stony meteorite breccias. Calcium-rich compound polymict breccias are those in which calcium-poor meteorite material is recognized. In some cases the foreign material appears to be carbonaceous meteorite material, and in other cases appears to be volatile-poor, calcium-poor meteorite material. Metal is present in small amounts in all(?), or nearly all, pyroxene-plagioclase achondrites, and it occurs in brecciated materials. Metal is inferred to have been introduced during brecciation and to have been derived from calcium-poor meteorite materials. Even the apparently unbrecciated eucrite, Moore County (Fig. 25a, b), contains minute metallic inclusions (Hess and Henderson, 1949). The inclusions were observed by Hess and Henderson to occur along concoidal fracture planes in plagioclase that lacks cleavage, which suggests that the metal was introduced after crystallization of the plagioclase of Moore County and at a time that the micro-fracturing occurred.

If metal is exogenetic, all pyroxene-plagioclase achondrites are technically compound polymict breccias. For the present, the only calcium-rich compound polymict breccias that are recognized are howardite and eucrite breccias which contain silicate fragments of calcium-poor meteorite material, or which contain rare gases and carbon

inferred to have been derived from carbonaceous meteorite materials.

With these exceptions, howardites are classed as restricted(?) polymict breccias and eucrites are classed as monomict(?) breccias, which reflects their general relative degree of brecciation and their relative contents of fragments of apparent diverse origin.

A number of eucrites may, with close examination, be revealed to be restricted polymict or compound polymict breccias. An example is the Juvinas eucrite, which megascopically appears only to be partly brecciated (Fig. 25c, d). A polished thin-section (Fig. 29; Juvinas No. 1 of M.B. Duke, U.S. Geological Survey) reveals the presence of tiny creamy white, possibly enstatite, spherules in a conspicuously brecciated part of the meteorite. The creamy spherules are isotropic, and they are enclosed by clear isotropic rinds of plagioclase(?) in which tiny black, vitreous-appearing flakes occur. The clear rinds locally are traceable into adjacent plagioclase glass that contains swirled trains of tiny vesicles and tiny black, vitreous-appearing flakes. The amorphous plagioclase is tentatively identified as maskelynite, which would indicate shock pressures on the order of 250 kb or more (Milton and DeCarli, 1963). The amorphous state of the creamy spherules also is inferred to be the result of shock. One subangular fragment of creamy silicate material is enclosed by a black vitreous fusion crust; within the fusion crust a large part of the fragment is stained or altered a dark brown. Tiny grains and very fine disseminations of metal are scattered through the brecciated rock and some are closely related, spatially, to the spherules and to the subangular fragment. In a plagioclase enclave adjacent to the fragment, parts of

Fig. 29.--White achondrite (enstatite?) spherules and fragment in Juvinas eucrite.

a, b, c. Spherules and fragment of amorphous enstatite(?) in brecciated material. Spherules are creamy-white and very finely granular. They are enclosed by clear shells of plagioclase(?) glass that contains black vitreous flakes of fused silicate. Foreign inclusions occur where crystallization texture of pyroxene and bladed plagioclase is disrupted. Largest spherule is 0.3 mm; sub-angular fragment to right is 0.2 mm wide. Note black fusion crust around the fragment, and that only part of the fragment is creamy white [a] reflected light; b) plane transmitted and reflected light; c) polarized transmitted and reflected light/.

d. Detailed view of large spherule showing glassy fusion crust containing flakes of black, vitreous, fused rock. The glassy shell can be traced to right into brecciated pyroxene and amorphous plagioclase that contains admixed black flakes of fused silicate. Extinction in plagioclase is undulatory [polarized transmitted and reflected light].

e, f. Three enstatite(?) spherules that appear to have been injected into pyroxene along fractures. Note the glassy crusts; the pale brown material enclosing the spherules is plagioclase(?) glass that contains myriads of tiny vesicles. The largest spherule is 0.2 mm in its longest dimension [e] plane transmitted and reflected light; f) polarized transmitted and reflected light/.

g, h. Sub-angular fragment of enstatite(?). Brown material to the right of the fragment is vesicle-laden plagioclase(?) glass. Part of the plagioclase crystal to the right of the fragment is amorphous. A metal fragment is present at the junction of the amorphous and crystalline plagioclase. In the detailed view, note the finely granulated appearance of the enstatite(?) and that the darkening of the fragment is the result of alteration, which may have occurred concomitantly with fragmentation and intrusion into brecciated Juvinas material. Black fusion crust encloses fragment. Fragment is 0.2 mm wide [g] polarized transmitted and reflected light; h) plane transmitted and reflected light/.

Polished thin-section, Juvinas No. 1, M. B. Duke, U. S. Geological Survey.



Fig. 29a.--General view of enstatite(?) spherules and fragment in Juvinas eucrite, reflected light.

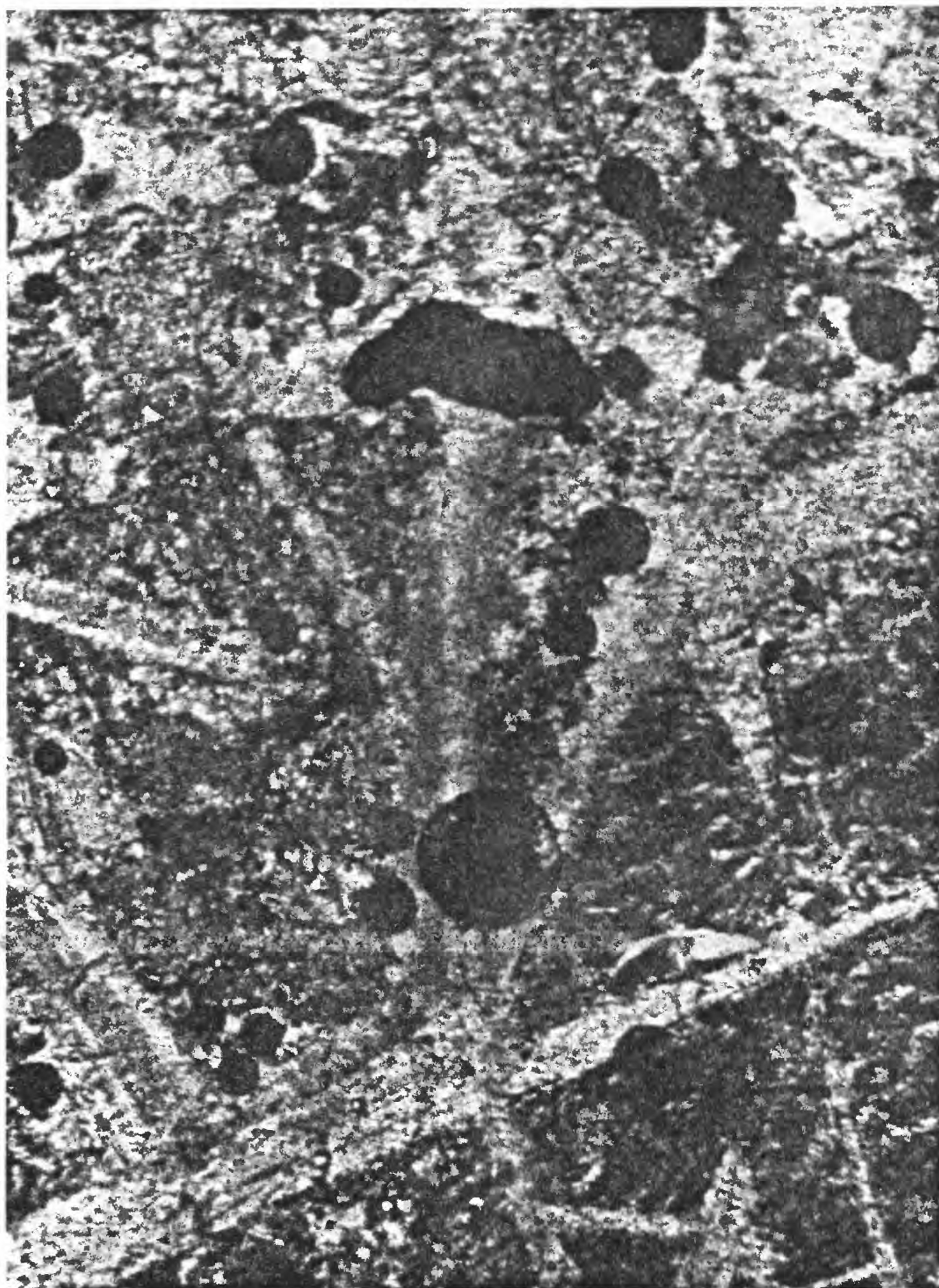


Fig. 29b.--General view of enstatite(?) spherules and fragment in Juvinas eucrite, plane transmitted and reflected light.



Fig. 29c.--General view of enstatite(?) spherules and fragment in Juvinas eucrite, polarized transmitted and reflected light.

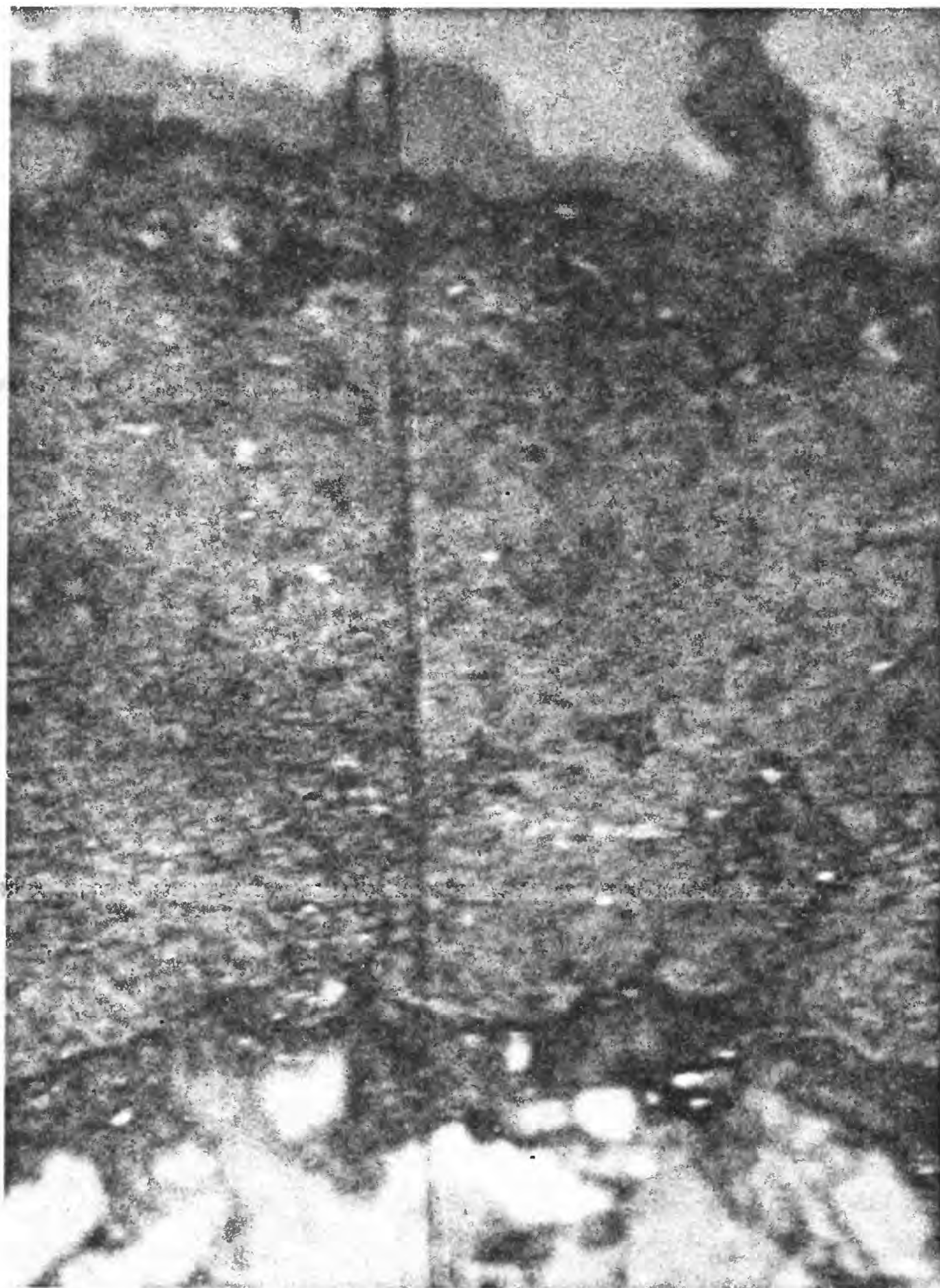


Fig. 29h.--Fragment of enstatite in Juvinas eucrite, detailed view, plane transmitted and reflected light.



Fig. 29g.--Fragment of enstatite in Juvinas eucrite, general view, polarized transmitted and reflected light.



Fig. 29f.--Enstatite(?) spherules in pyroxene of Juvinas eucrite, polarized transmitted and reflected light.



Fig. 29e.--Enstatite(?) spherules in pyroxene of Juvinas eucrite, plane transmitted and reflected light.

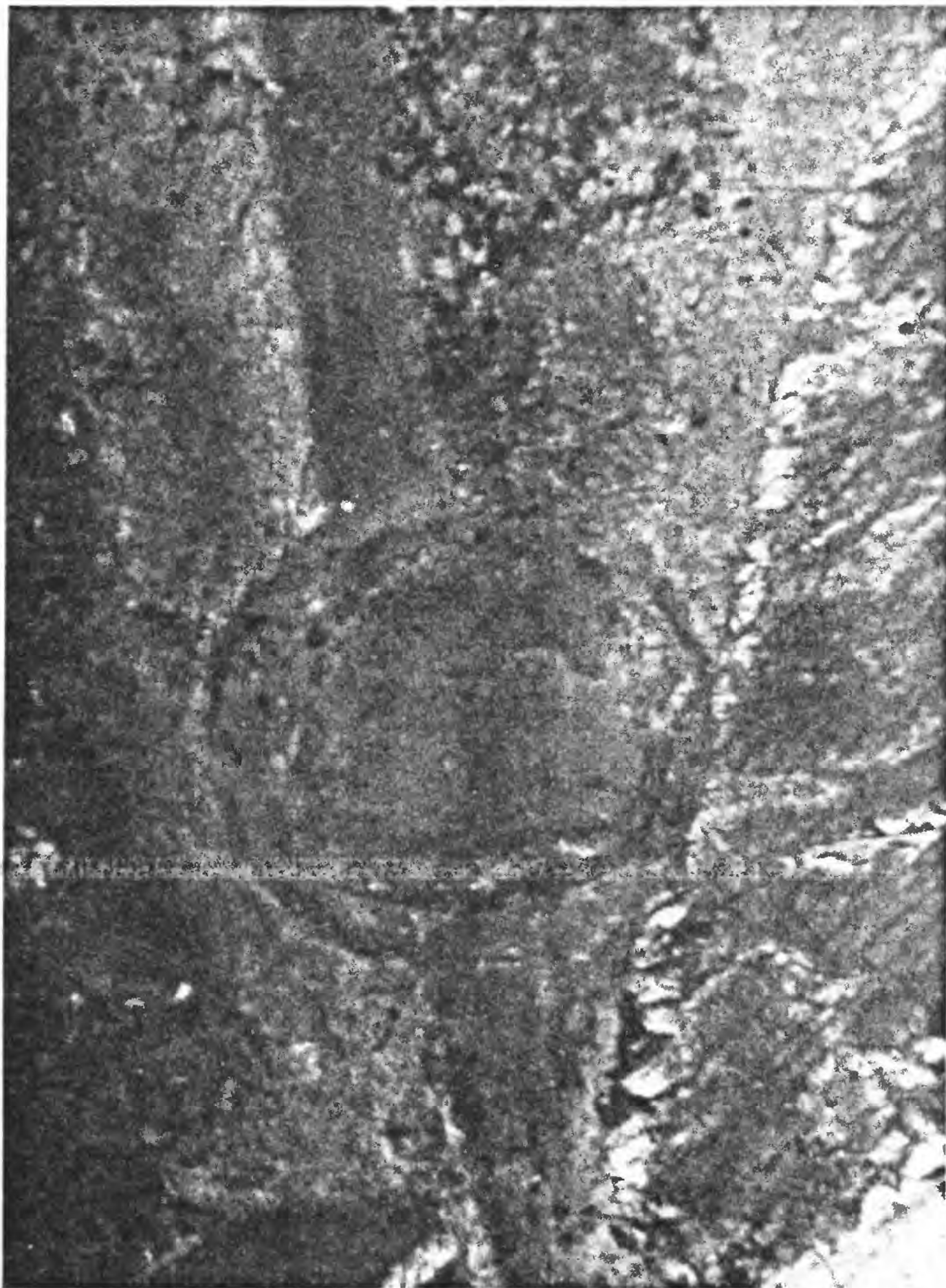


Fig. 29d.--Detailed view of large enstatite(?) spherule in Juvinas eucrite, polarized transmitted and reflected light.

the plagioclase are amorphous and parts of it are crystalline, and metal occupies a central juncture point. Metal is disseminated in the finely brecciated materials, and some appears to embay and invade brecciated pyroxene grains. From textural relations, the creamy spherules and the creamy fragment appear to have been injected into the pyroxene-plagioclase rock at the time of its brecciation. Finely disseminated black vitreous material, which is inferred to be shock-melted rock, also appears to have been intruded at the same time, and metal, which also is discordant to the crystallization textures, is inferred to have been injected with the foreign silicates.

Metal in some pyroxene-plagioclase achondrites in places appears to pre-date the last brecciation event. Relations described by Duke (1965b) for the Petersburg eucrite indicate that metal which encloses coarse, broken hypersthene grains has, in turn, been subjected to violent disruption, which is inferred from the presence of Neumann lines in the metal that encloses and apparently invades the brecciated pyroxene. The relations in Petersburg appear to be the result of two, or more, brecciation events.

Metal in the eucrites commonly is very low in nickel, less than one weight percent in most cases (Duke, 1965b). Exceptions occur. Kamacite of the Petersburg eucrite contains 3.5 weight percent Ni (Duke, 1965b), and metal in the Kapoeta howardite contains about 4.0 to 4.5 weight percent Ni (Fredriksson and Keil, 1963). Metal in the eucrites and in the howardites occurs principally as intergranular metal in breccia and locally as oriented inclusions in pyroxene (Duke, 1965b). Duke (1965b) considers the metal to be intrinsic. Alternatively, the

metal may have been mainly, if not entirely, derived from the calcium-poor meteorites and injected during brecciation events. The low but variable nickel contents of the disseminated metal may be due to loss of nickel from the metal during shock fusion and abrupt cooling, analogous to the apparent loss of nickel in metallic spherules around Meteor Crater (Mead and others, 1965). Metal in the eucrite and howardite breccias may have been derived principally from metal disseminated in chondritic material, and to a lesser extent from the low-nickel kamacite (α -iron) bands of Widmanstätten structure in the case of impact by "core" materials. High-nickel (γ -iron) lamellae are thin in most irons, and fused material derived from them would be expected to be very finely dispersed during a shock event, forming inconspicuous disseminations at best. Tiny nickel-rich droplets should be present in eucrite and howardite breccias where the metal has been derived from the impact of nickel-iron "core" materials. However, conspicuous nickel-rich droplets perhaps should not be expected to be produced during the impact fusion of the disseminated nickel-iron of the chondrites, because taenite is not a quantitatively important phase of the metal of the chondrites.

Tektites. Tektites are considered to be a special form of meteorite breccia. Atmospheric ablation features displayed by some tektites have been used as evidence for their extraterrestrial origin. The aerodynamically sculptured forms of the australites have been experimentally reproduced by Chapman and others (1962), and trajectories derived from the experimental work are reported to be compatible solely with a lunar origin (Chapman, 1964). Chemical, petrographic, and

abundance considerations cited by Chao (1963, 1964) make a terrestrial origin for the tektites extremely difficult, especially for the very young, extremely abundant australasian tektites, for which no terrestrial impact site that could serve as a source of material can be recognized.

An argument which has been used to support the concept of a terrestrial source for the tektites is that tektites display terrestrial minor element abundances (Mason, 1962a, p. 206; Chao, 1963, p. 80-82). However, except for some elemental abundances that appear to be anomalous to both terrestrial materials and to meteorites, for example the very high to high K, Rb, and Ba contents, the minor element abundances of the tektites appear to be as closely related to the pyroxene-plagioclase achondrites as they are to selected terrestrial materials.

A comparison of the abundances of 51 elements in australites, Henbury impact glass, and sub-greywacke by Taylor (1966) shows the virtual identity of these three materials, with the exceptions that the australites contain considerably more Ca and Sr, and considerably less of the calcophile elements Cu, Pb, Ti, In, and Bi. Taylor (1966) concludes that the evidence for the impact glass-parental sediment relationships suggests that the differences in composition between the tektites and the sub-greywacke are primary, and are not caused by the melting process. Taylor appeals to variations in the abundance of a calcium mineral and to low concentrations of sulfide in the parent material of the tektites to explain the differences. The elements shown by Taylor (1966) to be enriched and depleted in the australites

are those that are abundant and that are depleted in the pyroxene-plagioclase achondrites, which are rich in Ca and Sr, and poor in sulfides (Tables 3 and 4).

Australasian microtektites recently have been discovered from a number of ocean-sediment cores obtained from north of the Phillippine Islands, south of Australia, various parts of the Indian Ocean, and southeast of Madagascar (Cassidy and others, 1967). The known linear extent of the strewn field is about 11,000 km in a northeast-southwest direction. Cassidy and others (1967) report that some of the spherules are compositionally similar to the australasian tektites, but that some display lower SiO_2 contents and resemble basic terrestrial rocks and (calcium-rich) achondrites in composition. The australasian microtektites thus appear to bridge the compositional gap between the australasian tektites and "basaltic" terrestrial and extraterrestrial rocks. Cassidy and others (1967) have estimated that a minimum of 150 million tons of glassy spherules exist in the area of occurrence of the microtektites, and believe that this large mass rules out a terrestrial origin.

The distribution in extensive strewn fields, the great abundance, and the compositional characteristics, which include a close similarity in REE abundances for the heavier rare earths (Fig. 24c), suggest that the tektites are impact glasses derived from pyroxene-plagioclase achondrite materials. By analogy with terrestrial explosion and impact craters, the structural zone of formation of the tektites is inferred to be a shell of fused silicates developed between an outer fragmented zone that is marked principally by brecciation (and inferred

to be represented by the eucrites and howardites) and an inner zone that is characterized by intensive physical mixing of impacting bolide and invaded country rock (and inferred to be represented by the calcium-rich mesosiderites). Tektites display very high contents of Rb and K (Chao, 1963, Table 3), which have led investigators to propose a granitic source for the tektites. However, Rb and K are fairly abundant in the volatile-poor chondrites (Table 4), and from relations in polymict breccias, pyroxene-plagioclase achondrite materials appear to have been invaded by volatile-poor, calcium-poor meteorite materials. The chondrites may be the principal source of Rb and K in the tektites. Because they are fairly volatile, Rb and K probably can be lost from impacting materials as the result of shock fusion and driven into adjacent enclosing molten silicates where they could become trapped in glass as the result of abrupt cooling.

Dense Impactites

Chondrites. Some chondrite breccias are very dense, dark, and very fine-grained. Accretionary textures commonly are not well preserved in these chondrites, but evidence of mechanical deformation also, commonly, is not megascopically obvious. However, close examination has revealed evidence for mechanical deformation, for example in the Farmington meteorite, which is a black, tough, dense, monomict(?) hypersthene chondrite breccia (Buseck and others, 1966, Fig. 1). In Farmington, a fairly large, dark, very fine-grained "fragment" is in contact with dark, finely brecciated chondritic material. The dense "fragment" contains thin veinlets of metal and an elongate metal

fragment or strip, the ends of which are curled flaps that are nearly folded back on themselves. The metal strip is located very near the margin of the dense "fragment", and flaps of metal are folded away from the margin, into the matrix of the dense "fragment". A number of veinlets of metal occur in the "fragment", and these do not extend into the main mass of the meteorite. The contact between the "fragment" and the main mass of the meteorite is firmly welded. It is not knife-edged in sharpness as in the case of a discrete angular fragment that rests on "bedrock", but rather, the contact appears to be a narrow zone of abrupt transition between differently textured materials.

Disseminated metal in the main mass of Farmington, and in the black "fragment", shows irregular jagged forms in detail, and some metal is present as tiny spheroids that once were apparently molten (Buseck and others, 1966, p. 4); a violent origin by shock is proposed by Buseck and others to explain the brecciated micro-textures that they observed in both the main mass and in the black "fragment".

The relations suggest that the black "fragment" was not emplaced as a discrete fragment of pre-existing material, but rather was a temporarily fluidized mass of finely comminuted hypersthene chondrite material that contained finely disseminated molten metal and metal as softened fragments. The mixture of comminuted silicates and molten to softened metal appears, from the "aerodynamic" shape of the folded metal particle, to have moved toward and solidified against the brecciated hypersthene chondrite country rock or "bedrock". The textural relations do not support a magmatic origin for the development of brecciated textures in the main mass and in the dark inclusion in

Farmington. The textures, however, appear to be compatible with an origin by a violently disruptive event, such as could be generated during a collision or impact.

The dense tough nature of Farmington, and its disrupted textures, are analogous to textural characteristics of many mesosiderites. Both are considered here to be impactites generated very near, perhaps directly beneath, shock events, -- and in and near zones of mixing between impacting and impacted materials.

Mesosiderites. Twenty-four mesosiderites are known, and of these more than one-quarter are falls (Table 1). On the basis of falls, their abundance is nearly twice that of the pallasites. Most are dark and slaggy-appearing (Fig. 30). Their metal is unevenly and patchily distributed, and in some there is a flow-like structure in the metal.

The mesosiderites are classified on the basis of their silicates. Two principal groups are recognized: 1) a calcium-poor group, in which the silicates are solely those of the calcium-poor meteorites; and, 2) a calcium-rich group in which the silicates are pyroxene, calcic-plagioclase, and subordinate olivine. The calcium-poor mesosiderites are the original mesosiderites of the R.T.B. classification, and the calcium-rich mesosiderites are the grahamites of the R.T.B. classification (Brezina, 1904). A provisional classification of the mesosiderites is shown in Table 19.

Mesosiderites are composed of approximately equal amounts of nickel-iron and silicate. The nickel-iron does not form a network as in the pallasites, but rather is irregularly distributed in grains, threads, and nodules. The silicates commonly show a cataclastic

Fig. 30.--Morristown calcium-rich mesosiderite.

Slabbed surface showing dense, tough breccia consisting of irregular masses and threads of nickel-iron embedded in a dark matrix of calcium-rich achondrite. Metal veinlets display an apparent elongation or flow structure. Millimeter grid in background (Arizona State University Collection).



Fig. 30.--Morristown calcium-rich mesosiderite.

structure. Merrill (1896) noted the strongly cataclastic structure of Morristown, and observed that the feldspar was present as broken fragments, not as in a clastic rock but rather as in a crystalline variety of rock that had been subjected to dynamic agencies. Prior (1918) described a number of the calcium-rich mesosiderites, and he postulated that the agency for their origin was the magmatic intrusion of eucritic material by molten nickel-iron, which carried with it minor olivine. Prior recognized that the nickel-iron and the olivine were compositionally very similar to the pallasites.

Calcium-poor mesosiderites. Three examples of these, Bencubbin and Weatherford (compound polymict breccias), and Bondoc Peninsula (restricted(?) polymict breccia) will be discussed briefly.

Bencubbin has been described by Lovering (1962, p. 190-194), who recognized five types of materials. These are: 1) metal that occurs in nodules and masses of irregular outline (Lovering, 1962, Fig. 4); 2) intimately admixed white achondrite (enstatite) fragments; 3) dark, low-metal (about 5 percent) hypersthene chondrite inclusions (both 2 and 3 were noted to be similar to materials of the Cumberland Falls polymict enstatite achondrite association); 4) scattered, black, compacted inclusions consisting of incipient, flattened, fayalite-rich (Fa_{56}) olivine chondrules that are embedded in a dark, amorphous-looking matrix which contains abundant troilite, about 1 percent graphite, and less than 2 percent metal; and, 5) a single black, metamorphosed chondrite inclusion that contains more than 10 percent metal. Lovering (1962) noted that the most abundant chondritic inclusions in Bencubbin are the hypersthene chondrite "xenoliths", and the second most abundant are the

black, compacted, iron-poor graphitic inclusions. The nickel-iron displays no Widmanstätten pattern on etching, but rather is blotchy appearing (Simpson and Murray, 1932), a characteristic displayed by "rim" specimens of Canyon Diablo (Meteor Crater) iron which have apparently undergone heating due to shock (see Moore and others, 1967). Anorthite, reported as the result of chemical analysis by Simpson and Murray (1932), could not be detected visually by Lovering (1962).

Bencubbin has been re-examined by McCall (1967), who has reported that an enclave of hypersthene chondrite material is atypical in that its olivine is Fa_{19} and its pyroxene is entirely(?) pigeonite which is crystallized in substantial grains; the chemistry of the enclave is reported as being entirely typical of hypersthene chondrite material. A second enclave in Bencubbin investigated by McCall (1967) is reported to be enstatite chondrite material; the only silicate mineral in it is clino-enstatite, and the chondrules are very poorly formed and have incompletely crystallized central cores. Both the hypersthene and enstatite chondrite enclaves were found to contain small amounts of carbon. The enclaves described by McCall have characteristics of unequilibrated chondritic materials. Bencubbin thus may be inferred to contain near-surface materials of the enstatite and hypersthene chondrite bodies (Table 2; Fig. 23).

From textural evidence, Lovering (1962) concludes that the parent material of Bencubbin was an intimate mixture of pyroxene-olivine achondritic and various chondritic fragments, broadly comparable to the association observed in the Cumberland Falls meteorite. (The dark inclusions in the Cumberland Falls enstatite achondrite have been

identified by Binns (1967) as highly primitive, unequilibrated enstatite chondrite material.) Lovering (1962) notes that at some later stage the physical mixture of stony-meteorite types was intruded by a metal magma which caught up a number of chondritic and achondritic fragments as xenoliths. Lovering's description is heavily flavored by an underlying assumption that the mixtures are the results of magmatic processes that have taken place in a single parent body. However, if the mixture is interpreted in light of the proposed genetic classification (Table 2), Bencubbin can be considered to be compound polymict breccia consisting of hypersthene body, enstatite body, and possibly carbonaceous or pigeonite meteorite materials.

The Weatherford calcium-poor mesosiderite has been described by Mason and Nelen (1967) as a highly shocked breccia of nickel-iron and aubritic, or enstatite achondrite, silicates. Except for the lack of hypersthene material, Weatherford appears to be much like Bencubbin. In describing Weatherford at the 1967 Annual Meeting of the Meteoritical Society, Mason noted that it is also similar to the Cumberland Falls enstatite achondrite in that both contain blackened chondritic material having the approximate mineralogic composition of the iron-free olivine, forsterite. Mason and Nelen (1967) report 0.11 percent C, 1.69 percent H_2O^+ , and 0.56 percent H_2O^- in Weatherford. The water released above $1100^\circ C$ could have been terrestrially acquired water because Weatherford was a find that was plowed up. The possibility exists, however, that some of the water is extraterrestrial water which resides in layer lattice silicates associated with the carbonaceous materials -- materials that appear to have been emplaced at the time of brecciation. The

carbonaceous, water-bearing(?) material in Weatherford may have been either of primitive enstatite chondrite or of carbonaceous meteorite origin.

The relations in Bencubbin and Weatherford can be interpreted to be the result of mechanical mixing during impact or collision events. Evidence for two events appears to exist in Bencubbin. Evidence for one event is preserved in Weatherford (and Cumberland Falls) and it appears to be similar to one of the two mixing events of Bencubbin. The common event appears to have been impact of the inferred enstatite body by a carbonaceous meteorite or pigeonite chondrite body, which resulted in the emplacement of carbonaceous matter, fractionated rare gases (in the case of Weatherford; Anders, 1964, Table 8), and volatiles in nominally volatile-poor enstatite materials. The relicts of the carbonaceous or pigeonite meteorite material in Bencubbin would be the graphite-bearing chondritic material that is rich in sulfides, that is deficient in metal, and that has a high fayalite content in the chondrules, which is more characteristic of pigeonite than carbonaceous chondrite materials. In Bencubbin, some of the carbonaceous material also may have been derived from primitive, or unequilibrated, carbon- and rare gas-bearing enstatite and hypersthene chondrite materials at the time of a second mixing event. The second event, from descriptions of Lovering (1962), appears to have been accompanied by mobilization of metal that may have been derived from core materials of either or both the enstatite and hypersthene parent bodies.

The Bondoc Peninsula mesosiderite is a restricted(?) polymict breccia that consists of highly contorted metal which encloses and

intrudes brecciated hypersthene achondrite material (C.B. Moore, personal communication, 1966). Analysis of the hypersthene (H.B. Wiik, personal communication, 1966) has revealed no calcium. However, plagioclase feldspar has been reported for Bondoc Peninsula (Powell and Weiblen, 1967). The feldspar is not megascopically apparent in specimens in the Arizona State University Collection, and thus plagioclase must be only an accessory mineral, analogous to the accessory plagioclase of the hypersthene achondrites. If metal of Bondoc Peninsula can be demonstrated to belong to Ga-Ge group I (enstatite body) or Ga-Ge group III (bronzite body), Bondoc Peninsula could be reclassified as a compound polymict breccia.

Calcium-rich mesosiderites. The calcium-rich mesosiderites are structurally complex mixtures of calcium-rich and calcium-poor materials. They are considered by some workers to have close genetic affinities to the pyroxene-plagioclase achondrites, principally on the basis of $^{18}\text{O}/^{16}\text{O}$, and to have arisen from a common parent material through magmatic differentiation (Taylor and others, 1965; Duke and Silver, 1967). The interpretation that certain of the calcium-poor silicates are genetically related to the calcium-rich pyroxene-plagioclase achondrites as the result of magmatic processes in a parent body, has been discussed, and rejected, in Chapter 5. The data and interrelationships that are developed in Chapters 3, 4, and 5, which led to the correlations that are summarized in Table 2, indicate that on chemical grounds, calcium-poor and calcium-rich meteorites are genetically discrete materials. The following discussion summarizes some of the textural and mineralogical characteristics of the calcium-rich

mesosiderites, which need to be considered in evaluating their origin, - an origin that has not yet been fully explained.

In Vaca Muerta, Prior (1918) noted a cataclastic texture in which anorthite feldspar occurred in sharp edged fragments only, and in which pyroxene showed little in the way of crystal outline. He noted that the nickel-iron in Vaca Muerta encloses the fragmented materials and was the last constituent to consolidate. M.B. Duke (personal communication, 1967) has observed pieces of Vaca Muerta that are microscopically indistinguishable from terrestrial gabbro. Textural relations in Hainholz and Simondium, observed by Prior (1918), are similar to those in Vaca Muerta. In Mincy, Prior noted that the structure is much less cataclastic and that pyroxene occurs in rounded grains with the interstices filled with bladed feldspar; nickel-iron, as stringers, was observed to enclose the feldspar and pyroxene, and thus Mincy was also considered by Prior to be a mesosiderite. A thin section of Crab Orchard described by Prior (1918) displayed two parts that were in sharp division. In one part, which contained much metallic iron, the anorthite and pyroxene were observed to be broken into irregular fragments; in the other part, the anorthite and pyroxene formed a coarse-grained mozaic, much like a gabbro. Prior (1918, p. 169) concluded that the textural relations show the invasion and breaking up of a pyroxene and anorthite rock by nickeliferous iron.

The paragenetic relationships at places are more complicated than can be explained by simple intrusion. Lovering (1962, p. 183 and Fig. 1) observed in the Pinnaroo mesosiderite that the margins of large forsterite-rich olivine crystals (up to 2 cm in diameter) are intruded

and disrupted by the pyroxene-plagioclase achondrite groundmass. From this, Lovering (1962) concluded that the olivine crystals must have been xenocrysts in the basaltic achondrite "magma". The relations between the metal phase and the basaltic achondrite groundmass in Pinnaroo had earlier suggested to Alderman (1940) that both components were liquid at the same time, and that they solidified in situ. The textural relations in the mesosiderites thus are in part contradictory if they are considered to have resulted from magmatic intrusions in a parent body; they are not contradictory if they are considered to have resulted from impact brecciation and mixing, during which time the impacting bolide and part of the impacted country rock were brecciated and partly shock-melted, giving rise to the local development of mutual invasion textures. If a shock model is valid, the general conclusions of Prior (1918) would suggest that the pyroxene-plagioclase achondrites have served as the target materials for impacting pallasitic and nickel-iron materials.

Larger patches of metal in Vaca Muerta and Patwar contain well developed fine Widmanstätten structure, whereas metal of other mesosiderites contains irregular blebs and lamellae of very high-nickel taenite in relatively wide areas of kamacite (Powell and Weiblen, 1967). The Widmanstätten pattern, and the taenite, are very possibly relict from structures developed in typical irons. Determination of Ga and Ge from the larger patches of metal might serve to identify the metal with one of the Ga-Ge groups of irons.

Tridymite (< 3 kb, relatively high temperature SiO_2) appears to be a ubiquitous constituent of the mesosiderites. Duke (1963, p. 52)

reports that it is present in Estherville, and Powell and Weiblen (1967) have observed it in the six calcium-rich mesosiderites that they studied. In spite of the presence of free SiO_2 in the form of tridymite, the silicate phase of the mesosiderites is apparently enriched in Mg with respect to the calcium-rich achondrites (Table 3).

M.B. Duke (personal communication, 1967) reports that he has observed tridymite grains in Vaca Muerta that are crystal clear, perfect, and on the order of 2 mm in diameter; and that tridymite grains in Estherville also are commonly very large. Duke reports that tridymite occurs in Vaca Muerta in the centers of textures that are recognizably magmatic and that are not shock produced; and he notes that volatile minor elements in mesosiderites are not any more depleted than in howardites. Duke concludes that the fragmented texture of Estherville, including the paragenetic disequilibrium relations, indicate that Estherville was not molten but was recrystallized at rather high temperatures. Lastly, Duke notes that explaining the presence of tridymite in mesosiderites is no problem because all the pyroxene-plagioclase achondrites have free SiO_2 to begin with.

The foregoing indicates that several aspects of the problem of mesosiderite formation are not resolved. Textural relations described by Prior (1918) and by Lovering (1962) appear to be best interpreted in terms of mutual invasion, or mixing, of materials during impact events. The magmatic aspects described by M.B. Duke, above, require that a high temperature environment be generated in which the observed mineralogical and textural features could develop. Some of the features observed by Duke possibly could be post-impact features that developed well within a

high density mass, -- a mass that was elevated to high temperatures by shock and that then cooled fairly slowly at relatively low pressures.

On the basis of textural relations and correlations outlined in Table 2, the calcium-rich mesosiderites are classed as compound polymict breccias. They are interpreted to have been formed by the impact invasion of lunar country rock by metalliferous asteroidal materials, in events that also may have been responsible for their escape from the moon.

Classification of the Meteorite Breccias

A proposed classification of the meteorite breccias is outlined in Table 20, and is summarized in Appendices II and III. The classification was developed from evaluation of the meteorite breccias in terms of the proposed genetic classification of the meteorites (Table 2). Classification of brecciated meteorites with respect to the genetic classification results in some apparently internally consistent, and interrelated, groupings. The classification of the breccias is arranged so that compound polymict breccias appear under more than one heading. Furthermore, restricted(?) polymict breccias and monomict breccias can be raised in rank if additional work reveals new relations. The assignment of many meteorites to specific breccia groups is provisional at this time because the assignments of many were made on the basis of incomplete and sketchy descriptions in the literature. Some assignments were made on the basis of personal inspection. Essentially all of the polymict breccias of Wahl (1952) need to be re-examined. Unequilibrated chondrites such as Parnallee and Mezö-Madaras, which are discussed in

Table 20.--Preliminary classification of meteorite breccias.*

CLASS I. CALCIUM-POOR METEORITES

A. Carbon, water and rare gas-bearing breccias^{1/}1. Pigeonite association (restricted? polymict)^{2/}

- a. Chondrite (None)^{3/}
- b. Achondrite (5?)^{4/}

2. Hypersthene association^{2/}None^{5/}3. Bronzite association (compound polymict)^{2/}

- a. Chondrite (6)^{6/}
- b. Achondrite (1)^{7/}
- c. Pallasite (None?)
- d. Iron (2)^{8/}

4. Enstatite association (restricted? and compound polymict)^{2/}

- a. Chondrite (None?)^{9/}
- b. Achondrite (4)^{10/}
- c. Mesosiderite (2)^{11/}
- d. Iron (2)^{12/}

B. Breccias that apparently lack carbon, water, and rare gases

1. Chondrites

- a. Compound polymict breccia
 - 1). Hypersthene-enstatite mixtures (3?)^{13/}
 - 2). Hypersthene-bronzite mixtures (6?)^{14/}
 - 3). Bronzite-enstatite mixtures (3?)^{15/}
- b. Restricted(?) polymict breccia
 - 1). Pigeonite (None?)^{3/}
 - 2). Hypersthene (37)^{16/}
 - 3). Bronzite (18)^{17/}
 - 4). Enstatite (None)^{9/}

2. Achondrites

- a. Compound polymict breccia
 - 1). Enstatite-hypersthene mixtures (1)^{18/}

* See Appendix II for notes and references, and Appendix III for list of brecciated meteorites.

Table 20.--Continued

CLASS I. CALCIUM-POOR METEORITES

B. Breccias that apparently lack carbon, water, and rare gases2. Achondrites

- b. Restricted(?) polymict breccia
 - 1). Pigeonite-metal (ureilite) mixture (5?)4/
 - 2). Hypersthene-metal mixture (8)19/
 - 3). Enstatite-metal mixture (9?)10,20/

3. Stony-irons

- a. Mesosiderites (calcium-poor)
 - 1). Compound polymict breccia
 - a). Enstatite-hypersthene mixture (1)11/
 - 2). Restricted(?) polymict breccia
 - a). Enstatite-metal mixture (5)11,21/
 - b). Hypersthene-metal mixture (1)22/
 - c). Unclassified (2)23/
- b. Pallasites
 - 1). Restricted polymict (None?)
 - 2). Monomict (2⁺?)24/

4. Irons with silicate inclusions^{25/}

- a. Compound polymict breccia
 - 1). Metal (hypersthene)-silicate (enstatite) mixture
 - a). Brecciated hexahedrite (1)
- b. Restricted or compound(?) polymict breccia
 - 1). Enstatite association (Ga-Ge group I) (4)
 - 2). Hypersthene association (Ga-Ge group II) (2)
 - 3). Bronzite association (Ga-Ge group III and IV) (2)
 - 4). Inferred enstatite or hypersthene association (5)
 - 5). Inferred bronzite association (3)

CLASS II. CALCIUM-RICH METEORITES

A. Carbon, water, and rare gas-bearing breccias^{1/}1. Pyroxene-plagioclase achondrites^{26/}

- a. Howardite (4)27/
- b. Eucrite (1)28/

2. Tektites (?)^{29/}

Table 20.--Continued

CLASS II. CALCIUM-RICH METEORITES

B. Breccias that apparently lack carbon, water, and rare gases

1. Pyroxene-plagioclase achondrite^{26/}
 - a. Compound polymict breccia
 - 1). Howardite (3?)^{30/}
 - 2). Eucrite (4)^{31/}
 - b. Restricted(?) polymict breccia
 - 1). Howardite (7)^{32/}
 - c. Monomict(?) breccia
 - 1). Eucrite and shergottite (24)
2. Tektites(?)^{33/}
3. Mesosiderites (calcium-rich)
 - a. Compound polymict breccia^{34/}
 - 1). Enstatite-metal-eucritic mixture (None?)
 - 2). Hypersthene-metal-eucritic mixture (5)^{35/}
 - 3). Bronzite-metal-eucritic mixture (4)^{36/}
 - 4). Unclassified (7)
4. Chondrites with eucritic(?) inclusions
 - a. Compound polymict breccia
 - 1). Hypersthene chondrite-eucritic mixture (1?)^{37/}
 - 2). Bronzite chondrite-eucritic mixture (4?)^{38/}

the first section of this chapter, are recognized as accretionary rather than true polymict breccias. Until the individual meteorites are re-examined, the polymict assignments of Wahl (1952) are retained.

Volatile-rich Breccias

Breccias that contain structurally discordant carbonaceous material and associated volatiles in otherwise anhydrous high temperature silicates are classed as volatile-rich breccias. Water and rare gases are assumed to be held in layer lattice silicates that are associated with disseminated carbonaceous materials. The rare gases in some breccias, for example -- the water-bearing pigeonite achondrites (Table 3), are fractionated (Anders, 1964, Table 8). In this case, the source of the carbonaceous material may have been hydrated component 1 matrix material of the pigeonite chondrites, which display fractionated rare gases (Anders, 1964, Table 8). However, in some enstatite achondrites and howardites, the rare gases that are apparently associated with carbonaceous material are unfractionated, and the unfractionated gases may have been derived from primitive parent body materials of the carbonaceous meteorites (comets).

Thus, under the heading of carbon- and rare gas-bearing breccias resides material that may have been invaded either by volatile-rich cometary materials or by primitive, unequilibrated, hydrated, chondrite materials that resided in the outer or "crustal" parts of asteroidal bodies. A principal clue as to the origin of the volatile-rich materials may reside in the character of gases emplaced and trapped in the breccias. Unfractionated rare gases, gases in "solar" proportions, may

indicate a cometary origin, whereas fractionated or "planetary" gases may indicate an asteroidal origin.

Volatile-poor Breccias

Details regarding some of the breccias listed and discussed in Table 20 and Appendices II and III have been described in preceeding parts of this chapter. In a number of metalliferous breccias and in silicate-bearing irons, Ga and Ge values could prove useful for determining whether the silicate-metal mixtures are restricted polymict or compound polymict breccias.

Interpretation of Record in Breccias

Comet-asteroid and Interasteroidal Collisions, Breakup of Asteroids, and Formation of Lunar Basins

A large number of types of polymict breccias are possible. However, only a relatively few types of compound polymict breccias are known, and they tend to cluster into a few discrete groups or associations (Table 20). The brecciated materials appear to have resided principally in three parent bodies (Tables 2 and 20). From the polymict associations, the bodies probably had original configurations similar to that shown in Figure 23. Mixing appears to have occurred as the result of two comet-asteroid impacts, and a limited number of collisions between the inferred asteroidal bodies, and fragments of the bodies. The events that may be inferred directly from the polymict breccias, and indirectly from the gas-retention ages of stones and cosmic-ray exposure ages of the irons, appear to be major disruptions. The inferred bodies, and fragments of the bodies, were probably

perturbed into interasteroidal-, Mars-, and earth-crossing orbits as a result of the brecciation events.

Meteorite ages (Table 21) and the polymict breccias (Table 20) can be ordered with respect to the proposed genetic classification of the meteorites (Table 2). When so ordered, the timing, the probable causes, and the sequence of events in the fragmentation and breakup histories of the inferred asteroid parent bodies appear to be revealed (Table 22). Young ^4He ages, most of which are sharply discordant with K-Ar ages, have been used to estimate the ages of brecciation events in the stones. Short discordant ^4He ages are assumed to have been the result of preferential loss of He by shock. The assumption is supported in a few stones, such as the Bruderheim hypersthene chondrite and the highly shocked Farmington hypersthene chondrite, which show young, essentially concordant, K-Ar and ^4He ages (Appendix IV). A number of gas-retention ages have been reported for stones that may have been invaded by carbonaceous meteorite material, such as Norton County, Breitscheid, and Pultusk. The diversity in reported ages may reflect an irregular distribution of rare gases in the meteorites, which may be the result of emplacement of foreign rare gases during brecciation. For irons, $^{41}\text{K}/^{40}\text{K}$ cosmic-ray exposure ages have been used in most cases.

Irons of Ga-Ge groups III and IV, which are considered to be a single genetic group for reasons given in Chapter 3, have the oldest exposure ages, ranging from about 1440 to 2200 m.y. Irons of Ga-Ge group II first appear at about 1200 m.y. ago, and irons of Ga-Ge group I appear at about 900 m.y. ago (Tables 21 and 22). The abrupt appearance

of a number of irons at about 900 m.y. ago is inferred to record one major, and possibly one minor, interasteroidal collision (Table 22).

Irons of the enstatite and hypersthene bodies appear to have been extensively exposed at about 900 m.y. ago, and "stage two" in the formation of the Bencubbin mesosiderite may have occurred at this time. The enstatite body appears to have undergone an earlier invasion by carbonaceous meteorite or pigeonite chondrite material, which is inferred from paragenetic and age data from the carbon- and rare gas-bearing Norton County enstatite achondrite, and from "stage one" relations in the Bencubbin and Weatherford mesosiderites, and the Cumberland Falls enstatite achondrite. Carbon, troilite, and rare gases are inferred to have been intruded into core materials of the enstatite body during the earlier event, which is deduced from relations in the Ga-Ge group I Canyon Diablo, Toluca, and Odessa irons. The time of the inferred comet-asteroid brecciation event is uncertain, but it probably occurred before 1300 m.y. ago, and possibly before 1900 m.y. ago, which are gas-retention ages given for the Norton County enstatite achondrite.

The oldest major disruption event appears to have been the exposure of the core of the bronzite body, represented by irons of Ga-Ge groups III and IV, about 2200 m.y. ago. Initial fragmentation of the bronzite body also may have been the result of cometary impact, which is inferred from the carbon and the character of rare gases in the Pultusk and Breitscheid chondrites, and from shocked and rare gas-bearing irons of Ga-Ge groups III and IV.

Fragmentation history of asteroids. Events outlined in Tables 21 and 22 may be summarized as follows. Comet impacts are inferred to

have initially and apparently severely affected the bronzite and enstatite bodies, probably initially perturbing their orbits. One and possibly both events occurred before 2000 m.y. ago. Several impacts appear to have occurred on the hypersthene body in the interval 1000 to 2000 m.y. ago, possibly from impacts of fragments of bronzite and enstatite materials lost as the result of the inferred cometary impacts. The core of the hypersthene body was first exposed about 1200 m.y. ago, but major fragmentation of its core materials, as the result of a collision with the enstatite body, appears not to have occurred until about 910 m.y. ago. The bronzite body possibly became involved in a subsidiary collision at this time. Collision and fragmentation events became common (Table 22) following a possible collision between the bronzite and enstatite bodies at about 825 m.y. ago. There appears to have been a major collision between the bronzite and hypersthene bodies at about 700 m.y. ago, followed by major collisions between the enstatite(?), hypersthene and bronzite bodies at about 585 and 600 m.y. ago. Subsequent fragmentation events then occurred, principally between materials of the hypersthene and bronzite bodies. The youngest major events appear to have occurred at about 440 m.y. and 240 m.y. ago, although possible substantial events may have occurred to as recently as 75 m.y. ago. The fairly large number of events that post-date the times of the inferred major breakups may reflect a "comminution" of fragments of asteroidal bodies, and may have been responsible for the relatively great abundance of the hypersthene and bronzite chondrites.

Formation of lunar basins. The times of initial fragmentation of the bronzite and enstatite bodies, some 2000 m.y. ago or so, and the

apparent major breakups of the hypersthene, bronzite, and enstatite bodies at about 900, 700, and 600 m.y. ago, have interesting implications regarding the impact history of the earth and the moon, and the flux of asteroidal materials available for impact of the earth and the moon over the course of geologic time. The major lunar basins, which are of apparent impact origin on the basis of geologic considerations, almost certainly must owe their existence to the impact of extraordinarily large and massive bodies of materials. The only apparent sources are fragments of asteroidal bodies produced in the inferred collisions and breakups that are outlined in Tables 21 and 22.

On the basis of existing evidence in the meteorites, the oldest lunar basins could scarcely be more than about 2200 m.y. old. If a correlation exists between the apparent major asteroidal breakups and the formation of lunar basins, most of the lunar basins would be 900 m.y. old, and younger. Perhaps five of the six major lunar basins, those whose morphological appearances range from subdued to extremely fresh (Fig. 31), may have been formed in the past 900 m.y.

The basin underlying Mare Fecunditatis is the oldest of the major lunar basins. It is a relict or "ghost" basin, and no materials that are associated with its formation appear to be exposed at the lunar surface. The Fecunditatis basin may have been formed in the interval 1200 to 2200 m.y. ago.

Materials enclosing basins associated with Mare Nectaris and Mare Humorum exhibit about identical degrees of preservation and have fairly conspicuous outlines. The two basins, and possibly the basin associated with Mare Serenitatis, which has been extensively modified by

Fig. 31.--Index map of moon and full moon photograph

Prominent rays sketched approximately. Diffuse dark halo around Tycho and possibly similar halos around Anaxagoras, Aristarchus, Euctemon and Proclus are stippled. Outline of concealed basin "deep" of Mare Fecunditatis is shown in dotted outline. Full moon photograph, Mt. Wilson 100-inch telescope.

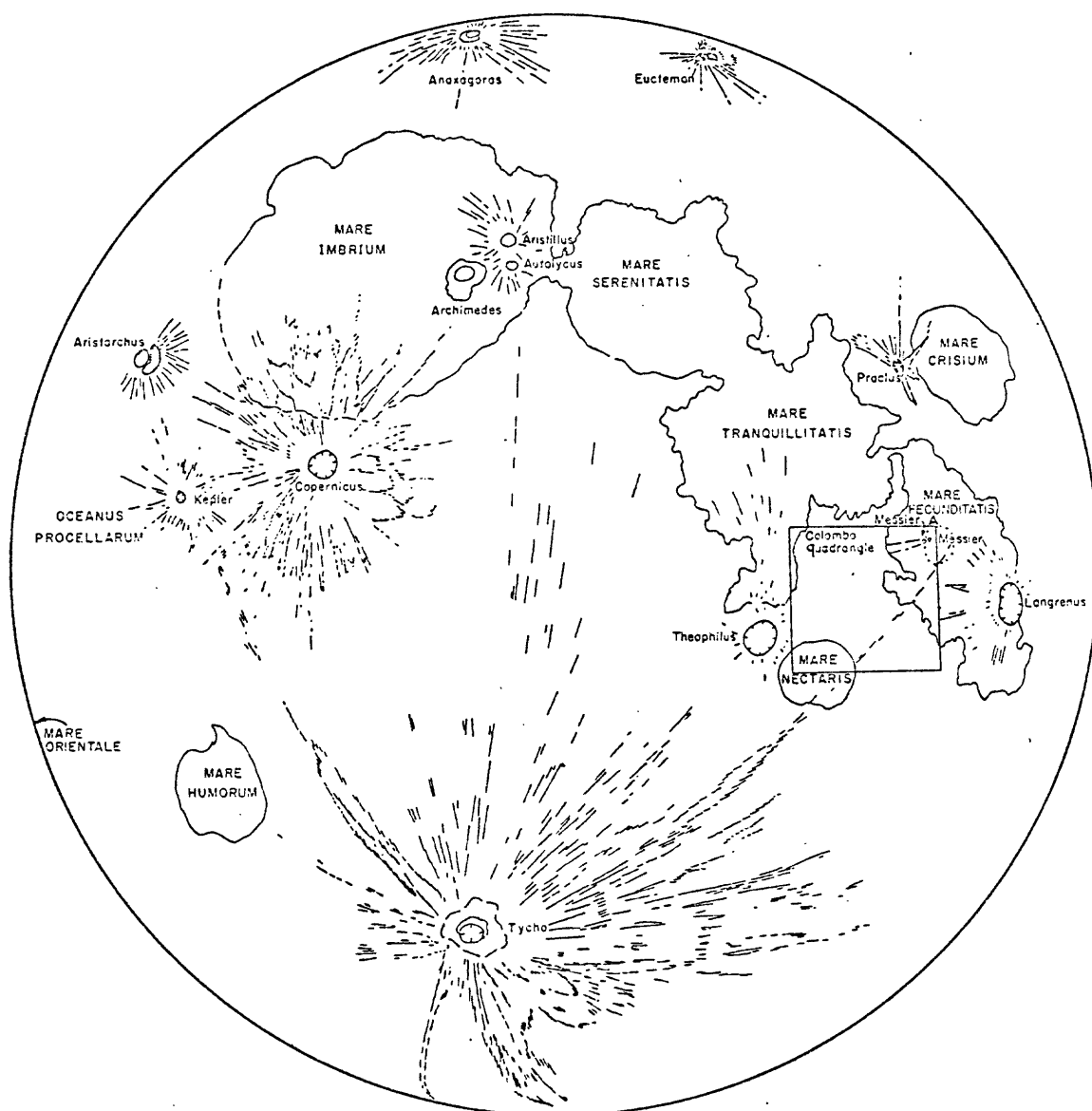


Fig. 31a.--Index map of moon.

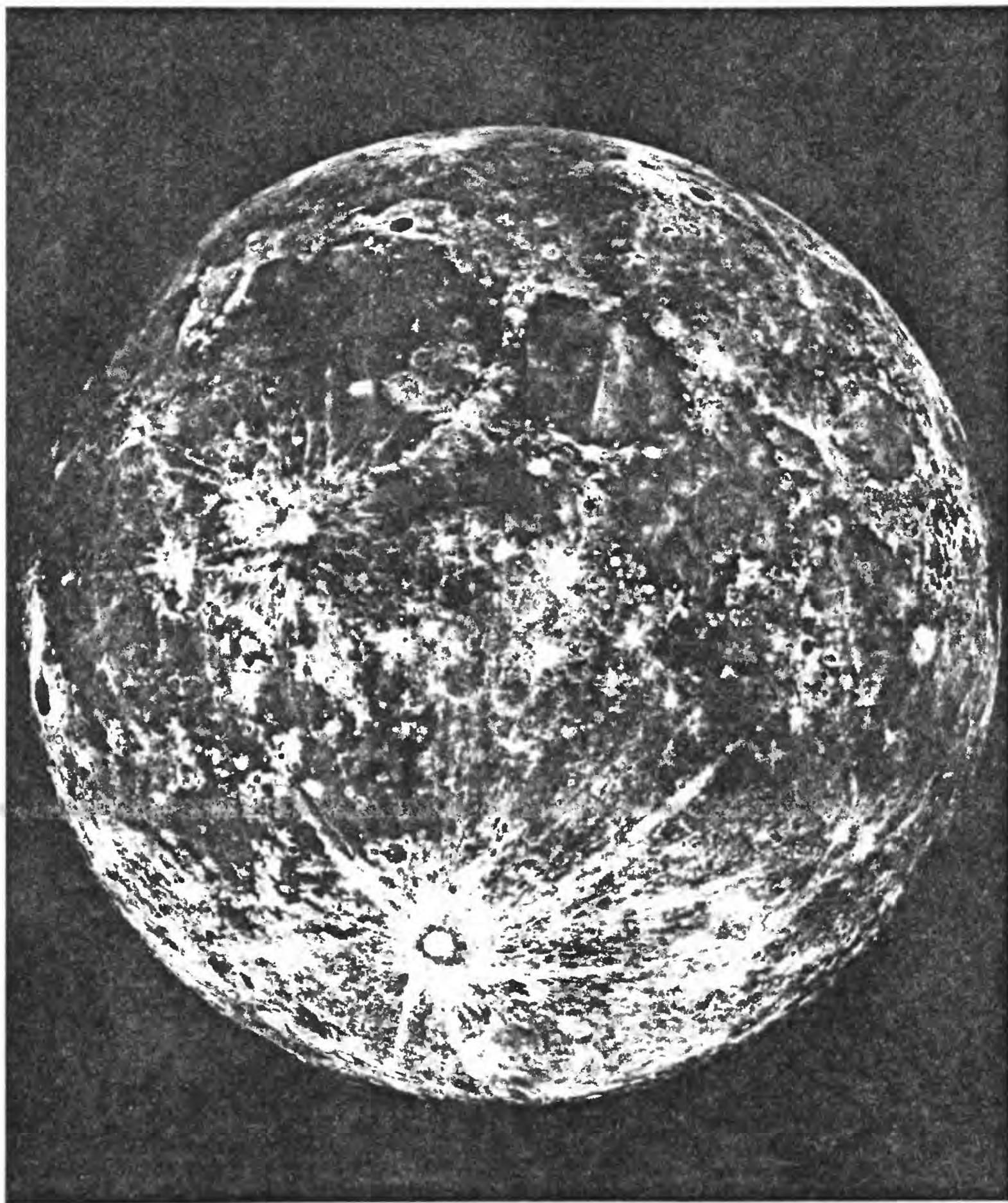


Fig. 31b.--Full moon photograph.

younger materials of the intersecting Imbrium Basin, may be considered to comprise an "old" group of basins. The "old" basin group perhaps formed after the first major breakups and may be about 900 m.y. old and less. The next younger basin is the well developed Crisium Basin, and the youngest, most prominent basin of the subterrestrial hemisphere is the fairly youthful appearing Imbrium Basin. The Crisium and Imbrium Basins may be related to the inferred breakups in the interval of about 580 to 700 m.y. ago, and they thus would be less than 700 and 600 m.y. old, respectively. However, the Imbrium Basin possibly may even be younger, and it might be related to the inferred 440 m.y. old collision event (Tables 21 and 22). The youngest major basin is the Orientale Basin, which is located on the leading or western edge of the moon (Fig. 31). It exhibits an exceedingly fresh appearance and may be related to the 220 m.y. old collision event. or possibly even to one of the younger events. It even may be less than 100 m.y. old. Although direct correlations cannot be made until materials are returned from one or more lunar basins, an interesting parallelism appears to exist between the general sequence in the development of the lunar basins and the general sequence in the inferred breakup history of the asteroids.

The correlations outlined above would indicate that pre-mare plains-forming materials of intermediate albedo that are seen, for example, in and near the Nectaris Basin, are less than about 900 m.y. old, and that the younger, dark mare materials, which are exposed in the floors of all basins, would be less than about 580 m.y. old (younger than the Imbrium Basin) and locally might be less than 100 m.y. old (younger than the Orientale Basin). The span of time that includes the

young Copernican System, the older Eratosthenian System, and the still older Archimedian Series of the Imbrian System, which post-dates formation of the Imbrium Basin, would fall in the interval of 0 to about 580 m.y. This interval of time, perhaps fortuitously, is essentially the same interval that is occupied by the Paleozoic, Mesozoic, and Cenozoic Eras of Earth.

The breakup history of the asteroids, if it has affected the moon in the manner discussed above, can hardly have gone unrecorded on earth. A next step is to integrate meteorite, lunar, and terrestrial information into a coherent, interrelated series of events in the impact history of the moon and the earth. An outline for the most recent of the events is discussed in the following section.

Recent Cratering of the Moon

A number of the polymict meteorite breccias listed in Table 20 may be interpreted to be lunar materials that have been driven from the moon by the impact of both cometary and asteroidal materials. The carbon-bearing and rare gas-rich howardites can be interpreted to be lunar uplands materials that have been invaded by cometary materials in one or more substantial impacts that occurred in the not very distant geologic past. Exposure ages for stones, except for the aubrites, are mostly a few tens of millions of years old, and only a few stones are as much as 50 m.y. old (Anders, 1964). The one carbon-bearing eucrite that is known, Haraiya, may be evidence that some mare materials also have been invaded by cometary materials. The existence of the fairly abundant calcium-rich mesosiderites, and of eucrites and howardites that

appear to contain materials derived from the bronzite, hypersthene, and enstatite bodies, may be considered evidence for the fairly recent impact of the lunar surface by chondritic, pallasitic, and metallic asteroidal materials.

The lunar surface is pock-marked with youthful ray craters of probable impact origin, but only a few are relatively large, about 100 km and more across (Fig. 31). Three large ray craters, Theophilus, Langrenus, and Copernicus, lie at approximately 10°N or 10°S latitude. A fourth prominent ray crater, Tycho, which is about 87 km across, lies at about 45°S latitude. A pair of fairly large ray craters, Anaxagoras and Euctomen, lie near the lunar north pole. A number of smaller, intermediate-sized ray craters, which include Aristarchus, Aristillus, Autolycus, Kepler, and Proclus, also are prominent in full moon illumination (Fig. 31). The very large ray craters would be expected to be the most likely sources of the howardites and eucrites, although the ray craters of intermediate size also could be sources of materials.

If the distinctive characteristics of certain meteorite breccias can be correlated with distinctive characteristics of the rim materials of certain lunar craters, then the composition and origin of the rim materials may be deduced, correlations become possible, and estimates of ages may be made. Some correlations seem possible. Detailed geologic mapping of the Colombo quadrangle of the moon (Fig. 31) using moderate and high resolution Lunar Orbiter photographs (Elston, in preparation; in press), has revealed the existence, in the maria and uplands, of youthful, dark to intermediate albedo halo craters of apparent impact origin.

Cratering by cometary materials. Messier and Messier A are a pair of elliptical dark halo craters, about 10 x 18 km, which lie near the central part of Mare Fecunditatis (Fig. 31). A pair of bright rays extends westward from Messier A across the maria to the Colombo uplands, a distance of more than 110 km. The ray material can be traced back to a position formerly occupied by wall material of an older crater that was partly destroyed during formation of Messier A. From this consideration, and from the braided character of fresh radial rim materials that are asymmetrically disposed in a north-south direction, Messier and Messier A are considered to be impact craters (Elston, in press). Except for their low albedo, the radial rim materials of the Messier craters are closely analogous to radial rim materials that enclose youthful bright halo and ray craters of probable impact origin. Crater wall materials of the Messier craters are fairly high in albedo, but the crater rim materials, which are low in albedo, are curiously smooth and contain only a few scattered blocks. The dark rim materials are anomalously smooth with respect to young bright halo craters, which display blocky and rubbly rim deposits. The rim materials of Messier are penetrated by two small younger craters that show that the smooth dark rim materials of Messier are underlain by normal mare material which displays a characteristic high albedo in the wall and rim materials of younger non-dark halo craters. The rim and fall-back(?) materials of Messier and Messier A appear diffusely darkened, and exhibit a smeared "out-of-focus" appearance in high resolution Lunar Orbiter photographs. The apparent comminution and the darkening of the Messier ejecta and fall-back(?) is attributed to the impact of dark, low density, easily

diffusible materials which rather thoroughly permeated the breccia and which possibly also were responsible for the apparent comminution as well as darkening; the impacting material may have been volatile-rich, icy, cometary material containing carbonaceous material (Elston, in press). In the meteorites, the diffusely darkened comminuted material of the rim deposits of the Messier craters appears to be most closely approximated by the light-dark structure that is exhibited by a few carbon- and rare gas-bearing howardites. In Kapoeta, the contact between pervasively darkened, carbon- and rare gas-bearing material, and lighter un-invaded howarditic material, can be seen to be extremely sharp and smooth in fine detail, and the light-dark contact is not marked by an obvious change in texture of the breccia (Signer and Suess, 1963). The darkening material must have been highly mobile, and its emplacement possibly was abrupt.

Several of the large and intermediate-sized craters contain dark halos in their rim materials. The most obvious dark halo encloses Tycho, and it irregularly encircles the crater, in part at some distance from the rim crest. In high resolution Lunar Orbiter photographs, materials of the dark halo appear to be smeared, diffusely darkened, and "out-of-focus". The materials appear to be virtually identical with the diffusely darkened, smooth rim and fall-back(?) materials of the Messier craters. If the dark halo materials of Tycho are inverted and returned to their assumed original positions in the area of the crater, they would lie in or near the path of penetration of the impacting body, where lunar bedrock could have been invaded by the impacting material. The author has proposed that Tycho was excavated by cometary impact,

and that the dark rim materials may be potential sources of water, rare gases, and carbon; volatiles may also be present in the form of a rather specially developed permafrost (Elston, in press).

Aristarchus is another ray crater that may have been formed by cometary impact. Cometary impact could explain the low albedo of its fairly smooth rim materials relative to the very great brightness of its crater wall and floor materials (Fig. 31).

The key to the identification of possible cometary impacts on the moon may be the development of a smooth, comminuted, diffusely darkened ejecta. Darkness of rim materials alone probably is an inadequate criterion. The impact of relatively dense, unequilibrated chondrite material containing carbon, such as pigeonite chondrite material, conceivably could result in the development of dark halo craters in which the ejecta is rubbly. Copernicus H, a small but conspicuous dark halo crater southeast of Copernicus (Fig. 31), may be such a crater (see high resolution Lunar Orbiter V photographs).

Tycho is inferred to have been produced by cometary impact on the basis of characteristics of its rim materials. Theophilus, Langrenus, and Copernicus, three very large ray craters near the lunar equatorial belt, show some darkening in their rim deposits. The rim deposits of these craters, however, do not appear to display the diffusely darkened aspect and the smooth, syrup-like texture that have been observed in the rim materials of Tycho and Aristarchus. Theophilus, Langrenus, and Copernicus thus may have been excavated by the impacts of asteroidal rather than cometary materials.

Tektites, and Lunar and Terrestrial Craters

Three of the four tektite strewn fields (American, European, and African) appear to have spatially related impact craters or crypto-explosion structures. The three fields and their structures lie in generally east-west lines. The fourth field (Australasian), which is the youngest and by far the most extensive of the tektite strewn fields, has no apparent associated terrestrial crater. The trend of its long axis is apparently NE-SW.

The origin of tektites has long been debated. A solution to the tektite problem should: 1) allow for a common mode of origin for all four tektite fields; 2) suggest an explanation for the origin of the terrestrial craters associated with three fields -- an origin that may be tested; 3) provide an explanation for the lack of an associated terrestrial crater with the fourth field; 4) provide an explanation for the E-W trends of three fields, and the NE-SW trend of the fourth field; 5) be generally compatible with chemical and age data for tektites and meteorites; 6) be compatible with lunar and terrestrial field geologic relationships; and, 7) possibly even allow for specific correlations between the tektite fields and lunar craters. The four tektite fields are discussed briefly in order of decreasing age. Following this, a correlation with lunar craters is proposed, a model for tektite and mesosiderite formation is suggested, and implications regarding the age of the lunar Copernican System are briefly discussed.

The American tektites and the Sierra Madera structure. Bediasites of east Texas have been found in gravels at the top of the Jackson group of late Eocene age, which indicates a possible post-Jackson age

(E.C.T. Chao and others, personal communication, 1961). Some bediasites are reported to occur in the Jackson group, which would then suggest that the Jackson group possibly extends into the Oligocene (Faul, 1966) because the bediasites have a K-Ar age of about 34 m.y. (Zähringer, 1963).

The Georgia tektites occur about 1250 km east of the bediasite locality, in gravels that unconformably overlie Eocene, Oligocene, and Miocene rocks, and they could have been derived from any of these rocks (Faul, 1966). Seven Georgia tektites and the Martha's Vineyard tektite, have been analyzed chemically for the major elements and for 22 minor elements (Cuttitta and others, 1967); they are compositionally similar to the bediasites.

The Sierra Madera crypto-explosion structure, near Fort Stockton in western Texas, lies about 700 km west of the bediasite locality. Sierra Madera consists of a central breccia lens, more than 1.5 km across. The breccia lens lies near the center of a circular, slightly structurally depressed basin that is about 13 km across. The small, central, structurally disrupted area, which contains shatter cones, is bordered by a complex faulted zone in which beds locally are displaced outward along low angle overthrust faults (Eggletton and Shoemaker, 1961). Recently completed mapping has revealed that the central brecciated area contains beds that are displaced radially inward and upward (Wilshire and others, 1967). This mode of displacement apparently was responsible for the structural and topographic elevation of the central part of the Sierra Madera structure. The breccia lens may have been central peak material that at one time underlay the floor of a now

eroded impact crater. Sierra Madera, from its relations to the surrounding Edwards Plateau, is possibly Eocene or younger in age. It and the Texas and Georgia tektite localities describe an essentially straight, east-west line that is about 2000 km long.

The European tektites and the Ries and Steinheim Basins. The moldavites and moravian tektites of Czechoslovakia have been reworked and occur in young gravels; they have been dated by K-Ar methods at about 14.9 m.y. (Gentner and others, 1963). The two strewn fields lie about 140 km apart on an east-west line. About 260 km west of the tektite fields, and lying on an essentially straight line, are the Ries and Steinheim Basins of Bavaria. The Nördlinger Ries is large, about 27 km in diameter; the much smaller Steinheim Basin is about 4 km in diameter. Identification of coesite (greater than 25 kb SiO_2) in breccias in the Ries Basin and recognition of suevite as an explosion-produced breccia (Shoemaker and Chao, 1961) has established the Rieskessel as an impact crater. Impact glass of the Ries Basin is approximately the same age as the moldavites (Gentner and others, 1963).

The African tektites and Bosumtwi Crater. The Ivory Coast tektites of Ghana are dated at about 1.3 m.y., as is the impact glass of Bosumtwi Crater (Gentner and others, 1963). Bosumtwi Crater lies about 300 km east-southeast of the strewn field. It is about 11 km in diameter, which is less than half the diameter of the Rieskessel, and it appears to be a bit smaller than the crater that may be inferred to have once overlain the Sierra Madera structure.

The Rb-Sr isochron for the Ivory Coast tektites differs from the isochron for the other tektites, and falls on the isochron for the

approximately 2 b.y. old suite of rocks that make up the region (Schnetzler and others, 1967). The coincidence indicated to Schnetzler and others (1967) that the Ivory Coast tektites are related to the phenomenon that formed Bosumtwi Crater. The Texas, Czechoslovakian, and Australasian tektites exhibit a 400 m.y. isochron (Schnetzler and others, 1967) which has not yet been explained in terms of either the terrestrial or lunar production of tektites. Because of this, the Rb-Sr correlation of the Ivory Coast tektites and the impact glass of Bosumtwi Crater cannot be used as definitive evidence for the terrestrial production of tektites, as has been proposed by Faul (1966). An alternative solution is that the Bosumtwi Crater glass includes material of the impacting bolide, and that elemental similarities existed between the bolide materials and the tektite materials. Such a relationship may be likely because nickel-bearing spherules have been discovered in Bosumtwi Crater suevite, which is indicative of the impact origin of the glass (El Goresy, 1966). The glass thus also should contain other materials, and elements, that have been derived from the impacting bolide. The one type of metal-bearing meteorite that contains silicates that are chemically related to the pyroxene-plagioclase achondrites and the tektites, is calcium-rich mesosiderite.

The Australasian tektites. The tektites of the Australasian strewn field, from K-Ar and fission track methods, are about 700,000 years old (Zähringer, 1963; Fleisher and Price, 1965). They occur, on land, in an extensive, apparent north-south trending belt that extends from China to southern Australia. Their marine extent, as micro-tektites, is from north of the Phillippine Islands to south of

Madagascar (Cassidy and others, 1967), a distance of about 11,000 km in a NE-SW direction. The Australasian microtektites range from tektite composition to a composition that is similar to basaltic rocks or (basaltic) achondrites (Cassidy and others, 1967). Their mass, estimated at a minimum of 150 million tons, essentially rules out a terrestrial source (Cassidy and others, 1967). No terrestrial crater is known that could be associated with this very young and very extensive tektite field.

Proposed origin for the Australasian tektite field. Evidence for the possible cometary origin of Tycho has been reviewed earlier. Tycho is one of the youngest ray craters on the moon. It lies at about 45°S latitude in the lunar uplands, and its ray system extends over much of the subterrestrial hemisphere of the moon (Fig. 31). The extensiveness of its rays indicates that the Tycho cratering event was extremely energetic, which could have been the result of a high speed impact such as would occur from a comet in a near-parabolic, retrograde orbit. A "new" cometary body in a near-parabolic orbit presumably would be in a nearly original accretionary condition, and presumably would consist largely of ices that had yet to be ablated by solar radiation. As seen in Lunar Orbiter IV and V photographs, extremely intense "volcanism" appears to have occurred in the floor of Tycho after impact; "ponds" occur in the rim materials; and the dark rim materials display flow-like textures. The features in the floor and rim materials may be due to the injection of large amounts of volatiles into brecciated bedrock at the time of impact. The impact-induced "volcanism" in the floor materials

conceivably would be augmented and sustained by excess volatiles to temperatures lower than those associated with a dryer "volcanism".

The lack of a dense core in a cometary body (Fig. 22; Table 2) would preclude the development of mesosideritic impactite material. A high energy impact, however, would be expected to fuse a large amount of lunar bedrock. Rim and ray materials of Tycho, which almost certainly are highly brecciated, are fairly symmetrically distributed around the crater. By analogy with terrestrial cratering experiments, materials in the central zone of fusion probably were ejected at higher angles from the crater than much of the brecciated ray and rim materials. For this reason, much of the Tycho ejecta that may be inferred to have attained escape velocity probably was lost from the central, most intensely shocked region of the crater, and would have left the moon in a direction that was nearly normal to the lunar surface. A mass or train of fused silicate droplets ejected from Tycho in a direction normal to the lunar surface would be injected into a path that lay at a relatively high angle to the plane of the earth-moon system. Such material would be available for capture by the earth at some relatively high angle to the equator.

The youthfulness of the Australasian tektite field and the relative youthfulness of Tycho; the NE-SW trend of the Australasian field and the 45°S latitude location of Tycho on the lunar surface; the abundance of the Australasian tektites and the apparent very highly energetic character of the Tycho event; the lack of a terrestrial crater for the Australasian tektites and lunar field geologic relations which suggest that Tycho was excavated by cometary impact (with no generation of

mesosideritic material) are characteristics that point to a genetic relationship between Tycho and the Australasian tektite field. If the correlation is valid, Tycho is about 700,000 years old.

Proposed origin for the American, European, and African tektite fields and their craters. An intriguing coincidence exists with regard to the relative size and relative age of the very large ray craters near the lunar equator, and the relative size and relative age of impact structures associated with the east-west trending tektite fields. Three large craters, Theophilus (~ 100 km), Langrenus (~ 130 km), and Copernicus (~ 95 km) lie about 10°N or 10°S latitude. Theophilus, which is marked by a faint ray pattern, is the oldest; Copernicus, with its bright ray pattern, is the youngest and it appears comparable in age with Tycho (Fig. 31). Materials ejected nearly normal to the lunar surface from these three craters would be in paths that would lie in or near the plane of the earth-moon system. The materials thus would be available for capture by the earth from overtaking or apparent retrograde orbits in and near this plane, which would give rise to east-west trending strewn fields.

A key question concerns the origin and character of the material that formed the terrestrial craters associated with the tektite fields. As suggested for Bosumtwi Crater, calcium-rich mesosiderite is the only type of metalliferous meteorite that contains silicates that can be related to both the pyroxene-plagioclase achondrites and the tektites. It is proposed that the Sierra Madera structure (13 km, and inferred to be about 34 m.y. old), the Ries Basin (27 km, and about 15 m.y. old), and Bosumtwi Crater (11 km, and about 1.3 m.y. old) were formed by the

impact of mesosideritic material that was ejected with tektite material from the lunar craters Theophilus, Langrenus, and Copernicus, respectively.

Dense mesosiderite is tough and could survive entry into the atmosphere as a fairly coherent mass, rather than be dispersed as a shower of fragments. Silicates of the mesosiderites are "basaltic", and they could be dispersed into terrestrial breccias and escape notice as extraterrestrial materials. The dispersal of metal from mesosideritic material during the terrestrial impact also may pose no special problem. Remnants of Canyon Diablo iron, which excavated Meteor Crater, are not obvious in the brecciated wall and fall-back materials, although tiny, commonly microscopic, droplets of metal locally may be found dispersed in the breccia. The irons that are preserved around Meteor Crater are rim and plains specimens that appear not to have taken part in the main cratering event. Suevite of the Ries and Bosumtwi Craters should be examined for relicts of mesosideritic material.

If mesosideritic material was the cause of the terrestrial cratering, the material that entered the atmosphere must have been accompanied by a train of tektites, which probably mostly fell short of the impact sites. The concomitant fall of tektites and mesosiderites would indicate that they were produced together and that they left the moon together, probably as a dense slug of metal and highly shocked silicates that was accompanied by a swarm of glassy particles.

The correlation proposed here is that Theophilus, Langrenus, and Copernicus were excavated by the impact of asteroidal materials, which presumably encountered the moon in overtaking orbits that lay in the

plane of the ecliptic. The correlations, if valid, have the effect of establishing an approximate absolute age limit for the Copernican System, which presently is defined solely on the basis of being able to discern ray material of probable impact craters having an albedo higher than that of background material. Theophilus, which exhibits faint rays and subdued radial rim materials, is one of the oldest recognized Copernican craters. If the proposed correlation is valid, the span of the Copernican System is approximately 35 million years. The Eratosthenian System, which includes relatively young craters that have "aged" sufficiently so that rays are no longer discernible, and the Imbrian System, which includes mare materials and pre-mare craters that post-date the formation of the Imbrium Basin, would thus lie in the interval of about 35 to perhaps about 580 million years.

APPENDIX I

Sources of data for Table 4 - Elemental Abundances of Meteoritic Materials.

Explanation:

<u>Calcium-poor</u>	<u>Calcium-rich</u>
Cc - Carbonaceous chondrite	Di-Ol - Diopside-olivine
Ca - Carbonaceous achondrite	Au - Augite
Pc - Pigeonite chondrite	Px-Plag - Pyroxene-plagioclase
Pa - Pigeonite achondrite	Ho - Howardite
Hc - Hypersthene chondrite	Eu - Eucrite
Ha - Hypersthene achondrite	
Bc - Bronzite chondrite	
Ec - Enstatite chondrite	
Ea - Enstatite achondrite	

The meteorite name is given where one to three meteorites are involved. Where one or more meteorites strongly affect an average value, alternate average values using all meteorites analyzed are shown in parentheses.

<u>Meteorite class</u>	<u>Number of meteorites</u>	<u>Meteorite name</u>	<u>Parts per million</u>	<u>Reference</u>
<u>CESIUM</u>				
<u>Calcium-poor</u>				
Cc	1	Mighei	0.12	Hey, 1966
Ca	1	Ivuna	0.18	"
Pc	1	Felix	0.045	"
Pa	-	--	---	
Hc	16		0.050	"
Ha	1	Johnstown	0.0076	"
Bc	13		0.0885	"
Ec	-	--	---	
Ea	1	Khor Temiki	0.060	"
<u>Calcium-rich</u>				
Di-Ol	-	--	---	
Au	-	--	---	
Px-Plag				
Ho	-	--	---	
Eu	4		0.0116	Hey, 1966; Duke, 1965a

APPENDIX I Continued

<u>Meteorite class</u>	<u>Number of meteorites</u>	<u>Meteorite name</u>	<u>Parts per million</u>	<u>Reference</u>
<u>RUBIDIUM</u>				
<u>Calcium-poor</u>				
Cc	2	Mighei, Murray	1.68	Hey, 1966; Smales & others, 1967; Murthy & Compston, 1965
Ca	2	Ivuna, Orgueil	2.28	"
Pc	3	Mokoia, Felix Lancé	1.33	Hey, 1966
Pa	-	--	---	
Hc	23		4.25	"
Ha	1	Johnstown	0.14	"
Bc	19 (20		3.77 4.29)	"
Ec	-	--	---	
Ea	2	Bishopville, Khor Temiki	1.79	"
<u>Calcium-rich</u>				
Di-01	-	--	---	
Au	-	--	---	
Px-Plag				
Ho	-	--	---	
Eu	4		0.23	Hey, 1966; Duke, 1965a
<u>POTASSIUM</u>				
<u>Calcium-poor</u>				
Cc	7		375	Hey, 1966
Ca	3	Alais, Ivuna, Orgueil	493	"
Pc	5 (6		444 604)	" "
Pa	1	Goalpara	60	"
Hc	51		872	"
Ha	2	Johnstown, Tatahouine	15	"
Bc	40 (41		810 834)	" "
Ec	5		756	"
Ea	5 (6		226 374)	" "
<u>Calcium-rich</u>				
Di-01	1	Nakhla	1020	"

APPENDIX I Continued

<u>Meteorite class</u>	<u>Number of meteorites</u>	<u>Meteorite name</u>	<u>Parts per million</u>	<u>Reference</u>
<u>POTASSIUM (Continued)</u>				
<u>Calcium-rich</u>				
Au	1	Angra	1600	Mason, 1962a
Px-Plag				
Ho	3		182	Hey, 1966
Eu	8		412	"
	(9		522)	"
<u>SODIUM</u>				
<u>Calcium-poor</u>			<u>Weight percent</u>	
Cc	11		0.40	Mason, 1963a
Ca	3		0.55	"
	(4		1.01)	"
Pc	7		0.40	"
Pa	2		0.32	Wood, 1963a
Hc	68		0.70	Mason, 1965
Ha	3		0.23	Mason, 1963d
Bc	36		0.64	Mason, 1965
Ec	11		0.66	Mason, 1966
Ea	4		0.98	Wood, 1963a
<u>Calcium-rich</u>				
Di-Ol	1	Nakhla	0.30	Prior, 1912
Au	1	Angra	0.19	Mason, 1962a
Px-Plag				
Ho	3		0.24	Mason, 1967b;
				Mason & Wiik, 1966a;
Eu	13		0.32	Urey & Craig, 1953
<u>LITHIUM</u>				
<u>Calcium-poor</u>			<u>Parts per million</u>	
Cc	1	Mighei	0.5	Hey, 1966
Ca	1	Orgueil	1.3	"
Pc	-	--	---	
Pa	-	--	---	
Hc	15		2.5	Hey, 1966
Ha	1	Tatahouine	0.81	"
Bc	9		2.8	"
Ec	1	Abee	1.3	"
Ea	-	--	---	
<u>Calcium-rich</u>				
Di-Ol	-	--	---	
Au	-	--	---	
Px-Plag				
Ho	-	--	---	
Eu	1	Sioux County	8	Fireman & Schwarzer, 1957

APPENDIX I Continued

<u>Meteorite class</u>	<u>Number of meteorites</u>	<u>Meteorite name</u>	<u>Parts per million</u>	<u>Reference</u>
<u>BARIUM</u>				
<u>Calcium-poor</u>				
Cc	2	Mighei, Murray	3.2	Hey, 1966
Ca	1	Orgueil	4.3	"
Pc	5		11.5	"
Pa	-	--	---	
Hc	62		11.3	"
	(70		25.6)	"
Ha	2	Johnstown, Shalka	3.2	Hey, 1966
Bc	41		8.1	"
	(46		26.7)	"
Ec	5		5.2	"
	(6		10.1)	"
Ea	2	Cumberland Falls, Norton County	8	"
<u>Calcium-rich</u>				
Di-Ol	1	Nakhla	11 (in pyroxene)	Duke, 1965a
Au	1	Angra	26.4	Schnetzler & Phil- potts, 1967
Px-Plag				
Ho	1	Bununu	18.5	Philpotts & others, 1967
	(2	Bununu, Binda	10.2)	Duke, 1965a
Eu	6		32	"
<u>STRONTIUM</u>				
<u>Calcium-poor</u>				
Cc	2	Murray, Cold Bokkeveld	9.7	Murthy & Compston, 1965; Hey, 1966
Ca	1	Orgueil	8.3	Murthy & Compston, 1965
Pc	6		18.1	Murthy & Compston, 1965; Hey, 1966
Pa	-	--	---	
Hc	33		16.8	Hey, 1966
Ha	1	Johnstown	3	"
Bc	21		12.1	"
Ec	5		18.2	"
Ea	1	Bishopville	12.2	"

APPENDIX I Continued

<u>Meteorite class</u>	<u>Number of meteorites</u>	<u>Meteorite name</u>	<u>Parts per million</u>	<u>Reference</u>
<u>STRONTIUM</u> (Continued)				
<u>Calcium-rich</u>				
Di-Ol	1	Nakhla	59.6	Pinson & others, 1965
Au	-	--	---	
Px-Plag				
Ho	1	Binda	37	Duke, 1965a
Eu	6		82.4	Duke, 1965a; Hey, 1966
<u>CALCIUM</u>				
<u>Calcium-poor</u>			<u>Weight percent</u>	
Cc	11		1.28	Mason, 1963a
Ca	4		1.03	"
Pc	7		1.74	"
Pa	2		0.56	Wood, 1963a
Hc	68		1.34	Mason, 1965
Ha	6		1.02	Mason, 1963d
Bc	36		1.25	Mason, 1965
Ec	11		0.94	Mason, 1966
Ea	4		0.65	Wood, 1963a
<u>Calcium-rich</u>				
Di-Ol	1	Nakhla	10.77	Prior, 1912
Au	1	Angra	6.06	Mason, 1962a
Px-Plag				
Ho	8		5.47	Urey & Craig, 1953
Eu	13		7.23	"
<u>MAGNESIUM</u>				
<u>Calcium-poor</u>				
Cc	11		12.76	Mason, 1963a
Ca	4		9.26	"
Pc	7		15.39	"
Pa	2		21.54	Wood, 1963a
Hc	68		15.17	Mason, 1965
Ha	7		15.92	Mason, 1963d
Bc	36		14.19	Mason, 1965
Ec	11		12.43	Mason, 1966
Ea	4		21.66	Wood, 1963a
<u>Calcium-rich</u>				
Di-Ol	1	Nakhla	7.24	Prior, 1912
Au	1	Angra	6.06	Mason, 1962a

APPENDIX I Continued

<u>Meteorite class</u>	<u>Number of meteorites</u>	<u>Meteorite name</u>	<u>Weight percent</u>	<u>Reference</u>
MAGNESIUM (Continued)				
Calcium-rich (Continued)				
Px-Plag				
Ho	8		7.09	Urey & Craig, 1953
Eu	13		5.10	"
<u>ALUMINUM</u>				
Calcium-poor				
Cc	11		1.16	Mason, 1963a
Ca	4		0.93	"
Pc	7		1.53	"
Pa	2		0.20	Wood, 1963a
Hc	68		1.33	Mason, 1965
Ha	5		0.80	Mason, 1963d
Bc	36		1.41	Mason, 1965
Ec	11		1.04	Mason, 1966
Ea	4		0.35	Wood, 1963a
Calcium-rich				
Di-Ol	1	Nakhla	0.92	Prior, 1912
Au	1	Angra	4.69	Mason, 1962a
Px-Plag				
Ho	8		0.53	Urey & Craig, 1953
Eu	13		0.69	"
<u>SILICON</u>				
Calcium-poor				
Cc	11		13.28	Mason, 1963a
Ca	4		10.36	"
Pc	7		15.39	"
Pa	2		18.13	Wood, 1963a
Hc	68		18.58	Mason, 1965
Ha	7		24.62	Mason, 1963d
Bc	36		16.93	Mason, 1965
Ec	11		18.05	Mason, 1966
Ea	4		25.17	Wood, 1963a
Calcium-rich				
Di-Ol	1	Nakhla	22.81	Prior, 1912
Au	1	Angra	20.77	Mason, 1962a
Px-Plag				
Ho	8		22.96	Urey & Craig, 1953
Eu	13		22.18	"

APPENDIX I Continued

<u>Meteorite class</u>	<u>Number of meteorites</u>	<u>Meteorite name</u>	<u>Weight percent</u>	<u>Reference</u>
<u>IRON</u>				
<u>Calcium-poor</u>				
Cc	8	FeS	5.46	Wiik, 1956 Mason, 1963a (Est. D.P.E.)
		FeO	15.59	
	11	Metal	0.15	
		Total	22.13	
Ca	3	FeS	10.7	Wood, 1963a Mason, 1963a
		FeO	8.02	
	4	Metal	0.11	
		Total	18.24	
Pc	5	FeS	3.87	Mason, 1963a
		FeO	18.90	
	7	Metal	2.34	
		Total	24.74	
Pa	2	FeS	---	Wood, 1963a
		FeO	9.89	
		Metal	8.13	
		Total	18.02	
Hc	68	FeS	3.86	Mason, 1965
		FeO	11.39	
		Metal	6.28	
		Total	21.53	
Ha	4	FeS	0.71	Urey & Craig, 1953
		FeO	12.47	
		Metal	0.79	
		Total	13.97	
Bc	36	FeS	3.35	Mason, 1965
		FeO	7.47	
		Metal	16.79	
		Total	27.61	
Ec	8	FeS	6.81	Wood, 1963a
		FeO	1.31	
		Metal	19.82	
		Total	27.94	
Ea	4	FeS	0.80	Wood, 1963a
		FeO	0.75	
		Metal	2.29	
		Total	3.84	

APPENDIX I Continued

<u>Meteorite class</u>	<u>Number of meteorites</u>	<u>Meteorite name</u>	<u>Weight percent</u>	<u>Reference</u>
<u>IRON</u> (Continued)				
Calcium-rich				
Di-Ol	1	Nakhla	FeS 0.11	Prior, 1912
			FeO 16.19	
			Metal ---	
			Total 16.30	
Au	1	Angra	FeS 0.80	Mason, 1962a
			FeO 7.92	
			Metal ---	
			Total 8.72	
Px-Plag				
Ho	8		FeS 0.38	Urey & Craig, 1953
			FeO 13.25	
			Metal 0.35	
			Total 13.98	
Eu	13		FeS 0.36	Urey & Craig, 1953
			FeO 12.83	
			Metal 1.18	
			Total 14.37	
<u>NICKEL</u>				
Calcium-poor				
Cc	8		NiO 1.23	Wiik, 1956
			Metal 0.16	
			Total 1.39	
Ca	3		NiO 0.92	Wiik, 1956
			Metal 0.02	
			Total 0.94	
Pc	5		NiO 0.26	Wiik, 1956
			Metal 1.08	
			Total 1.34	
Pa	2		Metal 0.15	Wood, 1963a
Hc	68		Metal 1.10	
Ha	4		Metal 0.03	Urey & Craig, 1953
Bc	36		Metal 1.63	
Ec	11		1.64	Mason, 1965
Ea	4		NiO 0.20	
			Metal 0.17	Wood, 1963a
			Total 0.37	

APPENDIX I Continued

<u>Meteorite class</u>	<u>Number of meteorites</u>	<u>Meteorite name</u>	<u>Weight percent</u>	<u>Reference</u>
<u>NICKEL (Continued)</u>				
<u>Calcium-rich</u>				
Di-Ol	1	Nakhla	---	Prior, 1912
Au	1	Angra	---	Mason, 1962a
Px-Plag				
Ho	8	Metal	0.10	Urey & Craig, 1953
Eu	13	Metal	---	"
<u>SCANDIUM</u>				
<u>Calcium-poor</u>			<u>Parts per million</u>	
Cc	2	Mighei, Murray	9.95	Hey, 1966
Ca	2	Ivuna, Orgueil	5.55	"
Pc	5		10.42	"
Pa	-	--	---	
Hc	4		8.59	"
Ha	2	Johnstown, Shalka	11.90	"
Bc	18		9.66	"
Ec	6		7.75	"
Ea	1	Norton County	9.00	"
<u>Calcium-rich</u>				
Di-Ol	2	Nakhla, Lafayette	66.00	"
Au	1	Angra	---	Mason, 1962a
Px-Plag				
Ho	1		19	Duke, 1965a
Eu	6		30.90	Duke, 1965a, Hey, 1966
<u>LANTHANIUM</u>				
<u>Calcium-poor</u>				
Cc	2	Mighei, Murray	0.34	Hey, 1966
Ca	2	Ivuna, Orgueil	0.19	"
Pc	2	Felix, Mokoia	0.40	"
Pa	-	--	---	
Hc	4		0.35	"
Ha	2	Johnstown, Shalka	0.03	"
Bc	3		0.31	"
Ec	2	Abee, Indarch	0.23	"
Ea	1	Norton County	0.21	"
<u>Calcium-rich</u>				
Di-Ol	2	Nakhla, Lafayette	1.67	"
Au	-	--	---	

APPENDIX I Continued

<u>Meteorite class</u>	<u>Number of meteorites</u>	<u>Meteorite name</u>	<u>Parts per million</u>	<u>Reference</u>
<u>LANTHANIUM</u> (Continued)				
Calcium-rich (Continued)				
Px-Plag				
Ho	-	--	---	
Eu	4		3.66	Hey, 1966
<u>YTTRIUM</u>				
Calcium-poor				
Cc	1	Mighei	1.77	"
Ca	2	Ivuna, Orgueil	1.56	"
Pc	2	Felix, Mokoia	2.43	"
Pa	-	--	---	
Hc	4		2.08	"
Ha	2	Johnstown, Shalka	0.72	"
Bc	1	Miller	2.09	"
Ec	2	Abee, Indarch	1.24	"
Ea	1	Norton County	2.09	"
Calcium-rich				
Di-Ol	2	Nakhla, Lafayette	3.78	"
Au	-	--	---	
Px-Plag				
Ho	-	--	---	
Eu	6		21.8	Hey, 1966; Duke, 1965a
<u>CERIUM</u>				
Calcium-poor				
Cc	2	Mighei, Murray	0.87	Hey, 1966
Ca	2	Ivuna, Orgueil	0.62	"
Pc	2	Felix, Mokoia	1.07	"
Pa	-	--	---	
Hc	4		1.36	"
Ha	-	--	---	
Bc	3		0.63	"
Ec	3		0.58	"
Ea	1	Norton County	0.81	"
Calcium-rich				
Di-Ol	2	Nakhla, Lafayette	5.83	"
Au	1	Angra	20.6	Schnetzler & Phil- potts, 1967
Px-Plag				
Ho	1		4.02	
Eu	4		7.32	Philpotts & others, 1967

APPENDIX II

Notes and References for Table 20

1. Carbon, water, and rare gases appear to have been derived either from little-metamorphosed chondritic materials of the same genetic group (restricted polymict), or introduced from carbonaceous meteorite (cometary?) material (compound polymict). Fractionated rare gases are associated with little-metamorphosed, unbrecciated chondrites (such as the pigeonite chondrites and unequilibrated ordinary chondrites), and thus may reflect gas loss during mild metamorphism. Unfractionated rare gases occur in some brecciated meteorites and irons, and are associated with shock effects (see discussion by Anders, 1964, p. 673-679). It is here inferred that the unfractionated rare gases are cometary in origin, and were introduced during comet-asteroid collisions.
2. Association of chondrite, achondrite, stony-iron and iron shown in proposed genetic classification of the meteorites (table 2).
3. Mokoia, Karoonda, and Vigarano are unbrecciated. Carbon, water, and rare gases are thus intrinsic to the component 1 matrix of these. All pigeonite chondrites show fractionated rare gas (Anders, 1964, table 8). This suggests that no carbonaceous meteorite material has intruded members of this class.
4. Dyalpur, Goalpara, and Novo Urei contain carbon and associated diamond (Vinogradov and Vdovykin, 1963); water (Wood, 1963a, table 10), and fractionated primordial rare gases associated with shock effects (Stauffer, 1961a) are reported for two of these. Anders (1964, p. 674) has suggested a collision event to explain the introduction of carbonaceous material and primordial rare gas. The fractionated character of the rare gases suggests that they and the hydrated carbonaceous material may have been derived from unmetamorphosed (crustal) pigeonite chondrite materials during an interasteroidal collision. Metal is associated with structurally discordant diamond-bearing carbonaceous material in Novo Urei (see Carter and Kennedy, 1964, fig. 7). Relations indicate that a source of metal, either from the pigeonite body or from another asteroidal body, was available for injection during brecciation. The ureilites are restricted polymict, and may be compound polymict breccias.
5. Fractionated primordial rare gas and shock effects are reported for a single hypersthene chondrite, Mezö-Madaras by J. Geiss (personal communication to Anders, 1964, table 8). This chondrite is one of the least metamorphosed of the hypersthene chondrites (L-3 of Van Schmus and Wood, 1967; Hh-2 of the proposed mineralogic-petrologic classification, table 9). The specimen of Mezö-Madaras in the Arizona State University Collection displays an essentially unbrecciated assemblage of

APPENDIX II Continued

components 1, 2, and 3. Jarosewich (1967) reports carbon and water in Mezö-Madaras. The primordial rare gases (and water) probably reside in component 1 material, which was incorporated in the material at the time of accretion.

6. Carbon and rare gases that are associated with the dark parts of light-dark structure, and in one case, diamond have been reported. Rare gases, both fractionated and unfractionated, are associated with carbon and shock effects (Anders, 1964, table 8, fig. 25, and p. 677-678). The unfractionated rare gases suggest cometary impact.

7. Achondrite fragment in Breitscheid compound polymict bronzite chondrite (see Wlotzka, 1963; Anders, 1964).

8. Weekeroo Station is a rare gas-rich, brecciated octahedrite that contains high Ar^{40} concentrations for which an age of about 10^{10} yr has been calculated (Rancitelli and others, 1967). Washington County is a rare gas-rich, nickel-rich ataxite (all nickel-rich ataxites are in Ga-Ge group IV; see Lovering and others, 1957). Washington County contains unfractionated rare gases associated with shock effects (Anders, 1964, table 8, and p. 678). Unfractionated rare gases suggest cometary impact.

9. All enstatite chondrites contain fractionated primordial rare gases and carbon (Zähringer and Gentner, 1960; Signer and Suess, 1963; Zähringer, 1962a; Anders, 1964, table 8). Of the ten enstatite chondrites known at least one (Indarch; specimen in the Arizona State University Collection) is essentially unbrecciated. It is relatively unmetamorphosed (E-4 class of Van Schmus and Wood, 1967; E-3 class of the proposed mineralogic-petrologic classification, table 9), and displays components 1, 2, and 3. Indarch is water-bearing (Wiik, 1956). The carbon, rare gases and water thus apparently are intrinsic to the component 1 matrix material of Indarch, and by extension to the component 1 matrix of the other enstatite chondrites. The lack of unfractionated gases suggests no invasion by carbonaceous meteorite (cometary) material.

10. Three aubrites are included here (Khor Temiki; Norton County; Pesyanoe), which contain large amounts of trapped "solar" (unfractionated) rare gases (Eberhardt and others, 1965). Water (Wood, 1963a, table 10) and carbon (C. B. Moore, personal communication, 1967) have been reported for some aubrites. The unfractionated rare gases in Pesyanoe (Anders, 1964, fig. 25) are inferred to have been derived from carbonaceous meteorite (cometary) material. A fourth carbon-bearing aubrite, Shallowater, contains a large amount of trapped fractionated rare gas (Eberhardt and others, 1965). Shallowater may contain rare gases and carbonaceous material derived from little-metamorphosed (crustal) enstatite parent body materials.

APPENDIX II Continued

11. The Bencubbin (Lovering, 1962) and Weatherford (Mason and Nelen, 1967) mesosiderites have silicates that are compositionally similar to the enstatite chondrites and achondrites, and they contain dark admixed materials of possible carbonaceous meteorite or enstatite chondrite origin. Weatherford contains fractionated rare gases (Stauffer, 1962) and carbon and water (Mason and Nelen, 1967). The fractionated rare gases suggest that Weatherford was invaded by enstatite chondrite material and is a restricted polymict breccia. Bencubbin contains admixed hypersthene chondrite material (McCall, 1967) and is a compound polymict breccia. Possibly related mesosiderites are listed in table 19.

12. High Ar^{40} contents (Fisher, 1965) occur in Canyon Diablo and Toluca irons (Ga-Ge group I; Lovering and others, 1957; Wasson, 1967b). The rare gases, and the carbon and troilite nodules (which locally are diamond-bearing; see Carter and Kennedy, 1964) are inferred to have been emplaced by the impact of a carbonaceous meteorite (cometary) body. See table 19 for possibly related materials.

13. Danville and Parnallee are described by Wahl (1952) as polymict breccias that contain fragments of "white chondrite". Preliminary examination of Parnallee (specimen No. 93a, Arizona State University Collection) reveals that it probably is not a polymict breccia, but rather that it is a coarse accretionary aggregate; component 3 materials in it appear to consist both of hypersthene and enstatite (iron-poor or iron-free) silicates, the duality being somewhat analogous to the two apparent component 3 materials observed in the pigeonite chondrite, Vigarano. Danville was not examined. Kelley, a white to gray brecciated hypersthene chondrite (Hey, 1966), contains white (enstatite?) fragments in a hypersthene chondrite matrix. It may be a brecciated version of Parnallee, and thus a monomict breccia; however, it could be a compound polymict breccia that correlates with other enstatite-hypersthene mixtures.

14. Three chondrites (Bandong; Jelica; Manbhoom) are reported by Wahl (1952) to contain fragments of amphoterite (hypersthene achondrite?) embedded among smaller fragments and splinters of olivine and bronzite, and to also contain fragments of several kinds of chondrites. Homestead is classed as a hypersthene chondrite by Mason (1963c) and a bronzite chondrite by Keil and Fredriksson (1964), who raised the question of a mixture. Ness County (1894) was classed as a hypersthene chondrite by Mason (1963c) and a bronzite chondrite by Knox (1963); a mixture is possible. Plainview, classed as a polymict brecciated veined intermediate bronzite chondrite by Hey (1966), is reported by Wahl (1952) to contain black chondrite and rodite (hypersthene achondrite?) fragments.

15. Hainaut is reported by Wahl (1952) to contain white chondrite (enstatite?) fragments, black fragments of chondrite and ophitic texture; white fragments may be analogous to those in Parnallee

APPENDIX II Continued

(Appendix II, footnote 13), and this meteorite may be a polymict bronzite-eucrite mixture. Leighton is reported by Wahl (1952) to contain angular fragments of white (enstatite?) chondrite. Pulsora is reported by Wahl (1952) to contain white (enstatite?) fragments, eucrite fragments, and gray fragments; white fragments may be analogous to those in Parnallee (Appendix II, footnote 13), and the presence of eucrite fragments suggest that this may be a bronzite-eucrite mixture.

16. Most of these are polymict breccias as listed by Hey (1966), many of which were described or listed by Wahl (1952). In Arriba, Wahl observed achondritic fragments of basic volcanic rock and crystalline igneous rock ("diogenite"); may be a hypersthene chondrite-eucrite mixture, or a hypersthene chondrite-achondrite mixture. Chandakapur is noted as a complex polymict breccia (Wahl, 1952). Harrison County, Ottawa, and Shelburne are reported to have a "diogenite" (hypersthene achondrite?) matrix (Wahl, 1952).

17. Most of these are polymict breccias as listed by Hey (1966), many of which were described or listed by Wahl (1952). Fleming and Ochansk contain fine grained microcrystalline fragments of basic volcanic rock (Wahl, 1952); may be bronzite-eucrite mixtures. Hugoton contains fragments of black chondrite (Wahl, 1952).

18. Cumberland Falls enstatite achondrite contains fragments of black chondrite material reported by Lovering (1962) to be metamorphosed hypersthene chondrite. Anders and Goles (1961) and Binns (1967) report inclusions of enstatite chondrite. Both may be present (see Appendix II, footnote 11).

19. The hypersthene achondrites, which nominally are monomict breccias and consist of large crystals of pyroxene in a finely crushed groundmass of pyroxene, are here considered to be restricted(?) polymict on the basis of accessory metal and troilite (see Mason, 1963d) in the breccias. Angular fragments of metal occur in the matrix of Johnstown (Arizona State University Collection) indicating a disruption and an injection of metal at the time of brecciation. Mason (1963d) notes that in Tatahouine, the only diogenite which shows an apparently uncrushed structure (but which is friable and which broke into innumerable pieces at the time of fall), that metal was observed to occur as thin plates on the surfaces of the pyroxene grains. The metal may have been derived from nearby core material.

20. All nine aubrites are tentatively included here. Metal appears to be a minor constituent in the brecciated parts of several (all?) aubrites, including the carbon-bearing aubrite, Norton County (Arizona State University Collection). The sparse metal appears to have been injected at the time of brecciation. It may have been derived from

APPENDIX II Continued

disrupted metalliferous enstatite(?) chondrite materials, from core material of the enstatite body, or from the impacting materials.

21. See table 19; and Appendix II, footnote 11.

22. Bondoc Peninsula mesosiderite; see table 19.

23. Budulan and Lujan(?) mesosiderites; see table 19.

24. Admire pallasite (University of Arizona Collection, specimen No. 8370; Eagle Station pallasite (Mason, 1962a, fig. 45).

25. See table 19.

26. Classification as to howardites and eucrites is from Mason (1967b). All howardites and eucrites technically may be compound polymict breccias if the metal and troilite that they contain are derived from calcium-poor meteoritic materials and were intruded during brecciation. As a generalization, the howardites appear to have undergone more extensive brecciation, probably as the result of multiple events, than the eucrites. The brecciation in eucrites commonly appears explainable as the result of a single brecciation event. In howardites and eucrites that appear to have undergone multiple brecciation, metal that may be inferred to have been introduced during earlier brecciation has undergone deformation in the later event.

27. Bununu is water-bearing (Jarosewich, 1967; Mason, 1967b); Frankfurt is carbon-bearing (Mason and Wiik, 1966b); Jodzie contains primordial rare gases (Mazor and Anders, 1967); Kapoeta contains rare gases, carbon, chondrules and layer lattice material (Zähringer, 1962b; Signer and Suess, 1963; Müller and Zähringer, 1966, and P. Ramdohr cited in foregoing). Müller and Zähringer (1966) suggest that Kapoeta was invaded by carbonaceous chondrite material. Jodzie also appears to have been invaded by a "carrier" of carbonaceous chondrite composition (Mazor and Anders, 1967).

28. Haraiya contains 0.25 percent C (C. B. Moore, personal communication, 1968), which is not megascopically apparent and is very finely disseminated through brecciated material.

29. Australasian tektites, which are tentatively correlated with the formation of the lunar crater Tycho by cometary impact.

30. Le Teilleul (includes La Vivionnere) contains eucritic fragments, "bronzite" fragments, and fragments not seen in other meteorites (Wahl, 1952). Pavlovka contains eucritic fragments and fragments of "bronzite" (Wahl, 1952). Yurtuk contains olivine of a fayalite composition (Kolomenskiy and Mikeyeva, 1963) that is found in the low-iron group of pallasites.

APPENDIX II Continued

31. Juvinas locally contains tiny spherules of white achondrite (enstatite?), bordered locally by black fusion crust and clear glassy rims of plagioclase; the spherules occur in breccia with disseminated metal, and shock-melted and transformed plagioclase (Polished thin section of M. B. Duke, U. S. Geological Survey). Luotolax contains unaltered to altered fragments, fragments of enstatite grains, and fragments of bronzite or "diogenite" (Wahl, 1952). Petersburg contains pieces of eucrite in dense matrix (Wahl, 1952). Two brecciation events are recorded by shocked metal that encloses brecciated pyroxene (see Duke, 1965a). Stannern contains metal that appears to have been intruded at the time of brecciation (see fig. 25g, h in text).

32. Mässing contains pieces of eucrite in dense matrix (Wahl, 1952).

33. The American, European and African tektite fields, and their related terrestrial craters, are tentatively correlated with the formation of the lunar craters Theophilus, Langrenus and Copernicus, respectively, from the impact of asteroidal materials.

34. See table 19.

35. Except for Mount Padbury, inferred from Fs content of pyroxene (see table 19).

36. Inferred from Fa content of olivine and Fs content of pyroxene (see table 19).

37. Arriba; see Appendix II, footnote 16.

38. Fleming(?); Hainaut(?); Ochansk(?); Pulsora(?); see Appendix II, footnotes 13 and 17.

APPENDIX III

List of Brecciated Meteorites Arranged in Genetic Groupings^{1/}

CLASS I. CALCIUM-POOR METEORITES

A. Carbon, water and rare gas-bearing breccias

1. Pigeonite association

a. Chondrite (None)

b. Achondrite

Dingo Pup Donga(?)^{2/}

Dyalpur

Goalpara

North Haig(?)^{2/}

Novo Urei

2. Hypersthene association (None)

3. Bronzite association

a. Chondrite

Breitscheid

Carcote^{3/}

Fayetteville^{4/}

Pultusk^{5/}

Pantar^{6/}

Tabor^{7/}

b. Achondrite

Fragment in Breitscheid

c. Pallasite (None?)

d. Iron

Weekeroo Station

Washington County

4. Enstatite association

a. Chondrite (None?)

b. Achondrite

Khor Temiki

Norton County^{9/}

Pesyanoë

Shallowater^{9/}

c. Mesosiderite

Bencubbin

Weatherford

d. Iron

Canyon Diablo

Toluca

APPENDIX III Continued

CLASS I. CALCIUM-POOR METEORITES

B. Breccias that apparently lack carbon, water and rare gases1. Chondrite^{10/}

a. Compound polymict breccias

1). Hypersthene-enstatite mixture

Danville	Parnallee(?)
Kelley	

2). Hypersthene-bronzite mixture

Bandong	Manbhoom
Homestead	Ness County (1894)
Jelica	Plainview

3). Bronzite-enstatite mixture

Hainaut	Pulsora
Leighton	

b. Restricted(?) polymict breccia

1). Pigeonite (None?)

2). Hypersthene

Aleppo	Mauritius
Arriba	Näs ^{11,12/}
Assam	New Almelo
Bremervörde	Norcateur
Borgo San Donnino	Orvinio
Chandakapur	Ottawa
Chantonay ^{11/}	Oubari
Drake Creek	Oviedo
Ensisheim	Rush Creek
Farmington ^{11,12/}	St. Mesmin
Harrison County	Santa Barbara
Hedjaz	Sevilla
Holman Island ^{13/}	Siena
Johnson City ^{11,12/}	Shelburne
Knyahinya	Shytal
Krähenberg	Soko-Banja
Ladder Creek ^{14/}	Vavilovka
Lalitpur	Waconda
Mangwendi	

3). Bronzite

Akbarpur	Hugoton
Canellas	Miller
Cangas de Oris	Monroe
Cashion ^{14/}	Ochansk ^{14/}
Coldwater ^{14/}	Sitathali
Cullison	Ställdalen ^{11/}
Fleming	Tulia
Gerona	Tysnes Island
Gnadenfrei	Weston

APPENDIX III Continued

CLASS I. CALCIUM-POOR METEORITES

B. Breccias that apparently lack carbon, water, and rare gases

1. Chondrite

- b. Restricted(?) polymict breccia
- 4). Enstatite (None)

2. Achondrite

- a. Compound polymict breccia
 - 1). Enstatite-hypersthene mixture
Cumberland Falls
- b. Restricted(?) polymict breccia
 - 1). Pigeonite-metal (ureilite) mixture
See list of ureilites, Class IAlb
 - 2). Hypersthene-metal mixture

Ellemeet	Roda
Garland	Shalka
Ibbenbühren	Tatahouine
Johnstown	
Manegaon	
 - 3). Enstatite-metal mixture

Aubres	Norton County
Bishopville	Pena Blanca Spring
Bustee	Pesyancee
Cumberland Falls	Shallowater
Khor Temiki	

3. Stony-irons

- a. Mesosiderites (calcium-poor)
 - 1). Compound polymict breccias
 - a). Enstatite-hypersthene mixture
Bencubbin
 - 2). Restricted(?) polymict breccia
 - a). Enstatite-metal mixture

Bencubbin ^{15/}	Udei Station
Enon	Weatherford ^{15/}
Mount Egerton	Winona
 - b). Hypersthene-metal mixture
Bondoc Peninsula
 - c). Unclassified
Budulan
Lujan(?)
- b. Pallasites
 - 1). Restricted polymict breccia (None?)
 - 2). Monomict
 - Admire
 - Eagle Station

APPENDIX III Continued

CLASS I. CALCIUM-POOR METEORITES

B. Breccias that apparently lack carbon, water, and rare gases

4. Irons with silicate inclusions

a. Compound polymict breccia

1). Metal (hypersthene)-silicate (enstatite) mixture

a). Brecciated hexahedrite (Ga-Ge group II)

Kendall County

b. Restricted or compound(?) polymict breccia

1). Enstatite association (Ga-Ge group I)

Campo del Cielo Odessa

Canyon Diablo Toluca

2). Hypersthene association (Ga-Ge group II)

Four Corners

Pitts

3). Bronzite association (Ga-Ge group III and IV)

Bishop Canyon

Weekeroo Station

4). Inferred enstatite or hypersthene association

Copiapo

Pine River

Linwood

Woodbine

Persimmon Creek

5). Inferred bronzite association

Colomera

Netchaveo

Kodaikanal

CLASS II. CALCIUM-RICH METEORITES

A. Carbon, water, and rare gas-bearing breccia

1. Pyroxene-plagioclase achondrite

a. Howardite

Bununu(?)

Jodzie

Frankfort

Kapoeta

b. Eucrite

Haraiya

2. Tektites(?)

B. Breccias that apparently lack carbon, water, and rare gases

1. Pyroxene-plagioclase achondrite

a. Compound polymict breccia

1). Howardite

Le Teilleul

Yurtuk(?)

Pavlovka

APPENDIX III Continued

CLASS II. CALCIUM-RICH METEORITES

B. Breccias that apparently lack carbon, water, and rare gases1. Pyroxene-plagioclase achondrite

a. Compound polymict breccia

2). Eucrite

Juvinas

Petersburg

Luotolax

Stannern

b. Restricted(?) polymict breccia

1). Howardite

Bholgati

Mässing

Binda

Washougal

Brient

Zmenj

Chaves

c. Monomict breccia

1). Eucrite and shergottite(S)

Adalia

Medanites

Bereba

Moore County

Bialystok

Nagaria

Cachari

Nobleborough

Chervony Kut

Nuevo Laredo

Emmaville

Padvarninkai(S)

Haraiya

Pasamonte

Ibitira

Peramiho

Jonzac

Serra de Magé

Kirbyville

Shergotty(S)

Lakangaon

Sioux County

Macibini

Zagami(S)

2. Tektites(?)

3. Mesosiderites (calcium-rich)

a. Compound polymict breccia

1). Enstatite-metal-eucritic mixture (None?)

2). Hypersthene-metal-eucritic mixture

Hainholz(?)

Vaca Muerta

Mount Padbury

Veramin

Patwar

3). Bronzite-metal-eucritic mixture

Dalgaranga

Lowicz

Estherville

Morristown

4). Unclassified

Barea

Mincy

Clover Springs

Pinnaroo

Crab Orchard

Simondium

Dyarrl Island

APPENDIX III Continued

CLASS II. CALCIUM-RICH METEORITES

B. Breccias that apparently lack carbon, water, and rare gases

4. Chondrites with eucritic inclusions

a. Compound polymict breccia

- 1). Hypersthene chondrite-eucritic mixture
Arriba(?)
- 2). Bronzite chondrite-eucritic mixture
Fleming(?) Ochansk(?)
Hainaut(?) Pulsora(?)

-
- 1/. References cited here supplement those given in table 20 and listed in Appendix II.
 - 2/. McCall and Cleverly (1967).
 - 3/. Diamond reported by Sandberger (1889).
 - 4/. Müller and Zähringer (1966).
 - 5/. See Anders (1964, p. 677).
 - 6/. Signer and Suess (1963); Wlotzka (1963).
 - 7/. Signer and Suess (1963).
 - 8/. Wlotzka (1963).
 - 9/. Norton County contains 0.040 percent carbon; Shallowater contains 0.135 percent carbon (C. B. Moore, personal communication, 1967).
 - 10/. Classification into hypersthene and bronzite classes are based on Fe content of olivine as listed by Mason (1963c).
 - 11/. Fredriksson and others (1963).
 - 12/. Buseck and others (1966).
 - 13/. Müller and Zähringer (1966).
 14. Knox (1963).
 - 15/. Also listed under Class IA⁴c

APPENDIX IV

Ages of Selected Stones and Irons used for Estimating the
Ages of Collision Events outlined in Table 21.

Hypersthene Body (Ga-Ge group II iron; hexahedrites and Ni-poor ataxites)

	<u>Age*</u>	<u>Reference</u>
Stone		
Zaborzika	4010; 2040	1
Khohar (dark)	---; 1980 (440)	2
St. Michel	4000; 1900	3, 1
Bruderheim	1850 (1650, 1850, 1900); 1830 (1100, 1270)	1, 4
Mocs	3750 (4300); 1750 (2320, 2400)	4
Dhurmsala	---; 1600	2
Arriba	---; 1550	2
Mezel	3100; 1300	5
Bluff	---; 1220	2
Iron		
Ponca Creek 1, 2	1205, 1180	a
Stone		
Long Island	---; 1110	2
Lissa	1970; 1100	1
Harleton	---; 1050	2
Peace River	1000, 960; ---	6, 7
New Concord	---; 920 (1000)	2
Walters	---; 910 (light and dark)	2
Iron		
Ainsworth	920	a
Arispe	905	a, b
Bendego	910	a
Carbo 5	850; 895	a, b, c

* Ages are in 10^6 yr. For stones, the ages are K-Ar; U, Th- ^4He , respectively. For irons, ages are $^{40}\text{K}/^{41}\text{K}$, except where otherwise noted.

APPENDIX IV ContinuedHypersthene Body (Ga-Ge II iron; hexahedrites and Ni-poor ataxites)

	<u>Age</u>	<u>Reference</u>
Stone		
Alfianello	770; 800, 840	1, 8
Zemaitkiemis	---; 770	2
La Lande	1650; 740	9, 2
Farmington	830; 710	1
Oberlin	---; 700	2
Pervomaisky (gray)	650; 630	10, 11
(black)	640, 1800; 630, 940	1, 10
Hayes Center	650, 650; 600, 450, 780	1, 2, 4
Bondoc Peninsula (mesosiderite)	---; 600	2
Taiban	---; 530	2
Goodland	---; 500	2
Iron		
Union (h) ⁼	500 (⁴ He)	d
Stone		
Potter	720; 470	1
Barratta	---; 460	2
Iron		
Iredell (h)	450	d
Stone		
Kunashek	530; 440	1
(McKinney)	(720-gray, 1200-black; 550-gray, 560-black)	12, 1
Ergheo	2320; 450, 320	1, 3)
Kingfisher	---; 440	2
Ramsdorf	---; 440	2
	420, 370; 430, 400	1, 2, 13
Iron		
Cedartown (h)	430	d
Stone		
Chantonmay (light)	---; 380	2
Iron		
Sikhote-Alin	355 (³¹ 0, ³⁶ Cl/ ³⁶ Ar)	a, e
Mount Joy (h)	350 (³⁶ Cl/ ²¹ Ne)	f

⁼ Hexahedrite

APPENDIX IV ContinuedHypersthene Body (Ga-Ge II iron; hexahedrites and Ni-poor ataxites)

	<u>Age</u>	<u>Reference</u>
Stone		
McKinney	2320; 320, 450	1, 2
Chateau Reynard	510; 300	1
Iron		
Sao Juliao (II- (anomalous)	270 ($^{36}\text{Cl}/^{21}\text{Ne}$)	b, f
Santa Rosa	260 (^4He)	b, d
Lombard (h)	260 ($^{36}\text{Cl}/^{21}\text{Ne}$); 205 (± 200 , $^{41}\text{K}/^{40}\text{K}$)	c, f
	295 \pm 200	a
Coya Norte (h)	250, 220 (^4He)	b, d, g
Tocopilla (h)	250	g
Keen Mountain (h)	220 (^4He); 200 120($^{36}\text{Cl}/^{21}\text{Ne}$)	d, g, f
Sandia Mountains (h)	210 ($^{36}\text{Cl}/^{21}\text{Ne}$); 140 (^4He)	b, h, d
Stone		
Paragould	---; 200	2
Iron		
Rio Loa (h)	160 (^4He)	d
Seeläsgen(?)	160 ($^{36}\text{Cl}/^{21}\text{Ne}$)	f
Sierra Gorda (h)	110 (^4He)	d
Forsyth County	75 (Ar)	b, i
Negrillos (h)	54 (^4He); 30	b, d, g
Braunau (h)	8 (Ar); 4.5 ($^{36}\text{Cl}/^{21}\text{Ne}$)	i, f
<u>Bronzite Body (Ga-Ge group III, IV irons)</u>		
Iron		
Deep Springs 1, 2 (IV)	2250, 2275	j, a
Williamstown (III)	2200 ($^{36}\text{Cl}/^{36}\text{Ar}$)	i
(" 1, 2	640, 660, 760 ($^{41}\text{K}/^{40}\text{K}$)	a
Stone		
Pultusk	3750, 3740, 3930; 1750, 1800, 3420, 3870	13, 14, 1, 2

APPENDIX IV ContinuedBronzite Body (Ga-Ge group III, IV irons)

	<u>Age</u>	<u>Reference</u>
Iron		
Clark County 2 (III anomalous)	1440	j, a
Stone		
Breitscheid	3330; 1350, 1530, 2500	15, 16, 2, 14
Texline	---; 1330	2
Iron		
Klondike (IV)	915	a
Tlacotepec (IV)	915	a
Mungindi (III)	820	a
Pinon 3, 2, 1 (III anomalous)	790, 780, 660	j, a
Delgate (III)	775	a
Maria Elena 1, 2 (IV)	745, 740	a
Wiley (Ni-rich ataxite)	740	a
Santa Apolonia (III)	730	a
Mount Edith (III)	710	a
Cowra (III)	710...1400	j, a
Norfolk (III)	700	a
Puente d'Zacate (III)	690	a
Grant 2, 3 (III)	675, 715	a
Anoka (III)	685	a
Norfolk (III)	685	a
Thunda (III)	680	a
Williamstown 1, 2 (III)	640, 660, 760	a
Cape of Good Hope (IV)	630	a
Grundaring (III)	630	a
Carlton 2, 1 (III)	625, 605	a
Treysa 4, a (III)	625, 615	a
Merceditas (III)	600	a
Sanderson (III)	590	a
Tamarugal (III)	585	a
San Angelo (III)	580	a
Trenton 1, 3 (III)	580, 565	a
Washington County (Ni-rich ataxite)	575	a

APPENDIX IV ContinuedBronzite Body (Ga-Ge group III, IV irons)

	<u>Age</u>	<u>Reference</u>
Stone		
Seres	---; 530, 510	13, 2
Iron		
Descubridora 1, 2 (III)	505, 515	a
Stone		
Bath	1170; 470	1
Iron		
Bristol (IV)	470	j, a
Moonbi (III- anomalous)	440...900	a
Hill City	435	a
Huizopa (IV)	430	a
Butler (anomalous)	420...850	j, a
Putnam County (IV)	410	a
Stone		
Beddlegert	2780; 400	13, 2
Iron		
Weaver Mountains (IV)	385	a
Yanhuitlan 2 (IV)	370	a
Iron River (IV)	360	a
Cambria(?)	350...700	a
Casas Grandes (III)	350 ($^{36}\text{Cl}/^{21}\text{Ne}$)	f, b
Charlotte 1, 2, 3 (IV)	340, 355, 320	a
Hoba (IV)	300	a
Tawallah Valley (IV)	245	a
(Sacramento Mountains (III)	235 ($^{41}\text{K}/^{40}\text{K}$); 185)	a, c
Glorieta Mountain (III)	230	b, a
Duchesne 2, 1 (IV)	220, 175	a
Dayton (III- anomalous)	215	a
Stone		
Rose City	1040; 200	1

APPENDIX IV ContinuedBronzite Body (Ga-Ge group III, IV irons)

	<u>Age</u>	<u>Reference</u>
Iron		
Sacramento Mountains (III)	185,235	a, c
Santa Catherina (III) (anomalous)	166	j, i
Admire (III-pallasite)	160 (^4He), 150	b, d, g
Wedderburn (III) (anomalous)	100...200	j, a
Chinga (Ni-rich ataxite)	110 (^4He)	d
Smithland (Ni-rich ataxite)	110 (^4He)	d
Stony-iron		
Colomera (pallasite)	75 ($^{36}\text{Cl}/^{21}\text{Ne}$)	f
Mesosiderite		
Estherville (lunar impact?)	64 ($^{36}\text{Cl}/^{21}\text{Ne}$) 62 ($^{39}\text{Ar}/^{38}\text{Ar}$)	e e
Iron		
Tucson (Ni-rich ataxite)	20 (Ar)	i

Enstatite Body (Ga-Ge group I iron)

Stone		
Norton County	2720 (4680-5090); 1330 (1910-1920)	1
Iron		
Aroos, 1, 2, 3	935, 905, 910	a
Mt. Ayliff(?)	920	a
Odessa	890	a
Bischtübe 1, 3a, 3b	805, 840, 835	a
Canyon Diablo	650, 610, 675	a
Toluca	600 ($^{36}\text{Cl}/^{21}\text{Ne}$)	f, 1
Osseo	490	a
Stone		
Norton County	220 (^4He)	17

APPENDIX IV ContinuedEnstatite Body (Ga-Ge group I irons)

	<u>Age</u>		<u>Reference</u>
Stone			
Pena Blanca Spring	53 (^3He)	38 (^{21}Ne)	17
Cumberland Falls	(13) "	49 "	17
Bishopville	47 "	43 "	17
Bustee	45 "	44 "	17
Pesyance	-- "	43 "	17
Khor Temiki	41 "	43 "	17
Shallowater	20 "	14 "	17
Aubres	(6) "	11 "	17

-
- | | |
|---|--|
| 1. Kirsten and others (1963). | 10. Gerling and Levski (1956). |
| 2. Hintenberger and others (1964). | 11. Heide (1957/1964/7). |
| 3. Geiss and Hess (1958). | 12. Gerling and Rik (1955). |
| 4. Hintenberger, Vilcsek, and Wänke (1964). | 13. Hintenberger, König, and Wänke (1962). |
| 5. Geiss and others (1960). | 14. Anders (1963). |
| 6. Baadsgaard and others (1964). | 15. Paneth (1959). |
| 7. Taylor (1964). | 16. Keil (1960). |
| 8. Reed and Turkevich (1957). | 17. Eberhardt and others (1965). |
| 9. Stauffer (1961b). | |
-
- | |
|-------------------------------------|
| a. Voshage (1967). |
| b. Lovering and others (1957). |
| c. Voshage and Hintenberger (1963). |
| d. Bauer (1963). |
| e. Schaeffer and Heyman (1965). |
| f. Vilcsek and Wänke (1963). |
| g. Signer and Nier (1962). |
| h. Lipschutz and others (1965). |
| i. Fisher and Schaeffer (1960). |
| j. Wasson (1967a). |
| k. Wasson (1966). |
| l. Wasson (1967b). |

REFERENCES CITED

- Alderman, A. R., 1940, A siderolite from Pinnaroo, South Australia: Royal Soc. South Australia Trans., v. 64, p. 109.
- Anders, Edward, 1963, Meteorite ages in Middlehurst, B. M., and Kuiper, G. P, eds.: The moon, meteorites and comets, the solar system, v. 4: Chicago, Univ. of Chicago Press, p. 402-495.
- _____, 1964, Origin, age and compositions of meteorites: Space Science Reviews, v. 3, no. 5/6, p. 583-714.
- Anders, Edward, and Goles, G. C., 1961, Theories on the origin of meteorites: Jour. Chem. Educ., v. 38, no. 2, p. 58-66.
- Baadsgaard, H., Folinsbee, R. E., and Cumming, G. L., 1964, Peace River meteorite: Jour. Geophys. Res., v. 69, no. 19, p. 4197-4200.
- Bauer, C. A., 1963, The helium contents of metallic meteorites: Jour. Geophys. Res., v. 68, no. 21, p. 6043-6057.
- Binns, R. A., 1967, Petrographic relationships between chondrites and achondrites (abs.): 30th Annual Meeting of the Meteoritical Society Program.
- Boström, Kurt, and Fredriksson, Kurt, 1966, Surface conditions of the Orgueil meteorite parent body as indicated by mineral associations: Smithsonian Misc. Coll., v. 151, no. 3, 39 p.
- Brandt, J. C., and Hodge, P. W., 1964, Solar system astrophysics: New York, McGraw Hill Book Co.
- Brezina, A., 1904, The arrangements of collections of meteorites: Am. Phil. Soc. Proc., v. 43, no. 176, p. 211-247.
- Buddhue, J. D., 1946, The average composition of meteoritic iron: Popular Astronomy, v. 54, no. 3, p. 149-152.
- Buseck, P. R., Mason, Brian, and Wiik, H. B., 1966, The Farmington meteorite - mineralogy and chemistry: Geochim. et Cosmochim. Acta, v. 30, no. 1, p. 1-18.
- Cameron, A. G. W., 1966, The accumulation of chondritic material: Earth and Planetary Science Letters, v. 1, no. 3, p. 93-96.

REFERENCES CITED Continued

- Carter, N. L., and Kennedy, G. C., 1964, Origin of diamonds in the Canyon Diablo and Novo Urei meteorites: *Jour. Geophys. Res.*, v. 69, no. 12, p. 2403-2421
- Cassidy, W. A., Glass, G., and Heezen, H. C., 1967, Physical and chemical properties of Australasian microtektites (abs.): Program of the 30th Annual Meeting of the Meteoritical Society.
- Chao, E. C. T., 1963, The petrographic and chemical characteristics of tektites in O'Keefe, J. A., ed: *Tektites*: Chicago, Univ. of Chicago Press, p. 51-94.
- , 1964, Some geologic occurrences of Australasian tektites, in *Astrogeologic studies annual progress report, Part C., cosmic chemistry and petrology*: U. S. Geol. Survey, p. 10-64.
- Chapman, D. R., 1964, On the unity and origin of the Australasian tektites: *Geochim. et Cosmochim. Acta*, v. 28, no. 6, p. 841-880.
- Chapman, D. R., Larson, H. K., and Anderson, L. A., 1962, Aerodynamic evidence pertaining to the entry of tektites into the earth's atmosphere: N.A.S.A. Tech. Rept. R-134.
- Cobb, J. C., and Moran, George, 1965, Gallium concentrations in the metal phases of various meteorites: *Jour. Geophys. Res.*, v. 70, no. 20, p. 5309-5311.
- Coulson, A. L., 1940, A catalogue of meteorites: *Geol. Survey India Mem.*, v. 75.
- Cuttitta, F., Clarke, R. S. Jr., Carron, M. K., and Ansell, C. S., 1967, Martha's Vineyard and selected Georgia tektites: new chemical data: *Jour. Geophys. Res.*, v. 72, no. 4, p. 1343-1349.
- Dodd, R. T. Jr., and Van Schmus, W. R., 1965, Significance of the unequilibrated ordinary chondrites: *Jour. Geophys. Res.*, v. 70, no. 16, p. 3801-3811
- Dodd, R. T. Jr., Van Schmus, W. R., and Koffman, D. M., 1967, A survey of the unequilibrated ordinary chondrites: *Geochim. et Cosmochim. Acta*, v. 31, no. 6, p. 921-951
- Dollfus, Audouin, 1962, The polarization of moonlight, in Kopal, Z., ed., *Physics and astronomy of the moon*: New York, Academic Press, p. 131-159.
- DuBois, R. L., and Elston, D. P., 1967, Remanent magnetism of several meteorite classes (abs.): *Am. Geophys. Union Trans.*, v. 48, no. 1, p. 165.

REFERENCES CITED Continued

- DuBois, R. L., and Elston, D. P., in preparation, Remanent magnetism in meteorites.
- DuFresne, E. R., and Anders, Edward, 1962, On the chemical evolution of the carbonaceous chondrites: *Geochim. et Cosmochim. Acta*, v. 26, p. 1085-1114.
- _____, 1963, Chemical evolution of the carbonaceous chondrites, in Middlehurst, B. M., and Kuiper, G. P., eds., *The moon, meteorites and comets, the solar system*, v. 4: Chicago, Univ. of Chicago Press, p. 496-526.
- Duke, M. B., 1963, Petrology of the basaltic achondrite meteorites: Unpublished PhD dissertation, California Institute of Technology.
- _____, 1964, Petrologic evidence consistent with a lunar model for the origin of basaltic meteorites (abs. title): *Am. Geophys. Union Trans.*, v. 45, no. 1, p. 86.
- _____, 1965a, Abundances of some lithophile elements in basaltic meteorites, hypersthene achondrites and diopside achondrites, in *Astrogeologic Studies annual progress report, Part C. cosmic chemistry and petrology*: U. S. Geol. Survey, p. 73-84.
- _____, 1965b, Metallic iron in basaltic achondrites: *Jour. Geophys. Res.*, v. 70, no. 6, p. 1523-1527.
- Duke, M. B., and Silver, L. T., 1967, Petrology of eucrites, howardites and mesosiderites: *Geochim. et Cosmochim. Acta*, v. 31, no. 10, p. 1637-1665.
- Eaton, J. P., and Murata, K. J., 1960, How volcanoes grow: *Science*, v. 132, no. 3432, p. 925.
- Eberhardt, P., Eugster, O., and Geiss, J., 1965, Radiation ages of aubrites: *Jour. Geophys. Res.*, v. 70, no. 18, p. 4427-4434.
- Eggleton, R. E., and Shoemaker, E. M., 1961, Breccia at Sierra Madera, Texas, in *Geological Survey Research 1961*, Prof. Paper 424-D: U. S. Geol. Survey, p. 151-153.
- El Goresy, Ahmed, 1966, Metallic spherules in Bosumtwi Crater glasses: *Earth and Planetary Science Letters*, v. 1, no. 1, p. 23-24.
- Elston, D. P., in press, Character and geologic habitat of potential deposits of water, carbon and rare gases on the moon: Water resources of the inner planets, Am. Astronautical Soc. National Specialists Meeting, 1968.

REFERENCES CITED Continued

- Elston, D. P., in preparation, Geologic map of the Colombo Region of the moon.
- Elston, D. P., and Holt, H. E., 1967, Development of increased reflectance in basaltic achondrites by brecciation and a possible relationship with lunar breccias (abs.): Program of the Annual Meeting of the Geological Society of America.
- _____ in preparation, Reflectance characteristics of lunar materials and stony meteorites in respect to brecciation and comminution.
- Faul, Henry, 1966, Tektites are terrestrial: *Science*, v. 152, no. 3727, p. 1341-1345.
- Fireman, E. L., and Schwarzer, D., 1957, Measurements of Li^6 , He^3 , and H^3 in meteorites and its relation to cosmic radiation: *Geochim. et Cosmochim. Acta*, v. 11, no. 4, p. 252-262.
- Fisher, D. E., 1965, Anomalous Ar^{40} contents of iron meteorites: *Jour. Geophys. Res.*, v. 70, no. 10, p. 2445-2452.
- Fisher, D. E., and Schaeffer, O. A., 1960, Cosmogenic nuclear reactions in iron meteorites: *Geochim. et Cosmochim. Acta*, v. 20, no. 1, p. 5-14.
- Fleisher, R. L., and Price, P. B., 1965, Fission track evidence for the simultaneous origin of tektites and other natural glasses: *Geochim. et Cosmochim. Acta*, v. 28, no. 6, p. 755-760.
- Fouché, K. F., and Smales, A. A., 1967, The distribution of trace elements in chondritic meteorites. 1. Gallium, germanium, and indium: *Chemical Geol.*, v. 2, p. 5-33.
- Fredriksson, Kurt, DeCarli, P. S., and Aaramae, A., 1963, Shock induced veins in chondrites, in Priester, W. ed.: *Space research III*, Amsterdam, North Holland Pub. Co., p. 974-983.
- Fredriksson, Kurt, and Keil, Klaus, 1963, The light-dark structure in the Pantar and Kapoeta stone meteorites: *Geochim. et Cosmochim. Acta*, v. 27, p. 717-739.
- _____ 1964, The iron, magnesium, calcium, and nickel distribution in the Murray carbonaceous chondrite: *Meteoritics*, v. 2, no. 3, p. 201-207.
- Fredriksson, Kurt, and Mason, Brian, 1967, The Shaw meteorite: *Geochim. et Cosmochim. Acta*, v. 31, no. 10, p. 1705-1709.

REFERENCES CITED Continued

- Fredriksson, Kurt, and Reid, A. M., 1965, A chondrule in the Chainpur meteorite: *Science*, v. 149, no. 3686, p. 856-860.
- Frey, F. A., and Haskin, Larry, 1964, Rare earths in oceanic basalts: *Jour. Geophys. Res.*, v. 69, no. 4, p. 775-780.
- Geiss, J., and Hess, D. C., 1958, Argon-potassium ages and the isotopic composition of argon from meteorites: *Astrophys. Jour.*, v. 127, no. 1, p. 224-236.
- Geiss, J., Oeschger, H., and Signer, Peter, 1960, Radiation ages of chondrites: *Zeitschr. Naturforsch.*, v. 15a, p. 1017-1017.
- Gentner, W., Lippolt, H. J., and Schaeffer, O. A., 1963, Argonbestimmungen an kaliummineralien -XI: die kalium-argon-alter der glaser des Nordlinger Rieses und der bahmisch-mahrischen tektite: *Geochim. et Cosmochim. Acta*, v. 27, no. 2, p. 191-200.
- Gerling, E. K., and Levski, L. K., 1956, Origin of inert gases in stone meteorites: *Doklady Akad. Nauk. SSR*, v. 110, p. 750.
- Gerling, E. K., and Rik, K. G., 1955, Bestimmung des alters von stein-meteoriten nach der argon methode: *Doklady Akad. Nauk, SSR*, v. 101, p. 433-435.
- Goldberg, Edward, Uchiyama, Aiji, and Brown, Harrison, 1951, The distribution of nickel, cobalt, gallium, palladium, and gold in iron meteorites: *Geochim. et Cosmochim. Acta*, v. 2, no. 1, p. 1-25.
- Goldschmidt, V. M., 1954, *Geochemistry*, Muir, A., ed.: London, Oxford University.
- Goldstein, J. I., and Short, J. M., 1967a, Cooling rates of 27 iron and stony-iron meteorites: *Geochim. et Cosmochim. Acta*, v. 31, no. 6, p. 1001-1023.
- _____, 1967b, The iron meteorites, their thermal history and parent bodies: *Geochim. et Cosmochim. Acta*, v. 31, no. 10, p. 1733-1770.
- Greenland, L., 1965, Gallium in chondritic meteorites: *Jour. Geophys. Res.*, v. 70, no. 16, p. 3813-3817.
- Greenland, L., and Lovering, J. F., 1965, Minor and trace element abundances in chondritic meteorites: *Geochim. et Cosmochim. Acta*, v. 29, no. 8, p. 821-858.

REFERENCES CITED Continued

- Hapke, Bruce, 1966, Optical properties of the moon's surface, in Hess, W. N., Menzel, D. H., and O'Keefe, J. A. eds.: The nature of the lunar surface, Baltimore, Johns Hopkins Press, p. 141-154.
- _____, 1968, Lunar surface: composition inferred from optical properties: *Science*, v. 159, no. 3810, p. 76-79.
- Hapke, Bruce, and Van Horn, Hugh, 1963, Photometric studies of complex surfaces, with applications to the moon: *Jour. Geophys. Res.*, v. 68, no. 15, p. 4545-4570.
- Heide, Fritz, 1957/[1964], *Meteorites* (translated by Edward Anders): Chicago, Univ. of Chicago Press.
- Henderson, E. P., and Perry, S. H., 1949, The Linwood (Nebraska) meteorite: *U. S. Nat'l Mus. Proc.*, v. 99, p. 357-360.
- Hess, H. H., and Henderson, E. P., 1949, The Moore County meteorite: a further study with comment on its primordial environment: *Am. Mineralogist*, v. 34, no. 7/8, p. 494-507.
- Hey, M. H., *Catalogue of meteorites*: Trustees of the British Museum, London, The Alden Press (Oxford) Ltd.
- Hintenberger, H., König, H., Schultz, L., Wänke, H., and Wlotzka, F., 1964, Die relativen produktionsquerschnitte für ^3He und ^{21}Ne aus Mg, Si, S, und Fe in steinmeteoriten: *Zeitschr. Naturforsch.*, v. 19a, no. 1, p. 88-92.
- Hintenberger, H., König, H., and Wänke, H., 1962, Über den helium- und neongehalt von steinmeteoriten und deren radiogene und kosmogene alter: *Zeitschr. Naturforsch.*, v. 17a, no. 12, p. 1092-1102.
- Hintenberger, H., Vilcsek, E., and Wänke, H., 1964, Zur frage der diffusionverluste von radiogenen und spallogenen: *Zeitschr. Naturforsch.*, v. 19a, no. 2, p. 219-224.
- Horan, J. R., 1953, The Murray, Calloway County, Kentucky, aerolite (CN=+0881, 366): *Meteoritics*, v. 1, no. 1, p. 114-121.
- Jarosewich, Eugene, 1967, Chemical analyses of seven stony meteorites and one iron with silicate inclusions: *Geochim. et Cosmochim. Acta*, v. 31, no. 6, p. 1103-1106.
- Jérémine, E., Orcel, J., and Sandréa, A., 1962, Étude minéralogique et structurale de la météorite de Chassigny: *Soc. Française Minéralogie et Crystallographie Bull.*, v. 85, p. 262-266.

REFERENCES CITED Continued

- Keil, Klaus, 1960, Fortschritte in der meteoritenkunde: Fortschr. Miner., v. 38, no. 2, p. 202-283.
- Keil, Klaus, and Fredriksson, Kurt, 1964, The iron, magnesium, and calcium distribution in coexisting olivines and rhombic pyroxenes of chondrites: Jour. Geophys. Res., v. 69, no. 16, p. 3487-3515.
- Kerridge, J. F., 1968, Occurrence of olivine in a Type I carbonaceous meteorite: Nature, v. 217, no. 5130, p. 729-730.
- Kirsten, T., Krankowsky, D., and Zähringer, J., 1963, Edelgas- und kalium-bestimmungen an einer grossen zahl von steinmeteoriten: Geochim. et Cosmochim. Acta, v. 27, no. 1, p. 13-42.
- Knox, Reed, Jr., 1963, The microstructure of several stony meteorites: Geochim. et Cosmochim. Acta, v. 27, no. 3, p. 261-268.
- Kolomenskiy, V. D., and Mikheyeva, I. V., 1963, The hypersthene and olivine of the Yurtuk meteorite: Meteoritica, v. 23 (Taurus Press, 1965), p. 77-88.
- Krankowsky, D., and Zähringer, J., 1966, K-Ar ages of meteorites, in Schaeffer, O. A., and Zähringer, J., eds.: Potassium argon dating, New York, Springer-Verlag, p. 174-200.
- Kvasha, L. G., 1948, Über einige typen von steinmeteoriten: Chem. Erde, v. 19, p. 124-136.
- Lipschutz, M. E., Signer, Peter, and Anders, Edward, 1965, Cosmic-ray exposure ages of iron meteorites by the $\text{Ne}^{21}/\text{Al}^{26}$ method: Jour. Geophys. Res., v. 70, no. 6, p. 1473-1489.
- Lovering, J. F., 1959, The magnetic field in a primary meteorite body: Am. Jour. Sci., v. 257, p. 271-275.
- _____, 1962, The evolution of meteorites - evidence for the coexistence of chondritic, achondritic, and iron meteorites in a typical parent meteorite body, in Moore, C. B., ed.: Researches on meteorites, New York, John Wiley and Sons, Inc., p. 179-198.
- Lovering, J. F., Nichiporuk, W., Chodos, A., and Brown, H., 1957, The distribution of gallium, germanium, cobalt, chromium, and copper in iron and stony-iron meteorites: Geochim. et Cosmochim. Acta, v. 11, no. 4, p. 263-278.
- McCall, G. J. H., 1965a, A meteorite of unique type from western Australia: the Mount Egerton stony-iron: Mineralog. Mag., v. 35, no. 270, p. 241-249.

REFERENCES CITED Continued

McCall, G. J. H., 1965b, New material from and a reconsideration of the Dalgara meteorite and crater, western Australia: Mineralog. Mag., v. 35, no. 271, p. 476-487.

____ 1966, The petrology of the Mount Padbury mesosiderite and its achondrite enclaves: Mineralog. Mag., v. 35, no. 276, p. 1029-1060.

____ 1967, The Bencubbin meteorite: W. Australia. A new study reveals enstatite and hypersthene chondrite enclaves in this enstatite-olivine stony-iron of unique type (abs.): Program of the 30th Annual Meeting of the Meteoritical Society.

McCall, G. J. H., and Cleverly, W. H., 1965, Newly discovered mesosiderite containing achondrite fragments: the Mount Padbury meteorite: Nature, v. 207, no. 4999, p. 851-852.

____ 1967, Two new ureilite finds from western Australia (abs.): Program of the 30th Annual Meeting of the Meteoritical Society.

Mason, Brian, 1962a, Meteorites: New York, John Wiley and Sons, Inc.

____ 1962b, The classification of the chondritic meteorites: Am. Mus. Novitates, no. 2085, 20 p.

____ 1963a, The carbonaceous chondrites: Sp. Sci. Rev., v. 1, p. 621-646.

____ 1963b, The pallasites: Am. Mus. Novitates, no. 2163, 19 p.

____ 1963c, Olivine composition in chondrites: Geochim. et Cosmochim. Acta, v. 27, no. 10, p. 1011-1023.

____ 1963d, The hypersthene achondrites: Am. Mus. Novitates, no. 2155, 13 p.

____ 1965, The chemical composition of olivine-bronzite and olivine-hypersthene chondrites: Am. Mus. Novitates, no. 2223, 38 p.

____ 1966, The enstatite chondrites: Geochim. et Cosmochim. Acta, v. 30, no. 1, p. 23-39.

____ 1967a, Extraterrestrial mineralogy: Am. Mineralogist, v. 52, no. 3/4, p. 307-325.

____ 1967b, The Bununu meteorite, and a discussion of the pyroxene-plagioclase achondrites: Geochim. et Cosmochim. Acta, v. 31, no. 2, p. 107-115.

REFERENCES CITED Continued

- Mason, Brian, 1967c, The Woodbine meteorite, with notes on silicates in iron meteorites: *Mineral. Mag.*, v. 36, p. 120-126.
- Mason, Brian, and Jarosewich, Eugene, 1967, The Winona meteorite: *Geochim. et Cosmochim. Acta*, v. 31, no. 6, p. 1097-1099.
- Mason, Brian, and Nelen, J., 1967, The Weatherford meteorite (abs.): Program of the 30th Annual Meeting of the Meteoritical Society.
- Mason, Brian, and Wiik, H. B., 1966a, The composition of the Barratta, Carraweena, Kapoeta, Moorefort, and Ngawi meteorites: *Am. Mus. Novitates*, no. 2273, 25 p.
- _____, 1966b, The composition of the Bath, Frankfort, Kakangari, Rose City, and Tadjera meteorites: *Am. Mus. Novitates*, no. 2272, 24 p.
- Mazor, Emanuel, and Anders, Edward, 1967, Primordial gases in the Jodzie howardite and the origin of gas-rich meteorites: *Geochim. et Cosmochim. Acta*, v. 31, no. 9, p. 1441-1456.
- Mead, C. W., Littler, Janet, and Chao, E. C. T., 1965, Metallic spheroids from Meteor Crater, Arizona: *Am. Mineralogist*, v. 50, no. 5/6, p. 667-681.
- Merrihue, C. M., 1966, Xenon and krypton in the Bruderheim meteorite: *Jour. Geophys. Res.*, v. 71, no. 1, p. 263-313.
- Merrill, G. P., 1896, On the composition and structure of the Hamblen County, Tennessee meteorite (Mossistown): *Am. Jour. Sci.*, ser 4., v. 2, no. 8, p. 149-153.
- _____, 1921, Notes on the meteorite of Estherville, Iowa, with especial reference to its included "Peckhamite" and probable metamorphic nature: *U.S. Nat'l Mus. Proc.*, v. 58, no. 2341, p. 363-370.
- Meunier, S., 1872, Analyse lithologique de la meteorite de la Sierra de Chaco. Mode de formation de la lagronite: *Acad. sci [Paris] Comptes rendus*, v. 75, p. 1547-1552.
- Milton, D. J., and DeCarli, P. S., 1963, Maskelynite - formation by explosive shock: *Science*, v. 140, no. 3567, p. 670-671.
- Moore, C. B., Birrell, P. J., and Lewis, C. F., 1967, Variations in the chemical and mineralogical composition of rim and plains specimens of the Canyon Diablo meteorite: *Geochim. et Cosmochim. Acta*, v. 31, no. 10, p. 1885-1892.
- Moore, C. B., and Lewis, C. F., 1965, Carbon abundances in chondritic meteorites: *Science*, v. 149, no. 3681, p. 317-318.

REFERENCES CITED Continued

- Morgan, J. W., and Lovering, J. F., 1965, Uranium and thorium in the Nuevo Laredo achondrite: Jour. Geophys. Res., v. 70, no. 8, p. 2002.
- Müller, O., and Zähringer, J., 1966, Chemische Unterschiede bei uredelgashaltigen steinmeteoriten: Earth and Planetary Science Letters, v. 1, no. 1, p. 25-29.
- Murthy, V. R., and Compston, W., 1965, Rb-Sr ages of chondrules and carbonaceous chondrites: Jour. Geophys. Res., v. 70, no. 20, p. 5297-5307.
- Nininger, H. H., 1942, The Enon, Ohio, meteorite (mesosiderite): Pop. Astron., v. 50, no. 10, p. 563-565.
- Olsen, Edward, 1967, Amphibole - first occurrence in a meteorite: Science, v. 156, no. 3771, p. 61-62.
- Paneth, F. A., 1959, Der meteorit von Breitscheid - I: Geochim. et Cosmochim. Acta, v. 17, no. 3/4, p. 315-319.
- Philpotts, J. A., and Schnetzler, C. C., 1967, Relationship between Serra de Mage and the normal brecciated achondrites considered in terms of rare-earth and barium concentrations and plagioclase compositions (abs.): Program of the 30th Annual Meeting of the Meteoritical Society.
- Philpotts, J. A., Schnetzler, C. C., and Thomas, H. H., 1967, Rare-earth and barium abundances in the Bununu howardite: Earth and Planetary Science Letters, v. 2, no. 1, p. 19-22.
- Pinson, W. H. Jr., Schnetzler, C. C., Beiser, E., Fairbairn, H. W., and Hurley, P. M., 1965, Rb-Sr age of stony meteorites: Geochim. et Cosmochim. Acta, v. 29, no. 5, p. 455-466.
- Powell, B. N., and Weiblen, P. W., 1967, On the petrology of mesosiderites (abs.): Program of the 30th Annual Meeting of the Meteoritical Society.
- Prior, G. T., 1912, The meteoric stones of El Nakhla el Baharia (Egypt): Mineral Mag., v. 16, p. 274-281.
- _____, 1916, On the genetic relationship and classification of meteorites: Mineral Mag., v. 18, p. 26-44.
- _____, 1918, On the mesosiderite-grahamite group of meteorites; with analyses of Vaca Muerta, Hainholz, Simondium and Powder Mill Creek: Mineral Mag., v. 18, no. 85, p. 151-172.

REFERENCES CITED Continued

- Prior, G. T., 1920, The classification of meteorites: *Mineralog. Mag.*, v. 19, no. 90, p. 51-63.
- Rancitelli, L., Fisher, D. E., Funkhouser, J., and Schaeffer, O. H., 1967, Potassium-Argon dating of iron meteorites: *Science*, v. 155, no. 3756, p. 999-1000.
- Reed, G. W., and Turkevich, A., 1957, Uranium, helium and the ages of meteorites: *Nature*, v. 180, p. 594-596.
- Richter, D. H., and Eaton, J. P., 1960, The 1959-60 eruption of Kilauea volcano: *The New Scientist*, v. 7, p. 994-997.
- Ringwood, A. E. 1961, Chemical and genetic relationships among meteorites: *Geochim. et Cosmochim. Acta*, v. 24, no. 3/4, p. 159-198.
- _____, 1966, Genesis of chondritic meteorites: *Rev. Geophysics*, v. 4, no. 2, p. 113-175.
- Sandberger, F. V., 1889, Eon neuer meteorit aus Chile: *Neues. Jahrb. Mineral.*, v. 12, p. 173-180.
- Schaeffer, O. A., and Heymann, D., 1965, Comparison of $\text{Cl}^{36}\text{-Ar}^{36}$ and $\text{Ar}^{39}\text{-Ar}^{38}$ cosmic-ray exposure ages of dated fall iron meteorites: *Jour. Geophys. Res.*, v. 70, no. 1, p. 215-224.
- Schmitt, R. A., and Smith, R. H., 1963, Implications of similarity in rare-earth fractionation of nakhlitic meteorites and terrestrial basalts: *Nature*, v. 199, no. 4893, p. 550-551.
- Schmitt, R. A., Smith, R. H., Lasch, J. E., Mosen, A. W., Olehy, D. A., and Vasilevskis, S., 1963, Abundances of the fourteen rare-earth elements, scandium, and yttrium in meteoritic and terrestrial matter: *Geochim. et Cosmochim. Acta*, v. 27, no. 6, p. 577-622.
- Schnetzler, C. C., and Philpotts, J. A., 1967, Angra dos Reis (stone): rare-earth and barium concentrations and their implications (abs (abs.): Program of the 30th Annual Meeting of the Meteoritical Society.
- Schnetzler, C. C. Philpotts, J. A., and Thomas, H. H., 1967, Rare-earth and barium abundances in Ivory Coast tektites and rocks from the Bosumtwi Crater area, Ghana: *Geochim. et Cosmochim. Acta*, v. 31, no. 10, p. 1987-1993.
- Shoemaker, E. M., Batson, R. M., Holt, H. E., Morris, E. C., Rennilson, J. J., and Whitaker, E. A., 1967, Surveyor V: television pictures: *Science*, v. 158, no. 3801, p. 642-652.

REFERENCES CITED Continued

- Shoemaker, E. M., and Chao, E. C. T., 1961, New evidence for the impact origin of the Ries Basin, Bavaria, Germany: *Jour. Geophys. Res.* v. 66, no. 10, p. 3371-3378.
- Signer, P., and Nier, A. O., 1962, The measurement and interpretation of rare gas concentrations in iron meteorites, in Moore, C. B., ed.: *Researches in meteorites*, New York, John Wiley & Sons, p. 7-35.
- Signer, P., and Suess, H. E., 1963, Rare gases in the sun, in the atmosphere, and in meteorites, in Geiss, J., and Goldberg, E. D. ed.: *Earth science and meteoritics*, Amsterdam, North-Holland Pub. Co., p. 241-272.
- Simpson, E. S., and Murray, D. G., 1932, A new siderolite from Bencubbin, western Australia: *Mineralog. Mag.*, v. 23, no. 136, p. 33-37.
- Smales, A. A., Mapper, D., and Fouché, K. F., 1967, The distribution of some trace elements in iron meteorites, as determined by neutron activation: *Geochim. et Cosmochim. Acta*, v. 31, no. 5, p. 675-720.
- Smith, E. J., Davis, L. Jr., Coleman, P. J. Jr., and Jones, D. E., 1965, Magnetic field measurements near Mars: *Science*, v. 149, no. 3989, p. 1241-1242.
- Stacey, F. D., and Lovering, J. F., 1959, Natural magnetic moments of two chondritic meteorites: *Nature*, v. 183, no. 4660, p. 529-530.
- Stacey, F. D., Lovering, J. F., and Parry, L. G., 1961, Thermomagnetic properties, natural magnetic moments and magnetic anisotropies of some chondritic meteorites: *Jour. Geophys. Res.*, v. 66, no. 5, p. 1523-1534.
- Stauffer, H. A., 1961a, Primordial argon and neon in carbonaceous chondrites and ureilites: *Geochim. et Cosmochim. Acta*, v. 24, p. 70-82.
- _____, 1961b, Cosmogenic argon and neon in stone meteorites: *Jour. Geophys. Res.*, v. 66, no. 5, p. 1513-1522.
- _____, 1962, On the production ratios of rare gas isotopes in stone meteorites: *Jour. Geophys. Res.*, v. 67, no. 5, p. 2023-2028.
- Taylor, H. P. Jr., Duke, M. B., Silver, L. T., and Epstein, S., 1965, Oxygen isotope studies of minerals in stony meteorites: *Geochim. et Cosmochim. Acta*, v. 29, no. 5, p. 489-512.

REFERENCES CITED Continued

- Taylor, H. P. Jr., and Epstein, S., 1963, O^{18}/O^{16} ratios in rocks and coexisting minerals of the Skaergaard intrusion, East Greenland: *Jour. Petrology*, v. 4, p. 51-74.
- Taylor, H. W., 1964, Gamma radiation emitted by the Peace River chondrite: *Jour. Geophys. Res.*, v. 69, no. 19, p. 4194-4196.
- Taylor, S. R., 1966, Australites, Henbury impact glass and subgreywacke: a comparison of the abundances of 51 elements: *Geochim. et Cosmochim. Acta*, v. 30, no. 11, p. 1121-1136.
- Tschermak, G., 1870, Der meteorit von Lodran: *Sitzber. Akad. Wiss.-Wien, Math.-naturw. Kl.*, v. 61, pt. 2, p. 465-475.
- Turkevich, A. L., 1968, (Chemical analyses of the Moon at the Surveyor V, VI, VII landing sites): Surveyor VII press conference, N.A.S.A. headquarters, Washington D.C., February 28, 1968.
- Turkevich, A. L., Franzgrote, E. J., and Patterson, J. H., 1967, Chemical analysis of the moon at the Surveyor V landing site: *Science*, v. 158, no. 3801, p. 635-637.
- Urey, H. C., 1964, A review of atomic abundances in chondrites and the origin of meteorites: *Rev. Geophysics*, v. 2, no. 1, p. 1-34.
- Urey, H. C., and Craig, H., 1953, The composition of the stone meteorites and the origin of meteorites: *Geochim. et Cosmochim. Acta*, v. 4, no. 1, p. 36-82.
- Van Schmus, W. R., 1967, Polymict structure of the Mezö-Madaras chondrite: *Geochim. et Cosmochim. Acta*, v. 31, no. 10, p. 2027-2042.
- Van Schmus, W. R., and Wood, J. A., 1967, A chemical-petrologic classification for the chondritic meteorites: *Geochim. et Cosmochim. Acta*, v. 31, no. 5, p. 747-765.
- Vilcsek, E., and Wänke, H., 1963, Cosmic-ray exposure ages and terrestrial ages of stone and iron meteorites derived from Cl^{36} and Ar^{39} measurements, in *Radioactive dating -- Proceedings of the Internat'l Atomic Energy Agency: Vienna*, p. 381-393.
- Vinogradov, A. P., and Vdovykin, G. P., 1963 *Almazy v kamennykh meteoritakh* [Diamonds in stony meteorites (with English abstract)]: *Geokhimiya*, no. 8, p. 743-750.

REFERENCES CITED Continued

- Voshage, H., 1967, Bestrahlungsalter und herkunft der eisenmeteorite: Zeitschr. Naturforschung, v. 22a, p. 477-506.
- Voshage, H., and Hintenberger, H., 1963, The cosmic-ray exposure ages of iron meteorites as derived from the isotopic composition of potassium and the production rates of cosmogenic nuclides in the past, in Radioactive dating -- Proceedings of the Internat'l Atomic Energy Agency: Vienna, p. 367-379.
- Wahl, W., 1952, The brecciated stony meteorites and meteorites containing foreign fragments: Geochim. et Cosmochim. Acta, v. 2, no. 2, p. 91-117.
- Wasson, J. T., 1966, Butler, Missouri: an iron meteorite with extremely high Ge content: Science, v. 153, no. 3739, p. 976-978.
- _____, 1967a, The chemical classification of iron meteorites: I - A study of iron meteorites with low concentrations of gallium and germanium: Geochim. et Cosmochim. Acta, v. 31, no. 2, p. 161-180.
- _____, 1967b, Chemical definition of genetic groups of iron meteorites: Preprint.
- Wasson, J. T., and Kimberlin, Jerome, 1967, The chemical classification of iron meteorites - II. Irons and pallasites with germanium concentrations between 8 and 100 ppm: Geochim. et Cosmochim. Acta, v. 31, no. 10, p. 2065-2093.
- Wesselink, A. J., 1948, Heat conductivity and the nature of the lunar surface: Bull. Astr. Inst. Netherlands, v. 10, p. 351-363.
- Wiik, H. B., 1956, The chemical composition of some stony meteorites: Geochim. et Cosmochim. Acta, v. 9, no. 5/6, p. 279-289.
- Wilshire, H. G., Cummings, David, Offield, T. W., and Howard, K. A., 1967, Geology of the Sierra Madera cryptoexplosion structure (abs.): Program of the Annual Meeting of the Geological Society of America.
- Wise, D. U., 1963, An origin of the moon by rotational fission during formation of the earth's core: Jour. Geophys. Res., v. 68, no. 5, p. 1547-1554.
- Wlotzka, F., 1963, Uber die hell-dunkel-struktur der urgashaltigen chondrite Breitscheid und Pantar: Geochim. et Cosmochim. Acta, v. 27, no. 5, p. 419-429.

REFERENCES CITED Continued

- Wöhler, F., 1860, Neue untersuchungen uber die bestandtheile des meteorsteines vom Capland: Sitzber, Aka. Wiss.-Wien, Math-naturw. kl, v. 41, p. 565-567.
- Wood, J. A., 1962, Metamorphism in chondrites: Geochim. et Cosmochim. Acta. v. 26, p. 739-749.
- _____, 1963a, Physics and chemistry of meteorites, in Middlehurst, B. M., and Kuiper, G. P., eds.: The moon, meteorites and comets -- the solar system, v. 4, Chicago, Univ. of Chicago Press, p. 337-401.
- _____, 1963b, On the origin of chondrules and chondrites: Icarus, v. 2, no. 2, p. 152-180.
- _____, 1967a, Olivine and pyroxene compositions in type II carbonaceous chondrites: Geochim. et Cosmochim. Acta, v. 31, no. 10, p. 2095-2108.
- _____, 1967b, Chondrites: their metallic minerals, thermal histories, and parent bodies: Icarus, v. 6, no. 1, p. 1-49.
- Zähringer, V. J., 1962a, Isotopie-effekt und haufigkeiten der edelgase in steinmeteoriten und auf der erde: Zeitschr. Naturforschung, v. 17a, no. 6, p. 460-471.
- _____, 1962b, Uber die uredelgase in den achondriten Kapoeta und Staroe Pesjanoe: Geochim. et Cosmochim. Acta, v. 26, no. 6, p. 665-680.
- _____, 1963, Isotopes in tektites, in O'Keefe, J. A., ed.: Tektites, Chicago, Univ. of Chicago Press, p. 137-149.
- Zähringer, V. J., and Gentner, W., 1960, Uredelgase in einigen steinmeteoriten: Zeitschr. Naturforschung, v. 15a, no. 7, p. 600-602.